

Non-invasive body condition monitoring and  
relationships between thermal responses and  
behaviour in captive and wild Nile crocodiles  
(*Crocodylus niloticus*)

by

Devon Marie Viljoen

10120263

Supervisor: Prof Edward Webb

Co-supervisors: Prof Jan Myburgh, Dr Christoff Truter, Prof Jeffrey Lang

Submitted in fulfilment of the academic requirements for the degree

PhD Animal Science

Faculty of Natural and Agricultural Sciences

University of Pretoria

June 2024

## DECLARATION

Full names of student: Devon Marie Viljoen

Student number: 10120263

I, Devon Marie Viljoen, hereby declare that all works and data sources not originating from my own efforts have been duly referenced and acknowledged in accordance with the requirements of the Faculty of Natural and Agricultural Sciences. This dissertation is the result of original research and has been composed by me. It is submitted in partial fulfilment of the requirements for the degree of Doctor of Philosophy (PhD) in Animal Science at the University of Pretoria. This dissertation has not been submitted as part of any previous work, but the following publications have resulted from chapters 3 and 4:

Viljoen, D., Webb, E., Myburgh, J., Truter, C., and Myburgh, A. (2023). Remote body condition scoring of Nile crocodiles (*Crocodylus niloticus*) using uncrewed aerial vehicle derived morphometrics. *Frontiers in Animal Science*, 4:1225396.

Viljoen, D. M., Webb, E. C., Myburgh, J. G., Truter, J. C., Lang, J. W., and Myburgh, A. (2023). Adaptive thermal responses of captive Nile crocodiles (*Crocodylus niloticus*) in South Africa. *Applied Animal Behaviour Science*, 106098.

## ACKNOWLEDGEMENTS

I would like to express my deepest gratitude to my supervisory committee for their unwavering support, insightful critiques, and encouragement throughout this journey. My heartfelt thanks go to Prof Edward Webb, Prof Jan Myburgh, Dr Christoff Truter, and Prof Jeffrey Lang for their invaluable guidance and mentorship, for sharing their expertise and constructive feedback, and for their enriching contributions to my research.

I am profoundly grateful to the Crocodile Specialist Group for their financial support, which was essential to my research. Their contribution has not only facilitated my work but has also underscored the importance of conservation efforts within this research field.

Special appreciation is extended to the farm owners, managers, and dedicated personnel for their involvement in this project. Their exceptional commitment and support that went above and beyond what was required have been instrumental in this work.

My sincere thanks to Danie Pienaar and his colleagues at SANPARKS Kruger National Park for their willingness to supply the data critical to the fifth chapter of this thesis. Their efforts and generosity are valued and greatly appreciated.

I am grateful to Dr Albert Myburgh for sharing his extensive drone knowledge and drone-piloting capabilities, which were intrinsic to multiple chapters of this work.

For the sixth chapter I am particularly thankful to Prof Hannes Van Wyk, whose expertise and recommendations were invaluable.

I also acknowledge the involvement of members at the University of Pretoria's Civil Engineering Department, whose ingenuity in setting up and crocodile-proofing the equipment has been crucial. Their assistance in the material and methods development, as well as the provision of the thermal drone, were indispensable to the success of my research. Thank you to Prof Wynand Steyn, Dr Andre Broekman, and Mr Derek Mostert for your parts in making these studies possible.

On a personal note, I wish to thank my family and friends for their love and encouragement. To my husband, your unwavering faith in me and your constant support have seen me to the end of this process.

## ABSTRACT

As ectotherms, crocodylians achieve and maintain a preferred body temperature by seeking or avoiding heat in the environment. Temperature management influences aspects of crocodile welfare, production, and reproduction, and strongly determines the success of crocodile farming operations. Concerns surrounding temperature management of commercially farmed Nile crocodiles in South Africa have been raised by the NSPCA (National Society for the Prevention of Cruelty to Animals). Wild Nile crocodiles in the Kruger National Park have been affected by pansteatitis outbreaks leading up to and during winter months since 2008. Cooler winter temperatures have been implicated as a potential contributor to the recurrence of this disease. This study evaluated minimally invasive Nile crocodile body condition assessments, thermal experiences and behaviours of wild and captive Nile crocodiles, and the effect of temperature on nest site selection in commercial settings. Non-invasive data capture techniques were employed and developed to ensure the crocodiles natural behaviours, and therefore thermal experiences, were not disrupted or altered. This included drones, an Internet of Things system of abiotic loggers, telemetry tracking and temperature logging systems, and iButtons.

Seven drone-based morphometrics were measured for 288 commercially farmed Nile crocodiles across two farms in South Africa, and a subsequent body condition assessment was conducted using two of these morphometrics. A small and relatively inexpensive drone (DJI Mavic Mini) was selected for this study, after a vigilance assessment concluded that it was minimally disruptive to normal crocodile behaviour. Crocodiles on one farm were slimmer than those on the other farm prior to the drone flights. Crocodile condition was assessed with the following UAV-captured measures: total length (TL), snout-hindlimb length (SHL), snout-neck length (SNL), neck width (NW), belly width (BW), total surface area (SA), and perimeter. A body condition index (BCI) was calculated for each crocodile by measuring the relationship between total length and belly width, with the equation:  $BCI = (BW/TL) * 10$ , derived from photogrammetrically processed orthophotos in GIS. The BCI values were then normalized to form a body condition score (BCS) with the equation:  $BCS = (BCI/1.27) * 4 + 1$ . The body condition score ranked crocodiles from 1–5, with 1 being thin or emaciated and 5 being fat or obese relative to other crocodiles. The majority of crocodiles in the study had a BCS of 3, with few animals scoring a 1 or 5. The farm housing noticeably thinner crocodiles prior to the study had no BCS 5 occurrences, while the other farm had no BCS 1 occurrences. This UAV-based body condition score could be applied to large wild or captive populations for a fast-paced health and welfare evaluation.

Thermal behaviours of captive Nile crocodiles on a commercial crocodile farm in South Africa were assessed using a method which transformed relative thermal maps (produced by a DJI Mavic 2 Enterprise Dual drone) into a predictive model where temperatures were derived to within 2.6 °C per pixel of a processed orthophoto. Thermal behavioural data was extracted from the drone imagery and juxtaposed with climate and abiotic thermal data from the pen. Site (concrete, water, nest, and grass/sand) selection by crocodiles varied with season, time of day, and daily climatic conditions. During high ambient and pen temperatures in summer crocodiles sought refuge in water bodies, which only accounted for 20% of the pens total surface area. During low ambient and pen temperatures in winter the crocodiles prioritized basking on the concrete and grass/sand areas, abandoning the water bodies. The results suggest a need for increased shading over the land areas during summer, and heating of the waterbodies during winter. These alterations would increase the amount of thermally viable areas within the pen, allowing the

crocodiles to exercise heat seeking and avoidance behaviours during both seasons. This method provides a non-invasive assessment of the pens design from a thermal perspective, which can then inform improved temperature management.

Thermal behaviours of 16 wild Nile crocodiles (233–429 cm TL) within Kruger National Park were assessed. Each crocodile was fitted with sensors that recorded external temperatures (attached onto the crocodiles' backs), internal temperatures (stomach), activity (accelerometer), and location (GPS coordinates). Internal body temperatures were strongly influenced by ambient air temperatures and humidity, as well as the immediate external environment temperature. Variations in internal temperatures and activity levels were dependent on sex, size, and season. Seasonal temperature (internal, external, and ambient) and activity level fluctuations varied significantly. Internal temperature averages were low from April to July. Activity means declined from March till May and remained relatively low before increasing again between November and December. Reduced internal temperature and activity levels coincided with outbreaks of pansteatitis, highlighting a potential correlation. As ectotherms, the environmental temperatures available to crocodiles play a critical role in successful thermoregulation and dependent biological processes (metabolism, digestion, reproduction, immune function, muscular function, development, and behaviour). This study expanded the parks understanding of the temperatures experienced by these wild crocodiles and will guide future management efforts with respect to thermal comfort and thermal opportunities.

Nile crocodile nesting behaviours were monitored over a single breeding season on a commercial farm in South Africa. Drones (a DJI Mavic Mini 2 SE and a Mavic 2 Enterprise Dual) were used for overhead behavioural and temperature monitoring, whilst iButtons were placed at ground level recording nest temperatures at various depths and locations around the breeder pen. The farm recorded the numbers of eggs laid and hatched in each nest. The complex interplay between climate, nest thermal properties, crocodile nesting behaviours, and pen layout was inspected. Nesting locations within the pen varied in orientation, thermal properties, distance from waterbodies, distance from a nearby tourist centre, and proportion of grass coverage. Significant variations in nest site selection occurred across nesting locations, with a distinct predilection for certain sections while others were scarcely utilized. Behavioural variations were also noted between sections when considering nest occupancy versus confirmed egg deposition. The characteristics for preferred nesting sites in farmed settings need to be identified and met to ensure that all nesting female crocodiles have sufficient nesting opportunities. Stress due to nest site competition could result in a decrease in laying and hatching success and is a welfare concern.

Given the thermal challenges faced by crocodiles during summer and winter seasons, and the variations in crocodile farm setups in South Africa, guidelines for dynamic and innovative management strategies of both farmed and wild populations are necessary. The findings of these studies inform both farming and conservation efforts regarding the thermal experiences of Nile crocodiles in South Africa. Farming regulations may require updating with regards to temperature/pen design and management, whereas wildlife management initiatives could benefit from wild Nile crocodile thermal experience awareness.

## OPSOMMING

As ektotermes, bereik en handhaaf krokodille 'n voorkeur-liggaamstemperatuur deur hitte in die omgewing te soek óf te vermy. Temperatuurbestuur beïnvloed aspekte van krokodille se welsyn, produksie en voortplanting, wat die sukses van krokodilboerderybedrywighede grootliks bepaal. Kommer oor temperatuurbestuur van Nylkrokodille wat kommersieël in Suid-Afrika geteel word, is deur die NDBV (Nasionale Raad van Dierbeskermingsverenigings) geopper. Wilde Nylkrokodille in die Kruger Nasionale Park is deur pansteatitis-uitbrake geaffekteer in die aanloop tot en gedurende die wintermaande, vanaf 2008. Koeler wintertemperature is geïmpliseer as 'n potensiële bydraende faktor tot die herhalende voorkoms van hierdie siekte. Hierdie studie het met minimaal indringende Nylkrokodil liggaamskondisiebegelings, en termiese ervarings en gedrag van Nylkrokodille geëvalueer, en die effek van temperatuur op die seleksie van nesplek in kommersiële omgewings. Nie-indringende datavasleggingstegnieke is gebruik en ontwikkel om te verseker dat die krokodille se natuurlike gedrag, en dus termiese ervarings, nie ontwrig of verander word nie. Dit het hommeluie, “The Internet of Things-stelsel” van abiotiese aantekenaars, telemetrie-opsporing, temperatuurregistrasiesistelsels en iButtons ingesluit.

Sewer hommeluig-gebaseerde morfometriese metings is gemeet vir 288 Nylkrokodille in kommersiële boerderye by twee plase in Suid-Afrika, en 'n daaropvolgende liggaamskondisiebegelings is uitgevoer met behulp van twee van hierdie morfometriese metings. 'n Klein en relatief goedkoop hommeluig (DJI Mavic Mini) is vir hierdie studie gekies, na 'n waaksaamheidsasessering gevind het dat dit minimaal ontwrigtend vir normale gedrag is. Op een van die plase, was die krokodille maerder as dié op die ander plase voor die evaluasies begin het. Die spektrum van maer tot vet krokodille is geassesseer deur die volgende UAV-vaslegging maatstawwe: totale lengte (TL), snoet tot agterpote lengte (SHL), snoet tot nek lengte (SNL), nek breedte (NW), pens breedte (BW), totale oppervlakte (SA) en omtrek. 'n Liggaamskondisie-indeks (BCI) is vir elke krokodil bereken deur die verwantskap tussen totale lengte en maagwydte, met die vergelyking:  $BCI = (BW/TL) * 10$ , afgelei van fotogrammetries verwerkte ortofoto's in GIS te meet. Die BCI-waardes is dan genormaliseer om 'n liggaamskondisietelling (BCS) te bereken met die vergelyking:  $BCS = (BCI/1.27) * 4 + 1$ . Die liggaamskondisietelling het krokodille van 1-5 gerangskik, 1 is 'n maer of uitgeteerde krokodil, en 5 is 'n vet of oorgewig krokodil in teenstelling met die ander krokodille. 'n BCS van 3 was die algemeenste tussen alle krokodille in die studie, met min diere wat 'n 1 of 5 behaal het. Die plaas waar krokodille met skraler abdominale omtreкке gehuisves was, het geen BCS 5 gevalle gehad nie en die plaas wat krokodille gehuisves het met wyer abdominale omtreкке, het geen BCS 1 gevalle gehad nie. Hierdie UAV-gebaseerde liggaamskondisietelling kan toegepas word op groot wilde of gevange bevolkings vir 'n vinnige gesondheids- en welsynsevaluering.

Termiese gedrag van gevange Nylkrokodille, op 'n kommersiële krokodilplaas in Suid-Afrika, is geassesseer deur gebruik te maak van 'n metode wat relatiewe termiese kaarte (geproduseer deur 'n “DJI Mavic 2 Enterprise Dual” hommeluig) in 'n voorspellings model omskep het waar temperature afgelei is tot binne 2.6 °C per pixel van 'n verwerkte ortofoto. Krokodil termiese gedrag data is onttrek uit die hommeluig beelde en saamgestel met klimaat en abiotiese termiese data uit die kraal. Materiaal (beton, water, nes, en gras/sand) seleksie deur krokodille het gewissel met seisoen, tyd van die dag en daaglikse klimaatstoestande. Tydens hoë omgewings- en hoktemperature in die somer het krokodille skuiling in watermassas gesoek, wat slegs 20% van die krale se totale oppervlakte uitmaak. Tydens lae omgewings-

en hoktemperatuur in die winter het die krokodille gekies om op die beton- en gras-/sandgebiede te bak, en die watermassas te verlaat. Die resultate dui op 'n behoefte aan verhoogde skaduwee oor die landgebiede gedurende die somer, en verhitting van die waterliggame gedurende die winter. Hierdie veranderinge sal die hoeveelheid termiese geskikte areas binne die kraal verhoog, wat die krokodille in staat stel om hittedoekende en vermydingsgedrag gedurende beide seisoene uit te oefen. Hierdie metode het die nie-indringende inspeksie van potensiële tekorte in die kraalontwerp vanuit 'n termiese perspektief moontlik gemaak, wat dan verbeterde temperatuurbestuur kan inlig.

Termiese gedrag van 16 wilde Nylkrokodille (233–429 cm TL) binne die Kruger Nasionale Park is geassesseer. Elke krokodil was toegerus met sensors wat eksterne temperatuur (aan die krokodil se rug vasgeheg), interne temperatuur (maag), aktiwiteit (versnellingsmeter) en ligging (GPS-koördinate). Interne liggaamstemperatuur is beïnvloed deur lug, temperatuur, en humiditeit, sowel as hul onmiddellike eksterne omgewings temperatuur. Variasies in interne temperatuur en aktiwiteitsvlakke was afhanklik van geslag, grootte en seisoen. Seisoenale temperatuur (intern, ekstern en omgewing) en aktiwiteitsvlakskommelings het aansienlik gewissel. Interne temperatuur gemiddeldes het besonder laag gedaal vanaf April tot Julie. Aktiwiteit gemiddeldes het skerp gedaal vanaf Maart tot Mei en het relatief laag gebly totdat dit weer tussen November en Desember toegeneem het. Verlaagde interne temperatuur- en aktiwiteitsvlakke stem ooreen met uitbrake van pansteatitis, wat 'n potensiële korrelasie beklemtoon. As ektoterme, speel die beskikbare omgewingstemperatuur vir krokodille 'n kritieke rol in suksesvolle termoregulering, en die afhanklike biologiese prosesse (metabolisme, vertering, voortplanting, immuunfunksie, spierfunksie, ontwikkeling en gedrag). Hierdie studie het die park se begrip van die temperatuur wat deur hierdie wilde krokodille ervaar word verbeter en sal toekomstige bestuurspogings rig ten opsigte van termiese gerief en termiese geleenthede.

Nylkrokodille se nesgedrag is oor 'n enkele broeiseisoen op 'n kommersiële plaas in Suid-Afrika gemonitor. Hommeltuie ('n "DJI Mavic Mini 2 SE" en 'n "Mavic 2 Enterprise Dual") is gebruik vir oorhoofse gedrags- en temperatuur monitering, terwyl iButtons op grondvlak geplaas is om nesttemperatuur op verskillende dieptes en plekke rondom die teelthok aan te teken. Die plaas het terselfdetyd die getalle van eiers wat gelê en uitgebroei is in elke nes aangeteken. Die komplekse wisselwerking tussen klimaat, die neste se termiese eienskappe, krokodil nesbesoek gedrag, en kraal uitleg is geïnspekteer. Die liggings van neste binne die krale het gewissel in terme van oriëntasie, termiese eienskappe, afstand vanaf waterliggame, afstand vanaf 'n nabygeleë toeristesentrum, en proporsie van gras bedekking. Beduidende variasies in nes seleksie het voorgekom tussen nesplekke, met 'n duidelike voorliefde vir sekere seksies, terwyl ander skaars benut is. Gedragsvariasies is ook tussen seksies opgemerk wanneer nesbesetting teenoor bevestigde eierproduksie oorweeg word. Die vereistes vir voorkeur-nesplekke in boerdery omstandighede moet oorweeg word en nagekom word om te verseker dat alle reproducerende vroulike krokodille voldoende nesgeleenthede het. Stres of mededinging tussen wyfies vir voorkeur nesplekke kan lei tot 'n afname in lê- en uitbroeisukses, en is 'n welsyn bekommernis.

Gegewe die termiese uitdagings waarmee krokodille gedurende die somer- en winterseisoene te kampe het, en die variasies in krokodilplaas fasiliteite in Suid-Afrika, is riglyne vir dinamiese en innoverende bestuurstrategieë van beide geboerde en wilde bevolkings nodig. Die bevindinge van hierdie studies lig beide boerdery- en bewaringspogings in oor die termiese ervarings van Nylkrokodille in Suid-Afrika. Boerderyregulasies moet moontlik opgedateer word met betrekking tot temperatuur/kraal ontwerp en bestuur, terwyl bewaringsinisiatiewe sal baat by die waarnemings oor wilde Nylkrokodille se termiese ervarings.



## TABLE OF CONTENTS

DECLARATION .....	1
ACKNOWLEDGEMENTS .....	2
ABSTRACT .....	3
OPSOMMING .....	5
TABLE OF CONTENTS.....	7
LIST OF TABLES.....	13
LIST OF FIGURES.....	15
LIST OF EQUATIONS .....	20
ABBREVIATIONS .....	22
UNITS.....	24
1. Focussed literature review.....	25
<b>1.1. CROCODILE FARMING .....</b>	<b>25</b>
<b>1.2. MORPHEMETRICS AND BODY CONDITION .....</b>	<b>26</b>
<b>1.3. THERMOREGULATION.....</b>	<b>27</b>
<b>1.4. BEHAVIOUR.....</b>	<b>29</b>
<b>1.5. NESTING .....</b>	<b>29</b>
<b>1.6. APPLICABLE TECHNOLOGIES.....</b>	<b>30</b>
<b>1.7. AIMS AND LAYOUT OF THE THESIS .....</b>	<b>31</b>
2. Material and methods development .....	33
<b>2.1. Drone model and flight altitudes for monitoring farmed Nile crocodiles (<i>Crocodylus niloticus</i>)</b>	<b>36</b>
2.1.1. Introduction .....	36
2.1.2. Materials and methods.....	36
2.1.3. Data analysis .....	37
2.1.4. Results.....	37
2.1.5. Discussion.....	39
2.1.6. Conclusions .....	40
<b>2.2. UAV-based morphometric measurements and body condition assessment .....</b>	<b>41</b>
2.2.1. Introduction .....	41
2.2.2. Materials and methods.....	41
2.2.3. Data analysis .....	43
2.2.4. Results.....	43



2.2.5. Discussion.....	43
2.2.6. Conclusions .....	43
<b>2.3. The transformation of relative temperature maps from a thermal drone (DJI Mavic 2 Enterprise Dual) into a thermal predictive model.....</b>	<b>44</b>
2.3.1. Introduction .....	44
2.3.2. Materials and methods.....	44
2.3.3. Data analysis .....	45
2.3.4. Results.....	45
2.3.5. Discussion.....	46
2.3.6. Conclusions .....	46
<b>2.4. IButton refurbishment: battery and housing replacement.....</b>	<b>47</b>
2.4.1. Introduction .....	47
2.4.2. Materials and methods.....	47
2.4.3. Results.....	50
2.4.4. Discussion.....	50
2.4.5. Conclusions .....	50
<b>2.5. Core body temperatures of farmed grower Nile crocodiles (<i>Crocodylus niloticus</i>) .....</b>	<b>51</b>
2.5.1. Introduction .....	51
2.5.2. Materials and methods.....	51
2.5.3. Data analysis .....	54
2.5.4. Results.....	54
2.5.5. Discussion.....	58
2.5.6. Conclusions .....	59
<b>2.6. IButton encapsulation integrity for core temperature measurement.....</b>	<b>60</b>
2.6.1. Introduction .....	60
2.6.2. Materials and methods.....	60
2.6.3. Data analysis .....	61
2.6.4. Results.....	61
2.6.5. Discussion.....	62
2.6.6. Conclusions .....	62
<b>2.7. Farmed Nile crocodile (<i>Crocodylus niloticus</i>) nest site selection assessment .....</b>	<b>64</b>
2.7.1. Introduction .....	64
2.7.2. Materials and methods.....	64



2.7.3. Data analysis .....	66
2.7.4. Results.....	66
2.7.5. Discussion.....	66
2.7.6. Conclusions .....	66
<b>2.8. Concrete consistency and colour effects on temperature .....</b>	<b>67</b>
2.8.1. Introduction .....	67
2.8.2. Materials and methods.....	67
2.8.3. Data analysis .....	68
2.8.4. Results.....	68
2.8.5. Discussion.....	70
2.8.6. Conclusions .....	71
<b>2.9. Thermal niches of Nile crocodiles (<i>Crocodylus niloticus</i>) in Kruger National Park.....</b>	<b>72</b>
2.9.1. Introduction .....	72
2.9.2. Materials and methods.....	72
2.9.3. Data analysis .....	73
2.9.4. Results.....	73
2.9.5. Discussion.....	73
2.9.6. Conclusions .....	74
<b>3. Remote body condition scoring of Nile crocodiles (<i>Crocodylus niloticus</i>) using Uncrewed Aerial Vehicle derived morphometrics .....</b>	<b>75</b>
<b>3.1. INTRODUCTION .....</b>	<b>75</b>
<b>3.2. AIMS AND HYPOTHESES.....</b>	<b>76</b>
<b>3.3. MATERIALS AND METHODS .....</b>	<b>77</b>
3.3.1. Aerial image acquisition and processing.....	77
3.3.2. Deriving morphometric data.....	77
3.3.3. UAV-based body condition assessment.....	79
<b>3.4. DATA ANALYSIS .....</b>	<b>79</b>
<b>3.5. RESULTS .....</b>	<b>79</b>
3.5.1. Deriving morphometric data.....	79
3.5.2. Body Condition Scores based on UAV-derived morphometrics .....	81
<b>3.6. DISCUSSION.....</b>	<b>83</b>
<b>3.7. CONCLUSIONS .....</b>	<b>84</b>
<b>3.8. CRITICAL EVALUATION AND RECOMMENDATIONS.....</b>	<b>84</b>



4. Adaptive thermal responses of captive Nile crocodiles ( <i>Crocodylus niloticus</i> ) in South Africa .....	85
<b>4.1. INTRODUCTION .....</b>	<b>85</b>
<b>4.2. AIMS AND HYPOTHESES.....</b>	<b>86</b>
<b>4.3. MATERIALS AND METHODS .....</b>	<b>86</b>
4.3.1. Animals, husbandry, and pen layout .....	86
4.3.2. Aerial image acquisition.....	87
4.3.3. Thermal mapping settings and workflow .....	88
4.3.4. Thermal image processing settings in ODM and QGIS .....	88
4.3.5. The thermal environment.....	89
4.3.6. Extracting crocodile behaviour and environmental temperature selection data .....	90
<b>4.4. DATA ANALYSIS .....</b>	<b>90</b>
<b>4.5. RESULTS .....</b>	<b>90</b>
4.5.1. Thermal map conversions.....	90
4.5.2. The thermal environment.....	91
4.5.3. Crocodile thermal behaviours and pen/material utilizations.....	92
4.5.4. Crocodile environmental temperature selections.....	94
<b>4.6. DISCUSSION.....</b>	<b>97</b>
4.6.1. Low-cost thermal mapping .....	97
4.6.2. Crocodile thermal behaviour and pen/material utilization .....	97
4.6.3. Crocodile environmental temperature selections.....	98
<b>4.7. CONCLUSIONS .....</b>	<b>99</b>
<b>4.8. CRITICAL EVALUATION AND RECOMMENDATIONS.....</b>	<b>99</b>
5. Thermal niches of wild Nile crocodiles ( <i>Crocodylus niloticus</i> ) in the Kruger National Park, South Africa .....	101
<b>5.1. INTRODUCTION .....</b>	<b>101</b>
<b>5.2. AIMS AND HYPOTHESES.....</b>	<b>103</b>
<b>5.3. MATERIALS AND METHODS .....</b>	<b>104</b>
5.3.1. Study site, materials, and animals .....	104
5.3.2. Climate data .....	105
5.3.3. Crocodile temperatures .....	105
5.3.4. Thermal behaviour inferences.....	106
5.3.5. Crocodile activity.....	107
<b>5.4. DATA ANALYSIS .....</b>	<b>107</b>



<b>5.5. RESULTS</b> .....	<b>108</b>
5.5.1. Climate data .....	108
5.5.2. Study animals .....	109
5.5.3. Individual variability in temperatures .....	110
5.5.4. Cohort variability in temperatures .....	115
5.5.5. Thermal behavioural inferences .....	119
5.5.6. Crocodile activity.....	122
<b>5.6. DISCUSSION</b> .....	<b>126</b>
5.6.1. Crocodile temperatures .....	126
5.6.2. Thermal behaviour inferences .....	128
5.6.3. Crocodile activity.....	129
<b>5.7. CONCLUSIONS</b> .....	<b>130</b>
<b>5.8. CRITICAL EVALUATION AND RECOMMENDATIONS</b> .....	<b>131</b>
6. Thermal profiles associated with nest site selection of Nile crocodiles ( <i>Crocodylus niloticus</i> ) on a commercial crocodile farm in South Africa.....	132
<b>6.1. INTRODUCTION</b> .....	<b>132</b>
<b>6.2. AIMS AND HYPOTHESES</b> .....	<b>133</b>
<b>6.3. MATERIALS AND METHODS</b> .....	<b>134</b>
6.3.1 Study site and animals .....	134
6.3.2. Nest depth evaluation.....	135
6.3.3. Thermal profiles within nests .....	136
6.3.4. Surface and faunal temperature variations .....	137
6.3.5. Crocodile pen and nest utilization .....	137
<b>6.4. DATA ANALYSIS</b> .....	<b>138</b>
<b>6.5. RESULTS</b> .....	<b>138</b>
6.5.1. Study site and animals .....	138
6.5.2. Nest depth evaluation.....	140
6.5.3. Thermal profiles within nests .....	141
6.5.4. Surface and faunal temperature variations .....	146
6.5.5. Crocodile pen and nest utilization .....	150
<b>6.6. DISCUSSION</b> .....	<b>154</b>
6.6.1. Nest depth evaluation.....	154
6.6.2. Thermal profiles within nests .....	154



6.6.3. Surface and faunal temperature variations .....	155
6.6.4. Crocodile pen and nest utilization .....	156
<b>6.7. CONCLUSIONS .....</b>	<b>156</b>
<b>6.8. CRITICAL EVALUATION AND RECOMMENDATIONS.....</b>	<b>157</b>
7. Concluding summary .....	158
8. References .....	160
9. Appendix .....	174

## LIST OF TABLES

**Table 1.** Scope and context of the methods developed for/alongside, and applied to, the chapters of this thesis.

**Table 2.** Descriptive statistics summary of all pen temperature measures and humidity.

**Table 3.** Morphometric measurements of the 10 grower Nile crocodiles in the study.

**Table 4.** Weekly visual effects of the HCl solution and encapsulated batteries during the month-long study period, and the pH measures before (“pH start”) and after (“pH end”) the batteries were in the solution.

**Table 5.** The mean saturated (“ $M_s$ ”) and unsaturated (“ $M_d$ ”) cube masses, compressive force applied to break the cubes, and the calculated compressive strength of each concrete mix.

**Table 6.** Descriptive statistics for the temperatures of the five concrete slabs and on-site air temperatures (°C).

**Table 7.** Descriptive statistics for the seven UAV-based morphometric measures ( $n = 288$ ).

**Table 8.** Correlations (all highly significant,  $P < 0.001$ ) between the UAV-based morphometric measures.

**Table 9.** Body condition frequencies per BCS rating.

**Table 10.** Descriptive statistics (°C) of positional temperatures (first half of the table) and crocodile back temperatures (second half of the table) per material type and season.

**Table 11.** Crocodile data at deployment: crocodile identification (ID), location of capture and release (post-logger placement), sex, and morphometric measures (cm) per crocodile.

**Table 12.** Descriptive statistics of Nile crocodile  $T_{b_{external}}$ 's (°C).

**Table 13.** Descriptive statistics of Nile crocodile  $T_{b_{internal}}$ 's (°C).

**Table 14.** Descriptive statistics of Nile crocodile  $T_{b_{external}}$ 's (“EXT”, in °C) and  $T_{b_{internal}}$ 's (“INT”, in °C) per sex of the crocodiles.

**Table 15.** Descriptive statistics of Nile crocodile  $T_{b_{external}}$ 's (“EXT”, in °C) and  $T_{b_{internal}}$ 's (“INT”, in °C) per meteorological and climatic seasons.

**Table 16.** Nest site divisions by section, orientation, number of nests per section, mean distance from the closest water body, and mean distance from the tourist walkway.

**Table 17.** Descriptive statistics for the temperatures (°C) recorded by iButtons deployed on dowels, ordered by section and depth (cm).

**Table 18.** Descriptive statistics for the temperatures (°C) recorded by iButtons deployed as singles, ordered by depth (cm).

**Table 19.** Descriptive statistics of drone-derived crocodile back temperatures, positional temperatures, surface temperatures of crocodile-occupied nests, crocodile SHLs, and climate variables on the day of the thermal flights (1 December 2022).



**Table 20.** Nest surface temperature (°C) descriptive statistics per nesting section between 07:00 and 15:00, on 1 December 2022.

## LIST OF FIGURES

**Figure 1.** Digital sketches of a crocodile showing morphometric measures, with dorsal (top) and ventral (bottom) views. Key: total length (TL), snout-vent length (SVL), head length (HL), belly width (BW), head width (HW), neck girth (NG), chest girth (CG), belly girth (BG), and tail girth (TG).

**Figure 2.** A line up of the drones assessed in the current study, arranged from largest to smallest, from left to right: a Matrice 300 RTK, a Mavic 2 Enterprise Dual, a Mavic Air 2, and a Mavic Mini.

**Figure 3.** Flight altitude, in metres, plotted against the average disturbance rating allocated to the various reactions of breeder (a) and grower (b) crocodiles to the drone's presence. The UAVs were given shorthand names for these plots: Mavic Mini = "Mini", Mavic Air 2 = "Air 2", and Mavic 2 Enterprise Dual = "Mavic 2".

**Figure 4.** Flight altitude, in metres, plotted against the sound level. The UAVs were given shorthand names for this graph: Mavic Mini = "Mini", Mavic Air 2 = "Air 2", Mavic 2 Enterprise Dual = "Mavic 2", and Matrice 300 RTK = "M300".

**Figure 5.** (a) Morphological features recognisable from UAV imagery that are required to capture the morphometric measurements for the current study. "A" Illustrates the conclusion of the dermal neck scutes required for the morphological measure SNL. "B" Illustrates to the circumcircle scute layer behind the hind legs, required for the morphological measure SHL. (b) Depicts morphometric measures captured as vector line layers in QGIS, colour codes: total length in yellow, snout-hindlimb length in blue, belly width in pink, neck width in green, and snout-neck length in orange. (c) Depicts morphometric measures captured as vector polygon layers in QGIS: perimeter shown by the black outline of the crocodile, and surface area shown by the gradient-coloured area that falls within the perimeter line.

**Figure 6.** Illustrates the deconstruction of an intact iButton to reveal the battery and printed circuit board. Image (a) depicts the outer stainless-steel cap having been filed through, (b) the plastic insert having been carefully filed through and the lower stainless-steel cap removed, (c) the plastic insert was gently peeled back, and the upper steel cap was removed to reveal the internals, and (d) the PCB viewed from the front, and the old battery inside a plastic frame connected to the grommet. Image (e) depicts the PCB layout where "A" and "C" represent the positive (anode) terminals, "B" the quartz crystal, "D" the negative (cathode or "ground") terminal, and "E" the integrated circuit. The opposing side of the PCB, as seen in figure 6c, represents the "data" terminal.

**Figure 7.** Illustrates the connections between the battery and the iButton PCBs, front (a) and back (b). Image (c) depicts an iButton after it has been sealed in heat shrink and clamped shut with the stranded wires available for configuration.

**Figure 8.** Reader unit modification showing (a) extension wires soldered onto the data and ground ("Gnd/-") electrical contacts at the back of the reader, and (b) the crocodile clips placed onto the wire ends to establish the electrical contact for the one-wire interface.

**Figure 9.** Pen layout (not to scale), depicting the water body placements (dark blue rectangles), the feeding gutter (light blue oval), the concrete encased temperature loggers (grey oblongs), and the placement of shade netting (rectangle with a dot-filled pattern).

**Figure 10.** Placement of loggers (iButtons in green and Hobo pendants in red) within the right-hand water body within the pen (not to scale). The dotted line indicates the chain onto which the iButtons were fitted, and the blue line depicts the water level. Depths are included and marked with arrows.

**Figure 11.** Mean hourly environmental and crocodile temperatures (a) and humidity (b) for the full study period.

**Figure 12.** Grower 1 (a) and grower 2 (b) core body temperatures plotted over the full study period. Dotted lines at 28 °C and 33 °C reference the recommended optimal  $T_{b_{internal}}$ 's for crocodile farming, and dashed lines at 20 °C and 35 °C indicate the recommended lower and upper limits of safe ambient temperatures for crocodilians. These allow the visualization of periods when the recorded temperatures fell outside of what are considered safe ranges.

**Figure 13.** The proportional substrate utilization within the pen on 22 February 2022, between the hours of 08:00 and 15:00. The values above each bar represent the total number of crocodiles in view for that timeslot.

**Figure 14.** Concrete slabs from left to right: granite, dolomite, chrome slag, aerated granite, and lightweight dolomite.

**Figure 15.** Mean monthly (a) and hourly (b) temperature recordings from the various concrete-encased loggers, as well as the control and on-site air temperatures. The hourly mean temperatures are also plotted for summer (c) and winter (d) seasons. A dotted line at 20 °C serves as a reference, facilitating easier comparison of temperature values across different conditions.

**Figure 16.** Repeat of figure 5.

**Figure 17.** (a) Scatterplot depicting the relationship between total length and snout-neck length of 288 farmed Nile crocodiles, and (b) scatterplot depicting total length and snout-hindlimb length of 288 farmed Nile crocodiles. Graphs a and b differentiate the crocodiles farm of origin, crocodiles from farm A are represented with “+” and crocodiles from farm B with “O”.

**Figure 18.** Nile crocodiles within each of the five different body condition scoring (BCS) categories. From left to right, a BCS from 1 to 5 as assessed and derived in the current study.

**Figure 19.** The decision tree identifying the morphometrics (other than TL and BW) that most decisively differentiated the crocodiles’ farm of origin.

**Figure 20.** Ground control point as captured in (a) red, green, and blue (RGB) and (b) greyscale by the DJI Mavic 2 Enterprise Dual. The RGB (a 12-megapixel CMOS sensor) and thermal (uncooled VOx microbolometer thermal sensor) sensors vary in their resolution, hence the image clarity variation.

**Figure 21.** Hourly ambient temperature (a) and relative humidity (b) for the four days included in the assessment.

**Figure 22.** LoRaWAN water (“Twater”) and concrete (shaded represented as “Tconcreteshade” and sunny represented as “Tconcretesun”) temperatures within the timespan of the flights. All plots contain a dashed line at 30 °C for reference.

**Figure 23.** Hourly proportional material use within the pen for all flights.

**Figure 24.** The proportions of heat avoidance (blue) and heat seeking (red) behaviours per material type in summer (a) and winter (b) seasons.

**Figure 25.** Mean hourly crocodile back temperatures (“ $T_{croc}$ ”, represented by dashed lines) and positional temperatures (“ $T_{position}$ ”, represented by solid lines) are plotted against time (corresponding to all flights on each date). Both season and daily climatic condition are accounted for in the graph’s colouration.

**Figure 26.** The relationship between crocodile back temperature and positional temperature selected by the crocodiles, for summer (a) and winter (b) seasons. The colouration of the plot indicates which material type the crocodiles were selecting for each datapoint.

**Figure 27.** (a) Map of South Africa highlighting Kruger National Park (KNP) in red, (b) map of KNP indicating the specific study site with a box, (c) study site at the confluence of the Olifants and Letaba Rivers into Masingir Dam. The Wireless Wildlife base station and repeater placements are depicted with red and green rhombuses, respectively.

**Figure 28.** Seasonal air temperatures from two metres above the Olifants-Letaba confluence (ERA5) from 2018–2020. Air temperatures per time of day (a), meteorological season (b), and climatic seasons (c) are depicted. Each boxplot displays the median (centre line), interquartile range (box edges), and  $1.5 \times IQR$  (whiskers). Points beyond the whiskers represent outliers. Means are represented by red rhombuses.

**Figure 29.** (a) Depicts a male (“M”) and female (“F”) Nile crocodiles’ hourly internal temperatures during a cool week in winter, (b) depicts the same male and female Nile crocodiles’ internal temperatures during a warm week in spring. The length measure refers to the crocodiles SVLs and is organized in descending order.

**Figure 30.** (a) Depicts the internal temperatures of five Nile crocodiles of varying size over a week in July 2018, (b) depicts the internal temperatures of four Nile crocodiles of varying size over a week in November 2018. The length measure refers to the crocodiles SVLs and is organized in descending order.

**Figure 31.** (a) Depicts the internal temperatures of one male and two female crocodiles over a week in October 2018, (b) depicts the internal temperatures of two males and one female crocodile over a week in September 2020. The length measure refers to the crocodiles SVLs and is organized in descending order.

**Figure 32.** Mean hourly (a) and monthly (b) internal (“ $T_{b_{internal}}$ ”), external (“ $T_{b_{external}}$ ”), and air (“ $T_{air}$ ”) temperatures. Time of day categories and day and nighttime categories are shown in plot “a” with dotted lines on the plot and sun and moon symbols below the hours on the x-axis. Meteorological and climatic seasons are shown in plot “b” with dotted lines on the plot and colourful droplet (rainy) and sun (dry) symbols below the months on the x-axis, respectively.

**Figure 33.** Mean monthly internal (a) and external (b) temperatures, for all crocodiles (black plot) and per sex (see legend). Meteorological and climatic seasons are shown with dotted lines on the plots and droplet (rainy) and sun (dry) symbols below the month numbers, respectively.

**Figure 34.** A proportional display of hourly inferred heating and cooling behaviours per sex of the crocodiles.

**Figure 35.** Mean hourly variations in temperature differences between internal (“ $T_{b_{int}}$ ”), external (“ $T_{b_{ext}}$ ”), and air temperature (“ $T_{air}$ ”) measurements across meteorological seasons. Time of day categories and day and night categories are shown with dotted lines on the plot and sun and moon symbols below the hours on the x-axis. Each season is represented by a unique colour and line texture for clarity. A horizontal line at  $y = 0$  indicates the baseline where there is no difference, facilitating the comparison of temperatures above and below this threshold.

**Figure 36.** Scatterplots of internal versus external temperatures (a), internal versus air temperatures (b), and external versus air temperatures (c).

**Figure 37.** The extent of riverine habitat-use by all male (a) and all female (b) Nile crocodiles from 2018–2020.

**Figure 38.** Mean hourly (a) and monthly (b) activity per season of the year. Male (M) and female (F) activities have been illustrated separately. Time of day categories and day and nighttime categories are shown in plot “a” with dotted lines on the plot and sun and moon symbols below the hours on the x-axis. Meteorological and climatic seasons are shown in plot “b” with dotted lines on the plot and droplet (rainy) and sun (dry) symbols below the month numbers, respectively.

**Figure 39.** Mean hourly activity per meteorological (a) and climatic (b) seasons of the year. (c) Depicts the mean hourly activity over the climatic seasons, with sex as an added element. Time of day categories and day and nighttime categories are shown with dotted lines on the plot and sun and moon symbols below the hours on the x-axis, respectively.

**Figure 40.** A not-to-scale diagram of the study site, showing the placements of nesting sections A–F. The walkway is represented with horizontal-lines, and the waterbodies are coloured blue.

**Figure 41.** Images of (a) the 3D printer holders, (b) dowel iButtons, and (c) single iButtons.

**Figure 42.** Hourly (a) air temperature ( $^{\circ}\text{C}$ ), (b) relative humidity (% RH), (c) solar radiation ( $\text{W}/\text{m}^2$ ), (d) wind speed (m/s), and (e) rainfall (mm) throughout the nesting period (October–December 2022). Solid lines represent the mean per hour.

**Figure 43.** Nest depth variables (shallowest egg, deepest egg, and nest depth) between coarse and fine sanded nests on a commercial Nile crocodile farm in South Africa. Each boxplot displays the median (centre line), interquartile range (box edges), and  $1.5 * \text{IQR}$  (whiskers). Points beyond the whiskers represent outliers.

**Figure 44.** Sand temperatures recorded at varying depths below ground level. Plot (a) depicts measurements from dowel iButtons placed at 10, 20, 30, and 40 cm below the surface, and (b) depicts temperatures from harvested nest sites, specifically at the depth of the deepest egg, using single iButtons. Each boxplot displays the median (centre line), interquartile range (box edges), and  $1.5 * \text{IQR}$  (whiskers). Points beyond the whiskers represent outliers and means are represented by red rhombuses.

**Figure 45.** Single iButton sand temperatures recorded in each nest orientation. Each boxplot displays the median (centre line), interquartile range (box edges), and  $1.5 * \text{IQR}$  (whiskers). Points beyond the whiskers represent outliers and means are represented by red rhombuses.

**Figure 46.** Daily sand temperature ranges of the dowel iButtons arranged by depth (a), single iButtons arranged by depth (b), and single iButtons arranged by orientation (c). Each boxplot displays the median (centre line), interquartile range (box edges), and  $1.5 * \text{IQR}$  (whiskers). Points beyond the whiskers represent outliers and means are represented by red rhombuses.

**Figure 47.** A stacked bar plot depicting the proportional pen area/substrate occupancy per hour of 1 December 2022, from the DJI Mavic 2 Enterprise Dual drone-produced imagery.

**Figure 48.** Depicts the hourly (a) air temperature ( $^{\circ}\text{C}$ ), (b) relative humidity (% RH), (c) wind speed (m/s), and (d) radiation ( $\text{W}/\text{m}^2$ ) on 1 December 2022.

**Figure 49.** Mean hourly nest surface temperatures by (a) nesting section, (b) nesting orientation, and (c) grass-cover status of the nesting site.

**Figure 50.** Mean hourly shading percentage over the nesting sites per (a) nesting section and (b) nesting orientation.

**Figure 51.** Proportional pen area/substrate use per time of the day, categorized into morning (before 11:00), midday (12:00–13:00), and afternoon (after 15:00).

**Figure 52.** The proportional nest site occupancy (a) and confirmed nesting successes (b) per nesting section.

**Figure 53.** SHL of the crocodiles occupying the various pen areas (a), nesting sections (b), and nesting orientations (c). Each boxplot displays the median (centre line), interquartile range (box edges), and 1.5 \* IQR (whiskers). Points beyond the whiskers represent outliers and means are represented by red rhombuses.

## LIST OF EQUATIONS

**Equation 1.** Sound meter readings, above background noise levels, of drones.

$$SL = \frac{SLM_x - \text{Background noise}}{2}$$

**Equation 2.** Body condition index calculation.

$$BCI = \left(\frac{BW}{TL}\right) \times 10$$

**Equation 3.** Body condition score calculation.

$$BCS = \left(\frac{BCI - 1.34}{1.27}\right) \times 4 + 1$$

**Equation 4.** Thermal map conversion.

$$y = 0.3593x + 5.16$$

**Equation 5.** Repeat of equation 2.

**Equation 6.** Repeat of equation 3.

**Equation 7.** Correlation between total length and snout-hindlimb length.

$$TL = SHL (1.91) + 0.08$$

**Equation 8.** Correlation between total length and snout-neck length.

$$TL = SNL (4.33) + 0.37$$

**Equation 9.** Correlation between snout-hindlimb length and snout-neck length.

$$SHL = SNL (2.25) + 0.17$$

**Equation 10.** Repeat of equation 4.

**Equation 11.** S-curve regression of the relationship between thermal drone measured crocodile back temperatures and selected substrate temperatures.

$$T_{\text{croc}} = e^{\left(3.861 + \frac{(-12.223)}{T_{\text{position}}}\right)}$$

**Equation 12.** S-curve regression of the relationship between thermal drone measured crocodile back temperatures and selected substrate temperatures, exclusively in summer.

$$T_{\text{croc}} = e^{\left(3.982 + \frac{(-15.652)}{T_{\text{position}}}\right)}$$

**Equation 13.** S-curve regression of the relationship between thermal drone measured crocodile back temperatures and selected substrate temperatures, exclusively in winter.

$$T_{\text{croc}} = e^{\left(3.842 + \frac{(-11.745)}{T_{\text{position}}}\right)}$$

**Equation 14.** S-curve regression of the relationship between internal body temperatures and external body temperatures.

$$Tb_{\text{internal}} = e^{(3.610 + (-9.806)/T_{\text{external}})}$$

**Equation 15.** S-curve regression of the relationship between internal body temperatures and external body temperatures.

$$Tb_{\text{internal}} = e^{(3.506 + (-7.366)/T_{\text{air}})}$$

**Equation 16.** S-curve regression of the relationship between external body temperatures and air temperatures.

$$Tb_{\text{external}} = e^{(3.839 + (-15.706)/T_{\text{air}})}$$



## ABBREVIATIONS

BCI	Body condition index
BCS	Body condition score
BG	Belly girth
BW	Belly width
$\beta$	Beta level
CITES	Convention on International Trade in Endangered Species of Wild Flora and Fauna
CMOS	Complementary metal oxide semiconductor
df	Degrees of freedom
e.g.	For example
F	F-value
GCP	Ground control point
GPS	Global positioning system
GSD	Ground sampling distance
HL	Head length
HW	Head width
i.e.	In other words
IoT	Internet of Things
KNP	Kruger National Park
LoRaWAN	Low-power wide-area network
NG	Neck girth
NSPCA	National Society for the Prevention of Cruelty to Animals
NW	Neck width
ODM	OpenDroneMap
P	P-value
PCB	Printed circuit board
QGIS	Quantum Geographic Information System
RGB	Red, green, and blue



SA	Surface area
SAWS	South Africa Weather Service
SD	Standard deviation
SE	Standard error
SHL	Snout-hindlimb length
SNL	Snout-neck length
SVL	Snout-vent length
Tb	Body temperature
Tb <sub>internal</sub>	External body temperature
Tb <sub>external</sub>	Internal or “core” body temperature
TG	Tail girth
TL	Total length
UAV	Uncrewed aerial vehicle
$\bar{x}$	Mean
$\chi^2$	Chi-square
z	Z-score



## UNITS

°C	Degrees Celsius
cm	Centimetre
kg	Kilogram
kg/m <sup>3</sup>	Kilogram per cubic metre
km	Kilometre
m	Metre
mm	Millimetre
MPa	Megapascal
m/s	Metres per second
m <sup>2</sup>	Metres squared
N	Newton
% RH	Relative humidity
W/m <sup>2</sup>	Watts per square metre
%	Percent

# 1. Focussed literature review

## 1.1. CROCODILE FARMING

Crocodile farming emerged following the over-exploitation of wild populations in the mid-20<sup>th</sup> century. The CITES (Convention on International Trade in Endangered Species of Wild Flora and Fauna, <https://cites.org>) protection acts, implemented in 1975, marked a turn towards conservation, with crocodile farming practices contributing to the preservation of the species (Hoffman *et al.*, 2000; Flint *et al.*, 2000; Bothma & Van Rooyen, 2005; MacGregor, 2006; Brien *et al.*, 2007; Wallace & Leslie, 2008; Tosun, 2013; Tosun, 2013; Mpofu *et al.*, 2015; Manolis & Webb, 2016). Crocodile farming employs closed system breeding for skin and meat production, where animals are not harvested from or returned to the wild (Bolton, 1989; MacGregor, 2006; Brien *et al.*, 2007; Ganswindt *et al.*, 2014). Crocodile skin is highly valued in luxury markets for its use in fashion items, and crocodile meat has been promoted as a healthy alternative due to its low sodium and high unsaturated fat content (Bolton, 1989; Hoffman *et al.*, 2000; MacGregor, 2006; Beyeler, 2011; Tosun, 2013). Crocodile farming practices have shifted towards more intensive and controlled environments to improve skin quality and animal welfare (Davis, 2001; Bothma & Van Rooyen, 2005; Mpofu *et al.*, 2015). Crocodiles in captivity have different housing and nutritional requirements than their wild counterparts. Farm/pen design, water quality, and feed management are critical for improving skin quality, maintaining welfare standards, and reducing stress and disease (Bolton, 1989; Brien *et al.*, 2007). Properly managed temperature, density, and hygiene are essential, with special attention to pen and pond design to prevent injury, promote health, and reduce stressors (Davis, 2001; Bothma & Van Rooyen, 2005; Brien, 2015). Breeder (mature or adult crocodiles) and grower (between one-year-old and harvest size) crocodile husbandry varies to accommodate differences in size and behaviour. Crocodile farming welfare is guided by evolving standards and practices, such as the five freedoms and the more recent five domains' models. These models provide guidelines for assessing and identifying improvements in nutrition, environment, health, behaviour, and mental state to ensure that animals thrive in captivity (Mellor, 2016; Mellor, 2017).

The Nile crocodile (*Crocodylus niloticus*) is one of the largest living reptilian species and is endemic to freshwater habitats across Africa and Madagascar (Bolton, 1989; Flint *et al.*, 2000; Bothma & Van Rooyen, 2005; MacGregor, 2006; Mpofu *et al.*, 2015). Although not considered an endangered species, the Nile crocodile remains conservation dependent with region-dependent protection under CITES (Flint *et al.*, 2000; MacGregor, 2006; Beyeler, 2011; Blessing *et al.*, 2014). Farming practices in South Africa began in the 1970s, evolving from extensive egg harvesting from the wild to more intensive, captive breeding methods (Else *et al.*, 1990; Flint *et al.*, 2000; Bothma & Van Rooyen, 2005; Mpofu *et al.*, 2015). Nile crocodile skins are classified as "classic leather" in international markets, and Nile crocodiles are one of the preferred species for luxury leather goods (Bothma & Van Rooyen, 2005; MacGregor, 2006). In South Africa, the NSPCA (National Society for the Prevention of Cruelty to Animals) plays a role in recommending improved welfare standards for farmed Nile crocodiles.

Efficient pen design for captive crocodile farming balances safety, hygiene, and sufficient space for the expression of natural behaviours. Smooth concrete (or plastic) flooring is synonymous in farming operations for minimizing skin damage and its thermal properties, although insulation may be needed in colder climates to prevent heat loss (Bolton, 1989; Bothma & Van Rooyen, 2005; Shilton *et al.*, 2014). Pen walls should be a metre high, minimum, with smooth finishes and neutral colours to prevent escape and to simulate a natural environment (Bothma & Van Rooyen, 2005). Walls can be designed to curve slightly

inward, and securely lockable gates are critical for handler and crocodile safety (Bolton, 1989; Brien *et al.*, 2007). Social separation within pens can be achieved with barriers, which reduce stress and minimize aggressive interactions (Davis, 2001; Brien *et al.*, 2007; Groffen *et al.*, 2013). General recommendations are that water bodies should comprise 50–70% of pens, with depths allowing crocodiles to stand and a gradual incline for easy haul-out. Ponds should be spacious enough for all crocodiles to submerge simultaneously, and regular cleaning and proper drainage maintain hygiene and minimize the risks of disease (Bothma & Van Rooyen, 2005; Brien *et al.*, 2007). Natural ponds have a greater propensity for hygiene, disease, and treatment related issues (Brien *et al.*, 2007) and are recommended against for these reasons. Water temperature is important in farming scenarios where air temperatures cannot be precisely controlled. Maintaining the water temperatures at optimums allows the crocodiles to seek out warmth/cooling when needed (Davis, 2001; Isberg, 2007; Shilton *et al.*, 2014; Brien, 2015). Overall, pen and pond design must consider the crocodiles physical and behavioural needs for optimal welfare and productivity.

## 1.2. MORPHEMETRICS AND BODY CONDITION

Morphometrics are measurements of body dimension and/or mass and are commonly used to assess both captive and wild crocodile populations. These measurements are of ecological importance as they provide individual and population-level information about size, growth, and health (Salem, 2011; Warner<sup>1</sup> *et al.*, 2016). A selection of morphometrics that are regularly used to monitor crocodiles include length, width, girth, and mass (Salem, 2011; Warner<sup>1</sup> *et al.*, 2016; Edwards *et al.*, 2017; Webb *et al.*, 2021). Total length (TL) is measured from the tip of the snout to the tip of the tail. TL is a quick measurement that can be measured or estimated from multiple angles, although tail tip loss can affect its accuracy. Snout-vent length (SVL) is measured from the tip of the snout to the third circumcircle scute layer of the tail which corresponds to the caudal margin of the cloaca. SVL requires the crocodile to be flipped onto its back which may be stressful but avoids potential tail tip loss errors. Head length (HL) is measured from the tip of the snout to the posterior ridge of the supraoccipital bone. These three length measures have been mathematically related to one another in a previous Nile crocodile study so that should only one be available the other two could be estimated (Warner<sup>1</sup> *et al.*, 2016). Belly width (BW) is the transverse measurement across the widest part of a crocodile's smooth ventral belly scutes. Head width (HW) is the transverse measurement across the widest part of the head. Belly girth (BG) is the circumference measurement around the widest part of the belly. Neck girth (NG) is the circumference measurement around the widest part of the neck between the head and shoulders. Chest girth (CG) is the circumference measurement around the widest part of the chest, just posterior to front legs. Tail girth (TG) is the circumference measurement around the widest part of the tail immediately posterior to the hindlegs (Salem, 2011; Warner<sup>1</sup> *et al.*, 2016; Edwards *et al.*, 2017; Webb *et al.*, 2021) (figure 1).

Body condition scores are a useful indicator of an individual animal's overall health and fitness. Factors such as diet, density, season, temperatures (ambient, air, and water), sex, and health status can all affect body condition (Zweig, 2003; Mazzotti *et al.*, 2012; Brandt *et al.*, 2016; Ojeda-Adame *et al.*, 2020). Body condition assessments generally incorporate measurements of length (i.e., TL, SVL, and HL) and volume (i.e., body mass, TG, NG, and CG). Fultons K is a common body condition index in aquaculture and has been used for crocodilians. This index assumes isometric growth and is considered useful for comparisons across populations (Zweig, 2003; Salem, 2011; Mazzotti *et al.*, 2012; Brandt *et al.*, 2016). Ojeda-Adame *et al.* (2020) proposed a more in-depth and hands-on condition scoring system for crocodilians that assessed

multiple morphological zones known to accumulate fat and skeletal muscle. Working with wild animal populations or very large individuals may necessitate more non-invasive methods. UAV-based body condition assessments have utilized measures such as straight-line body length, belly girth (estimated from belly widths), and surface area morphometrics. Such methods have been applied to Fur seals, Antillean manatees, and eastern North Pacific gray whales (Allan *et al.*, 2019; Soledade Lemos *et al.*, 2020; Ramos *et al.*, 2022).

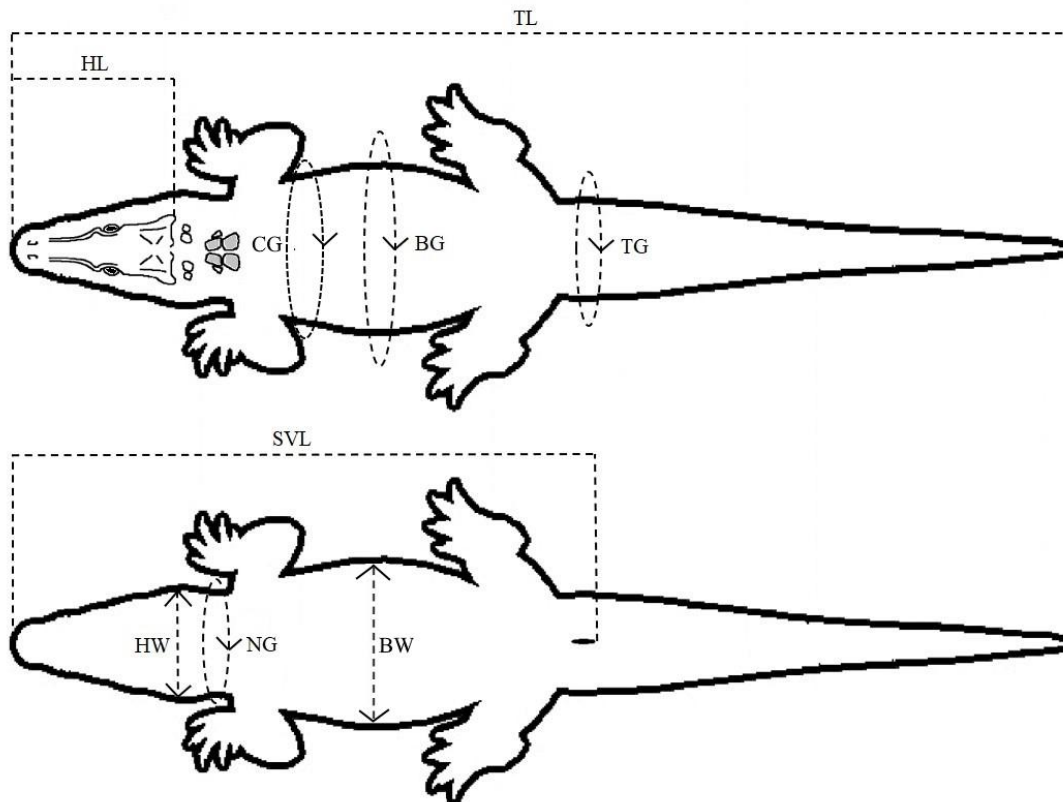


**Figure 1.** Digital sketches of a crocodile showing morphometric measures, with dorsal (top) and ventral (bottom) views. Key: total length (TL), snout-vent length (SVL), head length (HL), belly width (BW), head width (HW), neck girth (NG), chest girth (CG), belly girth (BG), and tail girth (TG).

### 1.3. THERMOREGULATION

Crocodiles are ectotherms, meaning their body temperatures rely heavily upon ambient temperatures available within their immediate environments (Lang<sup>2</sup>, 1987; Huchzermeyer, 2003; Bassetti *et al.*, 2014). Maintaining body temperatures within a “preferred” or optimal range, regardless of environmental temperature fluctuations, optimizes performance and is essential for survival (Lang<sup>2</sup>, 1987; Huchzermeyer, 2003; Seebacher, 2005; Bassetti *et al.*, 2014). Multiple biological processes depend on temperature maintenance, including metabolic processes, digestion, growth rates, and reproduction (Lang<sup>2</sup>, 1987; Huchzermeyer, 2003; Bothma & Van Rooyen, 2005; Bassetti *et al.*, 2014). Thermal preferences and tolerances are essential for survival and effective functioning but are not fixed. Preferred body temperatures change with size, age, reproductive status, nutritional condition, season, immediate

thermal environment, and ontogeny (Lang<sup>2</sup>, 1987; Seebacher & Grigg, 2001; Bassetti *et al.*, 2014; Telemeco *et al.*, 2017).

Various behavioural and physiological adaptations in reptiles, including crocodiles, determine the success of thermoregulation. Crocodiles actively engage in thermal behaviours such as basking, shuttling, posturing and gaping, while physiological mechanisms, including metabolism, heart rate, blood flow, and breathing occur intrinsically as a response to fluctuations in body temperature (Grigg & Alchin, 1976; Spotila *et al.*, 1977; Lang<sup>1</sup>, 1987; Seebacher, 1999; Seebacher & Grigg, 2001; Franklin & Seebacher, 2003; Seebacher, 2005; Downs *et al.*, 2008; Manolis & Webb, 2016; Price *et al.*, 2022). Basking involves lying in the sun to raise the body temperature (Lang, 1977; Downs *et al.*, 2008). Shuttling allows the selection of optimal temperatures along environmentally available thermal gradients; this is achieved by moving between either sunny and shaded or terrestrial and aquatic habitats (Lang<sup>1</sup>, 1987). Selecting specific orientations relative to the sun, posturing the body, and gaping have also been shown to aid thermoregulation (Spotila *et al.*, 1977, Terpin *et al.*, 1979; Seebacher, 1999). Thermal inertia effects in alligators showed that larger animals retained heat for longer periods and were less susceptible to short-term environmental temperature fluctuations (Colbert *et al.*, 1946).

Crocodile metabolic rates slow when environmental temperatures cool, allowing for extended survival without food as the animal's energy demands decrease. At constant low temperatures (10–20 °C) crocodiles cease feeding as food decomposition can occur in the stomach, potentially poisoning the animal (Colbert *et al.*, 1946; Lang<sup>2</sup>, 1987; Bolton, 1989). Heart rate modulation is a physiological mechanism for thermoregulation in ectotherms. Crocodile heart rates increase during basking which facilitates warming and decrease in cooler environments to assist heat retention (Grigg & Alchin, 1976; Franklin & Seebacher, 2003). Vasoconstriction near the skins surface conserves heat within the body and vasodilation increases heat loss to the crocodile's immediate environment (Grigg & Alchin, 1976; Seebacher & Franklin, 2007).

Previous studies have assessed how size, habitat, time of day, season, feeding status, reproduction, posture, and behaviour influences crocodilian thermoregulatory patterns (Lang<sup>2</sup>, 1987; Seebacher & Grigg, 1997; Grigg *et al.*, 1998; Seebacher, 1999; Glanville & Seebacher, 2006; Brien *et al.*, 2012; Bassetti *et al.*, 2014; Whitaker & Srinivasan, 2018). For the Nile crocodile, body temperature patterns and thermoregulatory behaviours in both wild and captive environments have been assessed, although the temperature recording methodologies varied (Loveridge, 1984; Downs *et al.*, 2008; Hocutt, 2022). Core body temperatures in wild, adult Nile crocodiles' range between 13.0–36.5 °C in winter (Downs *et al.*, 2008), and 15.0–36.4 °C between 10:00 and 17:00 in winter and spring (Hocutt, 2022). Monitoring temperatures in larger crocodiles is complicated by various factors including their size, movement between land and water, the temperatures experienced by the animal itself varying from that of the environment, and local climatic variations (temperature, humidity, radiation, and wind) (Cremieux *et al.*, 2005; Downs *et al.*, 2008; Bassetti *et al.*, 2014). Changes in environmental temperature can influence thermoregulatory activities, habitat ranges, breeding and nesting success, sex ratios, and overall survival (Lang<sup>2</sup>, 1987; Refsnider, 2012; Mainwaring *et al.*, 2017; Fukuda *et al.*, 2022).

In farmed settings, ambient temperatures between 17–35 °C are recommended, as constant temperatures above or below this range can be detrimental to crocodile health. Core body temperatures between 28–33 °C have been recommended for ideal growth and production of farmed grower crocodiles (Colbert *et al.*, 1946; Lang<sup>2</sup>, 1987; Bolton, 1989; Huchzermeyer, 2003; Bothma and van Rooyen, 2005;

CFAZ, 2012; Bassetti *et al.*, 2014). Temperature mismanagement is a potential stressor, impacting successful production and survival rates. Strict temperature controls are essential for younger crocodiles in intensively managed environments, while breeder crocodiles in natural pens experience ambient temperatures dictated by the prevailing local climate (Bolton, 1989; Huchzermeyer, 2003; Bothma and van Rooyen, 2005; Downs *et al.*, 2008; CFAZ, 2012).

#### 1.4. BEHAVIOUR

Crocodylian behaviour and social interactions are complex and influenced by both physical and chemical processes within the body. Crocodile social behaviours evolve with age, size, and gender (Lang<sup>1</sup>, 1987; Huchzermeyer, 2003). Previous studies indicate that captive crocodiles exhibit different social dynamics than their wild counterparts (Lang<sup>1</sup>, 1987). Farm conditions usually impose higher than natural densities which can impact growth and survival (Lang<sup>1</sup>, 1987; Huchzermeyer, 2003; Brien<sup>2,3</sup> *et al.*, 2013; Webb *et al.*, 2013).

Wild juvenile crocodiles form groups for safety when small, before eventually dispersing as competitive and dominance behaviours begin to emerge (Lang<sup>1</sup>, 1987; Huchzermeyer, 2003). Social hierarchies form in captivity where dominant individuals dictate feeding and space usage of subordinates, which in turn impacts the health and behaviour of those individuals (Lang<sup>1</sup>, 1987; Huchzermeyer, 2003; Brien<sup>1,2</sup> *et al.*, 2013; Webb *et al.*, 2013). Periodic sorting into size-similar groups is practiced by farmers to mitigate aggression and improve overall welfare in farming environments (Lang<sup>1</sup>, 1987; Morpurgo *et al.*, 1993; Cuijk, 2011; Webb *et al.*, 2013; Brien, 2015). Aggressive interactions in farming scenarios are unavoidable but can be reduced by maintaining similar sized groupings, providing suitable thermal environments, and sufficient space both on land and in the water for all individuals (Davis, 2001; Huchzermeyer, 2003; Brien<sup>1,2,3</sup> *et al.*, 2013; Pooley *et al.*, 2019).

Behavioural monitoring on farms can inform management strategies that ensure more natural behaviours are encouraged (Lang<sup>1</sup>, 1987; Bothma & Van Rooyen, 2005; Brien<sup>1,2,3</sup> *et al.*, 2013; Tosun, 2013). Ethograms have been used in multiple studies assessing crocodylian behaviours, and these should encompass as many aspects of both social and maintenance behaviours as possible (Cuijk, 2011; Brien<sup>1,2,3</sup> *et al.*, 2013). Repetitive disturbances such as capture, varying feeding regimes or diets, and approaching crocodiles closely can cause various changes in their natural behaviours, e.g., reduced appetites, impaired thermoregulation, disrupted social behaviour, and altered reproductive activities (Lang<sup>1,2</sup>, 1987). Regular feeding/cleaning schedules are necessary in captive situations to avoid these negative stress-effects (Lang<sup>1</sup>, 1987; Huchzermeyer, 2002; Bothma & Van Rooyen, 2005). Species specific stress-related behaviours in grower-sized crocodiles (e.g., piling, distress calls, and signs of dehydration) can be critical markers for monitoring welfare (CFAZ, 2012; Manolis & Webb, 2016; Mellor, 2016). Disease monitoring can also be incorporated into this type of behavioural monitoring as reduced immunity due to stress and/or poor management strategies (inappropriate temperatures, housing, feeding, hygiene protocols, and/or hierarchical antagonistic interactions) can lead to increased disease susceptibility (Huchzermeyer, 2002; Bothma & Van Rooyen, 2005; Beyeler, 2011).

#### 1.5. NESTING

Reproductive husbandry for commercially farmed crocodiles integrates breeding, incubation, and hatchling management. Sexual maturity is influenced by age, growth rates, and diet quality (Bolton, 1989;

Brien *et al.*, 2007; Magnino *et al.*, 2009; Lance *et al.*, 2015). Genetic diversity can be maintained by procurement/trade of breeding stock between farms. This is recommended to ensure captive populations do not become too closely related and continue to produce well (Bothma & Van Rooyen, 2005; Tosun, 2013). Wild and captive Nile crocodiles mate seasonally, with eggs laid in September–January in most of South Africa. However, this is dependent on climate and environmental conditions (Bolton, 1989; Swanepoel<sup>2</sup> *et al.*, 2000; Davis, 2001; Bothma & Van Rooyen, 2005). Incubation practices require precise temperature and humidity control, and careful handling to ensure hatchling viability (Bolton, 1989; Bothma & Van Rooyen, 2005; Tosun, 2013). Keeping records of breeding and hatching successes enable monitoring of trends and patterns, detection of issues, and inform better management (Bolton, 1989; Bothma & Van Rooyen, 2005; Tosun, 2013).

In commercial settings, successful breeding is influenced by the size, number, and sex ratio of crocodiles in a defined area. Wild male Nile crocodiles exhibit territorial behaviour across large stretches of aquatic habitat during mating seasons, whereas farmed males have less opportunity to disperse. Balanced sex ratios (eight females to one male) and enclosure designs which minimize breeding male conflicts will enhance fertility rates and minimize stress and aggression during breeding seasons (Bolton, 1989; Bothma & Van Rooyen, 2005; Verdade *et al.*, 2006; Brien *et al.*, 2007). Breeder pen stocking densities can be maximized via pool and enclosure shape/design and the presence of barriers (Verdade *et al.*, 2006; Brien *et al.*, 2007).

Nesting activities and behaviours can vary with species, temperature, day-length, location, female size and experience, and the number of competing females in the area (Kofron, 1989; Swanepoel<sup>2</sup> *et al.*, 2000; Refsnider, 2012; Murray *et al.*, 2020). Providing sufficient nesting areas and nesting material within a breeder pen will minimize fighting and maximize nesting success. Female Nile crocodiles select an appropriate nesting site and then dig 40–50 cm down into the soil (hole-nesters), where they then deposit between 30 and 90 eggs (Bolton, 1989; Bothma & Van Rooyen, 2005; Tosun, 2013). Nile crocodiles protect their nests for much of the incubation period (11–14 weeks), this is true of wild as well as farmed females which continue to guard their nesting sites even after egg removal (Bolton, 1989; Bothma & Van Rooyen, 2005; Tosun, 2013). Incubation temperatures determine hatchling fertility, future preferred body temperatures, and hatchling sex ratios due to the phenomenon of temperature-dependent sex determination (Lang<sup>2</sup>, 1987; Bothma & Van Rooyen, 2005; Tosun, 2013; Manolis & Webb, 2016; Murray *et al.*, 2020). Temperatures above 34 °C or below 31 °C produce predominantly female hatchlings, whereas intermediate temperatures tend to produce male hatchlings (Hutton<sup>2</sup>, 1987; Deeming, 2004; Bothma & Van Rooyen, 2005; López-Luna *et al.*, 2015).

Nest site selection and nesting success is dependent on temperature, soil, vegetative cover, nest site accessibility, and proximity to water (Murray *et al.*, 2020). The relationship between nesting behaviours and changing environmental conditions have been assessed for multiple nest-building reptilians, with particular interest in the long-term effects of climate change on nesting success, egg mortalities, and potential skewed sex ratios (Maciejewski, 2006; McGaugh & Jansen, 2011; Refsnider, 2012; Telemeco *et al.*, 2013; Hill *et al.*, 2015; Mainwaring *et al.*, 2017).

## 1.6. APPLICABLE TECHNOLOGIES

LoRaWAN technology, a critical component of the broader concept of Internet of Things (IoT) network, provides a data communication platform characterized by low power consumption, long-range

connectivity, high capacity, end-to-end security, broad coverage, and affordability. LoRaWAN communications, derived from Chirp Spread Spectrum technology, enable real-time data collection and remote monitoring of relevant study areas, organisms, and equipment (<https://www.thethingsnetwork.org>). The precise management of resources, livestock, and crop conditions improves decision making processes and operational efficiencies (Elijah *et al.*, 2018; Casas *et al.*, 2021). Wireless sensor networks like LoRaWAN are being incorporated into precision farming and sustainable agriculture practices, with potential for increased yields and health monitoring. Global population growth is driving enhanced farming strategies, and incorporating systems like LoRaWAN to monitor real-time effects within complex agricultural operations is expanding (Elijah *et al.*, 2018; Singh *et al.*, 2020; Casas *et al.*, 2021).

Small, sturdy, relatively affordable temperature loggers called iButtons have been extensively applied to thermal studies involving habitats, plants, and animals (Seebacher *et al.*, 2003; Downs *et al.*, 2008; López-Luna *et al.*, 2015; Smith *et al.*, 2015; Fawcett *et al.*, 2019). IButtons are capable of logging accurate temperatures over long recording periods and due to their small size are easily incorporated into environments and animal bodies (Smith *et al.*, 2015; Murray *et al.*, 2016). Their stainless-steel casings afford them a level of protection from damage and make them resistant to moisture, extreme temperatures, and dust. Further weatherproofing is achieved through encasement of iButtons in waterproofing materials such as rubberized coatings, wax, and epoxy (Robert & Thompson, 2003; Davies, 2005; Downs *et al.*, 2008; Brien *et al.*, 2012). These devices have been used to record external animal temperatures via adhesion to body surfaces or placement in tags (e.g., ear tags or collars), as well as internal temperatures via subcutaneous implantation or even feeding the loggers to the animals (Seebacher *et al.*, 2003; Davies, 2005; Downs *et al.*, 2008; Brien *et al.*, 2012; Moon *et al.*, 2021).

Drones or uncrewed aerial vehicles (UAV) have been used to monitor wild and captive animal populations, for both conservation and captive management purposes (Aubert *et al.*, 2021). The variable sensors and camera options available enable assessments of animal health, behaviour, distribution, habitat use, welfare, and productivity (Ezat *et al.*, 2018; Ramos *et al.*, 2022; de Kock *et al.*, 2021; Aubert *et al.*, 2021; Viljoen<sup>1,3</sup> *et al.*, 2023). Some advantages of UAV use in animal monitoring include access to generally inaccessible areas, non-intrusive surveying of shy or dangerous species, and fast-paced monitoring of large areas (Aubert *et al.*, 2021). Individual identification from drone imagery/video outputs could prove invaluable for farming practices as well as wild animal tracking (Andrew *et al.*, 2020; Desai *et al.*, 2022). Desai *et al.* (2022) performed individual identification of mugger crocodiles (*Crocodylus palustris*) using high resolution drone imagery. The ethical application of drone monitoring for animal species that may become aware of the drone's presence have been assessed and altitudes as well as size of the drones used can vary with study species (Hodgson & Koh, 2016; Bevan *et al.*, 2018). Although various drone models were employed and different crocodylian species assessed, altitudes in the range 40–50 metres above ground level have been suggested for crocodile studies (Bevan *et al.*, 2018; Ezat *et al.*, 2018; Aubert *et al.*, 2021; Myburgh *et al.*, 2021; Viljoen<sup>2</sup> *et al.*, 2023).

## 1.7. AIMS AND LAYOUT OF THE THESIS

The contents of this thesis assess thermal and behavioural experiences of captive and wild Nile crocodiles in South Africa. A material and methods development chapter precedes the main findings. It describes various assessments and methodologies developed which allowed the research resulting in the main findings assessments (chapters 3 to 6), or that occurred alongside or between those assessments. There

is a degree of repetition throughout this thesis for this reason. Although not always directly related to the main chapters, the details of the methods developed hold value for researchers involved in the fields of thermal and behavioural assessments for crocodiles.

Chapter 3 describes a UAV-based morphometrics data capture method to develop a rapid and non-invasive body condition scoring system. Breeder sized farmed Nile crocodiles were successfully ranked from emaciated to obese and the morphometrics that best delineated farm of origin (and therefore nutritional status) were assessed. Preceding this morphometric measurement and body condition scoring evaluation, a drone-vigilance assessment was conducted to identify which drone models and altitudes should be applied to drone assessments of breeder and grower-sized Nile crocodiles. The results for the vigilance assessment, presented in the materials and methods development chapter, dictated the size of crocodiles for which the morphometrics and body condition assessment was carried out.

Chapter 4 developed and applied a non-invasive thermal data capture technique to assess ambient temperatures and those selected by captive adult Nile crocodiles on a commercial farm in South Africa. Both thermal and behavioural data were extracted from thermal drone (Mavic 2 Enterprise Dual) imagery and juxtaposed with climate data from local weather stations and an on-site Internet of Things system. This methodology allowed the comparison of summer and winter thermal selections of farmed Nile crocodiles in a natural open-aired pen, highlighting pen design successes and shortfalls.

Chapter 5 evaluated the thermal profiles, behavioural patterns, and activity rhythms of adult Nile crocodiles in Kruger National Park from 2018 to 2020. The study providing data for this chapter commenced independently of the doctoral research. However, it was later incorporated due to its relevance to the overarching objectives of the thesis. It examines the thermoregulatory capabilities of wild crocodilians inhabiting the Letaba and Olifants Rivers by analysing core and surface body temperatures. The analysis also considers seasonal variations in body temperature and activity levels, considering recent Pansteatitis outbreaks affecting the population and the relevance of temperatures during the months of and leading into winter.

Chapter 6 assessed thermal and locational characteristics of preferred nesting sites and nest occupancy on a commercial crocodile farm in South Africa. Thermal data for the pen, the crocodiles within the pen, and the various pen substrates were collected using a thermal drone (Mavic 2 Enterprise Dual) (methodology as per Viljoen<sup>3</sup> *et al.*, 2023 and chapter 4 of this thesis). IButton temperature loggers were deployed at ground level to assess subsurface nest temperatures. The combination of surface thermal data with subsurface sand (within nest sites) thermal data allowed a more inclusive assessment of thermal factors affecting nest site selections. Nest site preferences of the crocodiles in this study were complex but quantifiable, and therefore manageable on farms.

## 2. Material and methods development

This chapter provides a detailed description of the methods employed to assess Nile crocodile thermal and behavioural experiences, as well as the development of fast-paced and non-invasive methodologies for monitoring the well-being of these animals in commercial production systems and in the wild. Wild crocodiles are elusive and difficult to handle due to their size and the risk of injury. The largest wild populations of Nile crocodiles reside within protected areas such as Kruger National Park (KNP), the Limpopo River outside of KNP, Lake St. Lucia, and Phongolo Nature Reserve (Isberg *et al.*, 2019). Captive crocodiles offer a more reliable means of assessment due to their housing in close quarters and sizes ranging from hatchling to breeder being available for research purposes. Various methods applied to captive crocodiles within this study are potentially applicable to wild crocodile studies. Both captive and wild Nile crocodile population assessments were carried out and the results are presented across four chapters. The following assessments and development of methods are described in detail:

- An assessment of available drone models and altitudes for monitoring farmed Nile crocodiles
- A drone-based morphometrics measurement and resulting non-invasive body condition scoring method
- The transformation of relative temperature maps from a thermal drone (DJI Mavic 2 Enterprise Dual) into a thermal predictive model for extracting temperature and behaviour of farmed Nile crocodiles
- The refurbishment of battery-depleted small temperature loggers (iButtons)
- An assessment of core body temperatures of farmed grower Nile crocodiles using rubber-coating encased iButtons and a simple force-feeding method
- An assessment of farmed Nile crocodile stomach pH and the survival of rubber and plastic logger coatings for a month-long period in similar pHs
- A drone-based assessment of nesting site preferences paired with a subsurface nest temperature evaluation using iButtons
- An assessment of colour and consistency effects on outdoor concrete temperatures by encasing LoRaWAN loggers in concrete slabs of various mix designs
- An assessment of the thermal experiences/behaviours and activity patterns of Nile crocodiles within the Kruger National Park using a selection of Wireless Wildlife ([www.wireless-wildlife.co.za](http://www.wireless-wildlife.co.za)) tracking devices

Ethical approval for these studies was granted by the University of Pretoria Animal Ethics Committee, reference number NAS327/2020. This approval covered all the methodologies employed and those developed in this study, except for those utilized in the research on wild crocodiles in the Kruger National Park. The Kruger National Park study clearances fell under SANParks project number GUILLJ1090.

Table 1 describes the methods developed in further detail and contextualizes the necessity of each assessment that occurred in connection with this PhD, the scope shorthand of “MD” stands for method development, and “Ch” refers to the chapters within the thesis document.

**Table 1.** Scope and context of the methods developed for/alongside, and applied to, the chapters of this thesis.

Method	Subjects	Context	Materials	Scope	Aims (A) and objectives (O)
2.1. Drone model and flight altitudes for monitoring farmed Nile crocodiles ( <i>Crocodylus niloticus</i> )	Farmed grower and breeder Nile crocodiles	This assessment preceded and informed chapters 3, 4, and 6	DJI Mavic Mini, DJI Mavic Air 2, DJI Mavic 2 Enterprise Dual, Matrice 300 RTK	MD1	A: Identify appropriate drone models and flight altitudes for farmed grower and breeder Nile crocodile assessments. O: Conduct a behavioural assessment to identify the least disruptive drone models and altitudes for body condition, thermal selections, and nest site selections studies.
2.2. UAV-based morphometric measurements and body condition assessment	Farmed breeder Nile crocodiles	This assessment resulted in chapter 3	DJI Mavic Mini	Ch3	A: Non-invasively capture morphometric data for captive breeder Nile crocodiles in South Africa, using a drone. O: Use UAV-derived morphometrics to estimate a fast-paced non-invasive body condition score.
2.3. The transformation of relative temperature maps from a thermal drone (DJI Mavic 2 Enterprise Dual) into a thermal predictive model	Farmed breeder Nile crocodiles	This method was applied in chapters 4 and 6	DJI Mavic 2 Enterprise Dual, ASSTech handheld infrared thermometer (ST653)	MD2 (Ch4 & Ch6)	A: Transform relative temperature maps (DJI Mavic 2 Enterprise Dual) into a thermal predictive model. O: Derive and apply an equation that converts the RGB values of resulting orthophoto pixels into predicted temperature values.
2.4. iButton refurbishment: battery and housing replacement	Nests and pen materials	Logger shortages necessitated rebuilds to continue with environmental monitoring in method 2.5 and chapter 6	Depleted iButtons (DS1921G-F5#), various electronic repair tools	MD3	A: Refurbish depleted iButtons donated to the PhD study amidst a nation-wide iButton shortage. O: Develop a refurbishment method for depleted iButtons for continued use in thermal studies. Deploy these iButtons for environmental monitoring purposes.
2.5. Core body temperatures of farmed grower Nile crocodiles ( <i>Crocodylus niloticus</i> )	Farmed grower Nile crocodiles	The failures that occurred during the assessment precluded its	iButtons (DS1921G-F5#) and refurbished iButtons	MD4	A: Assess the temperature selections of farmed grower Nile crocodiles under hyperthermia strain. O: Deploy a selection of internal (fed) and external (tail) iButtons in summer. Use refurbished iButtons for pen temperature monitoring. Assess the thermal selections of farmed



Method	Subjects	Context	Materials	Scope	Aims (A) and objectives (O)
2.6. IButton encapsulation integrity for core temperature measurement	Future studies utilizing iButtons for core body temperature monitoring in crocodiles	inclusion as a chapter This assessment addresses the former methods (2.6) failures and identifies improvements for future replications	Batteries with stainless steel casings like that of iButtons, HCl solution (pH = 2), pH meter	MD5	grower Nile crocodiles and how these correlated to the ambient climatic conditions. A: Address the setbacks encountered when force-feeding iButtons to farmed grower Nile crocodiles. O: Address the reason for iButton failure (encapsulations destroyed by stomach acids), identify the stomach acid pH to which the iButtons were originally exposed, conduct a laboratory assessment which identifies more appropriate future deployment guidelines for this encapsulation method.
2.7. Farmed Nile crocodile ( <i>Crocodylus niloticus</i> ) nest site selection assessment	Farmed breeder Nile crocodiles	This assessment resulted in chapter 6	DJI Mavic Mini SE, DJI Mavic 2 Enterprise Dual	Ch6	A: Assess thermal and locational influences on nest site selections on a commercial crocodile farm. O: Identify nest depths appropriate for temperature logger placements, place temperature loggers within randomly selected and excavated/active nest sites, apply predictive temperature model to assess surface level nest temperatures, monitor nesting behaviours, correlate all findings into an assessment of factors influencing nest site selections.
2.8. Concrete consistency and colour effects on temperature	-	The potential thermal suitability of coloured concretes for farming purposes was assessed	7x Tektelic Comfort Smart Room Sensors	MD6	A: Assess how altering the colour and consistency of concrete may affect temperatures. O: Mix similar concrete recipes whose primary aggregates vary in colour and cast LoRaWAN loggers into the centre of these blocks for thermal monitoring. Deploy the slabs and leave them out in the open for at least a month of each meteorological season.
2.9. Thermal niches of Nile crocodiles ( <i>Crocodylus niloticus</i> ) in Kruger National Park	Wild subadult and adult Nile crocodiles	This assessment resulted in chapter 5	Wireless Wildlife tracking system	Ch5	A: Explore the thermal selections, behaviours, and activity patterns of adult Nile crocodiles at KNP 2018–2020. O: Assess temperatures, behaviours, and activity of wild Nile crocodiles using a Wireless Wildlife system of devices.

## 2.1. Drone model and flight altitudes for monitoring farmed Nile crocodiles (*Crocodylus niloticus*)

### 2.1.1. Introduction

Drone presence and the resulting behavioural responses of UAV-surveyed species have been highlighted in previous studies (Bevan *et al.*, 2018; Ezat *et al.*, 2018; Aubert *et al.*, 2021). Saltwater crocodile (*Crocodylus porosus*) and West African crocodile (*Crocodylus suchus*) reactions to UAV presence have been assessed and flight altitudes of 50 m and 40 m were suggested for minimal disturbance, respectively (Bevan *et al.*, 2018; Aubert *et al.*, 2021). The current assessment identified the appropriate drone and flight altitudes for farmed grower (< 1.5 metres in total length) and breeder Nile crocodiles ( $\geq 1.5$  metres in total length). Four drone models available to the researchers at the time of the assessment were evaluated. An appropriate flight altitude was assessed for three of the drone models: a Mavic Mini (249 grams), a Mavic Air 2 (570 grams) and a Mavic 2 Enterprise Dual (899 grams). Drone sound outputs were recorded for these three drones. A Matrice 300 RTK (3600 grams) drone's sound output was also recorded, but this drone was not considered for crocodile monitoring on the farms due to its large size and high noise levels.

### 2.1.2. Materials and methods

Sound intensity for each drone tested was recorded with an Iso-Tech sound level meter (SLM 1352P). Each drone was flown to an altitude of 120 metres (m) above the sound level meter's position (placed in a quiet, empty parking lot on a windy day) and recordings occurred every 10 m of the drone's descent beginning at 100 m altitude and ending at 10 m altitude. Background noise levels were recorded before each flight began. Sound meter readings above background noise levels were expressed at each altitude by means of the equation:

$$SL = \frac{SLM_x - \text{Background noise}}{2}, \quad \text{Equation 1}$$

Where SL stands for "sound level",  $SLM_x$  refers to the sound level meters recording at "x" altitude, and Background noise refers to the background noise recorded before the flight.

The disturbance assessment was performed on a commercial crocodile farm in South Africa and flights were performed in the late morning when the crocodiles were exhibiting basking behaviour. For the vigilance assessment, each drone was flown to an altitude of 120 m at a distance from the pens to be monitored so as not to alert the crocodiles of the drone's presence. Each drone was then flown over a designated area in the pens, maintaining an altitude of 120 m. The drone's altitude was lowered 10 m at a time at a speed of < 1 m/s, stopping after each 10 m increment. Once the stopping altitude had been reached the drones were then flown forward, backward, left, and right (to account for the sound of propellers relative to the wind direction) for approximately 10 m in horizontal distance. All crocodile behaviours/reactions to the drone were recorded from 100 m to < 10 m above the crocodiles. Behaviours observed, seemingly as a direct result of the drone's presence, were recorded and rated on a scale of 0 (no reaction) to 5 (the most disruptive reactions). Each of the three drones was tested six times over different areas of two large breeder pens, and the ratings recorded per altitude were averaged. Grower pens were smaller in size and so testing multiple times over a single pen was avoided, each drone was tested three times over different grower pens and the ratings recorded per altitude were averaged. The disturbance ratings for the drone vigilance assessment were as follows: head raises or tilts in the direction of the drone (i.e., noticing the drone's presence) were rated with a score of 1, opening of mouths directed towards the drone (i.e., a potential warning sign) were rated with a score of 2, limb or bodily movements away from or towards the drone (i.e., the legs are pulled in towards the body, heads moved away from the drones area of approach, or there was a shift of

position either towards or away from the drone) were rated with a score of 3, walking away from the drone (and either laying down again further away or continuing to slowly move away from the drone) were rated with a score of 4, and scattering (where multiple if not all crocodiles hurriedly left the drones area in favour of water bodies) were rated with a score of 5. Ratings of 4 and 5 were considered particularly detrimental, causing both crocodile and potential data capture disturbances. Scores of 0–2 would be considered ideal for unimpeded capture of crocodiles in resulting orthophotos. The four drones studied were photographed alongside one another for a size comparison, this image is presented in figure 2.



**Figure 2.** A line up of the drones assessed in the current study, arranged from largest to smallest, from left to right: a Matrice 300 RTK, a Mavic 2 Enterprise Dual, a Mavic Air 2, and a Mavic Mini.

#### 2.1.3. Data analysis

Disturbance data was captured in Microsoft Excel<sup>®</sup> and the figures were created using this program. The data was then analysed SPSS (version 28.0.1.0, 142), using a generalized mixed model analysis, for the determination of significant differences ( $P < 0.05$ ). Breeder and grower reactions to the drones were assessed and discussed separately.

#### 2.1.4. Results

Breeder crocodile reactions, presented as a disturbance rating, varied with drone model ( $P < 0.001$ ,  $F = 10.97$ ,  $df = 2$ ) and flight altitude ( $P < 0.05$ ,  $F = 2.28$ ,  $df = 10$ ). Breeder reactions were correlated to drone altitudes ( $r = -0.77$ ,  $P < 0.001$ ). Breeder reactions elicited during the Mavic Mini flights differed significantly from those of the Mavic Air 2 and Mavic 2 Enterprise Dual ( $P < 0.001$ ). Breeder reactions did not differ significantly between the Mavic Air 2 and Mavic 2 Enterprise Dual flights ( $P > 0.05$ ). Of the drones assessed the Mavic Mini elicited the lowest disturbance rating over nearly all altitudes tested, with breeders noticing this drone only once it reached a 60 m altitude. The Mavic Mini did not produce disturbance ratings above 3 even when it was within 2 m of the breeder crocodiles' heads. The Mavic 2 Enterprise Duals disturbance ratings were steady below 2, until altitudes of 20 m and below were reached. The Mavic Air 2 drone showed a similar disturbance trend as the Mavic Mini; however, it produced higher disturbance ratings from breeder crocodiles at most flight altitudes when compared to the Mavic Mini.

Grower crocodile reactions varied with drone model ( $P < 0.05$ ,  $F = 6.27$ ,  $df = 2$ ) and flight altitude ( $P < 0.05$ ,  $F = 3.83$ ,  $df = 10$ ). Grower reactions were correlated to drone altitudes ( $r = -0.82$ ,  $P < 0.001$ ). Grower reactions elicited during the Mavic 2 Enterprise Dual flights differed significantly from those of the Mavic Air 2 ( $P < 0.05$ ) and Mavic Mini ( $P < 0.001$ ). Grower reactions did not differ significantly between the Mavic Air 2 and Mavic Mini flights ( $P > 0.05$ ). Of the drones assessed the Mavic 2 Enterprise Dual elicited the lowest disturbance rating for grower crocodiles at altitudes  $\geq 30$  metres,

after which the responses elicited became comparable to those of the other two drones. Grower crocodiles only noticed the Mavic 2 Enterprise Dual drone at an altitude of 40 m, whereas the other two drones were noticed almost immediately. All three drones elicited disturbance ratings as high as 5 in grower crocodiles when altitudes fell below 10 m. The Mavic Air 2 drone showed a similar disturbance trend to the Mavic Mini with grower crocodiles. Figure 3 depicts the results of the crocodile vigilance (represented by a disturbance rating) tests for breeder and grower sized crocodiles.

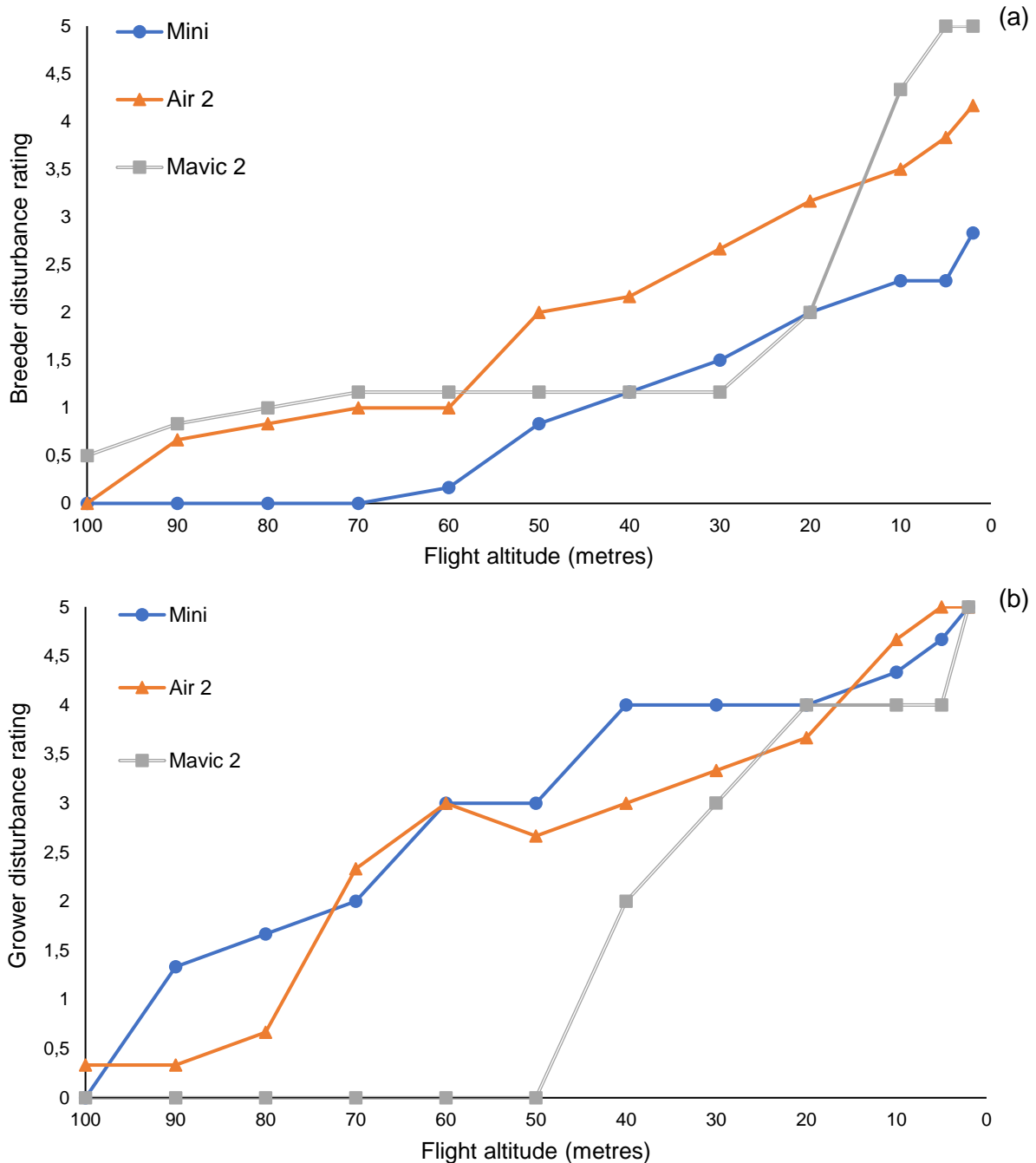


**Figure 3.** Flight altitude, in metres, plotted against the average disturbance rating allocated to the various reactions of breeder (a) and grower (b) crocodiles to the drone’s presence. The UAVs were given shorthand names for these plots: Mavic Mini = “Mini”, Mavic Air 2 = “Air 2”, and Mavic 2 Enterprise Dual = “Mavic 2”.

The drones varied in the altitudes at which they were first audible above background noise levels. The Mavic 2 Enterprise Dual registered above the background noise on the sound meter at lower altitudes when compared to the Mavic Air 2 and Mavic Mini. The Matrice 300's total noise output was the greatest, followed by the Mavic Air 2, the Mavic Mini, and finally the Mavic 2 Enterprise Dual. The sound levels of the drones differed as follows: the Mavic Mini differed significantly from the Matrice 300 ( $P < 0.05$ ), the Matrice 300 also differed significantly from the Mavic 2 Enterprise Dual ( $P < 0.01$ ), and the Mavic Air 2 differed significantly from the Mavic 2 Enterprise Dual ( $P < 0.05$ ). Both breeder and grower crocodile reactions to drone presence were positively correlated to drone sound levels ( $r = 0.72, P < 0.001$ ;  $r = 0.71, P < 0.001$ , respectively), which were negatively correlated to drone altitude ( $r = -0.82, P < 0.001$ ;  $r = -0.84, P < 0.001$ , respectively). The sound level recordings for the four drones are depicted in figure 4.

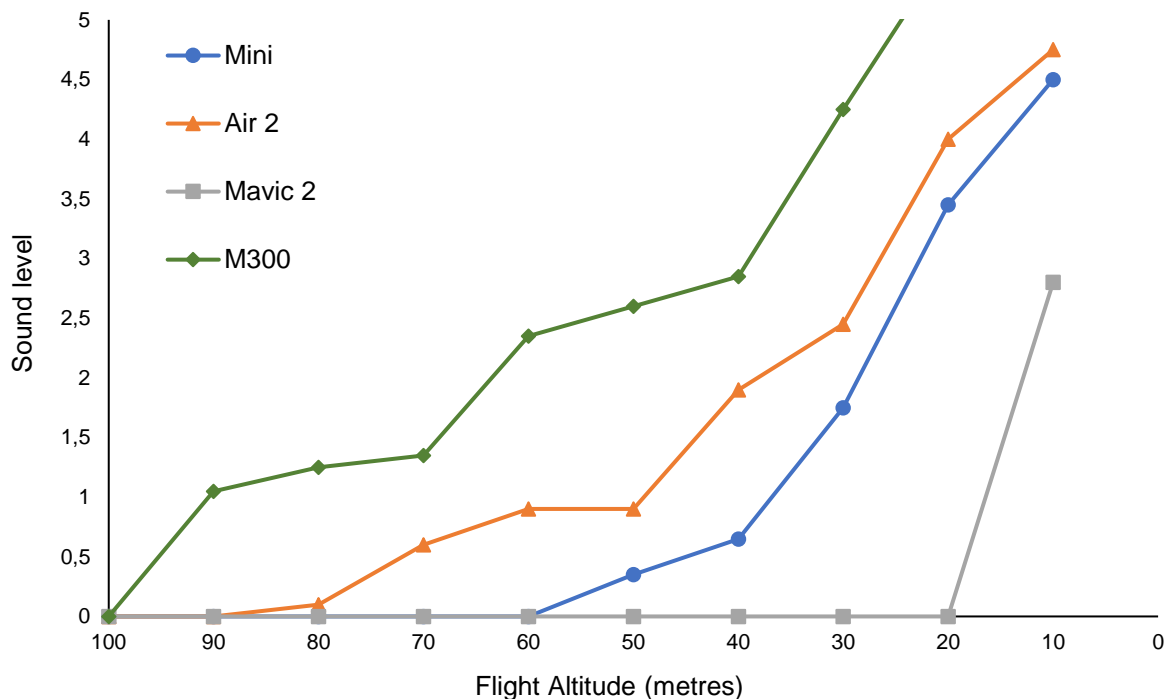


**Figure 4.** Flight altitude, in metres, plotted against the sound level. The UAVs were given shorthand names for this graph: Mavic Mini = “Mini”, Mavic Air 2 = “Air 2”, Mavic 2 Enterprise Dual = “Mavic 2”, and Matrice 300 RTK = “M300”.

#### 2.1.5. Discussion

Small consumer UAVs can be viable for crocodile population monitoring as they elicit minimal animal disturbance. The results of this disturbance assessment indicate that farmed breeder Nile crocodiles only reacted strongly to the presence of the drone once the noise of the UAV was audible above background noise levels. Although the Mavic 2 Enterprise Dual elicited very little response above 30 m altitudes, the Mavic Mini failed to elicit any class 4 or 5 disturbance responses for breeder sized crocodiles. This is noteworthy since class 4 or 5 disturbances impacted the physical positioning of the crocodiles. Such disruptions may have physiological consequences including disrupted thermoregulation, i.e., moving away from a basking position due to drone disturbance. The relatively low altitude achieved with the Mavic 2 Enterprise Dual, without eliciting high disturbance ratings in breeders, may be pertinent for wildlife studies where altitudes below 40 m are typically not required. The crocodiles assessed in this study were from a commercial farm where more human activity and

auditory disturbances (machinery and human-related noises) are expected than in natural settings, wild crocodiles may react differently to the drone models tested here.

The Mavic 2 Enterprise Dual was recalled (by the researchers) as having had a lower hum to its noise outputs than the smaller two drones assessed in this study. The sound level meter utilized only measured sound intensity of the drones, not pitch or sound wave frequencies. A previous study showed that higher pitched juvenile calls elicited greater responses from Nile crocodile females (Chabert *et al.*, 2015). Future studies of adult crocodile drone vigilance might consider pitch as well as sound intensity of the UAVs employed. The use of larger UAV platforms cannot be recommended based solely on noise outputs. The size of the drones likely impacted the disturbance ratings at lower altitudes, which could explain the sudden increase in disturbance ratings once the Mavic 2 Enterprise Dual descended below 30 m altitudes for breeders, and 40 m altitudes for growers. The single altitude for all assessed drones which elicited disturbance responses of 3 or lower for grower crocodiles was 50 m above ground surface level. The Mavic 2 Enterprise Dual drone achieved grower disturbance scores averaging 2 at 40 m; however, as the drone descended past this threshold, the disturbance ratings increased rapidly, catching up with those of the other drones. In this study, the Mavic Air 2 and the Mavic Mini drones elicited similar levels of disturbance in grower Nile crocodiles. Breeder crocodiles responded differently, exhibiting consistently lower disturbance levels to the Mavic Mini when compared to the Mavic Air 2.

#### 2.1.6. Conclusions

The results of the current study suggest that the Mavic Mini may be the preferred UAV (of the UAV models assessed) for breeder crocodile monitoring with minimal disturbance, provided it can cover the area under study. For grower crocodiles on the other hand the Mavic 2 Enterprise Dual, when flown at altitudes 40 m and higher, might be preferred. All drones tested elicited disturbance ratings below 3 at 50 m and higher for grower and breeder-sized crocodiles. The DJI Mavic Mini altitudes of  $\geq 40$  m did not elicit disturbance ratings greater than a 1 in breeders, and Myburgh *et al.* (2021) found geometric accuracy in orthophotographs produced from the DJI Mavic Mini and processed with ODM photogrammetry software at altitudes lower than 70 m above ground level. This assessment concludes that the Mavic Mini, flown at altitudes of 40–60 m above ground level would be ideally suited to a morphometrics and body condition study of farmed breeder Nile crocodiles. Grower crocodiles were more skittish around drones than their full-grown counterparts, and drone studies assessing animals  $< 1.5$  m in total length may consider flying at the highest altitudes which would suit their purposes so as not to stress these smaller crocodiles. These findings are like those of Bevan *et al.* (2018) and Aubert *et al.* (2021) who recommended flight altitudes of 50 m for Saltwater crocodiles (*Crocodylus porosus*) and 40 m for West African crocodiles (*Crocodylus suchus*), respectively. Both studies utilized DJI Phantom 4 Pro drones (1138 grams), which is larger than the Mavic 2 Enterprise Dual.

## 2.2. UAV-based morphometric measurements and body condition assessment

### 2.2.1. Introduction

This method aimed to non-invasively capture morphometric data for captive breeder Nile crocodiles in South Africa, using an uncrewed aerial vehicle (UAV). Two hundred and eighty-eight crocodiles were assessed at two commercial crocodile farms in South Africa. One of the farms crocodiles appeared slimmer at time of the flights, when compared to the other farms crocodiles. Due to the vast array of nutritional states of the crocodiles in this study, this method could be applied to captive or wild crocodile populations. The spectrum of thin to fat crocodiles was assessed by the following UAV-captured measures: total length (TL), snout-hindlimb length (SHL), snout-neck length (SNL), neck width (NW), belly width (BW), surface area (SA), and perimeter. The UAV-derived morphometrics were then used to produce a fast-paced and repeatable estimation of crocodile welfare, in the form of a body condition score (BCS).

### 2.2.2. Materials and methods

#### *Aerial image acquisition and processing*

A DJI Mavic Mini UAV with a 12-megapixel CMOS (complementary metal oxide semiconductor) sensor was used to survey four pens across two commercial crocodile farms (henceforth referred to as farm A and farm B) in South Africa with an estimated model error of < 25 mm (Myburgh *et al.*, 2021), i.e., all length measurements accurate to within 25 mm. The UAV was programmed to follow a predetermined flight path at an altitude of 40–60 metres (m) covering each area in a grid pattern, taking images with approximately 80% frontal and 70% side overlap over the surveyed area. These flight altitudes did produce a noticeable difference in image clarity. However, altitudes in this range are suitable for this method and maintain adequate accuracy as per Myburgh *et al.* (2021). The flights were programmed using the automated flight software [Dronelink](#). The flights were conducted between 10:00 and 11:00 on a relatively cold winter morning when the crocodiles were basking and could be photographed out of the water (Downs *et al.*, 2008). Each flight produced images which were processed into a single orthophotograph per flight at 1.42 cm resolution using OpenDroneMap (ODM, version 1.9.3 build 30). An Emlid Reach RS+ differential GPS and seven ground control points were used to ensure ground truthing of the orthoimages during processing. The resulting orthophotograph from ODM was imported into QGIS (version 3.16-Hannover) (QGIS Development Team, 2021) for morphometric data capture.

One hundred and forty-five crocodiles from farm A and 143 crocodiles from farm B were included in the analyses. These crocodiles included large growers (between one-year-old and harvest size) up to breeder (mature or adult crocodiles) sized individuals, ranging from > 1–4.8 m in TL. Crocodiles less than 1 m in TL were not included as data capture would have been complicated by orthophoto clarity and the tendency of smaller crocodiles to pile up which concealed body parts needed for the measurements. For consistency, only crocodiles that were lying motionless on the dry emergent area (i.e., basking) with their full bodies captured by the UAV imagery were used in the analyses, while crocodiles in motion or in the water bodies were not measured.

#### *Deriving morphometric data from UAV-based morphometrics*

Head lengths (HL) are traditionally measured using a standard tape measure, but from a UAVs perspective the HL measure can be problematic as the required features of measurement are difficult to detect in the images, especially in low-resolution imagery (Ezat *et al.*, 2018; Jordaan, 2021). HL can be adapted for UAV observations by measuring from the tip of the snout to the posterior margin of the four large dermal scute plates on the neck corresponding to the front limbs of the crocodile, henceforth referred to as snout-neck length (SNL). Snout-vent length (SVL) is a measure commonly used when the full length of a crocodile's tail cannot be accurately measured due to missing tail ends.

SVL cannot be precisely measured from UAV imagery as the caudal margin of the cloaca cannot be viewed dorsally on a crocodile (Myburgh, 2022). This measure can be adapted for UAV observations by measuring from the tip of the snout to the circumcircle scute layer immediately posterior to the back legs, henceforth referred to as snout-hindlimb length (SHL). Relationships between TL and SHL, and TL and SNL, have been proposed (Myburgh, 2022); however, correction factors have not been thoroughly tested on a range of crocodilian body sizes and conditions.

All morphometric data were derived with either a line-string layer or vector polygon layer in QGIS. Total length (TL) was measured by estimating the distance between the tip of the snout, following the curve of the animals back to the tip of the tail for those individuals where the tip of the tail could be clearly distinguished from the background (line-string layer in QGIS). In images of crocodiles where the tail did not terminate in a clear tip (indicating loss of tail) the individuals were excluded from the assessment. Snout-neck length (SNL) was measured by drawing a line (line-string layer in QGIS) from the tip of the crocodile's snout to the posterior margin of the large dermal scutes on the neck corresponding to the anterior origin of the front limbs. Snout-hindlimb length (SHL) was estimated by deriving the distance from the tip of the crocodile's snout to the last scute layer posterior to the crocodile's hind limbs (line-string layer in QGIS). The relationships between TL, SNL, and SHL were compared using linear regressions. Figure 5a identifies the morphological features for measuring the UAV-adapted morphometrics that replace SVL and HL (SHL and SNL, respectively) in this study. Neck width (NW) was measured by drawing a line across the widest part of a crocodile's neck, keeping perpendicular to the TL/SHL string layers. Belly width (BW) was measured with a line-string layer in QGIS across the widest part of the crocodile's stomach, keeping perpendicular to the TL/SHL string layers. Surface area (SA) was measured in QGIS using a vector polygon layer and outlining the crocodile's body. For the SA morphometric measurement, the tails were included as this is an area of fat deposition (Osthoff *et al.*, 2014), whereas the crocodiles' legs were not included as their positions were inconsistent from animal to animal. The perimeter was measured with the same vector polygon layer by extracting the length of the outline used to create the SA morphometric. The morphometric measures recorded in QGIS are depicted in figure 5b and 5c.

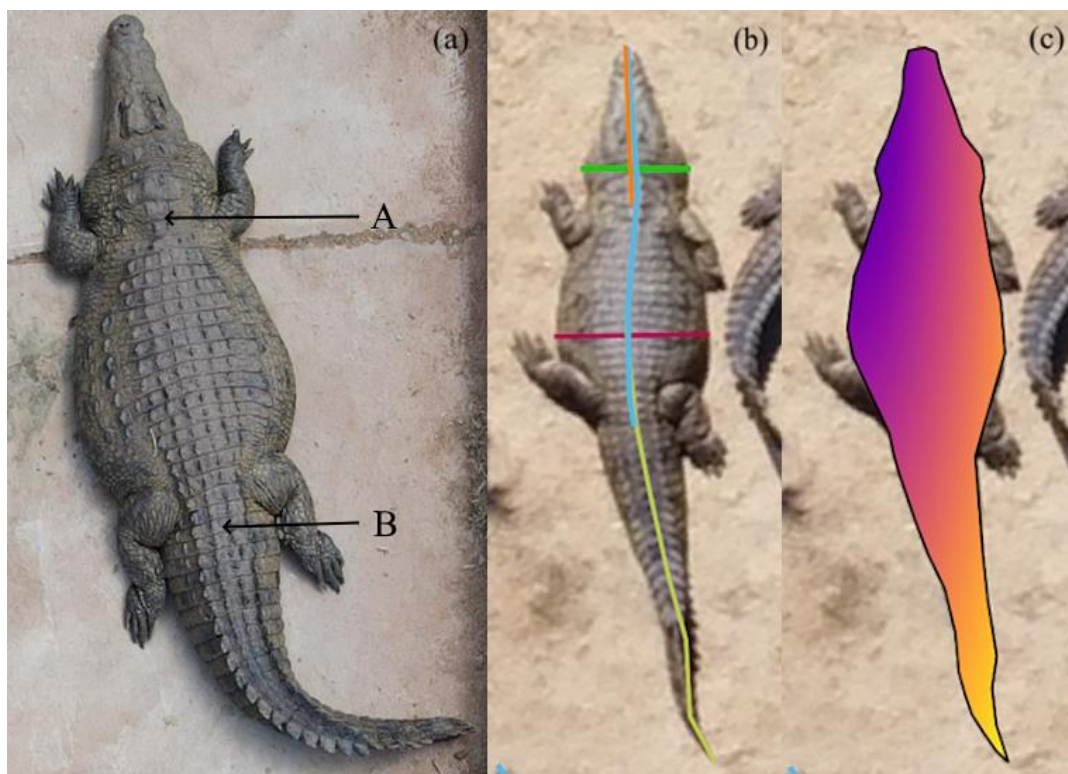


**Figure 5.** (a) Morphological features recognisable from UAV imagery that are required to capture the morphometric measurements for the current study. “A” illustrates the conclusion of the dermal neck scutes required for the morphological measure SNL. “B” illustrates to the circumcircle scute layer behind the hind legs, required for the morphological measure SHL. (b) Depicts morphometric measures captured as vector line layers in QGIS, colour codes: total length in yellow, snout-hindlimb length in blue, belly width in pink, neck width in green, and snout-neck length in orange. (c) Depicts morphometric measures captured as vector polygon layers in QGIS: perimeter shown by the black outline of the crocodile, and surface area shown by the gradient-coloured area that falls within the perimeter line.

#### *UAV-based body condition assessment*

A body condition index (BCI) was calculated using TL and BW by means of the equation:

$$BCI = \left( \frac{BW}{TL} \right) \times 10 \quad \text{Equation 2}$$

The BCI results were used to estimate a body condition score (BCS) by normalizing the BCI values and applying a rank between 1 and 5 (1 being a very low BCS and 5 a very high BCS) to create a score for each crocodile indicating its body condition in relation to all crocodiles measured in this study. This resulted in the following ‘standardized’ equation:

$$BCS = \left( \frac{BCI - 1.34}{1.27} \right) \times 4 + 1 \quad \text{Equation 3}$$

#### 2.2.3. Data analysis

All morphometric data were analysed in SPSS (version 28) using generalized linear mixed model analysis and discriminant analysis procedures. Pearson correlation coefficients, using a confidence interval of 95.0%, were calculated between variables. All data were analysed for the determination of significant differences ( $P < 0.05$ ). Linear regression analyses were performed in Microsoft Excel® to compare the relationships between total length, snout-hindlimb length, and snout-neck length. The relationships between these three measures were considered particularly important because similar measures have been traditionally used for population surveys. The body condition index (BCI) was calculated for each crocodile and then ranked on a scale of 1–5 using a min-max normalisation in Microsoft Excel®, producing the body condition score (BCS).

#### 2.2.4. Results

The seven morphometrics were successfully captured for 288 farmed Nile crocodiles and equations 2 and 3 yielded a range of body condition scores from 1 to 5, successfully identifying emaciated and overweight crocodiles. For detailed results, refer to chapter 3 of this thesis (Viljoen<sup>1</sup> *et al.*, 2023).

#### 2.2.5. Discussion

The variation in body condition scores between the two farms supports the credibility of the UAV morphometric measures. This method allowed a fast-paced, non-invasive and repeatable examination of the sizes and conditions of two captive Nile crocodile populations. This could easily be applied to wild crocodile populations and may therefore aid wildlife management and conservation efforts.

#### 2.2.6. Conclusions

Morphometric monitoring via UAVs is accessible, accurate, non-invasive, easily repeatable, and cost effective. The body condition scoring methods presented here could enable rapid assessments of population status for wild or captive crocodile populations. Replications of this method are recommended if assessing a particular group of crocodiles, thereby avoiding potential bias introduced by dominance behaviours determining the basking capabilities of subordinate individuals.

## 2.3. The transformation of relative temperature maps from a thermal drone (DJI Mavic 2 Enterprise Dual) into a thermal predictive model

### 2.3.1. Introduction

The method developed transformed relative thermal maps (produced by a DJI Mavic 2 Enterprise Dual drone) into a predictive model where temperatures were derived to within 2.6 °C per pixel of a processed orthophoto. The method was applied in chapter 4 (Viljoen<sup>3</sup> *et al.*, 2023) and chapter 6 and allowed fast paced and non-invasive monitoring of pen and external crocodile temperatures, as well as behavioural data from the crocodiles captured within the imagery.

### 2.3.2. Materials and methods

#### *Aerial image acquisition*

A DJI Mavic 2 Enterprise Dual drone was flown on a predetermined automated flight path using a third-party flight software package ([Dronelink](#)) at an altitude of 35 m with 85% side and frontal image overlap. The UAV covered an area of approximately 15000 m<sup>2</sup> in nine minutes. Between flights, all equipment was kept in an air-conditioned room (22 °C) to minimize drift from overheating of the uncooled thermal sensor, ensuring the starting temperature of the UAV was constant for each flight.

Six ground control points (GCPs) were distributed along the perimeter of the pen. The GCPs used were inexpensive square polystyrene platforms (60 cm x 60 cm) covered with aluminium foil and black paint as per Messina and Modica (2020). Aluminium foil has an emissivity of 0.03, creating sufficient contrast with black paint and adjacent pen materials, making it easily recognizable in thermal images (A.S.H.R.A.E, 2009; Messina & Modica, 2020). The GCPs were systematically positioned in predetermined positions around the perimeter of the pen for each flight, ensuring precise georeferencing of the resulting orthophotos based on established geospatial calibration methodologies.

#### *Thermal mapping settings and workflow*

The DJI Mavic 2 Enterprise Dual drone does not store the absolute temperature associated with the long wave infrared measurements captured by its thermal sensor. The DJI Pilot 4 interface was used to specify a greyscale colour palette, providing a linear conversion of thermal data (thermal range set between 5 °C and 65 °C) to red, green, and blue (RGB) variables (between 0 and 255; where, using the greyscale colour palette yielded equal colour values within all three colour bands) which were stored in the jpeg files associated with the thermal sensor. During flight, but not within the immediate perspective of the UAV, a handheld thermometer (ASSTech Process Electronics and Instrumentation handheld infrared thermometer, ST653) was used to measure the temperature of homogenous areas representing various materials outside the perimeter of the pen (and not within view of the crocodiles). The thermometers emissivity was set to 0.94 as per the instruction manual for the materials under study, i.e., concrete, brick, water, and sand. The distance from the thermometer to the materials measured was maintained at 1 m for all measures. Temperatures recorded by the thermometer were then used to elucidate the temperatures associated with the colour band value outputs of the resulting thermal orthophotos (equation 4).

#### *Thermal image processing settings in ODM and QGIS*

Processing parameter testing for the derivation of orthophotos from thermal images in OpenDroneMap (ODM) resulted in the selection of settings which differ from the standard “high resolution” option in the following ways: orthophoto resolution was set to the ground sampling distance (GSD) of the original images (11.16 cm/pixel in this case) and the lens selection was set to fisheye. RGB images were processed using the “default” settings in ODM with orthophoto resolution set to the GSD associated with the RGB images (1.42 cm/pixel). An Emlid reach RS+ differential GPS

was used to mark the position of each ground control point, ensuring all images aligned after photogrammetric processing. Where misalignment occurred, georeferencing was performed in QGIS (QGIS Development Team, 2021) using a linear conversion through a thin plate spline projection to resize and georeference each image into the correct position. Once the thermal images were aligned, the thermal orthophoto data was preserved as RGB image data ranging from 0 to 255 across the three colour bands. The steps to convert RGB thermal orthophotos into relative temperature maps were as follows:

1. Using the point creation tool in QGIS, a marker was placed at each location where temperature measurements were recorded with the handheld thermometer during flights.
2. Using the sample raster tool in the processing toolbox, the RGB data was derived from the thermal layer at each of the points across all thermal orthophotos.
3. The sampled points data were then exported to a spreadsheet, where the three RGB band values were averaged into a separate column. The measured temperatures taken with the handheld thermometer during flights were added next to the averaged RGB values.
4. A linear relationship was fitted to these two variables and an equation describing the relationship was derived.
5. A new relative temperature map of the area under survey was created for each flight using the raster calculator in QGIS, where the RGB values of the thermal orthophotos were set as “x” in the derived equation.

#### *Temperature and behavioural data extraction*

Data were extracted from the resulting processed imagery using point and polygon layers in QGIS (version 3.16 Hannover). Point layers were used to attain spot temperature approximations, e.g., point marker placement could output temperatures from the backs of each crocodile or the substrate temperatures which the crocodiles were selecting. Polygon layers were used to extract area and perimeter information from areas outlined within the imagery, thermal data for the outlined areas, and the spatial distributions of individual crocodiles per designated (polygons) area of the pen by combining the point and polygon layers with the “join attributes” function. Relative temperature maps were transformed with equation 4.

#### 2.3.3. Data analysis

The data were analysed in R (2022.12.0 Build 353) and IBM SPSS Statistics (version 28). A multivariate analysis of variance, two tailed partial correlations, Chi square, and regression analyses were performed. Bonferroni corrections were applied to post-hoc pairwise comparisons. Differences between variable means were analysed for the determination of significant differences at  $P < 0.05$ .

#### 2.3.4. Results

##### *Thermal map conversions*

The relationship between temperature measurements taken with the handheld thermometer ( $n = 330$ ) and colour information from the RGB bands ( $n = 330$ ) of the processed thermal orthophotos could be described through equation 4:

$$y = 0.3593x + 5.16 \quad (R^2 = 0.9454; P < 0.001), \quad \text{Equation 4}$$

Where  $y$  = temperature of the selected pixel, and  $x$  = average extracted value of the three RGB bands with an average absolute error of  $2.06 \pm 1.32$  °C and a root mean squared error of 2.6 °C.

This equation was applied, using the raster calculator function, to the grayscale versions of the orthophotos captured with the Mavic 2 Enterprise Dual drone over farmed Nile crocodile pens. The

equation was applied to each orthophoto pixel, and this information was then extractable using the point and polygon layers described previously.

#### 2.3.5. Discussion

The methodology described is a cost-effective alternative to more expensive proprietary software and larger UAV platforms, as well as a less invasive approach to temperature assessment via monitoring external body temperatures directly. This method provided sufficient resolution for distinguishing the thermal features of the respective breeding and basking areas for crocodiles on a commercial farm. This method was used to identify suboptimal thermal regimes which may be detrimental to crocodile welfare (Viljoen<sup>3</sup> *et al.*, 2023, or chapter 4) and allowed the assessment of preferred nesting sites which will inform future nest management strategies (chapter 6). An important feature of raster data is that it can be easily mathematically manipulated and partitioned to identify specific areas of interest. It can be used to detect changes in critical parameters and/or to identify areas requiring further investigation, saving analytical time and costs.

#### 2.3.6. Conclusions

A novel, non-disruptive, fast paced, and highly repeatable method of thermal and behavioural data capture was developed using a relatively affordable UAV platform equipped with a thermal camera (Mavic 2 Enterprise Dual).

## 2.4. IButton refurbishment: battery and housing replacement

### 2.4.1. Introduction

Thermocron iButtons are small, robust, reliable temperature logging systems (<https://www.thermochron.com/>). Although these devices are relatively inexpensive, they are designed for single-use applications, i.e., to be disposed of after the battery is discharged. Refurbishing these highly versatile loggers has been accomplished previously for the purposes of miniaturisation and use in small-animal studies (Robert & Thompson, 2003; Lovegrove, 2009). In the present study, the refurbishment of iButtons, rather than miniaturization, facilitated continued assessments amid nationwide supply constraints due to the COVID-19 pandemic, which precluded the timely procurement of new iButtons. A selection of used iButtons (DS1921G-F5#, some over a decade old) were donated for the study of thermal environments. The discharged batteries required replacement and by extension, refurbishment of the iButtons. Although the final product was larger in volume compared to an unaltered iButton, its functionality and water-resistance characteristics were maintained, whilst costs of battery replacements were kept to a minimum.

### 2.4.2. Materials and methods

#### *Deconstruction*

Careful deconstruction was required to separate the printed circuit board (PCB) and battery from the iButtons stainless steel enclosure (figure 6). The outer rim of the stainless-steel casings were filed through at three sections along the iButtons perimeter, using a small-diameter steel file. The two caps, which slot tightly into one another, were separated by a plastic insulating grommet which also served as a marker for when to terminate the filing process. After the grommet was filed through, the caps were pulled apart and the grommet peeled back with pliers to reveal the internal PCB assembly. The filed through stainless steel caps and the old batteries housed within their built-in plastic frames were discarded. The PCB chips were examined to identify the specific connections suitable for the attachment of a new battery.

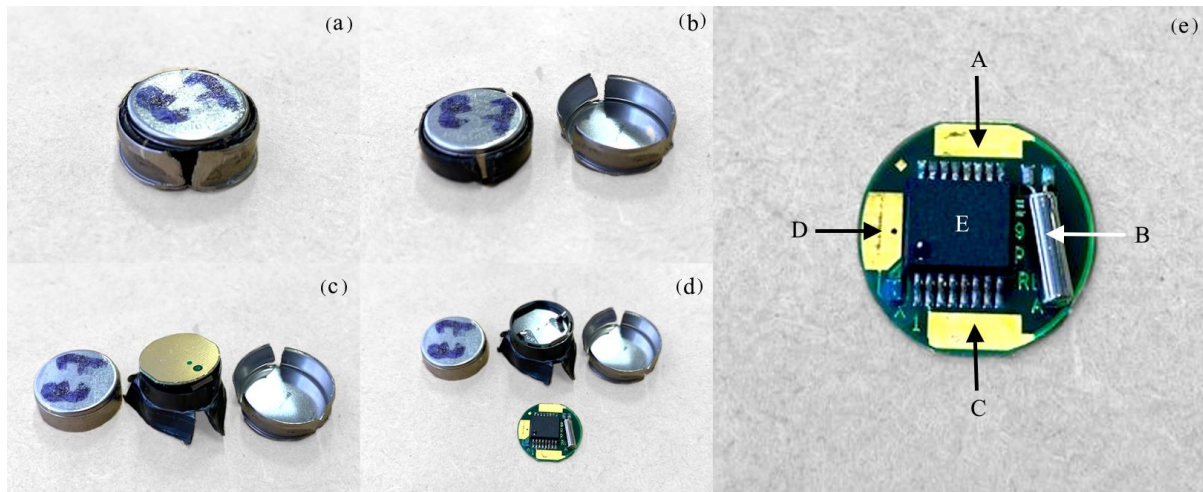


**Figure 6.** Illustrates the deconstruction of an intact iButton to reveal the battery and printed circuit board. Image (a) depicts the outer stainless-steel cap having been filed through, (b) the plastic insert having been carefully filed through and the lower stainless-steel cap removed, (c) the plastic insert was gently peeled back, and the upper steel cap was removed to reveal the internals, and (d) the PCB viewed from the front, and the old battery inside a plastic frame connected to the grommet. Image (e) depicts the PCB layout where “A” and “C” represent the positive (anode) terminals, “B” the quartz crystal, “D” the negative (cathode or “ground”) terminal, and “E” the integrated circuit. The opposing side of the PCB, as seen in figure 6c, represents the “data” terminal.

### Battery replacement

Suitable lithium coin cell batteries (Mantech Electronics CR1220-PAN3, BAT COIN LIT 3V 35mA VER-PCB) were procured to match the operating voltage of the iButtons, with a similar capacity. Batteries with solderable tabs were chosen to facilitate easier attachment to the PCB.

### Reconstruction

Two reconstruction configurations were considered, a “planar” configuration was selected over a “vertically stacked” one for ease of reconstruction. A stacked configuration was considered as a means of mimicking the shape of the formerly intact iButtons, where the new batteries would have been installed immediately adjacent and parallel to the PCB boards, possibly allowing the re-use of the remaining intact caps. The planar configuration positioned the batteries alongside the PCB boards as the solderable tabs did not require deformation using this configuration. As replicating the exact dimensions of the original, intact iButtons was not an essential objective, the planar configuration was selected. This facilitated rapid refurbishment of the iButtons in a planar form.

Colour-coded wiring was employed to distinguish between ground (blue wire) and data (yellow wire) connections (figure 7). Pre-tinning of the exposed wires and contact surfaces was performed to facilitate the soldering process, ensuring robust joint formation without excessive solder accumulation (Magnum 2002-80w, 350 °C). A short wire segment was employed to bridge the two positive electrical terminals, providing additional mechanical rigidity to the assembly. The primary purpose of the data (yellow) and ground (blue) wires was to facilitate the configuration and programming of the devices.

The refurbished iButtons were sealed with 12.7 mm diameter, glue-lined heat shrink tubing (RS Components, 481-1810) to establish a watertight seal on the logger ends. The heat shrink was cut to 60 mm segments, sleeved over the electronic assembly, and heated with a heat gun (Metabo, H16-500) on the lowest temperature setting. A small clamp applied a uniform clamping force to distribute the adhesive evenly at both ends, forming an effective water-resistant barrier ~10 mm in length (note the textured checkerboard pattern in figure 7c). The exposed wiring allowed for reprogramming of the iButtons. Small gauge, stranded wire exhibited improved mechanical stability compared to solid core wire, which tends to exhibit brittle characteristics post-soldering.

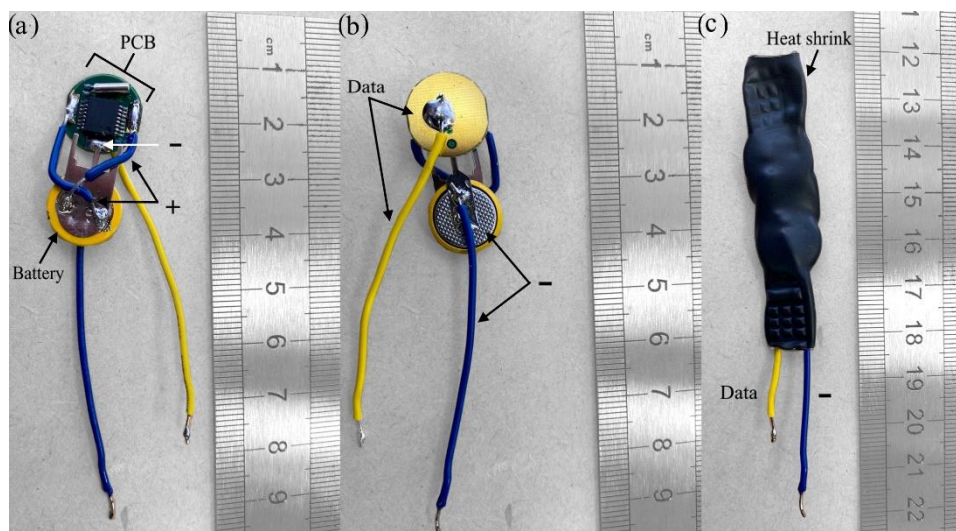


**Figure 7.** Illustrates the connections between the battery and the iButton PCBs, front (a) and back (b). Image (c) depicts an iButton after it has been sealed in heat shrink and clamped shut with the stranded wires available for configuration.

### Verification

One wire viewer software was used to read and configure the devices before deployment. Twenty refurbished iButtons were programmed to record data over a 24-hour period to assess their operational integrity. The devices underwent a simultaneous relocation sequence involving varying environmental conditions, including direct sunlight, a climate controlled indoor office setting, and a temperature controlled refrigerated environment. This procedure aimed to confirm and compare their functionality under different temperature exposures. All devices functioned as expected and recorded comparably uniform data without interruption throughout the day.

Depending on the deployment environment, the impact of the removal of the steel casing and addition of a layer of heat shrink on temperature recordings was unknown. Therefore, before deployment for any further studies, a two-day sequence of relocations was performed for two off-the-shelf and two refurbished iButtons. There were no significant differences in the temperatures recorded by these loggers ( $P = 0.98$ ).

### One wire viewer interface

The one-wire viewer interface, paired with a USB adaptor (Cold Chain Thermodynamics Multi Profile, CCTDmp/OT), facilitates data configuration and download from the iButtons by clipping the iButtons (in their unaltered form) into the reader (figure 8). After refurbishment, this was no longer viable; for the modified iButtons, direct access to the electrical conductors was required. Two colour-coded wires were soldered to the exposed data (black wire) and ground (green wire) electrical contacts beneath the data interrogator/reader. Crocodile clips were used to attach the respective data and power wires between the refurbished iButtons and data reader.

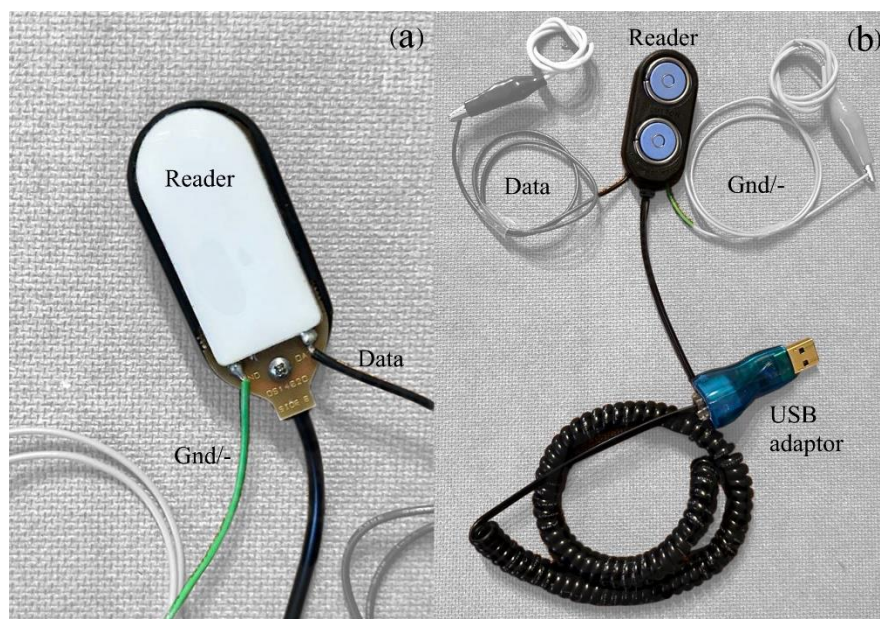


**Figure 8.** Reader unit modification showing (a) extension wires soldered onto the data and ground (“Gnd/-”) electrical contacts at the back of the reader, and (b) the crocodile clips placed onto the wire ends to establish the electrical contact for the one-wire interface.

### Final installation

Post-configuration, the exposed data and ground wire contacts of the iButtons were trimmed up to the heat shrink layer to prepare them for deployment. The terminated contacts were sealed with a removable layer of nail polish, serving as a low-cost sealant. This ensured the water-resistance of the contacts while allowing for their subsequent removal for data retrieval. The refurbished iButtons were deployed for environmental temperature monitoring.

#### 2.4.3. Results

Refurbished iButtons proved effective for recording the temperatures of solid mediums such as concrete and sand (chapter 2's MD 2.5 and chapter 6). However, their deployment for the measurement of water temperatures did not yield successful results. These results affirmed the devices water-resistant properties, as they successfully recorded concrete and sand temperatures in outdoor settings, which were subject to moisture.

#### 2.4.4. Discussion

The refurbished iButtons proved effective for recording the temperatures of solid mediums such as concrete and sand. The failure to monitor water temperatures indicates that the iButtons lacked the necessary waterproofing for sustained use in liquid environments.

#### 2.4.5. Conclusions

A selection of battery-depleted DS1921G-F5# iButtons were successfully refurbished and deployed into a crocodile pen for measurements of concrete temperatures, as well as into crocodile nests on a commercial farm for subsurface temperature recordings. Inexpensive materials and varsity-owned tools were used for the refurbishments, allowing the continuation of studies during a period of iButton shortages. Future studies should be cognizant of comparing the temperature recording capabilities of refurbished iButtons to off-the-shelf (already calibrated) iButtons and consider the effects that water-proof coatings might have on the refurbished iButtons recording capabilities.

## 2.5. Core body temperatures of farmed grower Nile crocodiles (*Crocodylus niloticus*)

### 2.5.1. Introduction

Core body temperatures ( $T_{b_{\text{internal}}}$ ) of grower Nile crocodiles (*Crocodylus niloticus*) on a commercial crocodile farm in South Africa were recorded over a single summer (December 2021–February 2022). The aim was to assess the temperature experiences of these animals and how these correlated to the ambient environmental temperatures (air, concrete, and water) and humidity. The generally recommended ambient temperatures for intensive crocodile farming are 17–35 °C, with continuous/unavoidable temperatures of 10–20 °C and > 35 °C being advised against for crocodile safety (Bolton, 1989; Bothma and van Rooyen, 2005; Bassetti *et al.*, 2014). Optimal  $T_{b_{\text{internal}}}$ 's between 28–33 °C have been suggested for farmed crocodilians (Colbert *et al.*, 1946; Huchzermeyer, 2003; CFAZ, 2012). Given the concerns raised about hyperthermia by the NSPCA regarding farmed crocodiles in South Africa, a study was conducted with particular interest in the maximum  $T_{b_{\text{internal}}}$ 's reached and whether these fall within an ethically acceptable range. Despite the study outcomes being negatively impacted by majority logger losses, the methodologies and results are reported in detail to facilitate learning and improvement in future studies.

### 2.5.2. Materials and methods

#### *Study site and materials*

The pen selected for the assessment was a 550 m<sup>2</sup> concrete pen with multiple water bodies. Two water bodies covered 44% of the total surface area, a feeding gutter covered 5%, and concrete covered the remaining 51%. Each water body sloped downwards to a maximum depth of 1 m. The feeding gutter was a long shallow (30 cm deep) pond designed to catch feed residue and thereby maintain the cleanliness of the main waterbodies. A shade net was present against one wall of the pen, covering 20% of the pens concrete area (figure 9). Other than the placement of temperature loggers, no further alterations were made to the pen. The farms regular feeding and cleaning schedules remained unchanged to avoid the potential of stressing the animals. Hourly air temperatures and humidity were recorded on site with a SenseCAP LoRaWAN Wireless Air Temperature and Humidity Sensor, placed in a permanently shaded area near the pen. A router (LtAPHD LR8 3xSIM2xmPCIe Wi-Fi LTE Router) and antenna (a LoRa 6.5dBi Antenna kit with 1m SMAF), responsible for relaying the sensor data to a Ubidots dashboard (<https://ubidots.com/>), were placed in a nearby building with a secure Wi-Fi connection.

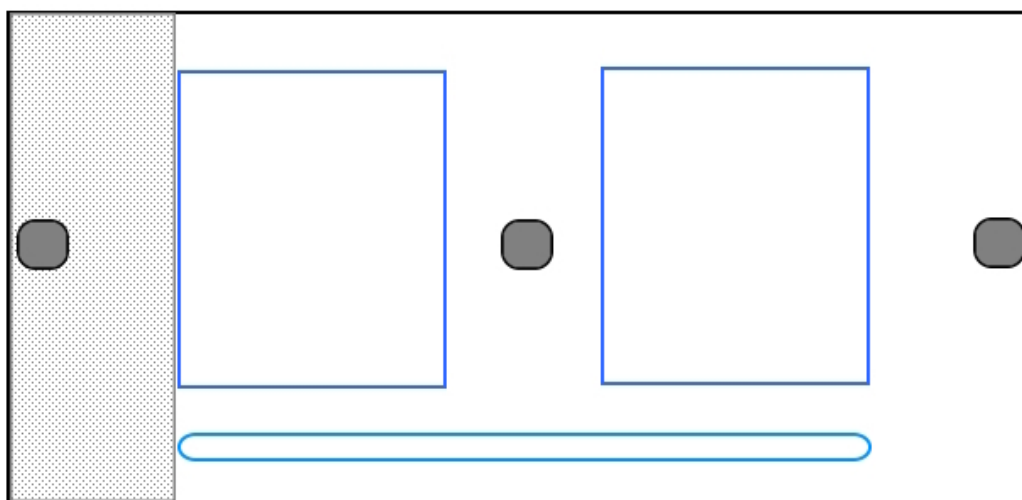


**Figure 9.** Pen layout (not to scale), depicting the water body placements (dark blue rectangles), the feeding gutter (light blue oval), the concrete encased temperature loggers (grey oblongs), and the placement of shade netting (rectangle with a dot-filled pattern).

Twelve refurbished Thermocron iButtons (DS1921G-F5) were deployed for concrete and water temperature measurements within the pen. These older iButtons had been donated to the study (Prof Hannes van Wyk, University of Stellenbosch) and had to be retrofitted due to battery failures (chapter 2's MD 2.4). Six locations were identified within the pen and two loggers deployed per location. Three of the locations were concrete areas within the pen, for which the iButtons were cast into concrete slabs (30 cm x 30 cm x 6 cm). Slab deployment, as opposed to placing iButtons on top of the existing concrete, ensured the loggers would not be eaten, moved, or need to be placed in such a way that would permanently alter the pen (e.g., drilling into the floor). Two iButtons were placed into each slab inside of a small section of copper piping for protection and easy removal when the slabs were cut open after the study. These slabs were mixed with a standard concrete recipe, as was likely used during pen construction (recipe for a seven-litre batch: 210 kg/m<sup>3</sup> water, 350 kg/m<sup>3</sup> cement, 924 kg/m<sup>3</sup> sand, 880 kg/m<sup>3</sup> aggregate, 2 kg/m<sup>3</sup> polypropylene fibres). The first slab location was below the only shade net in the pen, against a wall. The second was placed on the opposite end of the pen, against the opposite wall. The third was deployed in the middle of the pen, between the two waterbodies.

The remaining three iButton locations were within the one pond. These iButtons were deployed on a chain, secured in pairs, within carabiners at measured locations along the length of the chain so that each set of iButtons would measure three water locations: the first just below the surface of the water (~10 cm below the surface) next to the concrete, the second 0.5 m under the surface resting against the concrete wall of the pond, and the third at the very base of the pond (1 m below the water surface). The end of the chain that exited the water body was secured to a metal grate external to the pen, ensuring the chain would not move during the study. Two HOBO Pendant MX Temp (MX2201) loggers were also deployed to record water temperatures centrally in the water body. For protection from the crocodiles, these loggers were placed in a hollow aluminium pole secured in a large concrete base (150 kg) for stability (designed and built by members of the Civil Engineering department at the University of Pretoria). Holes were drilled into the aluminium pole at pre-defined locations for the insertion of the Hobo loggers at selected depths, allowing water temperature measurements just below the surface of the water and at 0.5 m below surface level (figure A1, A2). Figure 10 shows the placements of the water loggers within the waterbody. The iButton and Hobo logger deployments occurred in one waterbody only, this was the pond on the right-hand side when referring to figure 9.

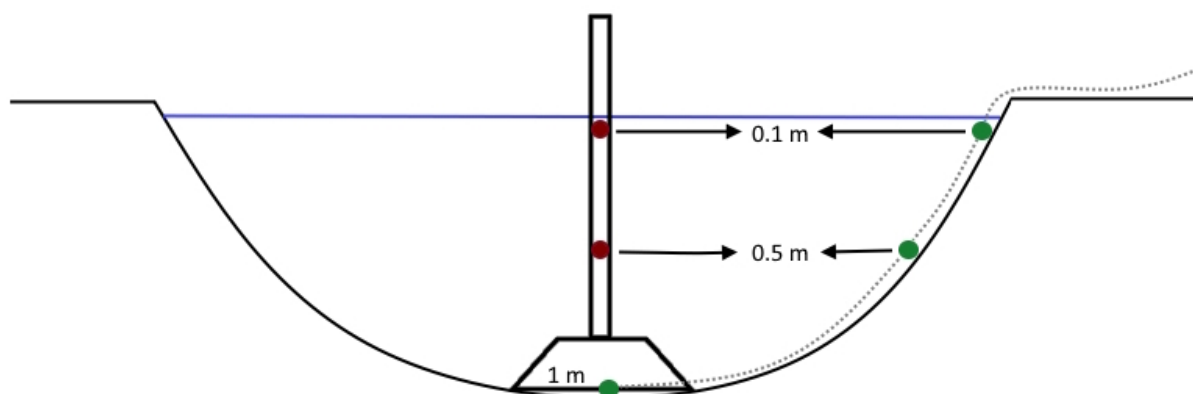


**Figure 10.** Placement of loggers (iButtons in green and Hobo pendants in red) within the right-hand water body within the pen (not to scale). The dotted line indicates the chain onto which the iButtons were fitted, and the blue line depicts the water level. Depths are included and marked with arrows.

#### *Crocodile measurements and body temperatures*

The farm manager estimated there were 500 crocodiles in the pen at the time of the assessment. All crocodiles within the pen had hatched on the farm and been treated similarly in terms of diet, housing,

and general husbandry practices before the study. Ten growers were captured by hand, their mouths secured shut with a thick elastic band, and their eyes covered. Each crocodile was marked (a brightly coloured dot of spray paint on the head), weighed, sexed, measured (morphometrics), tagged, disinfected at the tag sites, and fed a temperature logger, before being released. Each crocodile was placed into a breathable, woven garden refuse bag and the bag was then hooked onto a suspended scale (Camry, 25 kg capacity) to record its mass. The morphometric measurements collected for each animal were total length, snout-vent length, head length, and belly width (all measured with a flexible tape measure). The crocodiles were of a suitable size for sex determination via cloacal palpation (Ziegler & Olbert, 2007), which was carried out by a veterinarian (Prof J.G. Myburgh).

Crocodile  $T_{b_{\text{internal}}}$ 's were recorded with Liquid Armour encased iButtons (Thermochron, DS1922L-F5#) which were force-fed to the crocodiles during processing. Liquid Armour (<https://liquidarmour.co.za/>) is an air-dry, environmentally friendly, easily removable, synthetic rubberized coating produced in South Africa. The loggers were force-fed to the crocodiles using a simple method of rubber tubing of various strengths and diameters (figure A3). The first tube was a hard rubber tube and was the widest in diameter (4 cm). This tubing was used to tap each crocodile's snout which elicited a mouth opening response, at which time the tube was placed into the mouth of the crocodile which elicited a bite-down response. Once this tube was in place the crocodile's mouth was taped shut with duct tape (figure A4), and a second tube of soft rubber (3 cm diameter) was fed through the first. The soft rubber tubing was marked to identify the depth that the tube should travel (as approximated by a veterinarian) down the crocodile's oesophagus to reach the stomach (figure A5). Once the soft tubing was in place, two coated iButton loggers were placed into the tube and moved along it with the thinnest piece of tubing (2 cm diameter), also marked with the appropriate length for insertion. Two loggers were fed to each crocodile to increase the chances of data recapture should any of the loggers be passed by the crocodiles or malfunction. This method was adapted from previous studies which have used similar gastric intubation techniques on crocodylians (Loveridge, 1984; Janes & Gutzke, 2002; Brien *et al.*, 2012).

A third Liquid Armour encased iButton was also attached onto the tail of each crocodile, with the temperature recording side secured against the skin of the animal, to record external body temperatures ( $T_{b_{\text{external}}}$ 's). This was accomplished with a flattened, pill-shaped 3D printed iButton holder, with an iButton sized indentation into the one flattened side (4.2 cm x 2 cm x 1.3 cm). The holders were designed for the study as per tail dimensions which had been approximated from imagery from a subset of grower crocodile tails on the farm (figure A6). These holders were designed, printed, and supplied by the Civil Engineering department at the University of Pretoria. The holders, with iButtons glued into them, were coated in Liquid Armour for waterproofing. The holder was drilled through on the ends to allow the attachment of cable ties through holes in the scutes of the tail (figure A7). A tail punch was used for this purpose and the punched scutes disinfected once the loggers were attached (figure A8).

#### *Crocodile substrate selections*

A single day of flights over the grower pen gave insights into the substrate selections of the crocodiles during the day. A Mavic 2 Enterprise Dual drone was flown over the pen seven times on a hot summer's day (22 February 2022). These flights occurred as close to hourly as was manageable, delays in the hourly flights occurred due to overheating of the drone. The times flown were: 08:00, 09:00, 10:20, 11:30, 12:40, 13:40, and 15:00. In contrast to adult crocodiles, whose distinct thermal signatures facilitate individual identification against the background in thermal imagery (Viljoen<sup>3</sup> *et al.*, 2023), the grower crocodiles presented a challenge for such differentiation. This was likely due to their smaller size and/or their rapid thermal equilibrium with the surrounding environment, rendering

individual identification and therefore individual back surface temperature monitoring infeasible with the imagery produced in this specific study. It is acknowledged that shading was likely not accurately accounted for in the counts from the orthophotos since crocodile outlines could be easily seen through the shade netting in some images but not in others. Ponds also yield counting constraints as the crocodiles could not be seen unless near the surface. Visualization along the edges of the ponds were clear, whereas in the centre the waters opacity likely precluded perfectly accurate counts.

### 2.5.3. Data analysis

The data for this study were analysed in R (2022.12.0 Build 353). An analysis of variance, t-tests, and a Chi square analysis were performed. Bonferroni corrections were applied to post-hoc pairwise comparisons. Differences between variable means were analysed for the determination of significant differences at  $P < 0.05$  and highly significant differences at  $P < 0.001$ .

### 2.5.4. Results

#### *Study site*

The various concrete and water temperature-logging installations yielded little interest from the grower crocodiles. Often the animals were seen lying next to the concrete slabs and on occasion even over the top of the slabs. The farm manager reported that immediately after the water temperature logging pole was installed the crocodiles avoided the right-hand water body, but this behaviour had subsided by the next morning. The concrete slab underneath the shade netting received shade throughout the drone flights when compared to the other slabs. The concrete slab in the middle of the pen received no shading during the flights. The concrete slab against the right-hand wall of the pen received early morning shading (shading noted in 08:00 drone flight only). Of the 12 retrofitted iButtons deployed for concrete and water temperature measures, only the concrete encased iButtons survived the study period. Visual inspection revealed no signs of disruption or damage inflicted by the crocodiles on any of the retrofitted iButtons. Table 2 presents the descriptive statistics for the ambient temperatures and humidity within the pen during the study period.

**Table 2.** Descriptive statistics summary of all pen temperature measures and humidity.

Variable	Min	Max	Mean	SD	SE
Air temperature (°C)	12.7	34.9	23.3	4.82	0.11
Relative humidity (% RH)	17.7	100	62.8	18.16	0.40
Shaded concrete (°C)	14.5	31.5	22.3	3.31	0.07
Sunny concrete central (°C)	13.5	45.0	25.3	7.24	0.16
Sunny concrete wall (°C)	13.5	55.0	26.5	8.50	0.19
Water surface temperature (°C)	19.2	28.4	24.4	1.68	0.04
0.5m water temperature (°C)	19.0	29.4	24.9	1.99	0.04

Concrete and water temperatures recorded within the pen varied significantly from one another ( $P < 0.001$ ,  $F = 168.3$ ,  $df = 4$ ). The average temperatures recorded between sunny and shaded concretes varied significantly ( $P < 0.001$ ,  $t = 19.54$ ,  $df = 2797.2$ ), as did those recorded between the two sunny concretes ( $P < 0.001$ ,  $t = 4.75$ ,  $df = 3392.5$ ). The average deep and surface level water temperatures varied significantly ( $P < 0.05$ ,  $t = -8.55$ ,  $df = 3981.5$ ) from one another. Post hoc (Bonferroni) comparisons revealed that all concrete to water temperature comparisons varied significantly from one another (all  $P < 0.001$ ), except deep water temperatures and the temperatures recorded by the central sunny concrete slab ( $P > 0.05$ ).

*Crocodile measurements and body temperatures*

All 10 crocodiles in the study were female and their morphometric data is summarized in table 3.

**Table 3.** Morphometric measurements of the 10 grower Nile crocodiles in the study.

Crocodile	Mass (kg)	TL (cm)	SVL (cm)	BW (cm)
1	11.6	137.0	69.5	21.5
2	12.1	139.0	71.0	23.0
3	10.9	137.5	68.0	21.0
4	11.9	132.0	65.5	24.0
5	10.9	130.5	66.5	21.0
6	8.8	131.0	65.0	20.0
7	11.0	129.0	66.5	22.0
8	12.4	142.0	70.0	21.5
9	10.0	132.0	68.0	20.0
10	10.1	131.0	66.5	21.0

Of the 30 iButtons deployed among the 10 crocodiles, only 22 were recovered. Three of these were the loggers from the tails of the crocodiles; however, they were no longer attached to the tails. All three showed signs of having been chewed, only one had an iButton present and this iButton was dented and scratched, resulting in a loss of all  $Tb_{\text{external}}$  data. All 10 recaptured crocodile's tails showed signs that the loggers had been ripped off the tails, the cable ties having pulled free from the scutes. Nineteen of the 20 internal loggers were recovered, of these, eight still had signs of the Liquid Armour coating, although none were perfectly encapsulated as they had been at deployment. Three of the recovered iButtons had cracked open, the stainless-steel caps apparently dissolved in the crocodile's stomach acids (figure A9). Unfortunately, only three iButtons held data, and two of these were from a single animal, resulting in a loss of  $Tb_{\text{internal}}$  data for 8 out of the 10 study animals. The  $Tb_{\text{internal}}$  data from the two surviving iButtons is presented, these were from crocodiles 1 and 6 in table 3, these growers are henceforth referred to as "grower 1" and "grower 2".

Crocodile  $Tb_{\text{internal}}$ 's ranged from 16.5–37.0 °C ( $\bar{x}$  = 27.1 °C, SE = 0.08 °C for grower 1;  $\bar{x}$  = 25.8 °C, SE = 0.09 °C for grower 2), and these varied significantly between the two individuals ( $P < 0.001$ ,  $t = 10.54$ ,  $df = 4066.6$ ).  $Tb_{\text{internal}}$ 's were significantly impacted by air temperature ( $P < 0.001$ ,  $F = 7165.49$ ,  $df = 1$ ), relative humidity ( $P < 0.001$ ,  $F = 502.50$ ,  $df = 1$ ), concrete temperatures ( $P < 0.001$ ,  $F = 1274.96$ ,  $df = 1$  for the central slab;  $P < 0.001$ ,  $F = 2942.75$ ,  $df = 1$  for the slab against the wall;  $P < 0.001$ ,  $F = 1226.01$ ,  $df = 1$  for the shaded slab), and water temperatures ( $P < 0.001$ ,  $F = 114.68$ ,  $df = 1$  for the deep-water temperature;  $P < 0.001$ ,  $F = 64.72$ ,  $df = 1$  for the surface water temperature). Figure 11 shows the mean hourly temperatures (environmental and crocodile) and humidity recorded for the full study period.

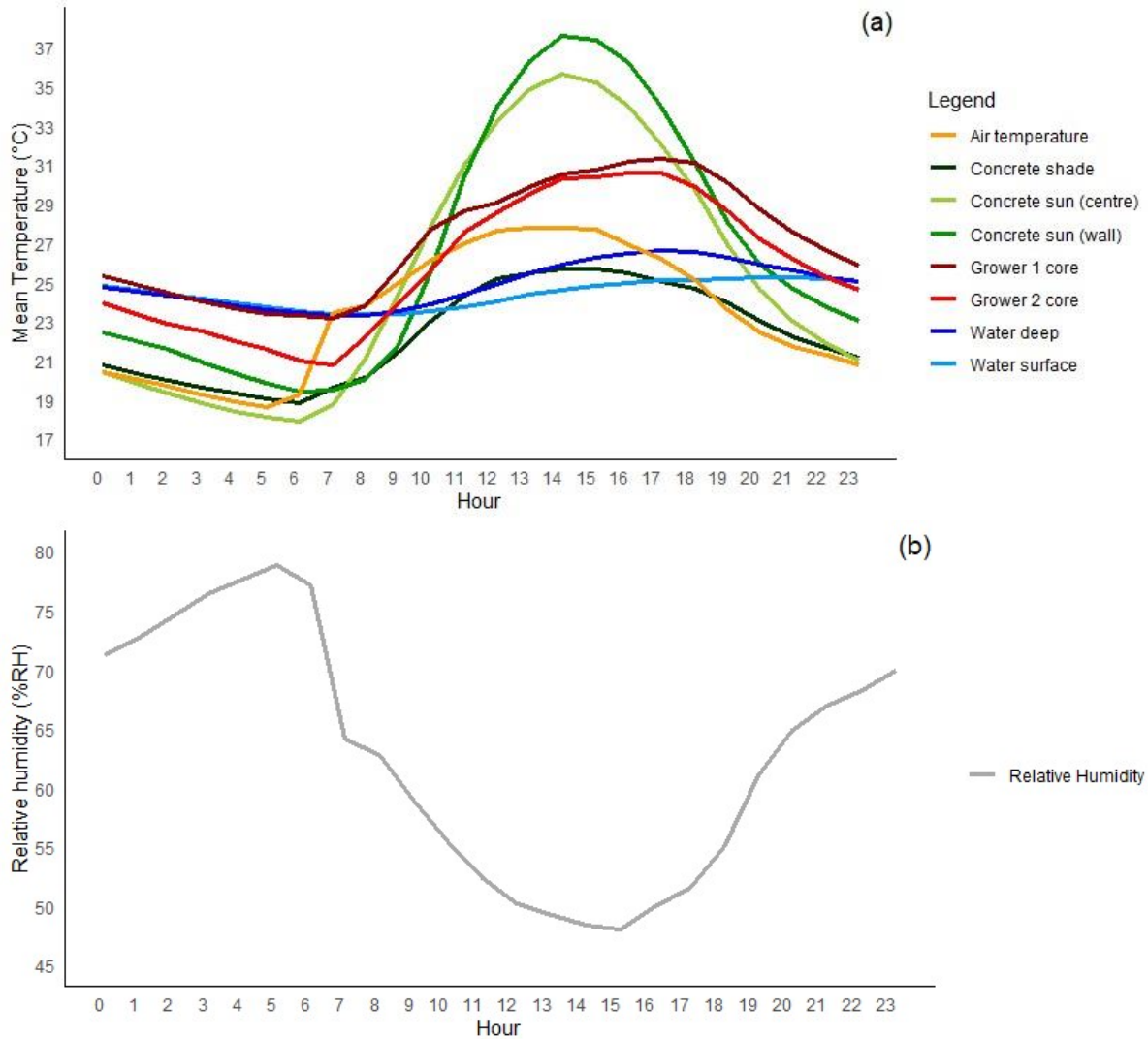


**Figure 11.** Mean hourly environmental and crocodile temperatures (a) and humidity (b) for the full study period.

The two growers were able to maintain mean  $T_{b_{internal}}$ 's within recommended ranges (28–33 °C) during the late morning to early evenings. There were, however, instances where  $T_{b_{internal}}$ 's reached  $\geq 34$  °C. Grower 1 reached a maximum  $T_{b_{internal}}$  of 35 °C, whereas grower 2 reached a maximum  $T_{b_{internal}}$  of 37 °C (figure 12). During the study period, grower 1 experienced 24 instances of  $T_{b_{internal}}$ 's reaching or exceeding 34 °C. The duration of these elevated temperature episodes ranged from 1–4 hours with an average duration of 1.6 hours per occurrence. Grower 2 experienced 13 instances of  $T_{b_{internal}}$ 's reaching or exceeding 34 °C for periods of 1–7 consecutive hours ( $\bar{x}$  = 1.8 hours). These occurrences were all limited to between 13:00 and 20:00.

$T_{b_{internal}}$ 's below the recommended farming minimum (28 °C) were more frequent than those above the recommended maximum (33 °C). Constant temperatures between 10–20 °C were assessed as these are known to suppress feeding behaviours in reptilians (Colbert *et al.*, 1946; Lang<sup>2</sup>, 1987; Bolton, 1989; Huchzermeyer, 2002). Grower 1 experienced eight instances of  $T_{b_{internal}}$ 's falling below 20 °C for periods of 1–11 consecutive hours ( $\bar{x}$  = 5.6 hours). These occurrences were all limited to between 21:00 and 10:00. Grower 2 experienced 31 instances of  $T_{b_{internal}}$ 's falling below 20 °C for periods of 1–16 consecutive hours ( $\bar{x}$  = 4.8 hours). These low temperature instances occurred at various hours of the day except 13:00–14:00.

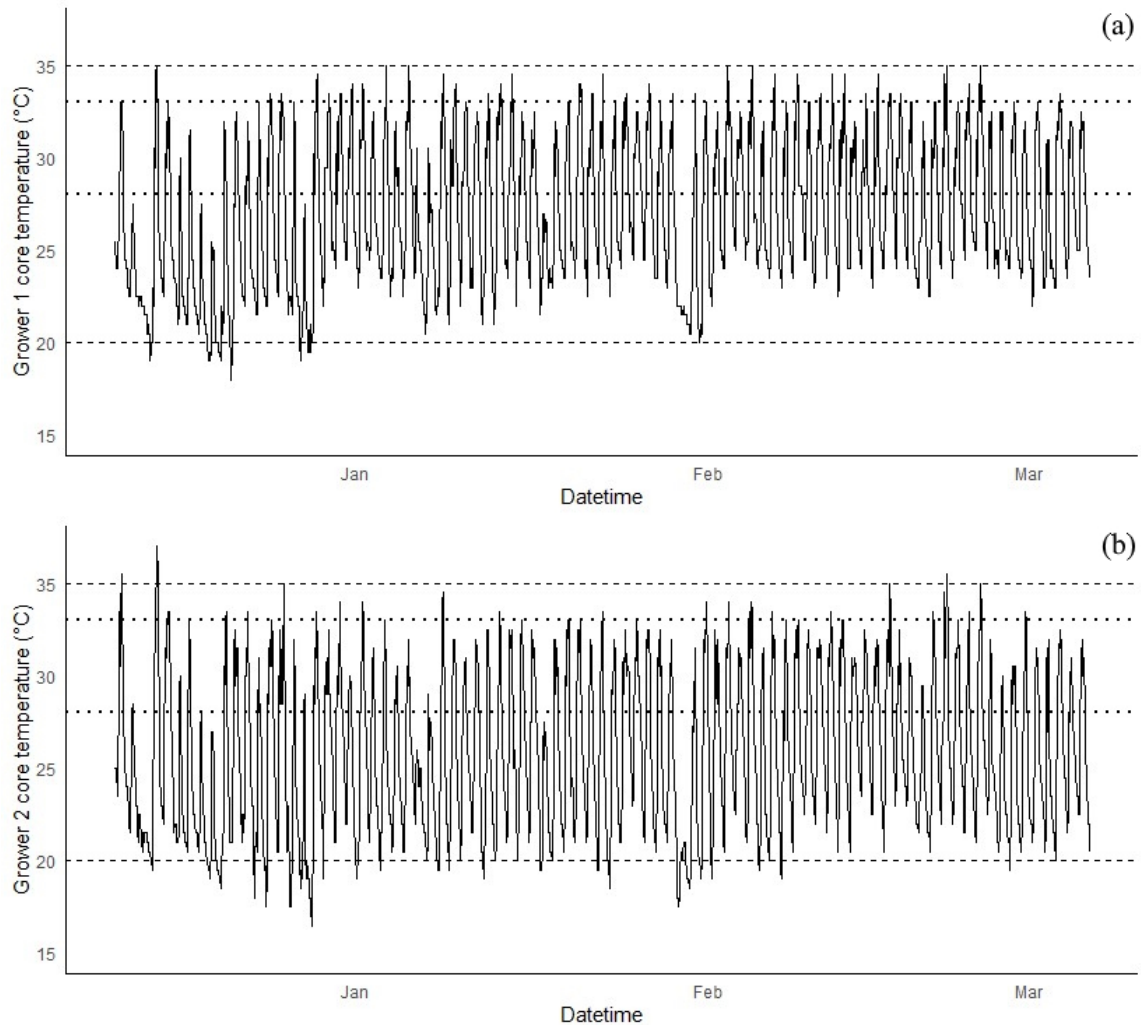


**Figure 12.** Grower 1 (a) and grower 2 (b) core body temperatures plotted over the full study period. Dotted lines at 28 °C and 33 °C reference the recommended optimal  $T_{b_{internal}}$ 's for crocodile farming, and dashed lines at 20 °C and 35 °C indicate the recommended lower and upper limits of safe ambient temperatures for farmed crocodilians. These allow the visualization of periods when the recorded temperatures fell outside of what are considered safe ranges.

#### *Crocodile substrate selections*

The drone flights assessing substrate use occurred on a relatively warm day within the summer season, giving a good idea of the thermal properties of, and the crocodiles' use of, the pen areas on a warm day. Ambient temperatures ranged from 27.3–32.2 °C ( $\bar{x}$  = 30.1 °C), and humidity from 30.8–56.6 % RH ( $\bar{x}$  = 44.1 % RH) during the flights. Both growers reached  $T_{b_{internal}}$  maximums of 33°C this day ( $\bar{x}$  = 28.9 °C for grower 1;  $\bar{x}$  = 27.8 °C for grower 2). Water temperatures ranged from 24.6–27.9 °C, and concrete temperatures ranged between 21.0–51.0 °C, during the flights. The total number of crocodiles within view varied significantly with flight time ( $P < 0.001$ ,  $F = 89.33$ ,  $df = 6$ ) and with area/substrate selections ( $P < 0.001$ ,  $F = 483.05$ ,  $df = 2$ ). Bonferroni post hocs revealed that the number of crocodiles counted varied between all substrate types (all  $P < 0.001$ ). Crocodile counts were highest at 09:00 (501 crocodiles counted) and lowest at 12:40 (218 crocodiles counted). A Chi-square test showed that the proportional substrate use varied between the drone flights ( $P < 0.001$ ,  $\chi^2 = 384.54$ ,  $df = 12$ ), indicating time of day effects on crocodile substrate preferences (figure 13).

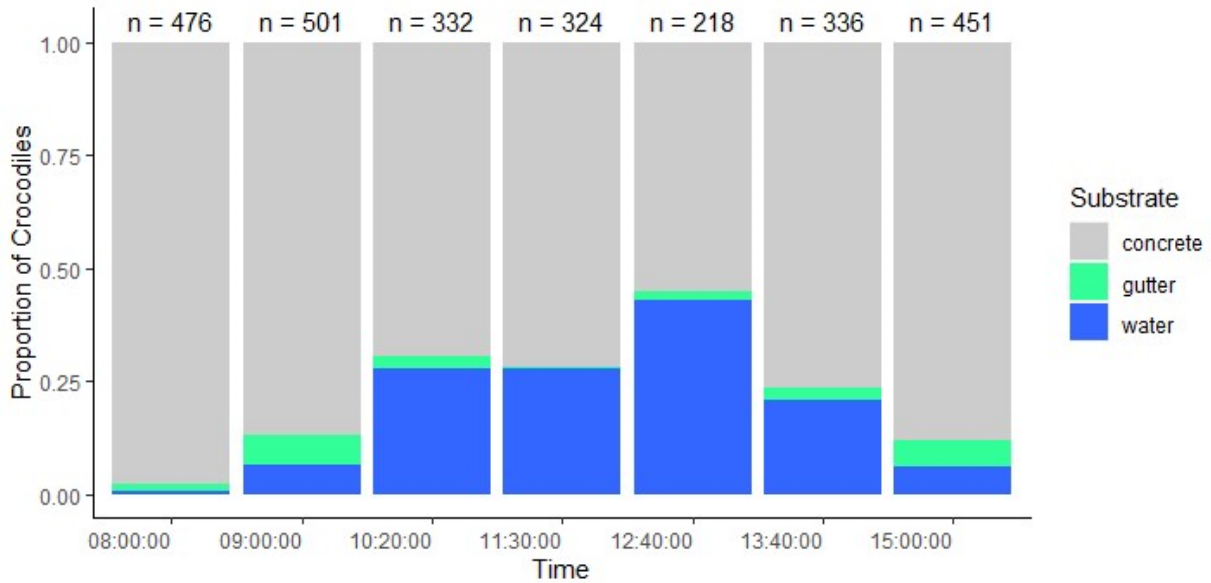


**Figure 13.** The proportional substrate utilization within the pen on 22 February 2022, between the hours of 08:00 and 15:00. The values above each bar represent the total number of crocodiles in view for that timeslot.

#### 2.5.5. Discussion

The thermal experiences of crocodiles in natural open-aired pens, such as in this study, are dependent on farm location, pen substrates, and the prevailing climatic conditions. Average air temperatures varied mostly within recommended ranges. However, temperatures cooler than 17 °C were reached in the evenings. Water temperatures (including minimums and maximums) for both deep and shallow loggers fell within recommended ranges throughout the study period. Shaded concrete temperatures fell mostly within recommended ranges, except for some evenings in December when temperatures fell below 17 °C. There were occasions where sunlit concrete areas of the pen reached temperatures as high as 55 °C, overtaking the upper recommended temperature limit (35 °C) frequently throughout the study period. On especially hot days, a few hours at these concrete temperatures could be detrimental to crocodiles.

Mean shaded concrete temperature maximums were comparable with those of mean water temperature maximums, whereas the minimums were lower for much of the day. It is notable that the NSPCA has suggested enforcing shade netting in open aired pens for crocodile farms in South Africa. In the current study, shaded concrete temperatures were significantly cooler, and based on the findings, shade netting implementations could be highly beneficial for farms struggling with hyperthermia in the summer months, offering another cooling option to the crocodiles other than water bodies. The extent (area coverage and shading efficiency) and orientational placement of shade netting in such instances may be of importance. There is minimal literature regarding effective shade provision assessments on crocodile farms in summer, this is a recommended avenue for future studies. Such studies should ensure there is always sufficient basking area alongside the shade provided, ensuring this natural behaviour is not limited.

The two grower crocodiles occasionally experienced  $T_{b_{internal}}$ 's higher than those recommended for crocodilians several times during the study, maintaining those temperatures for periods of 1–7 hours at a time. From a hyperthermia perspective this is concerning. Crocodiles rely heavily on the ambient temperatures within their environments to regulate their own body temperatures, the fact that both grower crocodiles endured higher than recommended  $T_{b_{internal}}$ 's indicates that there is a need to

expand the proportion of cooler areas within the pen, even if these are temporary measures for the summer months. The core temperatures of both crocodiles fell within recommended farming temperature ranges (but not recommended body temperature ranges) for the most part, attesting to the crocodiles' thermoregulatory capabilities. In terms of behaviour, the grower crocodiles exhibited a pattern of increased water utilization that intensified as daytime temperatures rose. Less crocodiles were in view as the air temperatures and therefore concrete temperatures rose during the daytime, likely pointing toward increased water and shade use at this time. These findings align with summertime observations of adult farmed Nile crocodiles (Viljoen<sup>3</sup> *et al.*, 2023). Such behaviour is typically associated with thermoregulatory practices, as the crocodiles seek to maintain optimal body temperatures amidst varying environmental conditions.

#### 2.5.6. Conclusions

During a single summer study period on a commercial crocodile farm in South Africa, the  $T_{b_{\text{internal}}}$ 's of two grower Nile crocodiles were monitored to assess the potential risks of hyperthermia. The thermal gradients within the pen encompassed the recommended ranges for crocodile farming, as well as temperatures outside of this range. Water temperatures and temperatures on shaded concrete surfaces closely aligned with the recommended ambient pen temperatures. In contrast, areas of concrete exposed to direct sunlight reached temperatures that could pose a threat to the crocodiles, should they remain there for extended periods. Despite the pen offering a wide gradient of ambient temperatures, including those recommended for commercial crocodile farming, a significant portion of the enclosure was uncovered concrete. Predominantly, the crocodiles succeeded in maintaining their  $T_{b_{\text{internal}}}$ 's within the generally advised farming limits (20–35 °C). There were, however, instances of temperatures rising above or, more regularly, falling below the recommended body temperature ranges (28–33 °C). As this study occurred in an open-aired pen subject to local climate, it was expected that the 28–33 °C  $T_{b_{\text{internal}}}$  range would not be strictly adhered to. Extended periods (up to seven consecutive hours) of core temperatures  $\geq 34$  °C were observed, this poses a potential hyperthermia risk. Consequently, the farm may benefit from implementing more extensive daytime shading solutions during summer months. Behavioural considerations are a valid avenue for incorporation into similar studies, as dominant and subordinate crocodiles have been shown to have differing thermal experiences (Lang<sup>1</sup>, 1987; Morpurgo *et al.*, 1993; Brien<sup>1,2</sup> *et al.*, 2013).

## 2.6. iButton encapsulation integrity for core temperature measurement

### 2.6.1. Introduction

After the previous study encountered setbacks when using Liquid Armour encapsulated iButtons (small temperature loggers) force-fed to farmed grower Nile crocodiles (1.3–1.4 metres total length) for core body temperature ( $T_{b_{\text{internal}}}$ ) monitoring on a commercial farm in South Africa, an assessment of the interaction between encapsulated iButton substitutes and a typical farmed crocodile stomach pH was conducted. Once the average stomach pH was identified, a laboratory assessment of two potential encapsulation materials that could survive those pHs was undertaken. The initial study was a season long  $T_{b_{\text{internal}}}$  assessment (chapter 2's MD 2.5), which endured an 85% failure rate of Liquid Armour encapsulated iButtons. Stomach pH was assessed on the farm shortly after the difficulties of the initial study, as a requirement for ethical clearances to be granted for the continuation of similar thermal assessments. Members of the Civil Engineering department at the University of Pretoria proposed, designed, and supplied 3D printed polypropylene capsules as a potential alternative to Liquid Armour. A chemical resistant glue was used to ensure these capsules were watertight. The viability of Liquid Armour and 3D printed polypropylene capsules as encapsulation materials for a month-long study of crocodile  $T_{b_{\text{internal}}}$ 's was assessed in a laboratory. The aim was to determine if the two encapsulations could survive a four-week period in a solution mimicking the acidic stomach environment, with the intention of repeating the initial study on a shorter time scale.

### 2.6.2. Materials and methods

#### *Crocodile stomach pH*

Shortly after the  $T_{b_{\text{internal}}}$  study, during routine culling at the commercial crocodile farms on-site abattoir, 20 crocodile stomachs were obtained for a stomach pH assessment. The digestive system of crocodiles is routinely removed and hygienically discarded by the abattoir. Twenty of these were weighed and set aside, and a pH meter (Hanna Instruments, HI8424) with a pH electrode (Hanna Instruments, HI1230B) was used to record the pH of the stomach contents within an hour of culling. The pH meter was calibrated before each use using a three-point calibration method according to the instruction manual, using Hanna branded buffer solutions.

#### *Encapsulations survival testing at stomach pH*

Due to a lack of surviving iButtons from the initial  $T_{b_{\text{internal}}}$  study, 24 coin-batteries (Rayovac PR44, 675) were used as substitutes for iButtons in the laboratory encapsulation tests. These batteries were selected specifically for their external design; like iButtons they were encased in two stainless steel caps with a rubber seal between the caps. Each battery was numbered and photographed on both sides before the voltage outputs were recorded using a digital multimeter (Major Tech MTD 10, 500V AC/DC DIY Multimeter). The smudging of the numbering, visual erosion of the steel caps, or the inability to measure voltage with the multimeter after the four weeks of submersion in the hydrochloric acid (HCl) solution would indicate that the encapsulations had failed to prevent the HCl reaching the batteries and/or short circuiting them. Ten batteries were encapsulated in Liquid Armour, each battery was double dipped, and the products recommended curing time adhered to per layer. Plasti Dip has been used in previous studies for waterproofing iButtons (Robert & Thompson, 2003; Brien *et al.*, 2012), Liquid Armour is similar to Plasti Dip and is produced in South Africa (<https://liquidarmour.co.za/>). Five more batteries were placed into 3D printed polypropylene capsules provided by the Civil Engineering department at the University of Pretoria, which were printed in two parts that clipped tightly into one another (figure A10). The seal was further reinforced with a chemical-resistant adhesive (Pratley Chemical Resistant Adhesive) along the edges to ensure the capsules remained watertight. Nine more batteries were included as controls and were not placed in the HCl solution but remained in a nearby container in the laboratory.

Three sterile glass beakers with HCl solution (mixed precisely to a pH of 2) were stored in a secure cabinet in a laboratory at the University of Pretoria's Agricultural Sciences building. The solutions were checked weekly and any changes to the batteries or the HCl solution were noted. The pH of the solutions was measured (Orion Star, A211 pH meter) at the placement and removal of the encapsulated batteries to monitor any changes during the assessment period. The pH meter was calibrated before each measurement as per the instruction manual. Long handled tongs were used to lower the encapsulated batteries into the HCl solution. Once the batteries were added the beakers were sealed with parafilm (figure A11), placed in a tray then on a shelf in the lab where they would not be disturbed. After one month of immersion, the batteries were extracted, rinsed with distilled water, and allowed to dry completely. The encapsulations were removed, and the batteries voltages were re-measured to assess their survival after exposure to a pH of 2. The Liquid Armour was removed by slicing through the coating with a craft knife and then peeling it away from the battery. The polypropylene capsules were carefully opened by cutting through the material at both ends using large wire cutters, taking care to avoid contact with the batteries. The capsules were then cracked open and separated with needle-nose pliers.

### 2.6.3. Data analysis

Statistical analyses were carried out in R (2022.12.0 Build 353), a single regression and correlation were performed to assess if the weight of the digestive systems (assumedly related to the weight of the crocodiles) were related to the pH measurements.

### 2.6.4. Results

#### *Crocodile stomach pH*

The crocodile stomach pHs ranged from 1.80–2.66 ( $\bar{x} = 2.13$ , SE = 0.04), the digestive systems weighed between 0.65 and 1.67 kg ( $\bar{x} = 1.23$ , SE = 0.06). There was no significant relationship or correlation between the digestive system masses and the pH recordings of the stomach contents ( $P > 0.05$ ).

#### *Encapsulations survival testing at stomach pH*

The 15 de-encapsulated batteries showed no sign of having contacted the HCl solution. The numbering was still present, and all batteries were readable by the multimeter after the month period had elapsed. The control HCl solution showed no changes in appearance over the four-week testing period. The HCl solution containing the polypropylene capsules showed no changes in appearance until the fourth week of the study when small precipitates could be seen in the HCl. The HCl solution containing the Liquid Armour encased batteries had a slight yellow tint to the solution at the end of the second week, this tint persisted until the end of the fourth week where precipitates could be seen in the solution. Table 4 summarizes the pH of the solutions measured before and after the assessment, as well as the weekly visual changes in appearance of the HCl solutions and encapsulated batteries.

**Table 4.** Weekly visual effects of the HCl solution and encapsulated batteries during the month-long study period, and the pH measures before (“pH start”) and after (“pH end”) the batteries were in the solution.

HCl	pH start	pH end	Week 1	Week 2	Week 3	Week 4
Liquid Armour	2.017	2.025	HCl clear and unchanged. No change to batteries.	HCl had a slight yellow tint. No change to batteries.	HCl tinted. No change to batteries.	HCl tinted and precipitates forming. No change to batteries.
Polypropylene	2.016	2.038	HCl clear and unchanged. No change to batteries.	HCl clear and unchanged. No change to batteries.	HCl clear and unchanged. No change to batteries.	HCl clear and precipitates forming. No change to batteries.
Control	2.016	2.018	HCl clear and unchanged.	HCl clear and unchanged.	HCl clear and unchanged.	HCl clear and unchanged.

#### 2.6.5. Discussion

Previous studies found that stomach pH in alligators (*Alligator mississippiensis*) and spectacled caimans (*Caiman crocodylus*) varied between 1.5 and 5.9, with variations between farmed and wild alligators as well as animals in the fed versus fasted state (Diefenbach, 1975; Keenan *et al.*, 2013). The pHs recorded during the present study fall within this range. Due to the farms pre-culling protocol for crocodiles in the present study, the crocodiles were in a fasted state at the time of the pH assessment. All 15 encapsulated batteries survived four weeks in a HCl solution of pH 2. The precipitations that occurred by the fourth week indicated the beginning of the encapsulations’ breakdown. The Liquid Armour beaker contained bright white sand-grain sized precipitates (figure A12), whereas the polypropylene capsule beakers precipitates were more translucent and varied in shape and size (figure A13). A period of longer than four weeks would likely begin to compromise the safety of the batteries (or iButtons). These results indicate that logging  $Tb_{\text{internal}}$ ’s of Nile crocodiles with iButtons encapsulated in the tested materials should be limited to a month.

Based on the difficulty in removal of the batteries from their polypropylene capsules at the end of the current study, it is plausible that these capsules may exhibit enhanced robustness when interacting with hard or sharp feed-objects in the stomach (e.g., chicken beaks, claws, or bone material) when compared to Liquid Armour. Mechanical grinding in the stomachs of the crocodiles is another factor that likely affects force-fed logger survival. One potential downside of the polypropylene capsules was the increase in size when compared to a Liquid Armour encapsulated iButton. The size of temperature loggers and their encapsulations in relation to the size of the crocodiles being assessed is worth considering when selecting and designing encapsulations (i.e., 3D printable versions) for similar studies.

#### 2.6.6. Conclusions

In conclusion, both encapsulations survived a month at a steady pH of 2.0 in a laboratory setting. The degradation of the encapsulation material started to occur at the end of the fourth week of the assessment. It is recommended for future Nile crocodile stomach pH or  $Tb_{\text{internal}}$  monitoring studies, where iButtons are force-fed to crocodiles, that logger encapsulation using Liquid Armour or polypropylene encapsulations be limited to a maximum month-long recording period. Fed versus

fasted states, feed composition, and other physiological factors inherent to the crocodile's gastrointestinal processes may also have contributed to the loss of loggers in the initial study. A study of stomach temperatures, gastric pH fluctuations, and mechanical grinding in farmed or wild, grower or breeder, Nile crocodiles is another potential avenue for future studies to investigate.

## 2.7. Farmed Nile crocodile (*Crocodylus niloticus*) nest site selection assessment

### 2.7.1. Introduction

The associations between various nest site selection parameters on a crocodile farm in South Africa were assessed, with particular emphasis on the role of temperature. A nest depth assessment was performed prior to the nest site selection study to determine the appropriate depths to monitor within nesting sites. A combination of drones and iButtons were used to monitor the nesting activities and nest site selection parameters over a single nesting season.

### 2.7.2. Materials and methods

#### *Nest depth evaluation*

Nest depths were evaluated early in the nesting season (October–December 2022) to identify the most appropriate depths for the assessment of the thermal profiles within nests in the pen that was eventually selected. Various depths within 32 nests, across three pens, were measured upon egg extraction. Egg extractions occurred daily in the early hours of the morning (05:00–07:00), when the crocodiles were least active, throughout the nesting season. A team of three experienced farm personnel identified nesting sites where digging/nesting by a crocodile had occurred. The procedures for egg collection were conducted in accordance with Section 7 of the South African National Standard for Crocodiles in Captivity (SANS, 2009). Following egg collections, the nests were raked flat, ensuring any new nest digging activity would be spotted the following day. Breeder pens on the farm were built between 1990–1996 and although river sand was used to fill all nesting sites, sand consistency variations were noticed during excavations. Of the 32 nests, 16 were from nests with coarse and loosely packed sand, and 16 were from nests with densely packed fine sand. The first measure was the depth of the last egg deposited (most shallow) by the nesting female, from the top of the egg to ground surface level. The second measure was the depth at which the first egg was deposited (deepest) by the nesting female, measured from the top of the egg to the ground surface level. These two measures were then used to determine the overall nest depth of the full nest (the difference between the deepest and shallowest egg depths). Two of the 32 nests had a single egg sitting at or just below ground level, > 10 cm away from the rest of the nest's eggs, these eggs were omitted.

#### *Thermal profiles within nests*

The subsurface thermal properties of a selection of nests were assessed using Liquid Armour coated iButtons (DS1921G-F50 Thermocron), secured in 3D printed iButton holders, and refurbished iButtons (chapters 2's MD 2.4). Liquid Armour (<https://liquidarmour.co.za/>) was used as a waterproofing agent for the iButtons. The iButton holders were printed with a Creality Ender-3 V2 3D printer, with PLA+ plastic; the holder design was publicly accessible on Thingiverse (design reference number: 2895204).

Twenty-four iButtons, secured in 3D printed iButton holders, were placed at different locations and orientations in various nests within a crocodile pen to assess the thermal properties at multiple depths within those nests. Based on the findings of the preliminary nest depth study, six nests were fitted with four iButtons each, at predetermined depths suited to fine sanded nests. These iButtons were cable-tied (via their 3D printed holders) onto brightly coloured (spray painted) wooden dowels and inserted vertically into the selected nests so that the shallowest iButton was 10 cm below ground level, and each following iButton another 10 cm deeper than the previous, up to 40 cm below ground surface level. The brightly coloured dowels ensured that the iButtons remained in place and should the dowel be exposed due to crocodiles digging in the vicinity they would be easily noticed by the farms nest attendees. The nests were checked daily, no dowels were dug up during the study. Nests containing these evenly spaced iButtons, from 10–40 cm below ground level, will be referred to as “dowel” nests.

Nine refurbished iButtons (chapter 2's MD 2.4.) were used to measure single-depth temperatures in randomly selected, confirmed nests, as the eggs were harvested. These single refurbished iButtons were tied (taped to a 3D printed holder) onto a length of brightly coloured rope and tagged using key tags. Single iButtons were inserted into confirmed nests during excavations. In each case, the depth of the deepest egg was measured and as the egg was removed, the iButton was placed into those eggs previous positions (with the colourful rope angled upward), and the nest was covered. The brightly coloured ropes facilitated easier extraction post-study owing to their visibility. The nests with these single loggers will be referred to as "single" harvested nests.

Due to the farms daily egg collection policy, eggs were not left in the nesting sites long enough for logger placements among them. Instead, this study evaluated the nesting environment and identified potential factors that influence nest site and nest depth selections by the nesting crocodiles.

#### *Surface and faunal temperature variations*

A single day of hourly flights from 07:00–15:00 was conducted with a Mavic 2 Enterprise Dual drone (899 grams) in early December (1 December 2022). The flights occurred at an altitude of 35 m above ground level and were initiated out of sight of the pen so as not to alert/stress the crocodiles. The flight path was programmed in a third-party flight software package ([Dronelink](#)) and was consistent throughout all flights. Ground control points, modelled after those used in Messina and Modica (2020), were arranged around the perimeter of the pen. The location of each ground control point was recorded with an Emlid Reach RS+ differential GPS, ensuring the precise alignment of the resulting imagery after photogrammetric processing. The method detailed in chapter 2's MD 2.3 describes the transformation of temperature maps allowing the prediction of temperatures per orthophoto pixel.

Once the resulting imagery was processed in OpenDroneMap (ODM, version 1.9.3 build 30) and imported into QGIS (version 3.16-Hannover) (QGIS Development Team, 2021), thermal data for the pen (all substrates), nesting sites (surface temperatures, area shading ratio, and grass growth effects) and crocodiles ("back temperatures"), were determined using point layers and zonal statistic extractions from polygon layers.

#### *Crocodile pen and nest utilization*

A DJI Mini 2 SE drone (249 grams) was flown once per week, on a randomly selected day of the week, in the morning (between 06:00 and 07:00) and afternoon (between 15:00 and 17:00) for seven weeks during the breeding/nesting season (October–December 2022). A midday flight (12:00–12:30) was included on three of these occasions. All flights occurred at an altitude of 35 m above ground level and were initiated out of sight of the pen.

Behavioural data (pen area utilization, nest occupancy, nest utilization, and nesting section/orientation preferences) were recorded using a combination of drone imagery and the farms nest records for the breeding/nesting season. "Nest occupancy" refers to the crocodiles occupying a nesting site during the observation periods, whereas nest "utilization" or "preference" refers to the committed use (i.e., confirmation of eggs being deposited, which were reflected by the farms nest records for the season) of a nesting site. Due to the unequal distribution of nests across sections, directly comparing nest occupancy and nest preferences would introduce bias, proportional comparisons were employed when comparing these two variables. The total number of nesting sites occupied and utilized per section were normalized by the total nest count within each section. This controlled for potential biases favouring sections with a greater number of nesting sites. The distances from each nest (measured from the nests entrance) to the closest water body and the tourist walkway were extracted from the drone imagery using line-string layers in QGIS. Crocodile positions and snout-

hindlimb lengths (SHLs) were recorded for each timeslot where possible using point and line-string layers in QGIS.

#### 2.7.3. Data analysis

The data were analysed in R (2022.12.0 Build 353) and IBM SPSS Statistics (version 28). Summary statistics were the starting point to all analyses to view the data distribution, identify potential outliers, and assess the fundamental characteristics of the data. In instances where categorical variables needed comparison, Chi-square analyses were employed. This was followed by normality determinations to ensure the assumptions for subsequent tests were met. Multivariate Analyses of Variance (MANOVA) were used to assess the effects of multiple factors on the dependent variables. Where these resulted in significant outcomes, post hoc (Bonferroni) were conducted to determine specific pairwise group differences. Mixed model analyses were then employed to ascertain if there was an enhancement in sensitivity when accounting for both fixed and random effects. Pearson product moment correlations and regression analyses were used to determine linear relationships between variables. All data were analysed for the determination of significant differences at  $P < 0.05$ , highly significant differences were noted if  $P < 0.001$ .

#### 2.7.4. Results

Various nest depths within 32 nests on a commercial crocodile farm in South Africa were recorded early in a breeding season, the outcomes of this assessment informed the thermal nest assessment that followed. Thermal properties of nesting sites (inside, and external to, the nests), as well as other potential factors that may affect nest site selection were successfully recorded and reflected upon in Chapter 6 of this thesis. The use of ground level temperature loggers as well as a predictive model applied to thermal drone (DJI Mavic 2 Enterprise Dual) imagery (Viljoen<sup>3</sup> *et al.*, 2023; or chapter 2's MD 2.2) resulted in a series of complex findings regarding temperature selections made by the female crocodiles. A second drone (DJI Mini 2 SE drone) was used to collect behavioural data throughout the nesting season. When paired with the farms nesting records for the season, this allowed the identification of preferred nesting areas throughout the pen that was assessed.

#### 2.7.5. Discussion

A complex interplay between temperature and behavioural mechanisms regarding nesting and nest site selection on the farm revealed a need for further investigations of farm-based factors that may affect nesting success. Farmed hatching successes are primarily incubator-dependent, but the thermal selections and general behaviours of nesting females were intricate. The application of these methods in a farmed setting are highly repeatable and repetitions may inform future management strategies.

#### 2.7.6. Conclusions

Understanding the thermal and behavioural factors that dictated nest site selections, and why certain nesting areas were preferred over others might inform nesting-area layout strategies for improved breeding efficiencies. Future studies of nesting site selections and behaviours should consider more in-depth behavioural monitoring during the nesting season, as well as yearly repetitions to broaden our understanding of what quantifiable factors have lasting effects on farmed Nile crocodile nest site selections.

## 2.8. Concrete consistency and colour effects on temperature

### 2.8.1. Introduction

Pen substrates on crocodile farms play a critical role in the health and welfare of the crocodiles. Concrete is robust and durable and offers a hygienic environment that is easy to clean and reduces the growth of harmful pathogens, ultimately resulting in higher skin qualities (Bolton, 1989; Bothma & Van Rooyen, 2005; Domone & Illston, 2010). As a result, concrete is widespread in the design and construction of crocodile pens (Huchzermeyer, 2003; Brien *et al.*, 2007; Blessing *et al.*, 2014). With recent hyperthermia concerns being raised by the NSPCA (Personal communication: Prof J.G. Myburgh, University of Pretoria), an assessment of how altering the colour and consistency of concrete may affect temperatures reached when subject to the same environmental conditions was undertaken. It was hypothesized that temperatures attained by less dense concretes would vary from those of denser concretes. Factors which might influence this include thermal conductivity, specific heat capacity, and insulation properties (Domone & Illston, 2010; Mlilwana & Kearsley, 2022). The colour of the concrete mixes was hypothesized to affect temperatures as well, with darker colours absorbing more heat and lighter colours reflecting more heat (Mlilwana & Kearsley, 2022). By exploring these thermodynamics on a small scale, using ingredients common in commercial concrete mixes to alter colour and consistency, the current study aimed to identify a practical concrete mix which may be better thermally suited for crocodile farming.

### 2.8.2. Materials and methods

Five LoRaWAN loggers (Tektelic Comfort Smart Room Sensor) were encased in concrete slabs (30 cm x 30 cm x 6 cm) of different formulae. Five concrete recipes were mixed, varying in their primary aggregates, which altered their colours and consistencies. All loggers were placed centrally within the concrete slab moulds and the concretes were mixed to pre-defined recipes compiled by Derek Mostert, a concrete specialist at the University of Pretoria. The five recipes are referred to in terms of their primary aggregates and consistency-altering additions: “granite”, “aerated granite”, “dolomite”, “lightweight dolomite”, and “chrome slag”. Polypropylene and steel fibres were added to the mixes to reduce shrinkage cracking and provide tensile strength, respectively. The “aerated granite” mixture was aerated with chryso foam, and the lightweight dolomite addition was praliperl perlite. The inclusion of aeration additives resulted in the lightweight dolomite and aerated granite exhibiting lower densities compared to their respective pure mixes, this also resulted in weaker strength properties. The strength of the concrete mixes in the current study are categorized as low-strength ( $\geq 10$  MPa) and high-strength (40–100 MPa) (Domone & Illston, 2010). In terms of colour, the granite and aerated granite slabs were lighter than the other recipes, followed by chrome slag; dolomite and lightweight dolomite slabs were the darkest in colour (figure 14).



**Figure 14.** Concrete slabs from left to right: granite, dolomite, chrome slag, aerated granite, and lightweight dolomite.

Two 100 mm x 100 mm cubes of each mixture were also moulded for compressive strength testing. The slabs and cubes spent seven days curing in a water bath before they were weighed, dried, re-weighed, and the cubes subjected to strength testing (table 5). Each slab was then marked (permanent

marker) with the appropriate mix name and deployed, out in the open, on University of Pretoria premises. The slabs remained in their deployed positions for just over a year (January 2022–February 2023), unprotected from all weather conditions. Two more loggers of the same brand and model were deployed, one as a control which remained in a drawer in a nearby office and another under a nearby roof recording air temperature. The differences between the concrete block temperatures are discussed in relation to season, climate variables, and colour of the slabs. Climate data was obtained from January–July 2022 from the South African Weather Services (SAWS), this supplemented that of the onsite loggers.

**Table 5.** The mean saturated (“M<sub>s</sub>”) and unsaturated (“M<sub>d</sub>”) cube masses, compressive force applied to break the cubes, and the calculated compressive strength of each concrete mix.

Concrete mix	M <sub>d</sub> (g)	M <sub>s</sub> (g)	Force (N)	Strength (MPa)
Granite	2350.50	2328.80	453.50	45.35
Dolomite	2589.55	2574.85	513.30	51.33
Chrome slag	2688.05	2677.67	618.35	61.84
Aerated granite	1727.95	1711.98	46.75	4.68
Lightweight dolomite	942.35	916.58	89.60	8.96

### 2.8.3. Data analysis

Statistical analyses were performed in R (2022.12.0 Build 353) and the data were analysed for the determination of significant differences at  $P < 0.05$  and highly significant differences at  $P < 0.001$ . An analysis of variance, t-tests, and partial correlations were performed to assess the variations between concrete temperatures and the effects of air temperatures on the concrete temperatures.

### 2.8.4. Results

Concrete temperatures of all slabs ranged from 0.3–55.0 °C, the descriptive statistics for the five concretes and the air temperatures in the immediate vicinity of the study are presented in table 6. The mean concrete temperatures in summer were 26.1 °C for granite, 27.5 °C for aerated granite, 28.6 °C for dolomite, 27.5 °C for lightweight dolomite, and 28.2 °C for chrome slag. The mean concrete temperatures in autumn were 21.0 °C for granite, 20.6 °C for aerated granite, 20.8 °C for dolomite, 20.6 °C for lightweight dolomite, and 21.9 °C for chrome slag. Mean concrete temperatures in winter were 16.0 °C for granite, 16.1 °C for aerated granite, 16.5 °C for dolomite, 15.7 °C for lightweight dolomite, and 16.7 °C for chrome slag. Mean concrete temperatures in spring were 25.1 °C for granite, 25.1 °C for aerated granite, 25.5 °C for dolomite, 25.0 °C for lightweight dolomite, and 25.9 °C for chrome slag.

**Table 6.** Descriptive statistics for the temperatures of the five concrete slabs and on-site air temperatures (°C).

Variable	Min	Max	Mean	SD	SE
Air temperature	2.00	36.00	20.25	5.79	0.02
Granite	0.30	50.30	22.46	9.82	0.05
Aerated granite	1.20	51.20	22.62	9.39	0.05
Dolomite	0.80	53.20	21.95	10.51	0.06
Lightweight dolomite	1.70	55.00	22.58	9.38	0.05
Chrome slag	1.50	53.00	23.44	10.04	0.06

The SAWS data showed ambient air temperatures varied from -1–33 °C ( $\bar{x}$  = 18.05 °C, SE = 0.016 °C), humidity ranged from 0–100 % RH ( $\bar{x}$  = 63.52 % RH, SE = 0.66 % RH), windspeeds varied from 0–5 m/s ( $\bar{x}$  = 1.23 m/s, SE = 0.003 m/s), and rainfall ranged from 0–29 mm ( $\bar{x}$  = 1.77 mm, SE = 0.036 mm) during the full study period. Concrete temperatures were very weakly correlated to ambient temperature ( $r$  = 0.061,  $P$  < 0.001), very weakly correlated to rainfall ( $r$  = -0.07,  $P$  < 0.001), weakly correlated to windspeed ( $r$  = -0.28,  $P$  < 0.001), and moderately correlated to humidity ( $r$  = -0.47,  $P$  < 0.001). Concrete temperatures varied with the mixes ( $P$  < 0.001,  $F$  = 110.17,  $df$  = 4), season ( $P$  < 0.001,  $F$  = 3869.63,  $df$  = 3), and hour of the day ( $P$  < 0.001,  $F$  = 4769.55,  $df$  = 1). Bonferroni post hocs for the mixes showed that temperatures for the chrome slag and dolomite slabs varied from those of all other mixes (all  $P$  < 0.001). Granite temperatures did not vary from those of aerated granite or lightweight dolomite, nor did the aerated granite and lightweight dolomite temperatures vary from one another ( $P$  > 0.05). Temperatures recorded by all concrete slabs varied significantly between all seasons (all  $P$  < 0.01). In summer, chrome slag and dolomite temperatures varied from all other concretes ( $P$  < 0.001) except each other ( $P$  > 0.05), lightweight dolomite and aerated granite temperatures varied from all other concretes ( $P$  < 0.05) except each other ( $P$  > 0.05), and granite temperatures varied from those of all other concretes ( $P$  < 0.05). In winter, chrome slag varied only from lightweight dolomite ( $P$  < 0.001), lightweight dolomite also varied from dolomite ( $P$  < 0.05), and granite and aerated granite did not vary from any other concretes ( $P$  > 0.05). Figure 15 shows the mean monthly and hourly plots of the concrete temperatures, as well as seasonal effects. Concrete temperatures were all strongly and positively correlated to on-site air temperatures (all  $r$   $\geq$  0.91, all  $P$  < 0.001). When assessing according to colour, where the dolomite and lightweight dolomite slabs were defined as “light” and the other slabs as “dark”, this significantly impacted the temperatures recorded ( $P$  < 0.05,  $t$  = 2.09,  $df$  = 14010). Specifically, the lighter slabs produced lower mean temperatures than the darker ones.

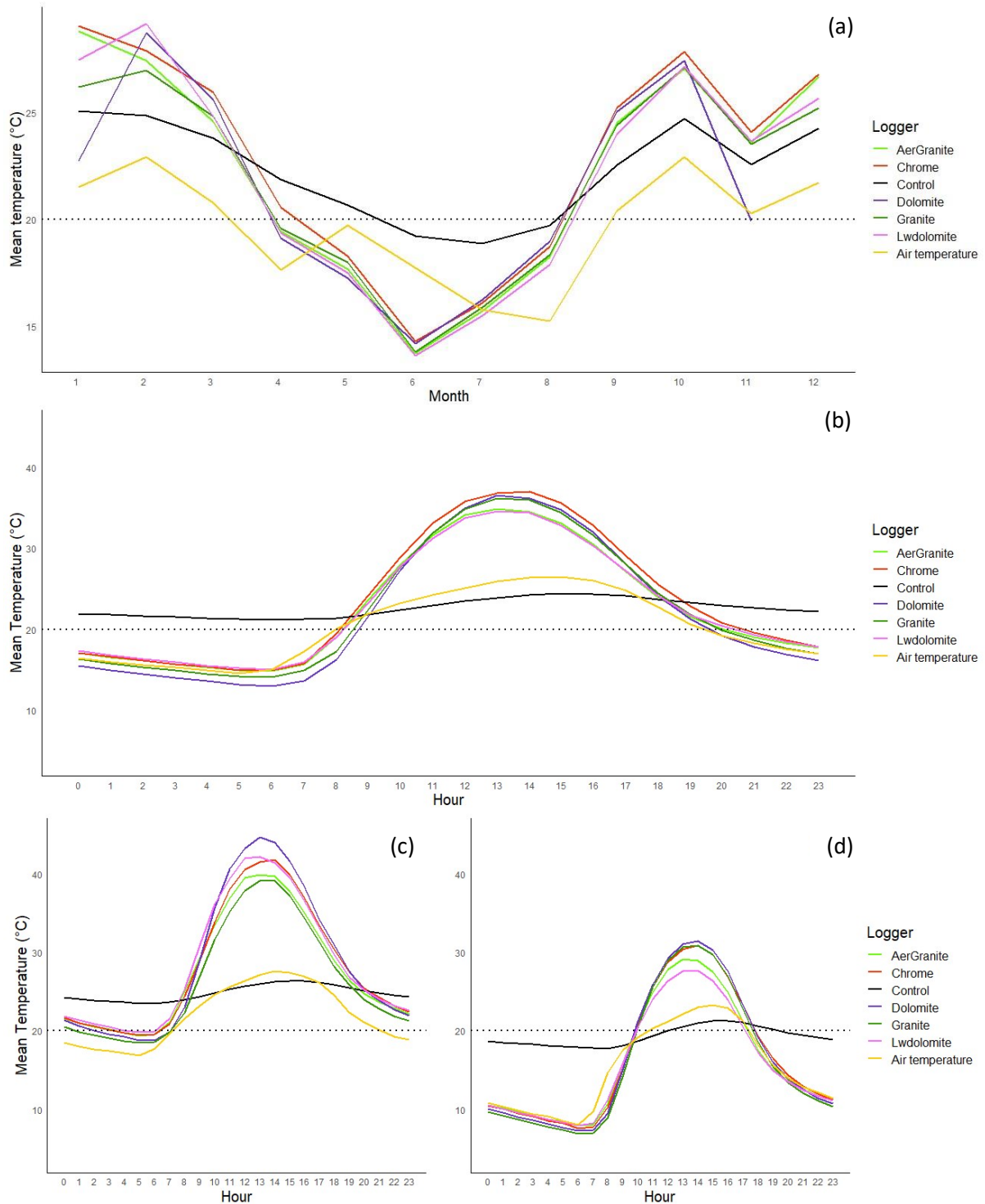


**Figure 15.** Mean monthly (a) and hourly (b) temperature recordings from the various concrete-encased loggers, as well as the control and on-site air temperatures. The hourly mean temperatures are also plotted for summer (c) and winter (d) seasons. A dotted line at 20 °C serves as a reference, facilitating easier comparison of temperature values across different conditions.

### 2.8.5. Discussion

Mean chrome slag temperatures were higher than other concretes during autumn and spring, closely followed by granite in autumn and dolomite in spring. Mean dolomite slab temperatures were higher than other concretes during summer and winter, followed by chrome slag and lightweight dolomite in summer, and chrome slag in winter. The lightweight dolomite slab presented the lowest mean

temperatures during all seasons except summer when it displayed the second highest mean temperatures. Although the chrome slag and dolomite slabs held higher mean temperatures during winter, which would likely be beneficial in a crocodile farm setting, these two concrete types would be ill-suited in summer months where they maintained higher temperatures than other concretes. The aerated granite and lightweight dolomite slabs tended to have mean temperatures consistently on the lower side (except for lightweight dolomite in summer); this was possibly due to their less dense consistencies and therefore altered insulation effects. From a practical perspective these less dense and therefore weaker concretes would likely not be incorporated into pen designs as they would not be as long-lived as their higher strength counterparts. The granite slabs' mean temperatures were the lowest recorded in summer, second highest in autumn, and mid-level in both winter and spring. During the daily peak in hourly on-site air temperatures, granite had the lowest mean temperature of all the mixtures in summer, whereas in winter it was comparatively warm if not warmer than all other mixtures except chrome slag.

#### 2.8.6. Conclusions

The granite-based concrete slab presented the preferable concrete type, for the purposes of this study, out of the assessed recipes. Characterized by light colouration and high strength, this concrete variant exhibited advantageous thermal characteristics which became clear when summer and winter temperatures were compared. Given the temperatures varied by only a few degrees, these mixes are likely not practical from a crocodile pen and thermoregulation perspective. Future studies assessing colour and strength of concretes and how this impacts temperature may consider colouration of concretes on a more extreme scale, or the application of surface level colourants that could be easily and safely applied on a seasonal basis to optimize the thermal properties of concretes within already-built pens.

## 2.9. Thermal niches of Nile crocodiles (*Crocodylus niloticus*) in Kruger National Park

### 2.9.1. Introduction

This study explored the thermal selections, behaviours, and activity patterns of subadult and adult Nile crocodiles (*Crocodylus niloticus*, 2.33–4.29 cm total lengths) at the confluence of the Letaba and Olifants Rivers within the Kruger National Park between 2018 and 2020. A selection of Wireless Wildlife tracking devices (<http://wireless-wildlife.co.za/products.html>), including base and relay stations for data retrieval and various temperature recording devices, were deployed.

### 2.9.2. Materials and methods

This study occurred at the confluence of the Letaba and Olifants Rivers, and into the Massingir Dam. Several solar and battery powered Wireless Wildlife base (WW-BS) and relay stations (WW-RS) were positioned along the banks of the study site. These were responsible for receiving data from temperature recording units attached/fed to the crocodiles in this study. Relay stations, which have an equivalent coverage footprint and serve as intermediaries to base stations, relayed telemetry data to the base stations for onward transmission to the operator via a global system for mobile communications (GSM) network.

Nine male and eight female wild Nile crocodiles in Kruger National Park were captured and fitted with a selection of Wireless Wildlife tracking devices. Each crocodile was fitted with a WW1500AS unit which encompassed a GPS device, a temperature logger, and a motion sensor. These units were attached by threading stainless steel strands subcutaneously underneath the nuchal rosettes at the back of each crocodile's neck (figure A21, A22), as per Brien *et al.* (2010). The GPS unit recorded latitudes and longitudes every six hours, whereas the motion sensor and temperature loggers were set up to record hourly. A second type of temperature logger (WW0500) was encased in dental acrylic and force-fed via gastric intubation, to be retained as pseudo-gastroliths, to each crocodile for internal temperature recordings (figure A23, A24). Similar methods for gastric intubation have been used for crocodylians in studies that fed loggers or performed stomach content collections (Loveridge, 1984; Janes & Gutzke, 2002; Brien *et al.*, 2012). This was accomplished using a hollow metal pipe, soft rubber tubing, adhesive tape, and a cloth. Each crocodile was prompted to bite down on the exterior of a large hollow metal pipe, which was covered in a softer but sturdy protective material to prevent potential movement/skidding and therefore damage to the crocodiles' teeth/mouth when biting down. Once the crocodile had a firm grip, the eyes were covered with a clean cloth and the mouth carefully taped shut. The soft rubber tubing, marked with length indicators for insertion depth estimation, was then inserted down the crocodile's throat until it reached the stomach. The dental acrylic encased WW0500 logger was then introduced through the soft tubing into the stomach. The tubing, tape, metal pipe, and eye-cloth were then carefully removed, and the crocodiles released. These internal/stomach/core body temperatures were recorded hourly. Downloadable ranges for the different devices varied due to their positioning and design. The externally placed loggers were readable up to a range of a few kilometres, the internals less so as they not only had a less effective antenna system (intentionally compact in design), but the signal would need to pass through the body of the crocodiles.

The motion sensor within the WW1500AS units measured hourly physical activity outputs of the crocodiles with an omnidirectional tilt and vibration sensor; the sensor outputted a "count rate" of tilts over time. The information provided did not indicate the type of activity being performed nor the rate of acceleration of the crocodiles, rather it showed the extent of the devices gravity displacement and therefore the intensity of the crocodile's "activity", at a point in time.

On-site climate data was not incorporated because the weather stations nearest the study site did not record historical weather data through much of the study period. The closest weather station with historical data was approximately 200 km away, in an area of KNP which is known to exhibit microclimatic variations distinct from those at the study site (Gertenbach, 1983; Venter & Gertenbach, 1986). For this reason, air temperatures for the study were attained from a global climate reanalysis dataset (European Centre for Medium-Range Weather Forecasts (ECMWF) fifth-generation high spatial resolution climate reconstruction platform (ERA5)), and no other climate data was incorporated to avoid biased results.

### 2.9.3. Data analysis

Statistical programs R (2022.12.0 Build 353) and IBM SPSS Statistics (version 28) were used to assess this dataset. Summary statistics allowed visualization of the distribution and the assessment of fundamental characteristics of the data. Variables were checked for multicollinearity to ensure the combination of related variables was avoided in the analyses that followed. T-tests were used to compare the means between groups. ANOVAs were used to compare means across different groups particularly when categorical variables were compared to continuous dependent variables. Regression analyses were employed to model the relationships between various temperature variables, offering insights into how changes in air and immediate ambient (“back”) temperatures affected  $T_{b_{\text{internal}}}$ 's. The relationships between variables were assessed with correlations; when there were potential additional variables that may have affected these relationships, partial correlations were employed. Generalized linear mixed models (GLMM) allowed exploration of the direct and indirect effects of environmental factors (air temperature), physiological measurements ( $T_{b_{\text{internal}}}$  and  $T_{b_{\text{external}}}$ ), physical attributes (TL), and activity levels of the study subjects on one another. Due to the unbalanced nature of the data, Bonferroni corrections were applied to all post hoc pairwise comparisons. All data were assessed for the determination of significant differences ( $P < 0.05$ ), and highly significant findings were also documented ( $P < 0.001$ ).

### 2.9.4. Results

Of the 17 crocodiles included in the original deployments, 12 had complementary internal and external temperature data ranging from 6 to 290 days ( $\bar{x} = 82$  days). In 9 of these 12 cases, the external loggers outlived their internal counterparts. It is postulated that this was due to either the expulsion of the internal loggers (as one such logger was later recovered near the waterline) or the eventual digestion of the protective coating applied, resulting in logger failure. Of the remaining five crocodiles, four had either only internal or external data recordings, and one crocodiles loggers failed to record altogether. These occurrences were likely due to logger failures/damage/expulsions, with the remaining loggers continuing their data capture without their temperature-logging counterparts. WW0500 and WW1500AS loggers both transmitted data that could be captured by any base or relay units in proximity, explaining the occurrence of crocodiles with periods of either only internal or external data. For detailed results, refer to chapter 5 of this thesis.

### 2.9.5. Discussion

The loggers attached to the crocodiles varied in their longevity, which appeared to be related to sex (and therefore size), where smaller (total length) crocodiles (usually females) maintained functioning loggers for longer periods than larger ones (usually males) did. Notably, the force-fed dental acrylic-encased loggers in this study outlasted the Liquid Armour and 3D-printed polypropylene capsule-encased loggers in the previously described methods chapters (MD 2.5 and 2.6). Occasional gaps in the data collected were another unforeseen outcome. The GPS coordinates, due to their error radius, were not necessarily useful in identifying whether the crocodiles were selecting land or water areas and so thermal behaviours had to be inferred from the crocodiles' temperatures and from climate

data (air temperature specifically). Assessment of the GPS data collected for this study is still a useful endeavour if territory and movement information is of interest.

#### 2.9.6. Conclusions

Future studies assessing long-term internal and external body temperatures and activity levels of wild Nile crocodile populations should consider adding more extensive behavioural and environmental condition monitoring methods into the planning process. Portable weather stations could be affixed within the study area, and water temperature loggers could be placed within water bodies at varying depths. Dental acrylic is recommended as a robust encasement material for studies where force-feeding of loggers for internal temperature monitoring is required. Behavioural monitoring of the individuals under study (whether that be mechanical or manual) would also expand our understanding of the crocodiles' use of substrates, impacts of social interactions, breeding behaviours, and nesting confirmations.

### 3. Remote body condition scoring of Nile crocodiles (*Crocodylus niloticus*) using Uncrewed Aerial Vehicle derived morphometrics

Viljoen, D., Webb, E., Myburgh, J., Truter, C., and Myburgh, A. (2023). Remote body condition scoring of Nile crocodiles (*Crocodylus niloticus*) using uncrewed aerial vehicle derived morphometrics. *Frontiers in Animal Science*, 4:1225396.  
<https://doi.org/10.3389/fanim.2023.1225396>

#### 3.1. INTRODUCTION

Frequent monitoring of wild Nile crocodile (*Crocodylus niloticus*) populations to gather demographic and management data can be complicated by their cryptic behaviour, occurrence in often inaccessible areas, and their semi-aquatic nature (Behangana *et al.*, 2017). In wild crocodile population surveys, it is often easier to observe larger animals, which are more reliably spotted and objectively classed into size categories (Behangana *et al.*, 2017; Utete, 2021; Aubert *et al.*, 2021). Until recently, crocodile population surveys relied exclusively on counts from fixed-wing aircraft and helicopters, or spotlight counts from boats at night; where waterways are accessible (Bayliss, 1987; Combrink, 2004; Ferreira & Pienaar, 2011; Wallace *et al.*, 2013). These methods are potentially disruptive, time consuming, require costly fuel and equipment, and may result in observer-biased size categorization (Elsey & Trosclair, 2016; Ezat *et al.*, 2018).

Uncrewed aerial vehicles (UAVs) have emerged as a valuable tool for conducting crocodile population and habitat surveys due to several advantages over traditional methods, including improved counting accuracy, cost-effectiveness, repeatability, reduced animal stress, and improved researcher safety (Aubert *et al.*, 2021). The efficacy of UAV surveys is constrained by the visibility of animals from above (Aubert *et al.*, 2021). Recent advancements in imaging sensor quality have resulted in higher-quality images, reducing the need for lower flight altitudes (Toffanin, 2019). Given sufficient drone batteries and suitable vehicle access to establish viable drone take-off and landing points, large areas can now be surveyed whilst producing clear enough images for accurate morphological measurements. Basking behaviour in open systems (e.g., bedrock based, mature river reaches), especially during the winter season, offers the ideal UAV monitoring scenario as many crocodiles leave the water between 10:00 and 17:00 to thermoregulate (Downs *et al.*, 2008). The effects of UAV presence, with a focus on auditory and visual disturbances, observer bias, ethical flight practices, and UAV-related animal behaviours, have been considered (Hodgson & Koh, 2016; Bevan *et al.*, 2018; Viljoen<sup>2</sup> *et al.*, 2023). The recommended flight altitudes for crocodilians range from 40 to 50 metres (m), depending on the imaging sensor used, to produce images with sufficient clarity and photogrammetric accuracy for crocodile population monitoring (Bevan *et al.*, 2018; Ezat *et al.*, 2018; Aubert *et al.*, 2021; Myburgh *et al.*, 2021).

Zoometric measures have ecological significance as they provide information about the size, growth, and health of individual crocodiles and populations (Salem, 2011; Warner<sup>1</sup> *et al.*, 2016). Several zoometric measurements are associated with crocodilians (Edwards *et al.*, 2017), a few of which can be recognized from the perspective of a UAV. Examples of standard morphometric measures for crocodiles are total length (TL: distance from the tip of the snout to the tip of the tail), snout-vent length (SVL: distance from the tip of the snout to the third circumcircle scute layer that corresponds to the caudal margin of the cloaca), head length (HL: distance from the tip of the snout to the posterior ridge of the supraoccipital bone) and belly width (BW: transverse measurement across the widest part

of a crocodiles smooth ventral belly scutes) (Warner<sup>1</sup> *et al.*, 2016; Edwards *et al.*, 2017; Webb *et al.*, 2021).

Despite the clear advantages of UAV-based crocodile population census, some factors limit the widespread application of the technique. In the case of UAV-based morphometrics, TL as a measure can be problematic due to the loss of tail ends, the difficulty in accurately distinguishing the thin tail tip from its surroundings, or due to partial submersion of a crocodile in water (Mazzotti *et al.*, 2012; Myburgh, 2022). Orthophotos with a ground sampling distance (GSD) > 3 cm/pixel can make sections of the tail difficult to distinguish. Previous studies have derived relationships between TL and SVL or HL of crocodiles as a means of accurately estimating TL from these more reliably captured measures. Morphometric measures hold importance for body condition and therefore welfare assessments, as well as population size estimates (Hutton<sup>1</sup>, 1987; Salem, 2011; Warner<sup>1</sup> *et al.*, 2016).

A body condition score is a measure of an animal's relative "fatness", from which health and well-being is inferred (Fujisaki *et al.*, 2009; Mazzotti *et al.*, 2012; Ojeda-Adame *et al.*, 2020). Body conditions of crocodiles have been assessed in multiple studies using Fultons index (K) which relates length to mass, which is considered useful for comparisons across populations (Zweig, 2003; Fujisaki *et al.*, 2009; Mazzotti *et al.*, 2012; Brandt *et al.*, 2016; Shirley *et al.*, 2017; Webb *et al.*, 2021). Ojeda-Adame *et al.* (2020) evaluated three condition score indices based on length and mass measurements of 26 American crocodiles (*Crocodylus acutus*), namely Fultons index, relative condition index, and scaled mass index, and suggested that the indices were difficult to interpret and potentially misleading. The proposed alternative was an in-depth condition score that assessed multiple morphological zones rather than assigning a relationship between length and volume measures (Ojeda-Adame *et al.*, 2020). For a hands-on assessment this is the recommended condition scoring method as it assesses regions of the body known to be affected by nutritional status.

Hands-on condition scoring techniques may not always be desirable or possible when working with wild populations or particularly large crocodiles. UAV-based body condition assessments have the advantage of being non-invasive and have been applied to Fur seals, Antillean manatees, and eastern North Pacific gray whales (Allan *et al.*, 2019; Soledade Lemos *et al.*, 2020; Ramos *et al.*, 2022). In these studies, straight-line body length, belly girth, and surface area, among other measures were considered. To our knowledge, no remote sensing body condition assessments have been attempted for crocodilians. A normalized UAV-based body condition score could be a useful health and well-being assessment tool in situations where large-scale assessments are required. These methods could be valuable in instances where rapid assessments of the well-being of a large crocodile population are required, a population is distributed over a large area, where crocodile populations occur in remote locations, or where capture/handling is not possible (i.e., capture difficulties, not wanting to cause the animals undue stress, or illness is suspected in a population).

In this study, the relationships between Nile crocodile morphometric measures derived from high resolution rectified UAV imagery were assessed. A logical combination of these measures for the assessment of well-being/health is derived and discussed, in the form of a body condition score. The relationships between several crocodile morphometric parameters were determined for use in future UAV-based crocodilian population monitoring studies.

### 3.2. AIMS AND HYPOTHESES

This study aimed to non-invasively capture morphometric data for captive breeder Nile crocodiles in South Africa, using an uncrewed aerial vehicle. The UAV-derived morphometrics were then used to estimate a fast-paced and repeatable estimation of crocodile welfare, in the form of a body condition score. It was hypothesized that UAV-based morphometrics could be reliably captured and used to

estimate a body condition score for Nile crocodiles. Due to the vast array of nutritional states of the crocodiles in this study, this method could be applied to captive or wild crocodile populations.

### 3.3. MATERIALS AND METHODS

Two hundred and eighty-eight crocodiles were assessed at two commercial crocodile farms in South Africa. One of the farms crocodiles appeared slimmer at time of the flights, when compared to the other farms crocodiles. The spectrum of thin to fat crocodiles was assessed with the following UAV-captured measures: total length (TL), snout-hindlimb length (SHL), snout-neck length (SNL), neck width (NW), belly width (BW), total surface area (SA), and perimeter.

#### 3.3.1. Aerial image acquisition and processing

A DJI Mavic Mini UAV with a 12-megapixel CMOS sensor was used to survey four pens across two commercial crocodile farms (henceforth referred to as farm A and farm B) in South Africa with an estimated model error of < 25 mm (Myburgh *et al.*, 2021), i.e., all length measurements accurate to within 25 mm. The UAV was programmed to follow a predetermined flight path at an altitude of 40–60 m covering each area in a grid pattern, taking images with approximately 80% frontal and 70% side overlap over the surveyed area. These flight altitudes did produce a noticeable difference in image clarity; however, altitudes in this range are suitable for this method and maintain adequate accuracy as per Myburgh *et al.* (2021). The flights were programmed using the automated flight software [Dronelink](#). The flights were conducted between 10:00 and 11:00 on a relatively cold winter morning when the crocodiles were basking and could be photographed out of the water (Downs *et al.*, 2008). Each flight produced images which were processed into a single orthophotograph per flight at 1.42 cm resolution using OpenDroneMap (ODM, version 1.9.3 build 30). An Emlid Reach RS+ differential GPS and seven ground control points were used to ensure ground truthing of the orthoimages during processing. The resulting orthophotograph from ODM was imported into QGIS (version 3.16-Hannover) for morphometric data capture (QGIS Development Team, 2021).

One hundred and forty-five crocodiles from farm A and 143 crocodiles from farm B were included in the analyses. These crocodiles included large growers (between one-year-old and harvest size) up to breeder (mature or adult crocodiles) sized individuals, ranging from > 1–4.8 m TL. Crocodiles less than 1 m in TL were not included as data capture would have been complicated by orthophoto clarity and the tendency of smaller crocodiles to pile up which concealed body parts needed for the measurements. For consistency, only crocodiles that were lying motionless on the dry emergent area (i.e., basking) with their full bodies captured by the UAV imagery were used in the analyses, while crocodiles in motion or in the water bodies were not measured.

#### 3.3.2. Deriving morphometric data

Head lengths (HL) are traditionally measured using a standard tape measure, from a UAVs perspective the HL measure can be problematic as the required features of measurement are difficult to detect in the images, especially in low-resolution imagery (Ezat *et al.*, 2018; Jordaan, 2021). HL can be adapted for UAV observations by measuring from the tip of the snout to the posterior margin of the four large dermal scute plates on the neck corresponding to the front limbs of the crocodile, henceforth referred to as snout-neck length (SNL). Snout-vent length (SVL) is a measure commonly used when the full length of a crocodile's tail cannot be accurately measured due to missing tail ends. SVL cannot be precisely measured from UAV imagery as the caudal margin of the cloaca cannot be viewed dorsally on a crocodile (Myburgh, 2022). This measure can be adapted for UAV observations by measuring from the tip of the snout to the circumcircle scute layer immediately posterior to the back legs, henceforth referred to as snout-hindlimb length (SHL). Relationships between TL and SHL, and TL and SNL, have been proposed (Myburgh, 2022); however, correction factors have not been thoroughly tested on a range of crocodilian body sizes and conditions.

All morphometric data were derived with either a line-string layer or vector polygon layer in QGIS. Total length (TL) was measured by estimating the distance between the tip of the snout, following the curve of the animals back to the tip of the tail for those individuals where the tip of the tail could be clearly distinguished from the background (line-string layer in QGIS). In images of crocodiles where the tail did not terminate in a clear tip (indicating loss of tail) the individuals were excluded from the assessment. Snout-neck length (SNL) was measured by drawing a line (line-string layer in QGIS) from the tip of the crocodile's snout to the posterior margin of the large dermal scutes on the neck corresponding to the anterior origin of the front limbs. Snout-hindlimb length (SHL) was estimated by deriving the distance from the tip of the crocodile's snout to the last scute layer posterior to the crocodile's hind limbs (line-string layer in QGIS). The relationships between TL, SNL, and SHL were compared using linear regressions. Figure 16a identifies the morphological features for measuring the UAV-adapted morphometrics that replace SVL and HL (SHL and SNL, respectively) in this study.

Neck width (NW) was measured by drawing a line across the widest part of a crocodile's neck, keeping perpendicular to the TL/SHL string layers. Belly width (BW) was measured with a line-string layer in QGIS across the widest part of the crocodile's stomach, keeping perpendicular to the TL/SHL string layers. Surface area (SA) was measured in QGIS using a vector polygon layer and outlining the crocodile's body. For the SA morphometric measurement, the tails were included as this is an area of fat deposition (Osthoff *et al.*, 2014), whereas the crocodiles' legs were not included as their positions were inconsistent from animal to animal. The perimeter was measured with the same vector polygon layer by extracting the length of the outline used to create the SA morphometric. The morphometric measures recorded in QGIS are depicted in Figure 16b and 16c.

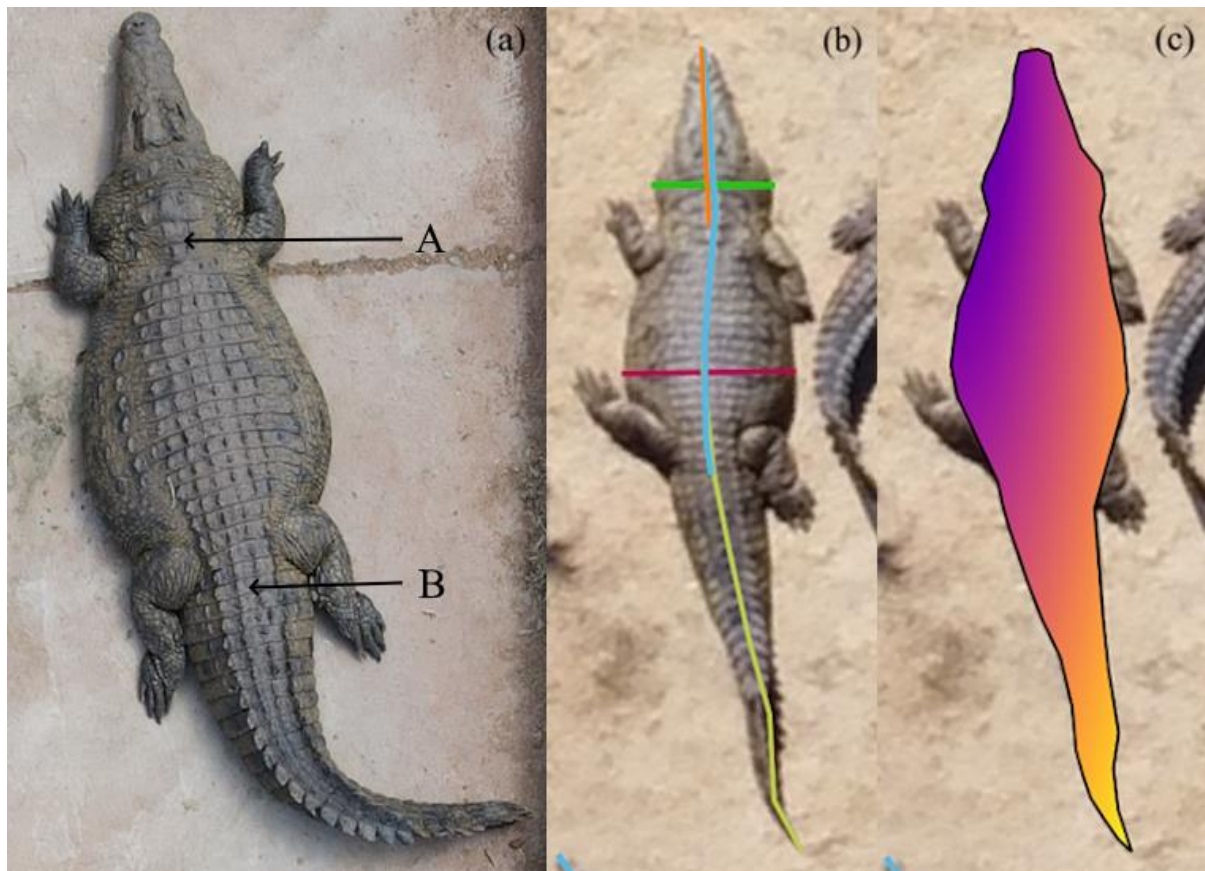


**Figure 16.** (a) Morphological features recognisable from UAV imagery that are required to capture the morphometric measurements for the current study. "A" illustrates the conclusion of the dermal neck scutes required for the morphological measure SNL. "B" illustrates to the circumcircle scute layer

behind the hind legs, required for the morphological measure SHL. (b) Depicts morphometric measures captured as vector line layers in QGIS, colour codes: total length in yellow, snout-hindlimb length in blue, belly width in pink, neck width in green, and snout-neck length in orange. (c) Depicts morphometric measures captured as vector polygon layers in QGIS: perimeter shown by the black outline of the crocodile, and surface area shown by the gradient-coloured area that falls within the perimeter line.

### 3.3.3. UAV-based body condition assessment

A body condition index (BCI) was calculated using TL and BW by means of the equation:

$$BCI = \left( \frac{BW}{TL} \right) \times 10 \quad \text{Equation 5}$$

The BCI results were used to estimate a body condition score (BCS) by normalizing the BCI values and applying a rank between 1 and 5 (1 being a very low BCS and 5 a very high BCS) to create a score for each crocodile indicating its body condition in relation to all crocodiles measured in this study. This resulted in the following 'standardized' equation:

$$BCS = \left( \frac{BCI - 1.34}{1.27} \right) \times 4 + 1 \quad \text{Equation 6}$$

## 3.4. DATA ANALYSIS

All morphometric data were analysed in SPSS (version 28) using generalized linear mixed model analysis and discriminant analysis procedures. Pearson correlation coefficients were calculated between variables. All data were analysed for the determination of significant differences ( $P < 0.05$ ). Linear regression analyses were performed in Microsoft Excel® to compare the relationships between total length, snout-hindlimb length, and snout-neck length. The relationships between these three measures were considered particularly important because similar measures have been traditionally used for population surveys.

Correlations among the morphometric measures were computed with confidence intervals of 95.0% in SPSS. A stepwise regression was used to assess which of the measures most accurately estimated the body condition of the crocodiles. Total length and belly width were excluded from this analysis because these variables were included in calculating the BCI. Three other morphometric measurements displayed significant ( $P < 0.05$ ) relationships with body condition: neck width, perimeter, and surface area. The body condition index (BCI) was calculated for each crocodile and then ranked on a scale of 1–5 using a min-max normalisation in Microsoft Excel®.

Assessing data from two farms whose crocodiles were in different nutritional states allowed the comparison of which morphometric parameters differed most significantly between slimmer and fatter Nile crocodiles over 1 m in TL. A decision tree analysis (adapted from the predictive model of de Kock *et al.* (2021)) was performed using R (version 4.1.2) to identify which parameters, aside from TL and BW, most accurately differentiated between the crocodiles at the two farms.

## 3.5. RESULTS

### 3.5.1. Deriving morphometric data

Seven UAV-based morphometric measures were captured for 288 farmed Nile crocodiles across two commercial crocodile farms in South Africa. The morphometrics measured were total length (TL), snout-hindlimb length (SHL), snout-neck length (SNL), neck width (NW), belly width (BW), surface area (SA), and perimeter. Figure 17 depicts various relationships between the UAV-based length morphometrics. The crocodiles in this study ranged from 1.05–4.79 m in TL, 0.53–2.48 m in SHL, 0.20–1.06 m in BW, 0.12–0.70 m in NW, 0.22–1.04 m in SNL, 2.21–10.23 m in perimeter, and from 0.13–

2.48 m<sup>2</sup> in SA. Table 7 summarizes the morphometric data collected for all crocodiles in the study. The following morphometric measures varied significantly ( $P < 0.05$ ) with farm of origin: SHL, BW, NW, SNL, and SA; as did BCI. TL did not vary significantly with farm, possibly because the crocodiles were selected for the study based on TL, ranging from  $> 1$  m up to breeder (full-grown) sized animals. All morphometric measures were strongly, positively correlated with one another (table 8).

**Table 7.** Descriptive statistics for the seven UAV-based morphometric measures ( $n = 288$ ).

Morphometric	Min	Max	Mean	SD	SE
TL (m)	1.1	4.8	2.8	0.7	0.0
SHL (m)	0.5	2.5	1.5	0.4	0.0
BW (m)	0.2	1.1	0.6	0.2	0.0
NW (m)	0.1	0.7	0.4	0.1	0.0
HL (m)	0.2	1.0	0.6	0.2	0.0
SA (m <sup>2</sup> )	0.1	2.5	0.9	0.5	0.3
Perimeter (m)	2.2	10.2	5.9	1.5	0.1

**Table 8.** Correlations (all highly significant,  $P < 0.001$ ) between the UAV-based morphometric measures.

	TL	SHL	BW	NW	SNL	SA	P
TL	1	0.983	0.994	0.923	0.953	0.952	0.998
SHL	-	1	0.976	0.902	0.954	0.928	0.985
BW	-	-	1	0.933	0.955	0.968	0.994
NW	-	-	-	1	0.930	0.955	0.924
SNL	-	-	-	-	1	0.944	0.954
SA	-	-	-	-	-	1	0.954
P	-	-	-	-	-	-	1

The relationships between TL, SNL, and SHL were assessed using a regression analysis. The resulting equations can be used to infer values that cannot be measured in the field from UAV imagery. The regression analyses between TL, SHL, and SNL were all significant ( $P < 0.05$ ) linear relationships and resulted in the following equations (rounded to two decimal places):

There was a strong correlation ( $R^2 = 0.97$ ) between the TL and SHL conforming to the equation:

$$TL = SHL (1.91) + 0.08 \quad \text{Equation 7}$$

There was a strong correlation ( $R^2 = 0.92$ ) between TL and SNL conforming to the equation:

$$TL = SNL (4.33) + 0.37 \quad \text{Equation 8}$$

There was a strong correlation ( $R^2 = 0.92$ ) between SNL and SHL conforming to the equation:

$$SHL = SNL (2.25) + 0.17 \quad \text{Equation 9}$$

Figures 17a and 18b show strong linear relationships between the length based morphometrics in this study, with  $R^2$  values of 0.92 and 0.97, respectively. The  $R^2$  values for farm A were greater than those of farm B for both morphometric comparisons. The equations describing the regressions between total length and snout-neck length were  $y = 4.51x + 0.17$  ( $R^2 = 0.97$ ) and  $y = 4.02x + 0.63$  ( $R^2 = 0.72$ ), for farms A and B respectively. The equations describing the regressions between total length and snout-hindlimb length were  $y = 1.95x + 0.05$  ( $R^2 = 0.99$ ) and  $y = 1.69x + 0.36$  ( $R^2 = 0.89$ ), for farms A and B respectively.

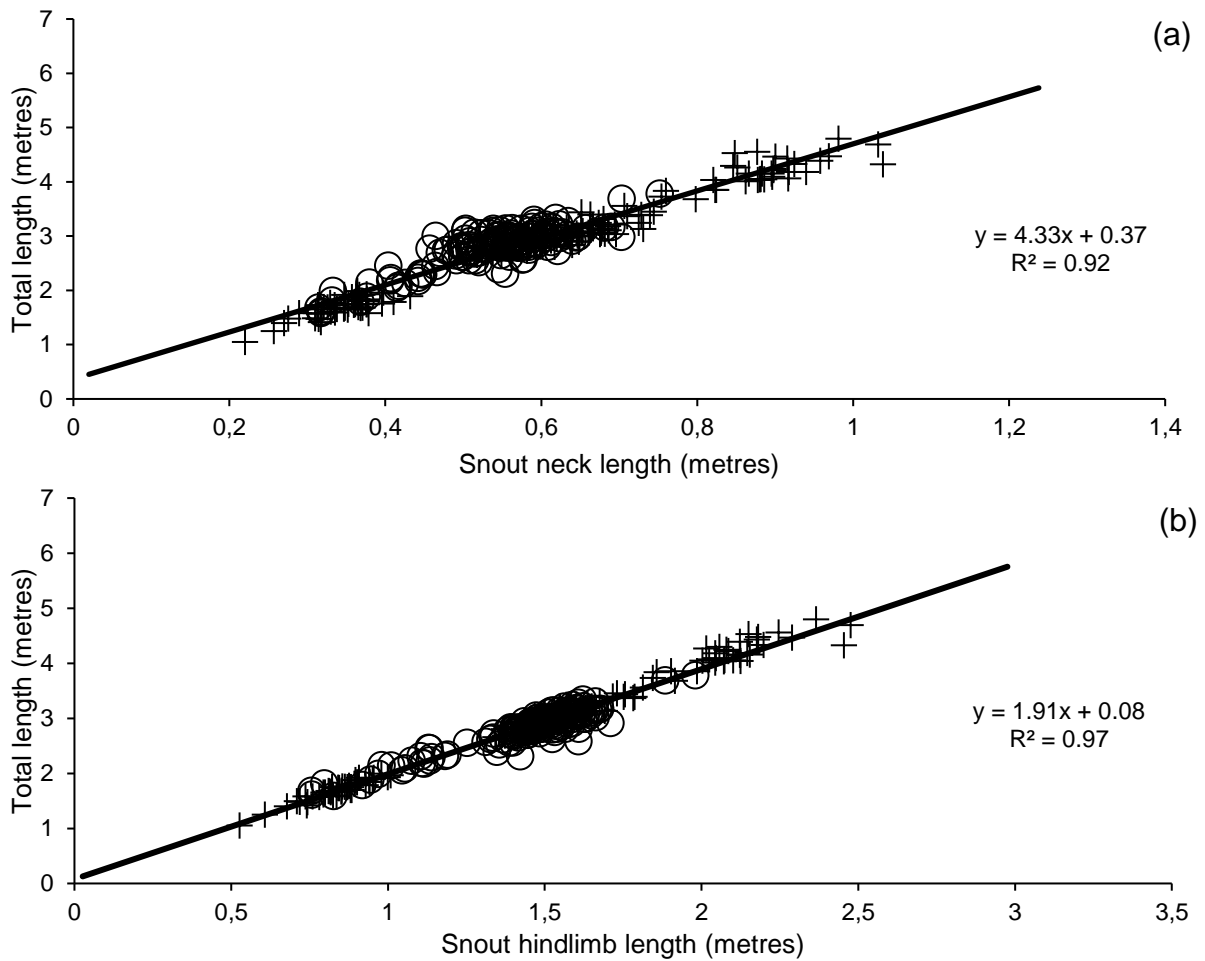


**Figure 17.** (a) Scatterplot depicting the relationship between total length and snout-neck length of 288 farmed Nile crocodiles, and (b) scatterplot depicting total length and snout-hindlimb length of 288 farmed Nile crocodiles. Graphs a and b differentiate the crocodiles farm of origin, crocodiles from farm A are represented with “+” and crocodiles from farm B with “O”.

### 3.5.2. Body Condition Scores based on UAV-derived morphometrics

The body condition index (BCI) calculation yielded an index range of 1.344–2.618 for both farms, where farm A’s BCIs ranged from 1.62–2.62 (rounded) with an average of 2.06 and farm B’s BCIs ranged from 1.34–2.40 (rounded) with an average of 1.90. A min-max normalization allowed the crocodiles to be ranked (BCS) from 1–5 based on their BCIs. Table 9 summarizes the outcome of this normalization and shows the range of body condition indices within each body condition score category.

Figure 18 presents a distribution of crocodiles within the five body condition score categories. Farm A, which was characterized by crocodiles with wider abdominal girths at the time of this assessment, had no crocodiles with BCS 1. Farm B, which was characterized by crocodiles with narrower abdominal girths at the time of this assessment, had no crocodiles with a BCS 5. Scores 1 and 2 are represented by images captured at a flight altitude of 60 m, and scores 3–5 are represented by images captured at a 40 m flight altitude.

**Table 9.** Body condition frequencies per BCS rating.

BCS	Number of crocodiles	Minimum BCI	Maximum BCI
1	4	1.344	1.465
2	60	1.532	1.821
3	160	1.827	2.136
4	60	2.140	2.451
5	4	2.511	2.618
Total	288	1.344	2.618

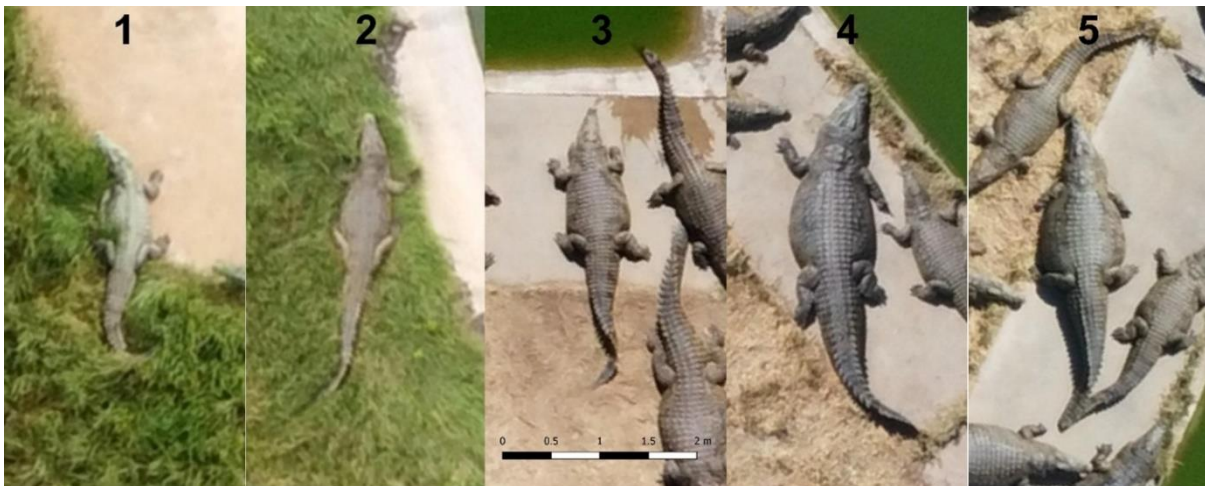


**Figure 18.** Nile crocodiles within each of the five different body condition scoring (BCS) categories. From left to right, a BCS from 1 to 5 as assessed and derived in the current study.

The decision tree in figure 19 depicts the UAV-derived morphometric measure boundaries (for the morphometrics other than total length and belly width) that determine which farm the 288 crocodiles measured belonged to. Neck width, followed by perimeter, surface area, and snout-hindlimb length were the four morphometrics that most effectively discriminated between the crocodiles' farm of origin.

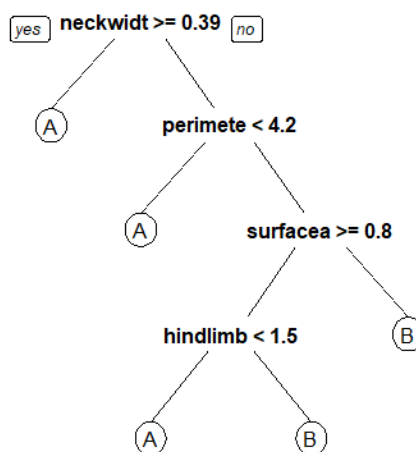


**Figure 19.** The decision tree identifying the morphometrics (other than TL and BW) that most decisively differentiated the crocodiles' farm of origin.

### 3.6. DISCUSSION

The current study assessed hundreds of farmed Nile crocodiles in a matter of days, at a relatively low cost. The crocodiles were counted, their morphometrics measured, and their health inferred through a body condition score developed with data generated from this work. The variation in body condition scores between the two farms lends credibility to the measures. This method allowed a fast-paced and repeatable examination of the sizes and conditions of two populations of captive crocodiles. This method has conservation value and could easily be applied to wild Nile crocodile populations.

When appropriate morphometric measures are used, UAVs enable accurate body condition analyses of crocodiles. The Nile crocodiles assessed in the present study represented a range of body condition states, covering a wide range of body conditions that may be encountered during wild crocodile population surveys. NW was not considered a viable metric for use in wild population surveys due to the difficulty of identifying the neck of crocodiles in lower resolution imagery (Myburgh, unpub. data). BW was considered a more suitable UAV-derived metric for estimating body condition, as it is easier to identify/measure and could be better suited for future applications of emerging technologies. Artificial intelligence, for example, requires distinguishable features for automated detection. Although SHL could be used for estimating body condition relationships, the use of TL was intentional because previous studies have used TL and its relation to other length-based morphometrics (SVL and HL traditionally, SHL and SNL in this study). Therefore, a UAV-based body condition score was calculated (equation 6) using TL and BW, which ranked the assessed crocodiles between 1 (comparatively thin) and 5 (comparatively fat). Applying this simple formula to UAV-derived imagery could offer an accurate, fast-paced, and non-invasive health and welfare monitoring tool for large wild or captive crocodile populations.

Relationships between various zoometric parameters for crocodylians have been investigated through traditional capture and measurement methods (Hutton<sup>1</sup>, 1987; Salem, 2011; Warner<sup>1</sup> *et al.*, 2016), but none have assessed UAV-derived morphometrics. Multiple equations for predicting UAV-based length morphometrics from one another were presented in the current study (equations 7–9), all with  $R^2$  values  $\geq 0.92$ . TL was more reliably estimated from SNL and SHL for farm A than from farm B, and it is postulated that variations in body condition status may have influenced the observed differences in R-squared values.

These equations can be useful in generating population-wide morphometric statistics, even when not all body parts of a Nile crocodile can be seen in UAV imagery. The strong positive and significant Pearson correlation coefficients between the length-based morphometric measures are likely indicative of allometric growth. Relating these morphometrics to body mass and manual morphometric measurements would add further precision to UAV-based morphometric data collections and body condition scoring in future studies.

Morphometrics measured in this study were only possible for crocodiles  $> 1$  m TL due to image distortion for smaller crocodiles (measurement landmarks not clearly visible), the tendency for smaller crocodiles to pile (especially in pens on commercial farms) and thereby prevent accurate measurements, and the skittish nature of small ( $< 1$  m TL) crocodiles impeding image quality. For farmed Nile crocodile populations specifically, the measurement of crocodiles  $< 1$  m in TL is still a potentially useful endeavour in terms of continuous morphometric and condition assessments if a viable method for surveying them can be developed.

Possible confounding factors for health predictions conducted through monitoring morphometrics (i.e., a body condition index/score) would be chronic diseases, toxicological problems, pathological changes, being gravid, and food availability. Pansteatitis for example, where crocodiles appear obese

due to the swelling of all fat depots (Lane *et al.*, 2013), would likely confound condition scoring within a population. To our knowledge, the effects of egg-bearing on crocodilian morphometric relationships have yet to be explored. Emaciation is suggestive of animals experiencing health or welfare issues; however, sightings of emaciated crocodiles are not uncommon in the wild (Swanepoel<sup>1</sup> *et al.*, 2000; Warner<sup>1,2</sup> *et al.*, 2016). The low BCS of 1 or 2 for farmed crocodiles may be a more natural state for wild crocodiles where feeding is infrequent, and health issues are not as controlled.

### 3.7. CONCLUSIONS

The potential uses of UAVs in wild and captive crocodile population monitoring are broad, from fast-paced counts to habitat monitoring and size estimations. Morphometric monitoring via UAVs is accessible, accurate, non-invasive, easily repeatable, and cost effective. The body condition scoring methods presented in this study could enable rapid assessments of population status for wild or captive crocodile populations. Given sufficient image clarity, neck width is not only a rapid measurement option but, according to outcomes of the decision tree analysis, is a potentially significant morphometric if comparing populations that vary in nutritional status or general well-being.

### 3.8. CRITICAL EVALUATION AND RECOMMENDATIONS

Future studies could consider assigning a cut-off value for “healthy” morphometrics per size class, which may differ for wild and farmed crocodiles, allowing the identification of discrepancies/differences between obese, emaciated, and gravid crocodiles. Considering pancreatitis specifically, this might allow particularly obese crocodiles to be identified as early warning signs of the disease. Future studies utilizing UAV-based morphometrics should also consider comparing UAV measures with true measures from captured crocodiles and including mass recordings to expand the UAV body condition methods capabilities and accuracy, as well as its comparison to traditionally measured body metrics.

## 4. Adaptive thermal responses of captive Nile crocodiles (*Crocodylus niloticus*) in South Africa

Viljoen, D. M., Webb, E. C., Myburgh, J. G., Truter, J. C., Lang, J. W., and Myburgh, A. (2023). Adaptive thermal responses of captive Nile crocodiles (*Crocodylus niloticus*) in South Africa. *Applied Animal Behaviour Science*, 106098. <https://doi.org/10.1016/j.applanim.2023.106098>

### 4.1. INTRODUCTION

Intensive communal pens in commercial crocodile farming are ubiquitous (Bothma & Van Rooyen, 2005), and there are a multitude of pen layouts within and across farms that facilitate husbandry practices, maintain production outputs, and optimize growth, survival, skin quality, and disease control (Bolton, 1989; Bothma & Van Rooyen, 2005; Verdade *et al.*, 2006). In addition to facilitating production, the artificial environment created by a pen determines animal welfare particularly with respect to thermal requirements. As ectotherms, crocodilians rely on environmental temperatures to maintain a “favourable” or “preferred” range of body temperatures ( $T_b$ ), which influences health, appetite, and metabolic rates (Lang<sup>1</sup>, 1987; Huchzermeyer, 2003; Bothma & Van Rooyen, 2005; Bassetti *et al.*, 2014). Crocodilians achieve and maintain a preferred  $T_b$  by selecting appropriate environmental temperatures, either seeking or avoiding heat by engaging in specific thermal behaviours (Lang<sup>2</sup>, 1987; Huchzermeyer, 2003; Downs *et al.*, 2008). Body temperatures differ among individuals and species, and are functions of nutritional or reproductive status, climatic conditions, social interactions, and ontogeny (Lang<sup>2</sup>, 1987; Seebacher & Grigg, 2001; Telemeco & Gangloff, 2021).

For intensive crocodilian farming, recommended ambient temperatures within pens range between 17 °C and 35 °C (Bolton, 1989; Bothma & van Rooyen, 2005; Bassetti *et al.*, 2014). Recommendations for optimal production and fitness tend toward the higher end of this range (Seebacher & Grigg, 2001; Huchzermeyer, 2002; Seebacher, 2005). Air temperature, humidity, solar radiation, windspeed and water temperature all play a role; this is incorporated into pen design features such as shading, water to land ratios, and floor materials where the crocodiles will spend much of their time basking (Lang<sup>2</sup>, 1987; Bolton, 1989; Huchzermeyer, 2003; Downs *et al.*, 2008; CFAZ, 2012). Strict temperature controls are essential for younger crocodiles in intensively managed environments, while breeder crocodiles in natural pens experience ambient temperatures dictated by the prevailing local climate (Bolton, 1989; Huchzermeyer, 2003; Bothma & van Rooyen, 2005; Downs *et al.*, 2008; CFAZ, 2012). Continuous ambient temperatures between 10 °C and 20 °C suppress feeding behaviours for multiple reptilian species, while consistent and unavoidable ambient temperatures exceeding 35 °C are considered lethal (Colbert *et al.*, 1946; Lang<sup>2</sup>, 1987; Bolton, 1989; Huchzermeyer, 2002). In addition to immediate environmental temperatures, optimal core  $T_b$ 's between 28 °C and 33 °C are recommended for crocodilians (Colbert *et al.*, 1946; Huchzermeyer, 2003; CFAZ, 2012). When optimizing pen climates, humidity levels of 60–90 % RH have been suggested in controlled farming environments (such as those for raising hatchlings). In contrast, natural pens, such as those for breeding groups, are subject to the local ambient humidity (Terpin *et al.*, 1979; Davis, 2001; Downs *et al.*, 2008).

Exceeding the acceptable ranges of farm temperatures and humidities can serve as significant stressors. Intensive crocodile farms have experienced hyperthermia-related mortalities in southern Africa, particularly during warmer months (Personal communication: Prof J.G. Myburgh, University of Pretoria). In South Africa, the NSPCA (National Society for the Prevention of Cruelty to Animals) issued warnings in respect of environmental temperatures for intensively farmed crocodiles. These warnings

emphasize the need for effective shade provision and maintaining water temperatures below air temperatures in summer, especially in shallow ponds that are not regularly replenished (Personal communication: Prof J.G. Myburgh).

In communal pens, how crocodiles behave affects production and survival. Often, a social hierarchy forms where dominant animals dictate feeding areas or restrict access to certain areas (Lang<sup>1</sup>, 1987; Morpurgo *et al.*, 1993; Brien<sup>1,2</sup> *et al.*, 2013). Agonistic behaviours ensue which can increase stress levels; poor management and increasing temperatures influence crocodile aggression (Pooley *et al.*, 2019). Social interactions that prevent subordinate individuals from maintaining optimal  $T_b$ 's likely influence growth and size (Grigg *et al.*, 1998; Seebacher & Grigg, 2001; Verdade *et al.*, 2006; Brien *et al.*, 2013<sup>1,3</sup>; Bassetti *et al.*, 2014). Management of density, feeding, size classes, and available thermal gradients is therefore important when farming crocodilians (Lang<sup>1</sup>, 1987; Morpurgo *et al.*, 1993; Manolis & Webb, 2016).

Crocodilian thermoregulatory behaviours include basking, gaping, shuttling, thermal posturing, and occasional burrowing during temperature extremes (Lang<sup>1</sup>, 1987; Seebacher & Grigg, 2001; Manolis & Webb, 2016; Price *et al.*, 2022). Crocodilians use diurnal basking to elevate  $T_b$ 's with minimal effort/energy costs, posturing and gaping to influence the rates of change in  $T_b$ 's, and shuttling and burrowing to select optimal temperatures along the thermal gradients available within their immediate environments (Spotila *et al.*, 1977; Terpin *et al.*, 1979; Lang<sup>1</sup>, 1987; Seebacher, 1999; Seebacher, 2005; Downs *et al.*, 2008). Behavioural assessments should encompass as many aspects of both social and maintenance behaviours as possible (Brien<sup>1,2,3</sup> *et al.*, 2013), and should be considerate of the animals so as not to alter behaviours. Monitoring temperatures in larger ectotherms is complicated by their size and movement between land and water (Lang<sup>2</sup>, 1987; Downs *et al.*, 2008; Bassetti *et al.*, 2014). The monitoring of thermal environments and behaviour of crocodiles have therefore been limited, although recent advances in drone technology enable novel and non-invasive methodological approaches.

This study presents a method for the derivation of thermal landscape maps using the DJI Mavic 2 Enterprise Dual drone, combined with open-source photogrammetry and GIS software (ODM version 1.9.3 build 30, and QGIS version 3.16-Hannover) (QGIS Development Team, 2021). The derived method, in conjunction with local weather station data and an Internet of Things (IoT) system of loggers, was used to monitor the thermal environment, temperature selections, and behaviour of breeder Nile crocodiles in a current commercial farm setting in South Africa.

#### 4.2. AIMS AND HYPOTHESES

This study aimed to assess the ambient temperatures and those selected by captive adult Nile crocodiles on a commercial farm in South Africa. Non-invasive data capture techniques were developed to ensure the crocodiles natural behaviours were not disrupted or altered. It was hypothesized that the thermoregulatory behaviours of farmed Nile crocodiles would vary significantly with season and that these variations could be effectively monitored using cost-effective equipment within a short time frame. This monitoring would enable the assessment of the utilization of different pen materials and based on their thermal properties, the subsequent development of recommendations to minimize hyperthermia risks under the conditions of a warming climate.

#### 4.3. MATERIALS AND METHODS

##### 4.3.1. Animals, husbandry, and pen layout

A large breeder pen (5020 m<sup>2</sup>) on a commercial crocodile farm in South Africa was monitored for this study. The pen housed 233 crocodiles ranging in snout-hindlimb lengths from 1.2–2.4 m, with an approximate sex ratio of one male to four or five females. The crocodiles studied had been housed in

the same enclosure since the early to mid-1990s, experiencing consistent rearing in terms of diet, housing, and general animal husbandry prior to this study. The standard pen setup was not altered further than the placement of LoRaWAN (Low-power wide-area network) loggers. Logger placement occurred over a one-day period, a month before any flights were conducted, with the assistance of farm personnel. The farms regular feeding and cleaning schedules remained unchanged for the study. Diets were also not modified so as not to stress the crocodiles or alter their regular behaviours. To maintain the comfort and socialization activities of the crocodiles, the personnel attending the pen were kept consistent. The pen contained a section of walkway from a neighbouring tourist centre. All drone flights were conducted on weekdays to ensure no tourists were present during the flights. The pen contained, and was divided up by, four main areas or material types: water, concrete, grass/sand, and nests. There were three water bodies within the pen, each surrounded by areas of concrete. The water bodies had a maximum depth of 2 m, and water levels were maintained year-round. There were also several areas that were a mix of sand and grassy patches, the ratio of these two material types varied with season and so for ease of analysis this area type will be referred to as grass/sand in the current study. Sections of the pen were cordoned using low brick walls and were filled with river sand. Crocodiles typically use these areas for nesting, and these will henceforth be referred to as “nests” to avoid confusion with sandy areas in the pen that are not used for nesting. Within the pen, shading was provided by scattered trees, a shade net, and pen perimeter walls. The extent of shading varied depending on the time of day.

#### 4.3.2. Aerial image acquisition

Uncrewed aerial vehicle (UAV) data was captured over four days, two summer days (26 January 2022 and 3 February 2022) and two winter days (12 August 2022 and 15 August 2022). Daily climatic condition was also noted, 26 January 2022 and 15 August 2022 were cool days (relatively) within their seasons, and 3 February 2022 and 12 August 2022 were warm days (relatively) within their seasons. Flights began in the morning and were conducted hourly, with a minimum of eight flights per day. The data were divided into morning and afternoon timeslots, based on the flights conducted, as follows: early morning between 07:30 and 09:59, late morning between 10:00 and 11:59, early afternoon between 12:00 and 13:59, and late afternoon between 14:00 and 15:59. For each flight ( $n = 33$ ), a DJI Mavic 2 Enterprise Dual drone was flown on the same, predetermined, automated flight path using a third-party flight software package ([Dronelink](#)) at an altitude of 35 m with 85% side and frontal image overlap. The UAV covered an area of approximately 15000 m<sup>2</sup> in nine minutes. Between flights, all equipment was kept in an air-conditioned room (22°C) to minimize drift from overheating of the uncooled thermal sensor, ensuring the starting temperature of the UAV was constant for each flight.

Six ground control points (GCPs) were distributed along the perimeter of the pen. The GCPs (figure 20) used in this study were inexpensive square polystyrene platforms (60 cm x 60 cm) covered with aluminium foil and black paint as per Messina and Modica (2020). Aluminium foil has an emissivity of 0.03, creating sufficient contrast with black paint and adjacent pen materials, making it easily recognizable in thermal images (A.S.H.R.A.E, 2009; Messina & Modica, 2020). The GCPs were systematically positioned in predetermined positions around the perimeter of the pen for each flight, ensuring precise georeferencing of the resulting orthophotos based on established geospatial calibration methodologies.

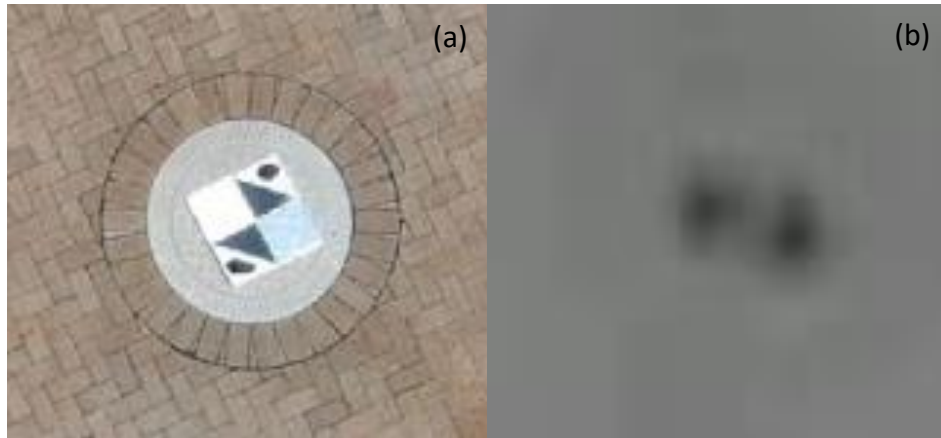


**Figure 20.** Ground control point as captured in (a) red, green, and blue (RGB) and (b) greyscale by the DJI Mavic 2 Enterprise Dual. The RGB (a 12-megapixel CMOS sensor) and thermal (uncooled VOx microbolometer thermal sensor) sensors vary in their resolution, hence the image clarity variation.

#### 4.3.3. Thermal mapping settings and workflow

The DJI Mavic 2 Enterprise Dual drone does not store the absolute temperature associated with the long wave infrared measurements captured by its thermal sensor. The DJI Pilot 4 interface was used to specify a greyscale colour palette, providing a linear conversion of thermal data (thermal range set between 5 °C and 65 °C) to red, green, and blue (RGB) variables (between 0 and 255; where, using the greyscale colour palette yielded equal colour values within all three colour bands) which were stored in the jpeg files associated with the thermal sensor. During flight, but not within the perspective of the UAV, a handheld thermometer (ASSTech Process Electronics and Instrumentation handheld infrared thermometer, *ST653*) was used to measure the temperature of homogenous areas representing various materials outside the perimeter of the pen (and not within view of the crocodiles). The thermometers emissivity was set to 0.94 as per the instruction manual for the materials under study i.e., concrete, brick, water, and sand. The distance from the thermometer to the materials measured was maintained at one metre for all measures. Temperatures recorded by the thermometer were then used to elucidate the temperatures associated with the colour band value outputs of the resulting thermal orthophotos (equation 10).

#### 4.3.4. Thermal image processing settings in ODM and QGIS

Processing parameter testing for the derivation of orthophotos from thermal images in ODM resulted in the selection of settings which differ from the standard “high resolution” option in the following ways: orthophoto resolution was set to the ground sampling distance (GSD) of the original images (11.16 cm/pixel in this case) and the lens selection was set to fisheye. RGB images were processed using the “default” settings in ODM with orthophoto resolution set to the GSD associated with the RGB images (1.42 cm/pixel). An Emlid reach RS+ differential GPS was used to mark the position of each GCP, ensuring all images aligned after photogrammetric processing. Where misalignment occurred, georeferencing was performed in QGIS using a linear conversion through a thin plate spline projection to resize and georeference each image into the correct position. Once the thermal images were aligned, the thermal orthophoto data was preserved as RGB image data ranging from 0 to 255 across the three colour bands. The steps to convert RGB thermal orthophotos into relative temperature maps were as follows:

1. Using the point creation tool in QGIS, a marker was placed at each location where temperature measurements were recorded with the handheld thermometer during flights.
2. Using the sample raster tool in the processing toolbox, the RGB data was derived from the thermal layer at each of the points across all thermal orthophotos.

3. The sampled points data were then exported to a spreadsheet, where the three RGB band values were averaged into a separate column. The measured temperatures taken with the handheld thermometer during flights were added next to the averaged RGB values.
4. A linear relationship was fitted to these two variables and an equation describing the relationship was derived.
5. A new relative temperature map of the area under survey was created for each flight using the raster calculator in QGIS, where the RGB values of the thermal orthophotos were set as “x” in the derived equation.

#### 4.3.5. The thermal environment

A LoRaWAN system recorded hourly ambient temperature, various material temperatures, and humidity throughout the pen. The system consisted of a router (LtAPHD LR8 3xSIM2xmPCIe Wi-Fi LTE Router), antenna (a LoRa 6.5dBi Antenna kit with 1m SMAF), humidity and temperature sensor (SenseCAP LoRaWAN Wireless Air Temperature and Humidity Sensor, placed in a permanently shaded area), and small temperature sensors (LHT65 LoRaWAN Temperature and Humidity Sensor). The router and antenna were placed close to the pen, in a room with a reliable Wi-Fi connection. The SenseCap sensor recorded hourly ambient temperatures and humidity from a shaded position near the pen. Three LHT65 sensors recorded hourly concrete temperatures in sunny and shaded areas of the pen, and 30 cm deep water temperatures.

Two LHT65 sensors were encased in concrete pyramids, these were mixed according to the standard concrete recipe/design detailed in chapter 2’s MD 2.5. The loggers were embedded centrally at the apex of the pyramid moulds (figure A14), and the pyramids were allowed to fully cure before deployment. One such pyramid was placed in a sunny area of the pen, with no cover, and another was placed in a shaded area under a tree. LHT65 sensors are equipped with a 1-metre-long extension cable that terminates in a waterproof probe, which transmits independent temperature data back to the sensor. The external cable of the third LHT65 logger was fed through the hollow centre of a steel pole, secured in a large concrete base (figure A15). This setup was designed and constructed by Mr Derek Mostert, a concrete specialist at the University of Pretoria. The heavy concrete base (150 kg) ensured the logger could not be easily moved around by the crocodiles, and the height of the pole ensured the logger remained safe from crocodile curiosity. An electronics-box was secured atop the pole and housed the LHT65 logger, and small holes along the length of the pole ensured water could flow through the setup. This allowed the logger itself to remain 2 m above water level, within range of the transceiver, whilst the probe was submerged 30 cm below the water surface. To reach the desired measurement location, the LHT65’s cable was extended by splicing an additional two metres of compatible cable. The extension was soldered and insulated to ensure durability. Every spliced joint was encased and sealed with various diameters of glue-lined heat shrink tubing (RS Components, 481-1775 & 481-1804 & 481-1810), providing a robust and waterproof connection (figure A16). A Metabo (H16-500) heat gun was used to seal the heat shrink layers, on the lowest setting. The completed extension was fully submerged in a bucket of water for a week prior to deployment to confirm its water-proofing capabilities.

These crocodile-proofing methods were designed and built with the assistance of members of the Civil Engineering department at the University of Pretoria. Accuracy configurations, data collection, and data visualization for the LoRaWAN loggers were obtained via a dashboard provided by Ubidots (<https://ubidots.com/>). South African Weather Service (SAWS) data (ambient temperature, relative humidity, and windspeed) and Weather Underground (<https://www.wunderground.com/>) data (radiation), from local weather stations within 12 km of the farm, were incorporated into the study to

supplement that of the LoRaWAN system. The radiation variable represents solar irradiance, i.e., the total radiant energy received per unit area of the Earth's surface.

#### 4.3.6. Extracting crocodile behaviour and environmental temperature selection data

Data were extracted from the resulting processed imagery using point and polygon layers in QGIS (version 3.16 Hannover). Point layers were used to attain temperature measurements for the back of each crocodile and the position of the crocodile. This was accomplished by placing a point layer marker centrally on the back of each crocodile in view and another point layer marker next to the crocodile, on the material the crocodile was selecting (figure A17, A18). If a crocodile was positioned over two material types, the point was placed on the primary material type the crocodile was occupying. Back temperatures and the corresponding selected positional temperatures were compared across season, allowing the assessment of the thermal options selected by these captive crocodiles. A regression analysis was also performed to deduce the accuracy with which these temperatures could be inferred from one another. A polygon layer was used to distinguish areas of the pen based on material type. Each material was outlined with the polygon layer tool and numbered; perimeter and area information were also extracted with this layer type. Crocodile material (water, concrete, nests, or grass/sand) selections and use of the various pen areas were assessed per time of day and season to deduce thermoregulatory behaviours.

Heat avoidance and heat seeking behaviours were intuited from the crocodile's back temperatures relative to those of the materials they were selecting. When the temperature of the crocodile's back was lower than that of the selected material, this was designated as "heat seeking" behaviour. Conversely, if the temperature of the crocodile's back was higher than that of the material the crocodile was selecting, this was designated as "heat avoidance" behaviour. In cases where the two corresponding temperatures were equal, no thermal behaviour was inferred. It was assumed that crocodile behaviours would be primarily driven by temperature, to avoid confounding the findings, the assessments occurred externally to the breeding season and to feeding/cleaning days. It is important to note that crocodile back temperature was used as an approximate indicator of the body temperature of the crocodile; it is not equivalent to the core temperature or deep body temperature of the crocodiles under consideration. Rather, a crocodile's back temperatures provided a thermal value for direct comparison with the surface temperature of the substrate upon which it was positioned.

## 4.4. DATA ANALYSIS

The data for this study were analysed in R (2022.12.0 Build 353) and IBM SPSS Statistics (version 28). A multivariate analysis of variance, two tailed partial correlations, Chi square, and regression analyses were performed. Bonferroni corrections were applied to post hoc pairwise comparisons. Differences between variable means were analysed for the determination of significant differences at  $P < 0.05$  and highly significant differences at  $P < 0.001$ .

## 4.5. RESULTS

### 4.5.1. Thermal map conversions

The relationship between temperature measurements taken with the handheld thermometer ( $n = 330$ ) and colour information from the RGB bands ( $n = 330$ ) of the processed thermal orthophotos could be described through equation 10:

$$y = 0.3593x + 5.16 \quad (R^2 = 0.9454; P < 0.001), \quad \text{Equation 10}$$

Where  $y$  = temperature of the selected pixel, and  $x$  = average extracted value of the three RGB bands with an average absolute error of  $2.06 \pm 1.32$  °C and a root mean squared error of 2.6 °C.

#### 4.5.2. The thermal environment

Hourly ambient temperatures and relative humidity from the closest national weather station (SAWS) are depicted in figure 21. Ambient temperatures and relative humidity data during the flights ranged from 10.6–35.3 °C and 18.6–61.7 % RH, respectively. Ambient temperature varied significantly with season ( $P < 0.001$ ,  $F = 19371$ ,  $df = 1$ ) and had significant effects on crocodile back temperatures ( $r = 0.28$ ,  $P < 0.001$ ) and positional temperatures ( $r = 0.23$ ,  $P < 0.001$ ). Relative humidity varied significantly with season ( $P < 0.001$ ,  $F = 12771$ ,  $df = 1$ ) and had significant effects on crocodile back temperatures ( $r = -0.38$ ,  $P < 0.05$ ) and positional temperatures ( $r = -0.31$ ,  $P < 0.05$ ).

Windspeed (SAWS) ranged from 0.0 to 3.6 metres/second (m/s) throughout the flight periods, with a mean of 0.8 m/s (1.2 m/s in summer, and 0.4 m/s in winter). Windspeed varied significantly with season ( $P < 0.001$ ,  $F = 906.6$ ,  $df = 1$ ) and had a significant effect on crocodile back temperatures ( $r = 0.27$ ,  $P < 0.001$ ) and positional temperatures ( $r = 0.21$ ,  $P < 0.001$ ). Radiation (<https://www.wunderground.com/>) ranged from 65.0 to 952.3 watts/metres squared ( $W/m^2$ ) throughout the flight periods, with a mean of 489.3  $W/m^2$  (487.1  $W/m^2$  in summer, and 490.9  $W/m^2$  in winter). Although the radiation did not vary significantly between summer and winter seasons ( $P = 0.42$ ,  $F = 0.66$ ,  $df = 1$ ), it did have a significant influence on crocodile back temperatures ( $r = 0.22$ ,  $P < 0.001$ ) and positional temperatures ( $r = 0.18$ ,  $P < 0.001$ ).

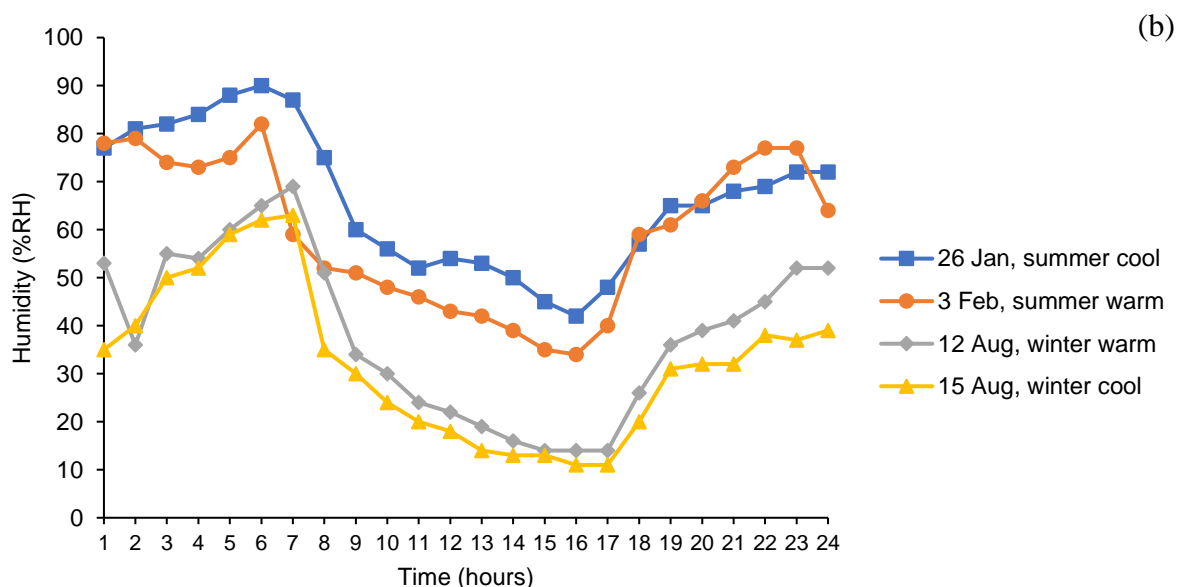
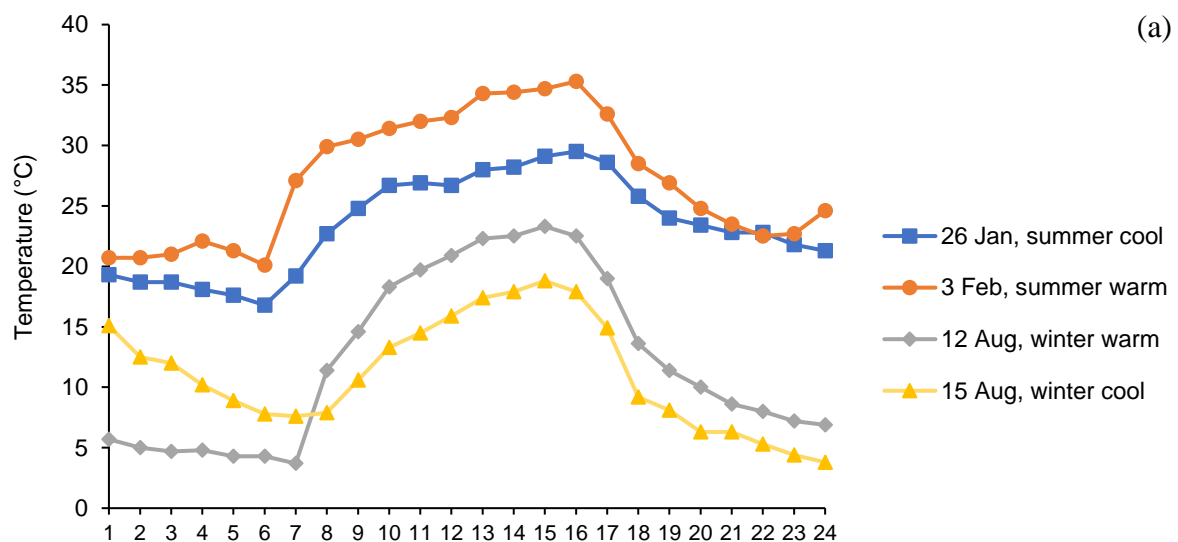


**Figure 21.** Hourly ambient temperature (a) and relative humidity (b) for the four days included in the assessment.

Water temperatures varied significantly between summer and winter seasons ( $P < 0.001$ ,  $F = 4377$ ,  $df = 1$ ) and had a significant effect on crocodile back temperatures ( $r = 0.36$ ,  $P < 0.001$ ) and positional temperatures ( $r = 0.28$ ,  $P < 0.001$ ). Sunny concrete temperatures varied significantly between summer and winter seasons ( $P < 0.001$ ,  $F = 4106$ ,  $df = 1$ ) and had a significant effect on crocodile back temperatures ( $r = 0.35$ ,  $P < 0.001$ ) and positional temperatures ( $r = 0.28$ ,  $P < 0.001$ ). Shaded concrete temperatures varied significantly between summer and winter seasons ( $P < 0.001$ ,  $F = 6556$ ,  $df = 1$ ) and had a significant effect on crocodile back temperatures ( $r = 0.22$ ,  $P < 0.001$ ) and positional temperatures ( $r = 0.16$ ,  $P < 0.001$ ). Figure 22 depicts the water and concrete (sunny and shaded) temperatures recorded by the LoRaWAN loggers, within the timespan of the flights. Daily climatic condition, between seasons and within each season, significantly affected water and concrete temperatures ( $P < 0.001$ ).

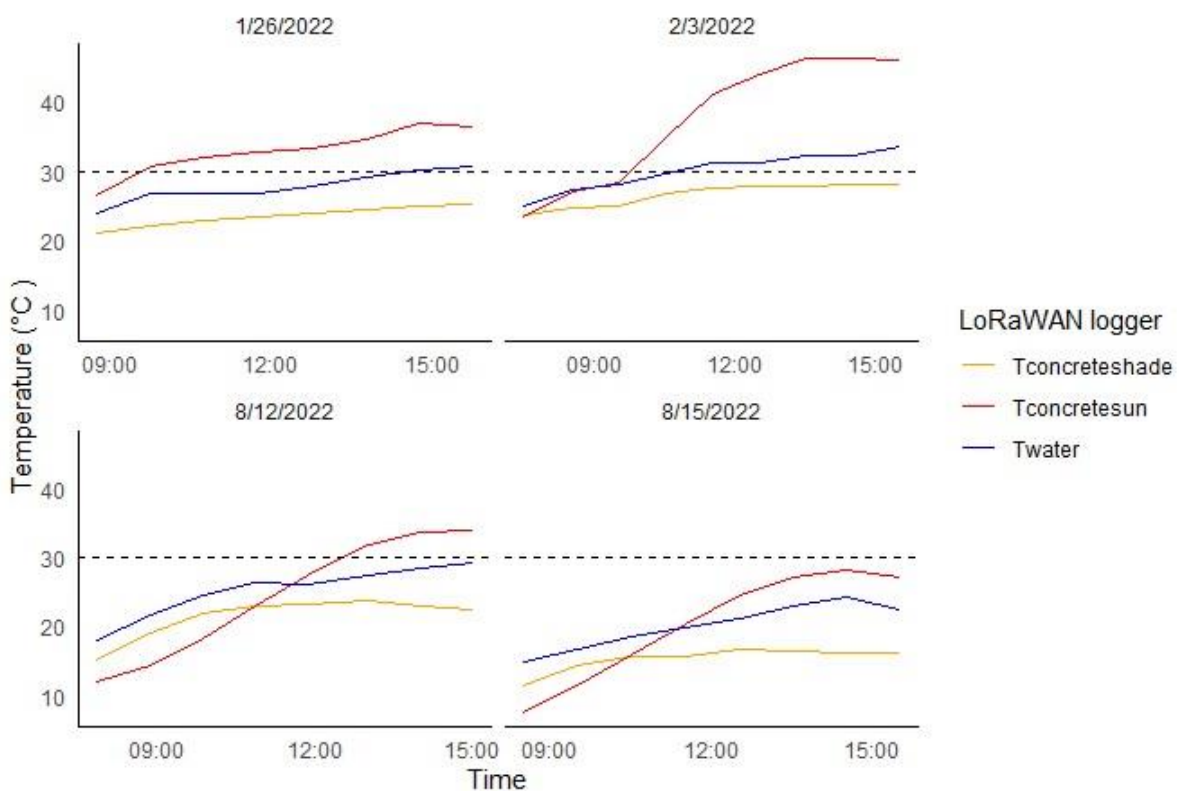


**Figure 22.** LoRaWAN water (“Twater”) and concrete (shaded represented as “Tconcreteshade” and sunny represented as “Tconcretesun”) temperatures within the timespan of the flights. All plots contain a dashed line at 30 °C for reference.

#### 4.5.3. Crocodile thermal behaviours and pen/material utilizations

The proportional layout of the pen calculated from UAV imagery was as follows: water bodies 22.5%, nests 19.1%, concrete 26.2%, and grass/sand 32.2%. The number of crocodiles visible from the UAV imagery during each flight varied from 111 to 233. An average of 151 crocodiles could be viewed in the imagery captured during the summer flights, compared to an average of 214 crocodiles captured during winter flights. Both time of day and season were significant ( $P < 0.001$ ,  $\chi^2 = 2607.5$ ,  $df = 96$ ) in determining the number of crocodiles counted, with the greatest number of crocodiles counted during the early morning winter flights and the lowest during late afternoon summer flights. The proportion of crocodiles located on the various materials during each set of flights are plotted in figure 23. Daily

climatic condition and season both had a significant effect on the proportional use of the material types within the pen ( $P < 0.001$ ,  $\chi^2 = 2017$ ,  $df = 9$ ).

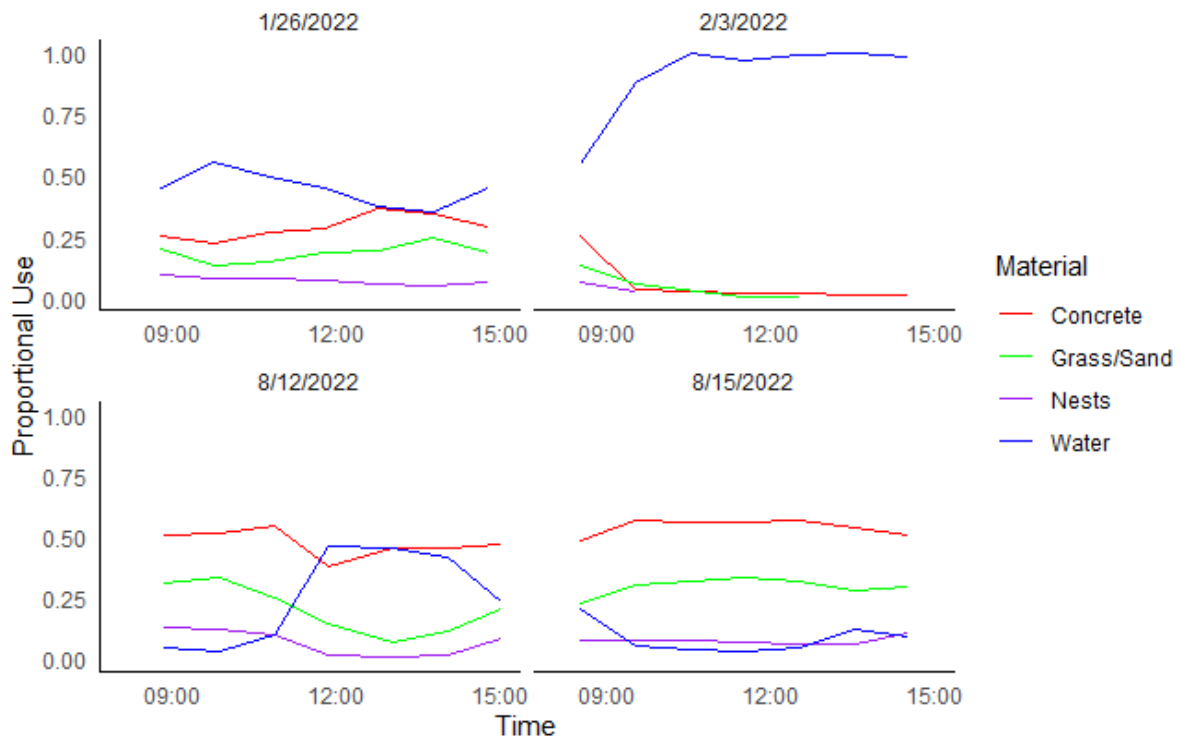


**Figure 23.** Hourly proportional material use within the pen for all flights.

To assess thermal behaviour, the crocodile back temperatures and corresponding positional temperatures were compared, and two behaviours were inferred. The first was “heat seeking” (i.e., attempting to warm up), and the second was “heat avoidance” (i.e., attempting to cool down). A generalized linear model analysis revealed these thermal behaviours were significantly affected by ambient temperature, relative humidity, water temperature, windspeed, radiation, and sunlit-concrete temperatures (all  $P < 0.001$  except radiation which had  $P = 0.003$ ). Time of day, season, and daily climatic conditions all significantly ( $P < 0.05$ ) affected thermal behaviours expressed. The proportions of the behaviours expressed in winter varied significantly with time of day ( $P < 0.001$ ,  $\chi^2 = 102.3$ ,  $df = 3$ ), specifically between early morning and all other times of the day. In summer, the proportions of the behaviours expressed varied significantly ( $P < 0.001$ ,  $\chi^2 = 22$ ,  $df = 3$ ) between early morning and early afternoon and late afternoon, with early afternoon behaviours also varying from late morning behaviours.

Crocodile back temperatures and positional temperatures varied significantly with thermal behaviours ( $P < 0.001$ ,  $F = 241.7$ ,  $df = 1$ ;  $P < 0.001$ ,  $F = 5762.8$ ,  $df = 1$ , respectively). Incorporating season into these models showed that it too exhibited a significant effect on crocodile back temperatures ( $P < 0.001$ ,  $F = 133.7$ ,  $df = 1$ ) and positional temperatures ( $P < 0.001$ ,  $F = 176.2$ ,  $df = 1$ ). All pairwise comparisons of crocodile back temperature, across behaviour within each season, as well as across seasons within each behaviour, differed significantly (all  $P < 0.001$ ). All pairwise comparisons of positional temperature across behaviour within each season, as well as across seasons within each behaviour, also differed significantly (all  $P < 0.001$ ).

The thermal behaviours exhibited varied significantly ( $P < 0.001$ ,  $\chi^2 = 1190$ ,  $df = 3$ ) between the materials selected by the crocodiles, this held true for both summer ( $P < 0.001$ ,  $\chi^2 = 719.5$ ,  $df = 3$ ) and winter ( $P < 0.001$ ,  $\chi^2 = 1084.3$ ,  $df = 3$ ) seasons. Figure 24 shows the proportional behaviours exhibited

per material type for summer and winter seasons. The selected materials, in order of most to least frequented, for cooling behaviours in the summer were water > nests > grass/sand > concrete. The selected materials, in order of most to least frequented, for heating behaviours in summer were the opposite of the cooling materials order for that season. Winter material selections, in order of most to least frequented, for cooling behaviours were water > concrete > nests > grass/sand. The selected materials, in order of most to least frequented, for heating behaviours in winter were again reversed for that season.

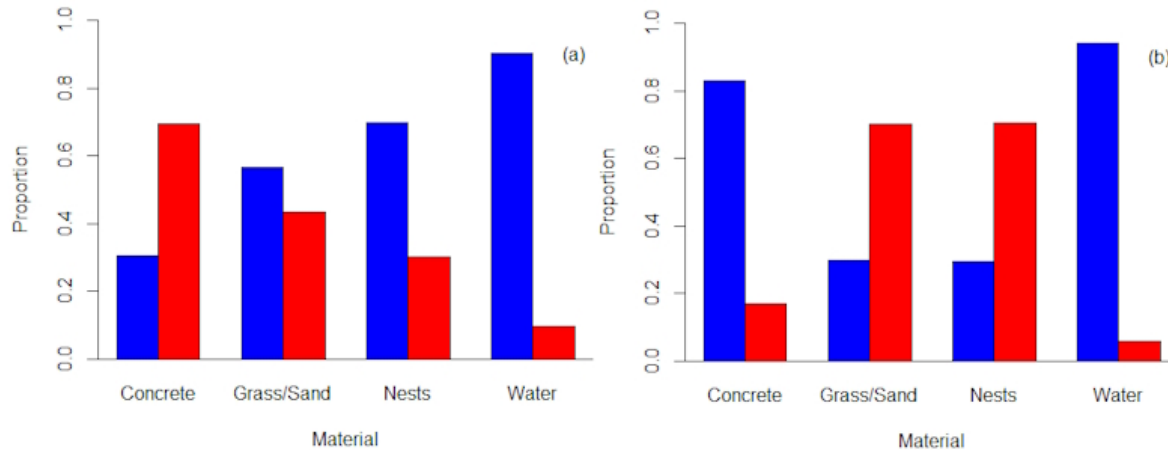


**Figure 24.** The proportions of heat avoidance (blue) and heat seeking (red) behaviours per material type in summer (a) and winter (b) seasons.

Where intuited behaviours were non-conclusive (i.e., constituting neither heating nor cooling activities) the proportions of this “neutral” temperature state were spread over the pen materials in the following selections: 82% water bodies, 10% concrete, 6% grass/sand areas, and 2% nest areas. Only 3.4% of all the crocodiles measured for this study fell into this “neutral” temperature category.

#### 4.5.4. Crocodile environmental temperature selections

Crocodile back surface temperatures over all flights and seasons ranged from 10.2–49.6 °C, with a mean of 30.4 °C. The positional temperatures selected by the crocodiles over all flights ranged from 10.6–66.6 °C, with a mean of 28.7 °C. Crocodile temperatures in winter ranged from 10.2–49.6 °C ( $\bar{x}$  = 29.9 °C), whilst in summer crocodile temperatures ranged from 20.6–47.0 °C ( $\bar{x}$  = 31.1 °C). Positional temperature selections ranged from 20.6–66.6 °C ( $\bar{x}$  = 29.3 °C) in summer and from 10.5–55.9 °C ( $\bar{x}$  = 28.2 °C) in winter. Crocodile back and positional temperatures varied significantly with daily climatic condition ( $P < 0.001$ ,  $F = 88.7$ ,  $df = 1$ ;  $P < 0.001$ ,  $F = 66.6$ ,  $df = 1$ , respectively). Mean hourly crocodile back temperatures and corresponding positional temperatures are plotted per season and daily climatic condition in figure 25.

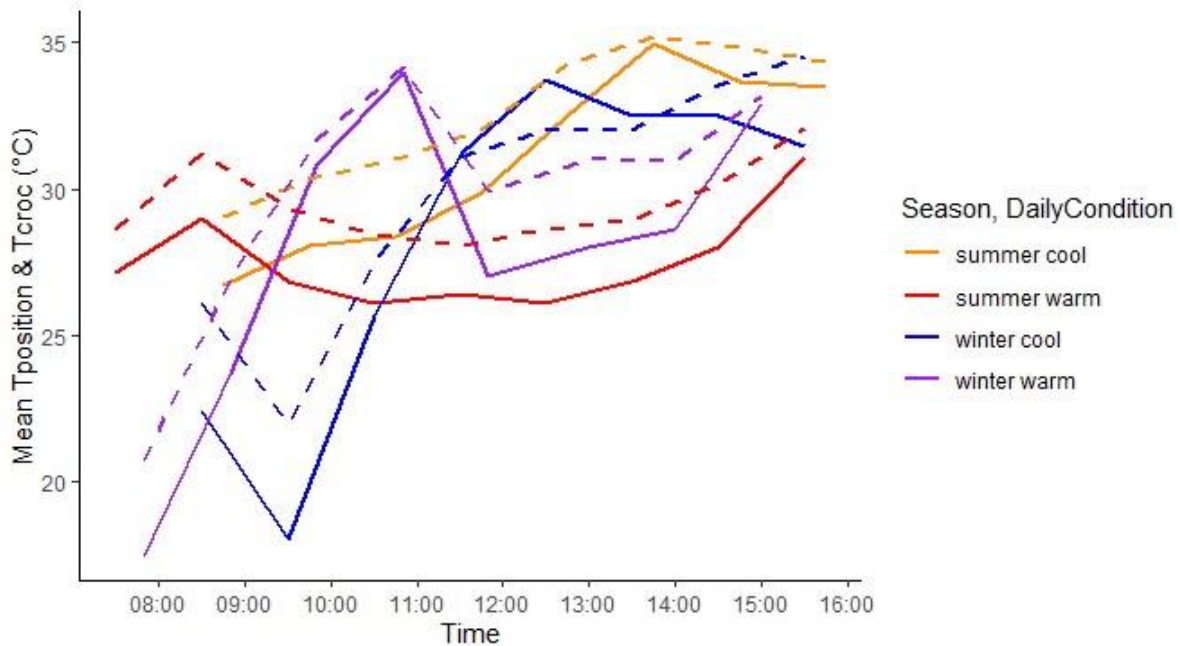


**Figure 25.** Mean hourly crocodile back temperatures (“Tcroc”, represented by dashed lines) and positional temperatures (“Tposition”, represented by solid lines) are plotted against time (corresponding to all flights on each date). Both season and daily climatic condition are accounted for in the graph’s colouration.

**Table 10.** Descriptive statistics (°C) of positional temperatures (first half of the table) and crocodile back temperatures (second half of the table) per material type and season.

Material	Summer				Winter			
	Min	Max	Mean	SD	Min	Max	Mean	SD
Concrete	23.1	57.0	36.9	5.8	10.5	49.1	25.9	7.0
Grass/sand	20.7	53.0	32.9	7.2	13.4	55.9	35.3	9.1
Nests	20.6	66.6	31.3	9.7	13.5	54.1	35.6	10.3
Water	21.1	33.5	26.1	1.9	10.5	27.4	19.1	2.8
Concrete	23.1	47.0	34.4	3.6	11.3	43.6	30.1	5.3
Grass/sand	22.8	43.6	33.7	3.9	15.6	49.6	31.5	5.4
Nests	20.6	43.4	33.7	5.3	13.9	45.5	31.0	6.6
Water	22.2	40.7	29.4	3.7	10.2	37.9	25.6	6.0

Positional temperatures selected by the crocodiles in this study are tabulated (table 10) for seasons and material types available within the pen. These temperatures were all derived from UAV imagery, and the water temperatures reflect only the surface-water temperatures. Positional temperatures were significantly affected by material selection ( $P < 0.001$ ,  $F = 767.4$ ,  $df = 3$ ) and season ( $P < 0.001$ ,  $F = 806.1$ ,  $df = 1$ ). In summer, positional temperature selections varied significantly between all material types (all  $P < 0.001$ , except nests and grass/sand where  $P = 0.004$ ). In winter, this variation remained significant (all  $P < 0.001$ ) except between grass/sand and nests ( $P = 0.86$ ).

Crocodile back temperatures in this study are tabulated (table 10) for the seasons and material types available within the pen. Crocodile back temperatures were significantly affected by material selection ( $P < 0.001$ ,  $F = 176.2$ ,  $df = 3$ ) and season ( $P < 0.001$ ,  $F = 582.1$ ,  $df = 1$ ). In summer, back temperatures of crocodiles in the water varied significantly from back temperatures of crocodiles occupying all other material types (all  $P < 0.001$ ). There was no significant variation between back temperatures of

crocodiles occupying concrete, nests, or grass/sand areas in this season. In winter, the back temperatures of crocodiles occupying water bodies varied significantly from those occupying other materials (all  $P < 0.001$ ); however, there was also a significant difference in back temperatures of crocodiles occupying concrete and grass/sand areas ( $P < 0.05$ ). Back temperatures of crocodiles occupying nests in winter did not vary significantly from those of crocodiles occupying concrete or grass/sand areas of the pen ( $P > 0.05$ ).

A curve estimation analysis in SPSS confirmed that the relationship between crocodile back temperatures and positional temperatures was best modelled by an S-curve, the resulting equation is presented in equation 11. Equation 12 describes the relationship when exclusively summer data was assessed, and equation 13 when exclusively winter data was assessed.

$$T_{\text{Croc}} = e^{\left( \frac{3.861 + (-12.223)}{T_{\text{position}}} \right)}, (R^2 = 0.54; P < 0.001) \quad \text{Equation 11}$$

$$T_{\text{Croc}} = e^{\left( \frac{3.982 + (-15.652)}{T_{\text{position}}} \right)}, (R^2 = 0.44; P < 0.001) \quad \text{Equation 12}$$

$$T_{\text{Croc}} = e^{\left( \frac{3.842 + (-11.745)}{T_{\text{position}}} \right)}, (R^2 = 0.57; P < 0.001) \quad \text{Equation 13}$$

Figure 26 depicts the relationship between crocodile back temperatures and the corresponding positional temperatures that the crocodiles were selecting for both summer and winter seasons. Correlation coefficients of  $r = 0.64$  ( $P < 0.05$ ) in summer and  $r = 0.70$  ( $P < 0.05$ ) in winter indicate a strong positive relationship between the two variables for both seasons.

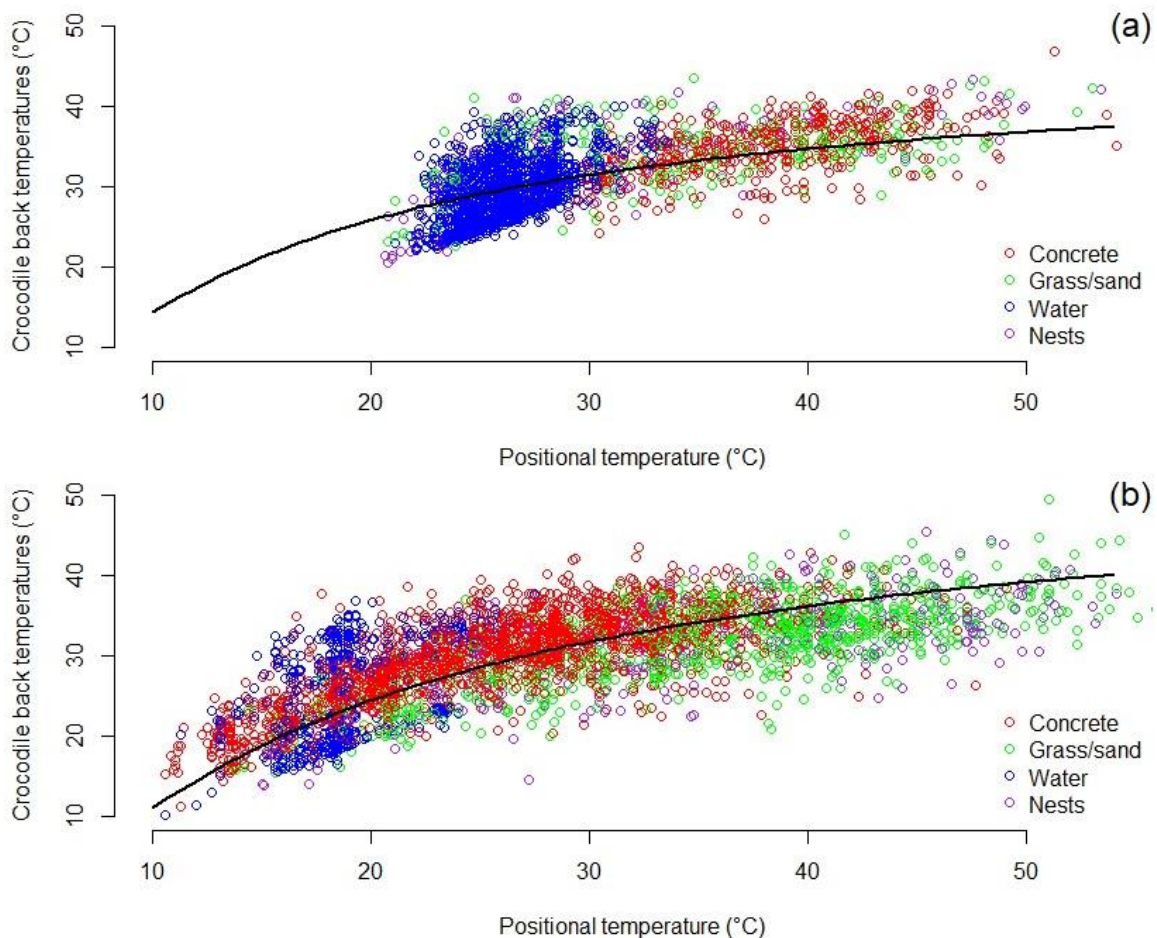


**Figure 26.** The relationship between crocodile back temperature and positional temperature selected by the crocodiles, for summer (a) and winter (b) seasons. The colouration of the plot indicates which material type the crocodiles were selecting for each datapoint.

## 4.6. DISCUSSION

### 4.6.1. Low-cost thermal mapping

The methodology described here is a cost-effective alternative to more expensive proprietary software and larger UAV platforms, as well as a less invasive approach to temperature assessment via monitoring external body temperatures directly. For the current study, it provided sufficient resolution for distinguishing the thermal features of the respective areas available to crocodiles in a pen on a commercial farm. This method could be used to identify suboptimal thermal regimes which may be detrimental to crocodile welfare. This approach could be applied to hotspot detection in commercial settings. An important feature of raster data is that it can be easily mathematically manipulated and partitioned to identify specific areas of interest. It can be used to detect changes in critical parameters and/or to identify areas requiring further investigation, saving analytical time and costs.

### 4.6.2. Crocodile thermal behaviour and pen/material utilization

The average number of crocodiles visible per season and time of day can be attributed to thermoregulatory activities/behaviours. Even within a season, the changing daily thermal regimes vastly affected the crocodiles' selection of an appropriate micro-environment. For example, on a warm summer day  $\geq 85\%$  of the crocodiles in view selected waterbodies between 09:30 and 15:30. The land temperatures in the pen were seemingly too hot, and the water bodies became the only refuge from these temperatures. Wild crocodiles similarly utilize aquatic environments extensively during the summer season, shuttling between land and water to thermoregulate their body temperatures. A potential welfare issue in commercial crocodile farming practices is the density of the population being confined to limited aquatic spaces, necessitating aggregation to mitigate overheating. Wild crocodiles can spatially distribute themselves, maintaining thermoregulation activities while simultaneously maintaining individual spacing. Farmed crocodiles do not necessarily have this same distribution opportunity. Consequently, the provision of sufficient thermal gradients (e.g., increased shaded areas within the pen during the summertime) on land, and over waterbodies, may be an effective alternative from both a thermoregulatory and social perspective.

With fewer crocodiles captured in the summer imagery, the assumption could be made that the uncaptured crocodiles missing from the imagery were also occupying the water bodies or shaded regions of the pen and were therefore out of sight. Overall, warmer summer temperatures resulted in the crocodiles exercising a greater degree of heat avoidance behaviours by retreating to the water. Conversely, the cool winters day showed  $\leq 12\%$  of the crocodiles in view selecting water bodies between 09:30 and 15:30. For this seasonally cool day in winter, water temperatures were "too cool" and the land areas were preferred by the crocodiles. Overall, cooler winter temperatures resulted in the crocodiles exhibiting heat seeking behaviour via basking on land areas where these materials functioned as heat sources as the day warmed up. Of the four pen materials assessed, the sandy nesting areas were the least frequented material type. This area comprised close to a fifth of the total pen area and a quarter of the total land-area available to the crocodiles, yet only 6.75% of the crocodiles utilized this area over all seasons and timeslots.

Significant variation in heat seeking and heat avoidance behaviours between the early morning timeslot and all other timeslots was likely due to the thermal properties of the pen materials, with land-based materials acting as heat sources once they had accrued enough warmth, and the water

bodies acting as heat sinks (Lang<sup>1</sup>, 1987). Once the land temperatures warmed sufficiently, the crocodiles basked from late morning, which concurs with previous Nile crocodile basking assessments (Downs *et al.*, 2008).

Although there is a general lack of confirmation regarding the exact thermoregulation link to cardiac shunting (Grigg and Alchin, 1976; Hicks, 2002; Seebacher & Franklin, 2004; Porter *et al.*, 2016), it is possible that partially submerged crocodiles may have been thermally “shunting” heat received through the peripheral parts of the body that were in direct sunlight (note: to be captured for analysis in this study, a portion of the crocodile, either the back or the head, had to be visible within the water body) directly into the water. For the “neutrally” behaving crocodiles this could explain the maintenance of back temperatures closely matching those of the water bodies they were selecting. Alternatively, the thermal camera resolution may not have been able to capture the variation between the portion of the crocodile’s body visible to that of the water surrounding the animal. It is also possible that the surface temperature of the crocodile when wet would reflect that of the water because the animal may have submerged recently.

#### 4.6.3. Crocodile environmental temperature selections

The crocodiles maintained back temperatures within a narrow/restricted range, relative to the wide range of environmental/material temperatures available. Apart from area/material selections (via shuttling between land and water) and climate conditions, physiological processes (cutaneous vasodilation/vasoconstriction and altered heart rates) and thermoregulatory behaviours (gaping and posturing) may also have contributed to the crocodiles back/body temperature ranges (Grigg & Alchin, 1976; Seebacher, 1999; Hicks, 2002; Porter *et al.*, 2016). The variation between environmental and crocodile back temperatures suggests that even when seasonal climatic factors are considered, crocodiles were consistently able to maintain back temperatures below 50 °C.

The lack of significant variation in back temperatures for crocodiles selecting materials other than water, in summer specifically, points towards a thermally restrictive pen environment. This suggests the higher temperatures available throughout the on-land portions of the pen in summer, alongside the increased ambient temperature and humidity, may have minimized the crocodile’s ability to select the appropriate land-based material for optimal thermoregulation. This interpretation is consistent with the observations of increased numbers of crocodiles occupying the waterbodies in summer and the lower numbers of crocodiles captured in UAV imagery during this season. In contrast, the significant variation in winter crocodile back temperatures between all material types except grass/sand and nests, and grass/sand and concrete, can be explained by the seasonal sparseness of the grassy patches, causing thermal similarity between these material types. Proportionally, land-based pen areas were used more in winter than in summer. This result suggests that summer temperatures may render these areas too hot, resulting in the crocodiles retreating to the water to maintain suitable back/body temperatures.

On average, crocodile back temperature means were higher than positional temperature means. This held true for all dates and times except between approximately 11:30 and 14:00 on the cool winter day, where positional temperature means increased above crocodile back means. The strong positive correlations between crocodile temperature and crocodile positional temperature for both seasons is indicative of heat seeking behaviour, and the known dependence of ectotherms on their environmental temperatures. In this case, the crocodiles made use of the various material substrates to seek or avoid warmth by manoeuvring between the variable thermal gradients available to them. The range of positional thermal options was relatively narrow in the summer season, starting at around 20 °C (compared to the 10 °C starting point in winter) and concluding at approximately 50 °C (as a posed to 55 °C in winter). Notably, the lowest available material/positional temperatures closely

corresponded to the lowest back temperatures in both seasons. However, when positional temperatures rose above approximately 20 °C in winter and 25 °C in summer, the crocodile back temperatures began to level off, few animals reached back temperatures  $\geq 40$  °C. This levelling off might indicate the upper boundary of Nile crocodile thermal comfort. An  $R^2$  value of 0.54 suggests that 54% of the variability in crocodile back temperatures could be explained by the pen material choices in their immediate ambient environments, lending importance to the management of thermal gradients available to crocodiles via the pen materials. The lower  $R^2$  value for summer, when compared to winter, suggests that the crocodiles back temperatures in winter were more predictably modelled from ambient pen temperatures. The range of back temperatures was narrower in summer than in winter but the range of positional temperatures between both seasons was comparable. This finding concurs with the crocodile behaviours studied. In summer, the crocodiles were more actively selecting temperatures within the pen by shuttling between land and water, increasing the variability between the observed back and positional temperatures. In winter, longer periods of basking on land were observed, reducing the variability in the observed back and positional temperatures, and likely contributing in the greater  $R^2$  value in the resulting regression equations.

#### 4.7. CONCLUSIONS

A novel, non-disruptive, fast paced, and highly repeatable method of thermal and behavioural data capture was developed using a relatively affordable UAV platform equipped with a thermal camera (Mavic 2 Enterprise Dual), combined with an IoT system of data loggers. This study assessed the external back temperatures and corresponding positional temperature selections of farmed, breeder sized, Nile crocodiles on a commercial farm in South Africa. It focused on winter versus summer seasonal differences in the thermal regimes available within a breeding pen, and how the captive crocodiles thermally selected appropriate microenvironments within the pen. In particular, the study examined whether warm summer temperatures provided adequate heat avoidance opportunities.

The NSPCAs warnings regarding overheating of farmed crocodiles in South Africa are concerning. Not only does hyperthermia compromise animal health and welfare, but with the varied crocodile farm setups the need for individual farm assessments and possible pen alterations is a sizeable undertaking. The pen assessed in the current study had multiple water bodies and a large land-based area for the crocodiles to move between. During high ambient and pen temperatures in summer, crocodiles sought refuge in water bodies. The results suggest that pen materials (and their thermal properties) are important determiners of crocodile thermal comfort. Farmers should ensure that sufficient basking and heating spaces are available for all crocodiles in winter, and sufficient water/cooling areas for full submersion and shallow lounging are available in summer. Effective shade provision over both land and water areas should be considered during the summer months. Appetites, digestion, growth, and health (Lang<sup>2</sup>, 1987; Huchzermeyer, 2003; Bothma & Van Rooyen, 2005; Bassetti *et al.*, 2014) are important determinants of crocodilian thermal selection, and require appropriate management.

#### 4.8. CRITICAL EVALUATION AND RECOMMENDATIONS

Future studies utilizing thermal UAVs for assessing environmental thermal regimes, and the thermal responses of crocodiles (or other species) within those environments, might consider recording internal/core Tb and subcutaneous belly/back skin temperatures alongside the surface back temperatures. This could yield valuable information regarding internal body temperatures and a better understanding of the mechanisms and dynamics of crocodile thermoregulation. Expanding the observation periods to include nighttime data and historical data on thermally related mortality and breeding/nesting would enhance our understanding and inform best practises for pen-temperature management and design. From a farming perspective, identifying the areas of the pen that are most

thermally “desirable” throughout annual climatic cycles would inform future pen designs in order to enhance optimal thermal conditions in farm settings.

## 5. Thermal niches of wild Nile crocodiles (*Crocodylus niloticus*) in the Kruger National Park, South Africa

### 5.1. INTRODUCTION

Crocodiles are the largest living reptile species, playing a vital role in the ecosystems they inhabit, acting as apex predators that maintain ecological balance (Ashton, 2010; Lane *et al.*, 2013). Nile crocodiles (*Crocodylus niloticus*) are widespread across Africa and Madagascar (Huchzermeyer, 2003). Kruger National Park (KNP), located in northeastern South Africa, is among the continent's largest game reserves (spanning almost two million hectares) and harbours a significant population of Nile crocodiles (Joubert, 2007). Nile crocodiles hold a keystone position in the KNP ecosystem (Joubert, 2007; Ashton, 2010). Excessive hunting in the 1900s threatened Nile crocodile populations, prompting protective measures under the Convention on International Trade in Endangered Species of Wild Fauna and Flora (CITES) (Kyalo, 2008; Lane *et al.*, 2013). While these protective measures safeguard the crocodiles within KNP, contemporary threats persist, notably water pollution, both within and external to the park's boundaries (De Villiers & Mkwelo, 2009; Ashton, 2010; Booyens *et al.*, 2013). Mining, agriculture, wastewater treatment processes, and industrial activities have been identified as contributors to the deteriorating water quality in the region (Ashton *et al.*, 2001; Ashton, 2007; Hobbs *et al.*, 2008; De Villiers & Mkwelo, 2009; Dabrowski & De Klerk, 2013). The Olifants River in particular, has been acknowledged as one of southern Africa's most polluted rivers, in need of drastic improvements in monitoring efforts (De Villiers & Mkwelo, 2009; Ashton, 2010). The Nile crocodile population within the Olifants River gorge in KNP has recently suffered due to recurring pancreatitis outbreaks, first documented between 2008 and 2009 when almost 200 crocodile fatalities were reported (Ashton, 2010; Ferreira & Pienaar, 2011; Booyens *et al.*, 2013). Recurrences leading up to and during the cooler winter months suggest that low temperatures could be a contributing factor (Ashton, 2010; Ferreira & Pienaar, 2011; Lane *et al.*, 2013). Alterations to the riverine environment, such as the raising of the Massingir Dam Wall in 2006 which resulted in sediment trapping in the gorge and altered food webs, ultimately amplified pollutant concentration upwards through the food chain, potentially exacerbating the pancreatitis events (Osthoff *et al.*, 2010; Lane *et al.*, 2013; Booyens *et al.*, 2013; Huchzermeyer *et al.*, 2017). Although no definitive causation has been identified (water pollution, dietary changes, sediment build-up, and/or cold temperature stress), the outbreak has had a prolonged impact on the Olifants gorge crocodile population (Nieuwoudt *et al.*, 2009; Lane *et al.*, 2013).

As ectotherms, crocodiles rely upon environmental temperatures to maintain their body temperatures ( $T_b$ ) within a preferred range (Lang, 1987; Huchzermeyer, 2003; Bassetti *et al.*, 2014). This  $T_b$  maintenance is essential for survival and multiple biological aspects, i.e., metabolic processes, efficiency of digestion, growth rates, and reproduction (Lang, 1987; Huchzermeyer, 2003; Bothma & Van Rooyen, 2005; Bassetti *et al.*, 2014). Thermal preferences and tolerances, i.e., the range of temperatures within which an animal can survive and effectively function, are not fixed.  $T_b$  ranges vary with season, size, age, reproductive status, nutritional status, social interactions, and ontogeny (Lang, 1987; Grigg *et al.*, 1998; Seebacher & Grigg, 2001; Bassetti *et al.*, 2014; Whitaker & Srinivasan, 2018). For example, American alligators (*Alligator mississippiensis*) and mugger crocodiles (*Crocodylus palustris*) showed less variable and higher  $T_b$ s following feeding (Lang 1977; Whitaker & Srinivasan, 2018). American alligators, saltwater crocodiles (*Crocodylus porosus*), and freshwater crocodiles (*Crocodylus johnstoni*) have displayed compromised thermoregulation capabilities when social and aggressive interactions were recorded (Lang 1977; Seebacher & Grigg, 2001). Reproductive broad snouted caimans (*Caiman latirostris*) exhibited higher  $T_b$  than their non-reproductive counterparts in a study by Bassetti *et al.* (2014). Diurnal  $T_b$  amplitudes of saltwater crocodiles were inversely related

to their mass, with large crocodiles achieving higher Tb than smaller individuals (Grigg *et al.*, 1998). Cooling and heating rates were notably higher in smaller (total length) Nile crocodiles (Hocutt, 2022). Nile crocodile maximum Tb's surpassed ambient maximum temperatures during the day but showed a delay in daily Tb extremes (both minima and maxima) relative to the corresponding ambient temperature minima and maxima (Hocutt, 2022). Crocodylian thermal preferences have been suggested as inversely related to their thermal environments (Lang, 1987). Persistent ambient temperatures ranging from 10–20 °C inhibit feeding behaviours in various reptilians, while those exceeding 35–39 °C are considered lethal (Colbert *et al.*, 1946; Lang, 1987; Bolton, 1989). In the context of global climate change, understanding the thermal tolerances of species like crocodylians becomes crucial. Changes in temperature can influence thermoregulatory activities, habitat ranges, breeding and nesting success, sex ratios, and overall survival (Lang, 1987; Refsnider, 2012; Mainwaring *et al.*, 2017; Fukuda *et al.*, 2022).

A combination of behavioural and physiological traits contributes to successful thermoregulation. Thermal behaviours (e.g., basking, shuttling, posturing, and gaping) are actively carried out by crocodiles, whereas physiological mechanisms (e.g., rates of metabolism, heart rate changes, blood flow alterations, and breathing rates) occur naturally within the body because of changes in Tb (Grigg & Alchin, 1976; Spotila *et al.*, 1977; Lang, 1987; Seebacher *et al.*, 1999; Seebacher & Grigg, 2001; Franklin & Seebacher, 2003; Seebacher, 2005; Downs *et al.*, 2008; Manolis & Webb, 2016; Price *et al.*, 2022). Basking is a thermoregulatory behaviour that involves laying out in the sun for extended periods of time, raising Tb's with minimal effort (Lang, 1977; Downs *et al.*, 2008). By moving between sunny and shaded or land and water areas, also known as shuttling, crocodiles can select temperatures along environmentally available thermal gradients (Lang, 1987). Body orientation, relative to the sun, and posturing have also been shown to aid in Tb regulation (Seebacher *et al.*, 1999). Gaping aids thermoregulation via evaporative cooling from the exposed surface area of the mouth, although the consensus is that gaping influences head rather than full-body temperatures (Spotila *et al.*, 1977; Terpin *et al.*, 1979). Larger crocodiles can retain heat for longer periods, this thermal inertia effect means they are less affected by short term environmental temperature changes (Colbert *et al.*, 1946). Physiologically, Tb changes alter metabolic rates. Cooler environmental temperatures will result in the slowing of a crocodile's metabolism, thereby reducing the energy requirements for that animal and extending the survival period without food. Crocodiles stop feeding at constant cooler temperatures as the ingestion of food before cold spells can result in food rotting in the stomach, ultimately poisoning the crocodile (Colbert *et al.*, 1946; Lang, 1987; Bolton, 1989). Crocodile heart rates become elevated during basking periods, which inadvertently assists with the warming of the body, and heart rates drop when environmental temperatures drop (e.g., at night) which assists with prolonged heat retention (Grigg & Alchin, 1976; Franklin & Seebacher, 2003). Vasoconstriction and vasodilation near the skin surface has also been suggested as a physiological mechanism by which crocodylians can alter changes in Tb. Increased blood flow near the skin can allow increased heat loss to the immediate environment, whereas reduced blood flow near the skin would conserve heat (Grigg & Alchin, 1976; Seebacher & Franklin, 2007).

Several studies have monitored wild Nile crocodile activity and behaviour in various locations in South Africa, namely Ndumo Game Reserve, Lake Ngezi in Zimbabwe, Flag Boshielo Dam, and the Lake St Lucia estuarine system (Hocutt *et al.*, 1992; Strauss *et al.*, 2008; Combrink, 2014; Calverley & Downs, 2015). Movement patterns, home range sizes, diurnal rhythms, homing capabilities, migrations, and reproductive behaviours of Nile crocodiles have been elucidated from wildlife tracking and telemetry technologies (Cloudsley-Thompson, 1964; Hocutt *et al.*, 1992; Strauss *et al.*, 2008; Combrink, 2014; Calverley & Downs, 2015). Nile crocodile activity levels have been shown to vary diurnally, seasonally, and between adult and subadult individuals. Size, age, and reproductive status impact Nile crocodile

movement patterns and home range sizes. Larger home ranges and more frequent movements across larger areas have been associated with larger individuals (Combrink, 2014). Increased mobility and space use were also related to nesting behaviour in females, which exhibited nest guarding and hatchling liberation behaviours (Combrink, 2014; Calverley & Downs, 2015). Transmitter survival durations were lower than expected in such studies, and this was related to logger placements (with tail placements being advised against), size (total length), and reproductive status of the crocodiles. Smaller crocodiles and non-gravid females maintained active loggers for longer periods in these studies (Strauss *et al.*, 2008; Calverley & Downs, 2015). Crocodile activity levels are related to temperature and therefore season. In cooler conditions the cost of physiological maintenance decreases allowing long periods of inactivity, whereas warmer conditions are linked to increased activity and food requirements (Manolis & Webb, 2013; Combrink, 2014).

The thermoregulatory patterns of multiple crocodylian species, varying in sizes and habitats, have been extensively investigated (Lang, 1977; Seebacher & Grigg, 1997; Grigg *et al.*, 1998; Seebacher *et al.*, 1999; Glanville & Seebacher, 2006; Brien *et al.*, 2012; Bassetti *et al.*, 2014; Whitaker & Srinivasan, 2018). For the Nile crocodile specifically, limited research has been performed describing internal Tb patterns and thermoregulatory behaviours in both wild and captive environments (Loveridge, 1984; Downs *et al.*, 2008; Hocutt, 2022). Further research is required describing the thermal niches of Nile crocodiles within Kruger National Park, aiming not only to comprehend the physiological and behavioural adaptations preceding the coolest months but also to establish a historical baseline of how these animals are responding to current climatic conditions. This investigation provided critical insights into wild Nile crocodile thermoregulation strategies and behavioural modifications in response to evolving environmental temperatures.

## 5.2. AIMS AND HYPOTHESES

This study elaborates on the thermal experiences/behaviours and activity patterns of Nile crocodiles within the Kruger National Park between 2018 and 2020. There was a focus on seasonal variation, given that the former pansteatitis outbreaks occurred leading up to and during the winter months. It was hypothesized that temperature and activity patterns would vary with time of day, month, season, and between different sex and size classes. The internal ( $T_{b_{\text{internal}}}$ ) and external ( $T_{b_{\text{external}}}$ ) body temperatures of Nile crocodiles, as ectotherms, were expected to exhibit predictable trends in relation to air temperatures, with variations influenced by season and sex/size of the individuals.

### 5.3. MATERIALS AND METHODS

#### 5.3.1. Study site, materials, and animals

The study was conducted at the confluence of the Letaba and Olifants Rivers, within the Kruger National Park (KNP), South Africa (figure 27). The Letaba-Olifants confluence is an important ecological and hydrological junction within the park making it a point of interest for management strategies and in the current study, an assessment of the thermal experiences of Nile crocodiles.

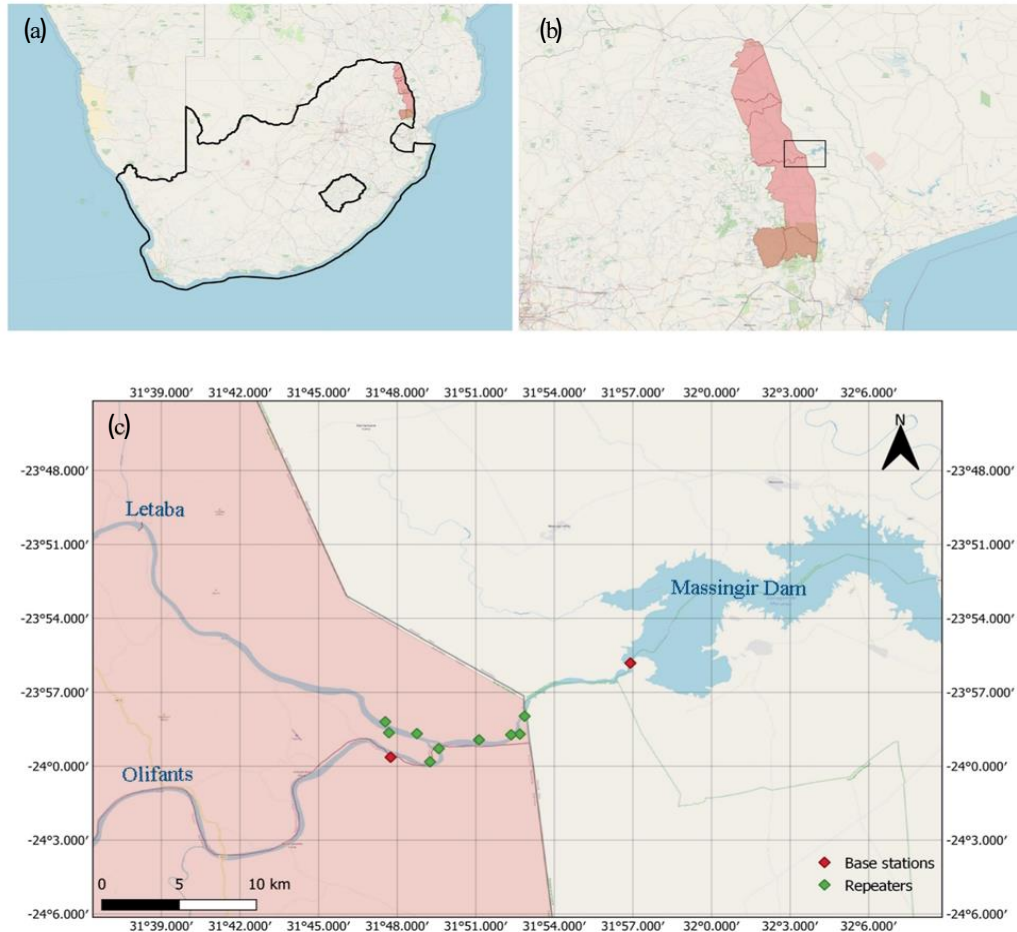


**Figure 27.** (a) Map of South Africa highlighting Kruger National Park (KNP) in red, (b) map of KNP indicating the specific study site with a box, (c) study site at the confluence of the Olifants and Letaba Rivers into Massingir Dam. The Wireless Wildlife base station and repeater placements are depicted with red and green rhombuses, respectively.

Seventeen Nile crocodiles were captured along the Olifants-Letaba River system, between 2018 and 2020. Each crocodile was captured using either a baited cage trap or a noose (figure A19, A20). Standard crocodile capture and handling procedures were followed as per Combrink *et al.* (2012). The following steps were taken in the processing of each crocodile, as per standard operating procedures: capture, immobilization, sex identification, scute marking, transmitter attachment/force-feedings, morphometric measurements, and release. Seven standard morphometrics were collected with a flexible standard tape measure (Warner<sup>1</sup> *et al.*, 2016; Edwards *et al.*, 2017; Webb *et al.*, 2021). Total length (TL) was measured from the tip of the snout to the tip of the tail, snout-vent length (SVL) from the tip of the snout to the caudal margin of the cloaca, head length (HL) from the tip of the snout to the posterior ridge of the supraoccipital bone, and head width (HW) the transverse measurement across the widest part of the crocodile's head. Neck girth (NG) was the circumference measurement

taken around the thickest part of the neck, belly girth (BG) the circumference measurement taken around the thickest part of the belly, and tail girth (TG) the circumference measurement taken around the thickest part of the tail.

### 5.3.2. Climate data

Ambient temperature data from the Olifants-Letaba confluence was incorporated via the European Centre for Medium-Range Weather Forecasts (ECMWF) fifth-generation high spatial resolution climate reconstruction platform (ERA5). The ERA5 platform outputs satellite data from two metres above “ground” level, giving the most spatially accurate temperature data near the study site. No further climate variables were included in the study as the local weather stations did not store historical data for the study period. The closest station that had historical data was in Skukuza (approximately 200 km away), which was previously shown to vary micro climatically from the study site (Gertenbach, 1983; Venter & Gertenbach, 1986). Year-to-year weather variations and climate change is another factor impacting uncertainties in the appropriateness of using data from other areas within the park (Dube & Nhamo, 2020; <https://www.krugerpark.co.za>). A statistical comparison with the ERA5 air temperature data and that of the Skukuza weather stations air temperature data ultimately ruled out the use of this dataset, with significant variations found throughout all seasons.

Seasonal variations were assessed throughout the current chapter, the seasons as defined for South Africa as well as rainy and dry seasons within KNP were compared. Seasons in South Africa are defined as summer (December–February), autumn (March–May), winter (June–August), and spring (September–November); these will henceforth be referred to as “meteorological” seasons. Rainy and dry seasons within KNP are defined as November–April and May–October, respectively (Sutherland *et al.*, 2018); these will henceforth be referred to as “climatic” seasons. Differentiating these season “types” was necessary as the seasons within KNP are known to deviate from those conventionally defined for South Africa. Season types were analysed independently to circumvent multicollinearity concerns. When time of day comparisons were made these were defined by the following categories: morning as 06:00–11:00, afternoon as 12:00–17:00, evening as 18:00–23:00, and night as 00:00–05:00. When day versus nighttime comparisons were made these were defined by the following categorizations, based upon the presence/absence of the sun: day was defined as 06:00–17:00 and night as 18:00–05:00.

### 5.3.3. Crocodile temperatures

Several solar and battery powered Wireless Wildlife base (WW-BS) and relay stations (WW-RS) were positioned along the banks of the study site (figure 27c). A further base station was mobile, its location is not mapped for this reason. These were responsible for receiving data from temperature recording units attached/force-fed to the crocodiles in this study. Relay stations, which have an equivalent coverage footprint and serve as intermediaries to base stations, relayed telemetry data to the base stations for onward transmission to the operator via a global system for mobile communications (GSM) network.

Nine male and eight female wild Nile crocodiles in Kruger National Park were captured and fitted with a selection of Wireless Wildlife tracking devices (<http://wireless-wildlife.co.za/products.html>). Each crocodile was fitted with a WW1500AS unit which encompassed a GPS (global positioning system) device, a temperature logger, and a motion sensor. These units were attached by threading stainless steel strands subcutaneously underneath the nuchal rosettes at the back of the crocodiles’ necks (figure A21, A22), as per Brien *et al.* (2010). The GPS unit recorded latitudes and longitudes every six hours, whereas the motion sensor and temperature loggers were programmed to record hourly. A second type of temperature logger (WW0500) was encased in dental acrylic and force-fed, to be retained as pseudo-gastroliths, via gastric intubation to each crocodile for  $T_{b_{\text{internal}}}$  recordings (figure

A23, A24). Similar methods for gastric intubation have been used for crocodylians in studies that fed loggers or performed stomach content collections (Loveridge, 1984; Janes & Gutzke, 2002; Brien *et al.*, 2012). This was accomplished using a hollow metal pipe, soft rubber tubing, adhesive tape, and a cloth. Each crocodile was prompted to bite down on the exterior of a large hollow metal pipe, which was covered in a soft but sturdy protective material to prevent potential movement/skidding and therefore damage to the crocodiles' teeth/mouth when biting down. Once the crocodile had a firm grip, the eyes were covered with a clean cloth and the mouth carefully taped in place. The soft rubber tubing, marked with length indicators for insertion depth estimation, was then inserted down the crocodile's throat until it reached the stomach. The dental acrylic encased WW0500 logger was then introduced through the soft tubing into the stomach. The tubing, tape, metal pipe, and eye-cloth were then carefully removed, and the crocodiles released. Of the 17 crocodiles, one was not fitted with an internal logger due to rejection on the first feeding attempt, this crocodile was released without an internal logger for this reason. All other crocodiles were successfully fitted with both external and internal loggers. Downloadable ranges for the different devices varied due to their positioning and design. The externally placed loggers were readable up to a range of a few kilometres, the internals less so as they not only had a less effective antenna system (intentionally compact in design) but the signal would need to pass through the body of the crocodiles.

Of the 17 crocodiles included in the original deployments, 12 had complementary  $T_{b_{\text{internal}}}$  and  $T_{b_{\text{external}}}$  data ranging from 6–290 days ( $\bar{x} = 82$  days). In nine of these 12 cases, the external loggers outlived their internal counterparts. It is postulated that this was due to either the expulsion of the internal loggers (as one such logger was later recovered near the waterline) or the eventual digestion of the protective coating applied, resulting in logger failure. Of the remaining five crocodiles, four had either only internal or external data recordings, and one crocodile's loggers failed to record altogether. These occurrences were likely due to logger failures/damage/expulsions, with the remaining loggers continuing their data capture without their temperature-logging counterparts. WW0500 and WW1500AS loggers both transmitted data that could be captured by any base or relay units in proximity, explaining the occurrence of crocodiles with periods of either only internal or external data.

To compare the crocodiles by size in a series of individual plots of  $T_{b_{\text{internal}}}$ , the crocodiles were categorized as follows: small classified as < 150 cm SVL, medium classified as 150–200 cm SVL, and large classified as > 200 cm SVL. Due to the possible loss of tail ends that can impact TL measures, SVLs were included in individual plots as an indicator of crocodile size. Mass is a key factor in crocodylian thermal regulation due to thermal inertia effects (Colbert *et al.*, 1946; Lang, 1977). Approximate masses were predicted from SVLs based on the inverse of the equation from Hutton<sup>1</sup> (1987). The categories mentioned above collate to approximate masses of < 100 kg for small sized individuals, 100–200 kg for medium-classed individuals, and > 200 kg for large-classed individuals.

Heating and cooling rates were determined by quantifying the rate of temperature change per unit of time. The difference in temperature between consecutive readings was calculated and then divided by the time interval between these readings. Given the minor variations in logging intervals, this method adjusted for the slight discrepancies in the timestamp precision of the loggers. A maximum allowable interval of 75 minutes and minimum allowable interval of 45 minutes between consecutive readings was established to maintain the integrity of the data whilst accommodating the loggers timestamp variations. This ensured the derived heating and cooling rates accurately reflected temperature changes over time.

#### 5.3.4. Thermal behaviour inferences

The relationships between crocodile body ( $T_{b_{\text{internal}}}$  and  $T_{b_{\text{external}}}$ ) and air temperatures offered insights into the thermoregulatory behaviours of the crocodiles.  $T_{b_{\text{internal}}}$  and  $T_{b_{\text{external}}}$  body temperature

comparisons were indicative of direct thermoregulation, where the differences were largest might indicate periods of thermal stress (overheating or overcooling), and the relationship between the two variables was used to construe basking behaviour.  $T_{b_{\text{external}}}$  and air temperature comparisons reflect microhabitat selections (sunny versus shaded or land versus water selections by the crocodiles) and large variations between the variables would suggest heat retention by the crocodiles.  $T_{b_{\text{internal}}}$  and air temperature comparisons were indicative of physiological thermoregulation, where consistency between the variables showed the crocodiles thermoregulation abilities and inconsistencies indicated deviations from the normal thermal behaviours (e.g., metabolic or reproductive status effects).

Comparing these temperature variables involved calculating the difference between them and then plotting this to visualize daily, monthly, and seasonal trends in thermoregulatory behaviours/experiences. The predictability of the relationships between the temperature variables ( $T_{b_{\text{internal}}}$ ,  $T_{b_{\text{external}}}$ , and air) were also assessed using a regression analysis. The relationship between  $T_{b_{\text{internal}}}$  and  $T_{b_{\text{external}}}$  was of particular interest. Heat seeking and avoidance behaviours were inferred from the relationship between these temperatures, if the result was positive (i.e.,  $T_{b_{\text{internal}}} > T_{b_{\text{external}}}$ ) the crocodile was assumed to be “cooling” or “heat avoiding” and if negative (i.e.,  $T_{b_{\text{external}}} > T_{b_{\text{internal}}}$ ) the crocodile was assumed to be “heating” or “heat seeking”. The placement of the WW1500AS loggers on the posterior region of the crocodiles’ necks should be noted when interpreting the results. Although these loggers were positioned close to the skin, the temperatures recorded were likely influenced by immediate environmental changes resulting from thermoregulatory behaviours such as immersion into water (shuttling) or prolonged exposure to the sun (basking).

#### 5.3.5. Crocodile activity

The motion sensor within the WW1500AS units measured hourly physical activity outputs of the crocodiles with an omnidirectional tilt and vibration sensor, which outputted a “count rate” of tilts over time. The information provided did not indicate the type of activity being performed nor the rate of acceleration of the crocodiles, rather it showed the extent of the devices gravity displacement and therefore the intensity of the crocodile’s “activity” at a point in time. Activities such as walking, running, swimming, digging, and hunting were likely to be captured; however, no distinction between the type of activity recorded was possible. Due to the unbalanced nature of the data, regarding both the extent of data available varying per individual and the lack of consecutive dates for comparisons, these results are not presented on an individual basis to avoid potential biases.

The GPS units recorded six-hourly latitudes and longitudes, with an approximate error radius of five metres. This allowed the mapping of the riverine environment utilization by the crocodiles but precluded the ability to consistently or precisely identify whether the crocodiles were occupying land or water areas. For these reasons the GPS data will, for the most part, not be addressed in the current study.

#### 5.4. DATA ANALYSIS

Statistical programs R (2022.12.0 Build 353) and IBM SPSS Statistics (version 28) were used to assess the current dataset. Summary statistics allowed visualization of the distribution and the assessment of fundamental characteristics of the data. Variables were checked for multicollinearity to ensure the combination of related variables was avoided in the analyses that followed. T-tests were used to compare the means between groups, and ANOVAs to compare means across different groups particularly when categorical variables were compared to continuous dependent variables. Regression analyses were employed to model the relationships between various temperature variables, offering insights into how changes in air and immediate ambient (“back”) temperatures affected  $T_{b_{\text{internal}}}$ ’s. The relationships between variables were assessed with correlations; when there were potential additional variables that may have affected these relationships partial correlations were employed.

Generalized linear mixed models (GLMM) allowed exploration of the direct and indirect effects of environmental factors (air temperature), physiological measurements ( $T_{b_{\text{internal}}}$  and  $T_{b_{\text{external}}}$ ), physical attributes (TL), and activity levels of the study subjects on one another. Due to the unbalanced nature of the data, Bonferroni corrections were applied to all post hoc pairwise comparisons. All data were assessed for the determination of significant differences ( $P < 0.05$ ), and highly significant findings were also documented ( $P < 0.001$ ).

## 5.5. RESULTS

### 5.5.1. Climate data

Air temperatures varied from 8.5–45.4 °C ( $\bar{x} = 24.2$  °C, SE = 0.02 °C) for the full study period. Air temperatures for 2018–2020 are depicted in figure 28, across the various times of the day, meteorological seasons, and climatic seasons. Air temperatures varied from 16.7–41.3 °C ( $\bar{x} = 26.9$  °C, SE = 0.03 °C) in summer, 11.8–38.3 °C ( $\bar{x} = 24.2$  °C, SE = 0.03 °C) in autumn, 8.3–38.0 °C ( $\bar{x} = 20.3$  °C, SE = 0.03 °C) in winter, and 9.9–45.4 °C ( $\bar{x} = 24.7$  °C, SE = 0.03 °C) in spring. Rainy season air temperatures varied between 12.9–41.5 °C ( $\bar{x} = 26.3$  °C, SE = 0.02 °C) and dry season temperatures between 8.3–45.4 °C ( $\bar{x} = 21.7$  °C, SE = 0.02 °C). Air temperatures varied between meteorological and climatic seasons ( $P < 0.001$ ,  $F = 4139.50$ ,  $df = 3$ ;  $P < 0.001$ ,  $F = 9754.87$ ,  $df = 1$ , respectively), all post hoc (Bonferroni) comparisons were highly significant (all  $P < 0.001$ ). Air temperatures varied with time of day ( $P < 0.001$ ,  $F = 7881.53$ ,  $df = 3$ ), all times of the day varied significantly from one another (all  $P < 0.001$ ) in this regard.

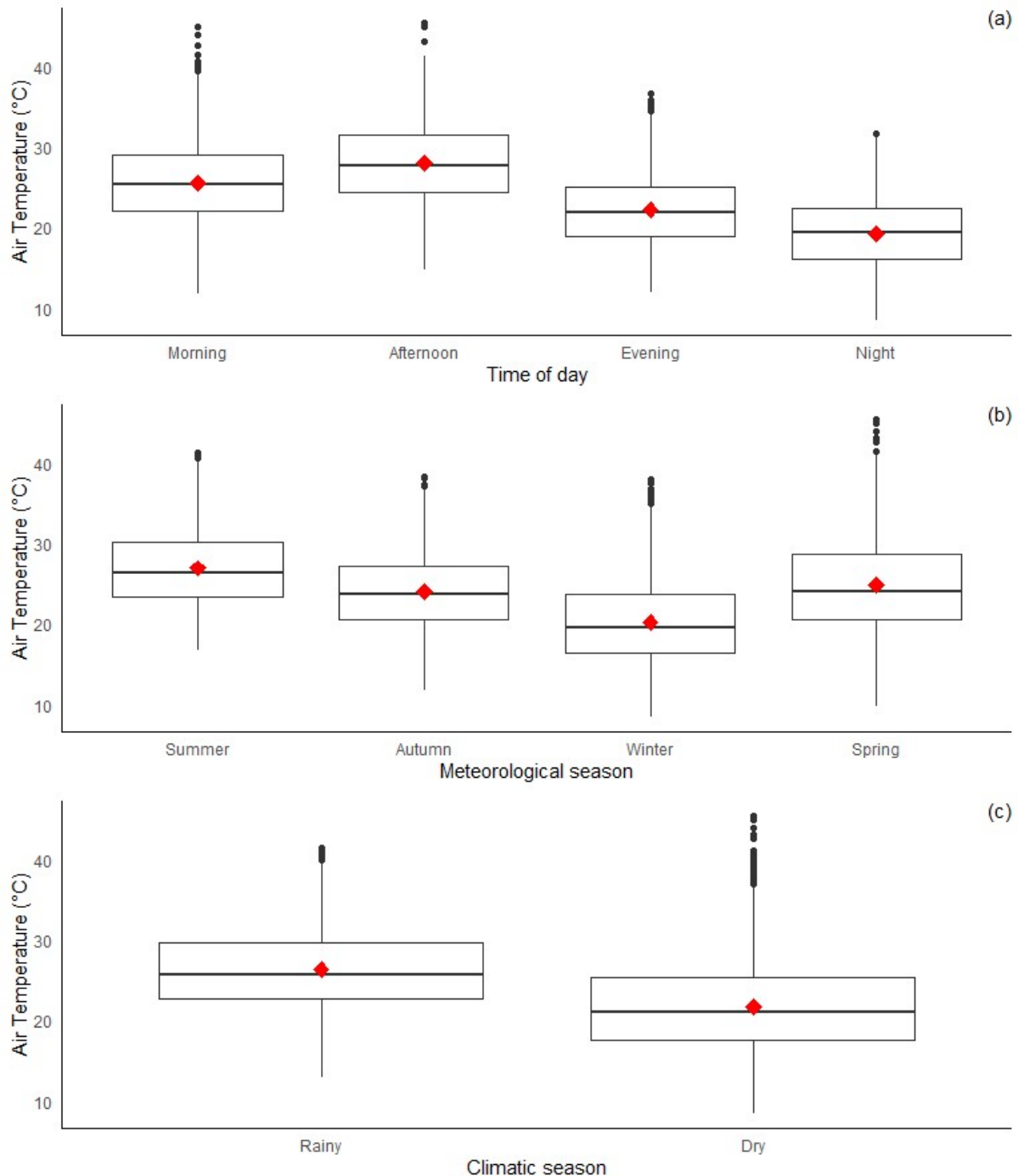


**Figure 28.** Seasonal air temperatures from two metres above the Olifants-Letaba confluence (ERA5) from 2018–2020. Air temperatures per time of day (a), meteorological season (b), and climatic seasons (c) are depicted. Each boxplot displays the median (centre line), interquartile range (box edges), and 1.5 \* IQR (whiskers). Points beyond the whiskers represent outliers. Means are represented by red rhombuses.

### 5.5.2. Study animals

Table 11 summarizes the data collected at logger deployments. Male and female crocodiles ranged from 281–429 cm ( $\bar{x} = 367.8$  cm, SE = 0.5 cm) and 233–309 cm ( $\bar{x} = 293$  cm, SE = 0.1 cm) in TLs, respectively. Male crocodiles had significantly longer TLs than females ( $P < 0.001$ ,  $t = -156.49$ ,  $df = 21932$ ). All morphometrics were strongly and positively correlated with one another, with all  $r \geq 0.93$

( $P < 0.001$ ) except between tail girth and the other morphometrics where the correlations varied between  $r = 0.58$  and  $r = 0.69$  (all  $P < 0.001$ ).

**Table 11.** Crocodile data at deployment: crocodile identification (ID), location of capture and release (post-logger placement), sex, and morphometric measures (cm) per crocodile.

ID	Capture location	Sex	TL	SVL	HL	HW	NG	BG	TG
1	Moz border Olifants gorge	Male	336.5	178	44.5	24	84	140	90
2	Moz border Olifants gorge	Male	410	228	56	32.5	120	149	98.5
3	Olifants river upstream confluence	Female	278	149	39.5	21.5	74	117	71
4	Potholes Olifants trails camp	Male	429	207	57	32	120	182	122
5	Letaba upstream confluence	Female	309	161	41	22.5	81.5	111	78.7
6	Moz border Olifants gorge	Female	287	147.5	38	19.3	71	111	73
7	Moz border Olifants gorge	Male	302	155	39	19.5	77.5	108	70.5
8	Olifants river upstream confluence	Female	233	125	33.5	16.5	57.5	85	59
9	Olifants river upstream confluence	Female	303	166	42.5	24	84	123	31
10	Letaba potholes	Female	294	165	40.5	23	83	116	71
11	-	Female	303	174	43	23.5	89	141	79
12	Letaba, 1 km upstream from confluence	Male	281	148	38	18	72	107	68
13	300 m downstream confluence	Male	289	161	41.5	22	82	128	78
14	Olifants	Male	421	225	57	32	125	166	120.5
15	Letaba	Female	257	136	37	19	67.5	94.5	29
16	Letaba	Male	428.5	246.5	61	37	138.5	167	114
17	Letaba	Male	413	233	60	38	111	154.5	99

\* Mozambique referred to as “Moz” in table.

### 5.5.3. Individual variability in temperatures

Crocodile  $T_{b_{\text{internal}}}$ 's ranged from 14.53–37.07 °C ( $\bar{x} = 24.11$  °C, SE = 0.02), and  $T_{b_{\text{external}}}$  from 7.88–46.58 °C ( $\bar{x} = 23.90$  °C, SE = 0.02). Although there was a strong positive correlation between  $T_{b_{\text{internal}}}$  and  $T_{b_{\text{external}}}$  ( $r = 0.59$ ,  $P < 0.001$ ), these temperatures varied significantly from one another ( $P < 0.001$ ,  $t = -30.26$ ,  $df = 22939$ ). Tables 12 and 13 present the descriptive statistics for the external and internal temperature loggers per individual crocodile. The full complement of data available per logger was assessed regardless of whether one temperature logger outlasted its counterpart. The mean number of days for which data was present varied with the sex of the crocodiles. Females and males averaged

98 and 58 days of available internal logger data, and 420 and 105 days of external logger data between 2018 and 2020, respectively. There was not sufficient data to test the significance of these differences.

**Table 12.** Descriptive statistics of Nile crocodile  $T_{b_{external}}$ 's ( $^{\circ}C$ ).

ID	n	Min	Max	Mean	SD	SE
1	1865	10.66	36.41	20.43	5.08	0.12
2	1662	11.55	35.12	20.51	4.40	0.11
3	5341	10.31	38.05	24.37	4.55	0.06
4	4034	10.89	43.86	23.13	5.16	0.08
5	3381	11.22	39.74	22.85	5.46	0.09
6	12424	8.46	42.47	23.67	5.57	0.05
7	2029	10.19	36.07	20.81	5.13	0.11
8	19335	7.88	42.03	23.76	5.01	0.04
9	9491	7.88	42.25	24.41	4.95	0.05
10	8895	9.96	43.44	24.57	4.56	0.05
11	4816	10.89	46.58	25.44	4.86	0.07
12	6316	9.47	43.01	25.35	5.21	0.07
13	972	10.08	43.86	24.80	6.07	0.19
<b>Total</b>	<b>80561</b>	<b>7.88</b>	<b>46.58</b>	<b>23.90</b>	<b>5.18</b>	<b>0.02</b>

**Table 13.** Descriptive statistics of Nile crocodile  $T_{b_{internal}}$ 's ( $^{\circ}C$ ).

ID	n	Min	Max	Mean	SD	SE
2	1633	15.90	34.13	23.55	3.65	0.09
3	1320	18.57	33.76	24.67	2.88	0.08
4	4000	16.39	33.20	24.69	3.31	0.05
5	3348	14.62	34.50	22.89	3.60	0.06
6	2054	14.53	34.68	23.46	4.54	0.10
7	860	15.49	33.01	21.59	4.15	0.14
8	839	17.16	34.50	25.02	3.94	0.14
9	357	19.08	36.07	25.43	3.45	0.18
10	6824	15.82	36.99	23.77	4.62	0.06
11	902	17.09	33.01	25.86	3.14	0.10
12	136	23.01	31.42	26.72	2.48	0.21
13	667	17.82	37.07	25.90	3.72	0.14
14	678	18.67	31.73	24.11	3.19	0.12
15	1991	17.46	32.62	24.09	3.05	0.07
16	1682	17.60	32.32	26.24	2.90	0.07
<b>Total</b>	<b>27291</b>	<b>14.53</b>	<b>37.07</b>	<b>24.11</b>	<b>3.96</b>	<b>0.02</b>

Selected individual  $T_{b_{internal}}$  plots highlight individual variations as well as validate cohort-level statistical findings (section 5.4.4) regarding the effects of meteorological season, size, and sex (figures 29, 30, and 31, respectively). Two crocodiles with the longest consecutive internal temperature recordings (IDs 4 and 5) were compared from July–November 2018. Diurnal  $T_{b_{internal}}$  patterns followed and lagged those of air temperatures, and there was a seasonal shift in thermal regimes between winter and spring. The two crocodiles maintained visually similar daily mean  $T_{b_{internal}}$ 's during winter

(July–August), although their thermal regimes varied in that crocodile 5’s daily minimum  $T_{b_{internal}}$ ’s were generally lower and daily maximums were generally higher than those of crocodile 4. In the spring months (September–November) crocodile 5’s thermal regime exhibited consistently lower  $T_{b_{internal}}$ ’s compared to that of crocodile 4. These variations are represented in figure 29, where the hourly internal temperatures are plotted for both individuals for a week in July 2018 and a week in September 2018. Crocodile 4’s  $T_{b_{internal}}$ ’s averaged 20.76 °C and crocodile 5’s averaged 20.43 °C during the winter week (figure 29a). Comparatively, crocodile 4’s  $T_{b_{internal}}$ ’s averaged 26.29 °C and crocodile 5’s 23.66 °C during the spring week (figure 29b). The average  $T_{b_{internal}}$  increase, indicative of the crocodiles heating rates, was 1.13 °C per hour in winter (1.38 °C/h for ID 5 and 0.88 °C/h for ID 4) and 0.52 °C per hour in spring (0.44 °C/h for ID 5 and 0.61 °C/h for ID 4). Cooling rates, reflected by the average decrease in  $T_{b_{internal}}$ ’s, were 0.45 °C per hour in winter (0.34 °C/h for ID 5 and 0.55 °C/h for ID 4) and 0.28 °C per hour in spring (0.25 °C/h for ID 5 and 0.31 °C/h for ID 4).

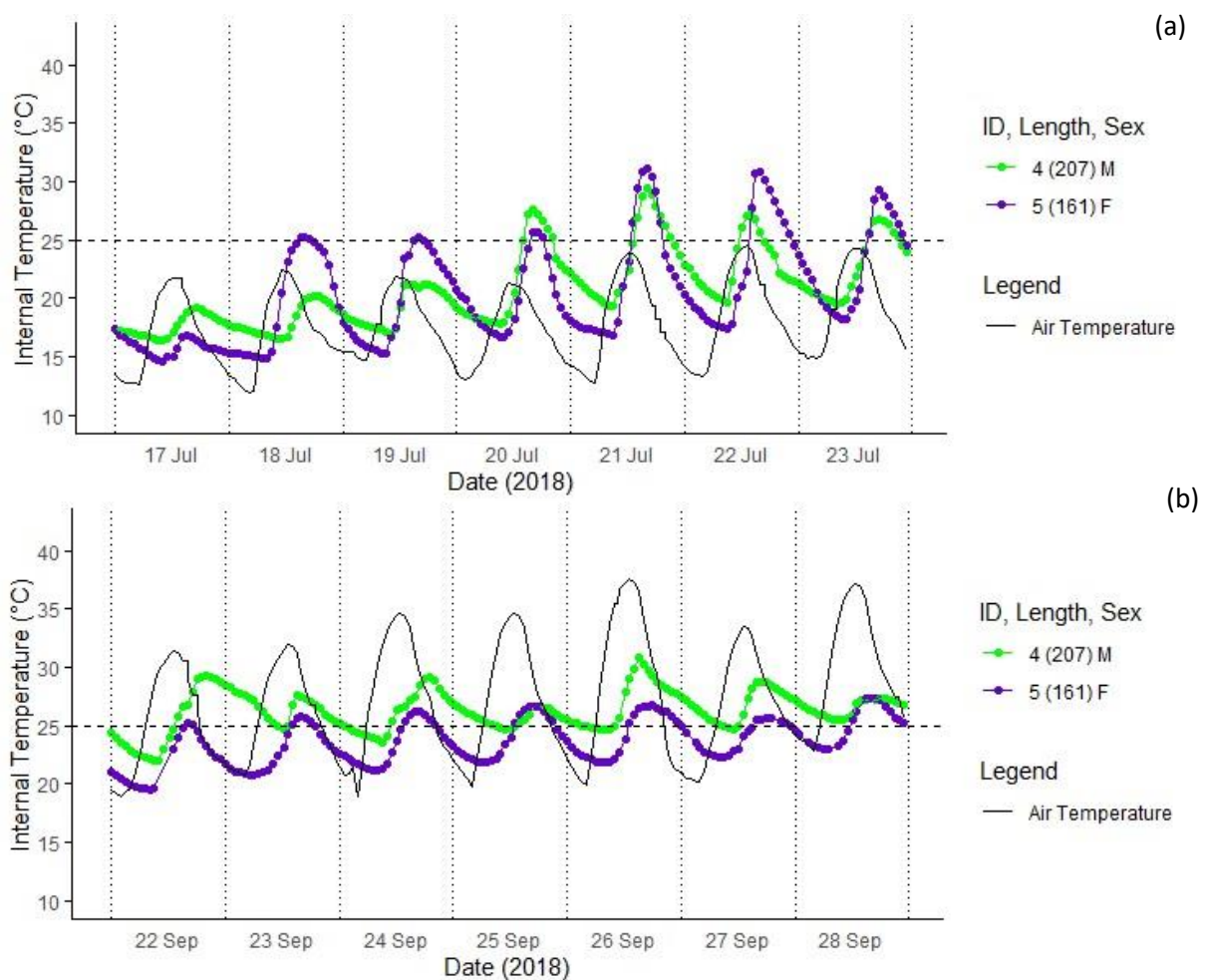


**Figure 29.** (a) Depicts a male (“M”) and female (“F”) Nile crocodiles’ hourly internal temperatures during a cool week in winter, (b) depicts the same male and female Nile crocodiles’ internal temperatures during a warm week in spring. The length measure refers to the crocodiles SVLs and is organized in descending order.

Plots comparing  $T_{b_{internal}}$ ’s of crocodiles varying in size (small: < 150 cm SVL, medium: 150–200 cm SVL, and large: > 200 cm SVL) are depicted in figure 30. Both plots had relatively warmer and cooler days which were considered when reporting  $T_{b_{internal}}$ ’s and heating and cooling rates. The week from 10–16 July contained two cool days (15–16 July), as did the week from 16–22 November (19 and 22 November). Five crocodiles (IDs 2, 4, 5, 6, and 7) were compared over a week in July 2018 (figure 30a)

and four crocodiles (IDs 3, 4, 5, and 10) over a week in November 2018 (figure 30b). A large crocodile (ID 4) managed to maintain higher minimum daily temperatures than the other crocodiles for five days of the week in July. The other large crocodile (ID 2) in the July plot maintained equal or higher maximum daily temperatures with ID 4 for five out of the seven weekdays, and slightly higher daily minimums than the smaller crocodiles for five of the seven weekdays plotted. The two medium sized crocodiles (IDs 5 and 7) had comparatively similar  $T_{b_{\text{internal}}}$  patterns. The small crocodiles (ID 6) daily minimums were comparable with those of the two medium-sized crocodiles. The small crocodile's daily maximums were among the highest for all crocodiles represented for the full week. Individual variations in maximum daily  $T_{b_{\text{internal}}}$ 's were clear throughout the week plotted in July 2018 (e.g., ID 4 achieved the highest maximum daily temperature on 11 July yet was among if not the lowest on all other plotted days), whereas the daily minimums were more consistent within the size categories defined.

For the week in November, the large-classed crocodile's (ID 4)  $T_{b_{\text{internal}}}$  daily minimums were greater than those of the other crocodiles represented, and the daily maximums higher or equal to those of the other crocodiles for four out of the seven weekdays. The medium-classed crocodile's (ID 10)  $T_{b_{\text{internal}}}$ 's were relatively low for the first four days of the represented week, then higher on the fifth day before dropping back to lowest on the sixth day again. The two medium-classed crocodiles were not as comparable as those of the July comparison, one crocodile (ID 5) outperformed the other regarding  $T_{b_{\text{internal}}}$ 's for five of the seven days represented. The smallest crocodile (ID 3) in the November plot had a similar thermal regime to that of the one medium sized crocodile (ID 5); however, it tended to outcompete the other medium sized crocodile (ID 10).

The mean  $T_{b_{\text{internal}}}$ 's for the various sized crocodiles in these plots averaged 21.73 °C (ranged from 21.21–22.32 °C) in July and 26.37 °C (ranged from 25.54–27.50 °C) in November. When assessing the relatively warmer days of the week in July the mean  $T_{b_{\text{internal}}}$ 's averaged 22.93 °C (ranged from 22.09–23.74 °C) on the warmer days and 18.72 °C (ranged from 18.43–19.04 °C) on the cooler days. For figures 30a and 30b the week-long heating rates were 1.45 °C and 0.46 °C, and the week-long cooling rates were 0.56 °C and 0.26 °C, respectively. Heating and cooling rates on the warmer days of the plotted week in July were 1.59 °C per hour and 0.66 °C per hour, respectively. Heating and cooling rates on the cooler days of this week were 0.85 °C per hour and 0.29 °C per hour, respectively. Heating and cooling rates on the warmer days of the plotted week in November were 0.48 °C per hour and 0.27 °C per hour, respectively. Heating and cooling rates on the cooler days of this week were 0.44 °C per hour and 0.24 °C per hour, respectively.

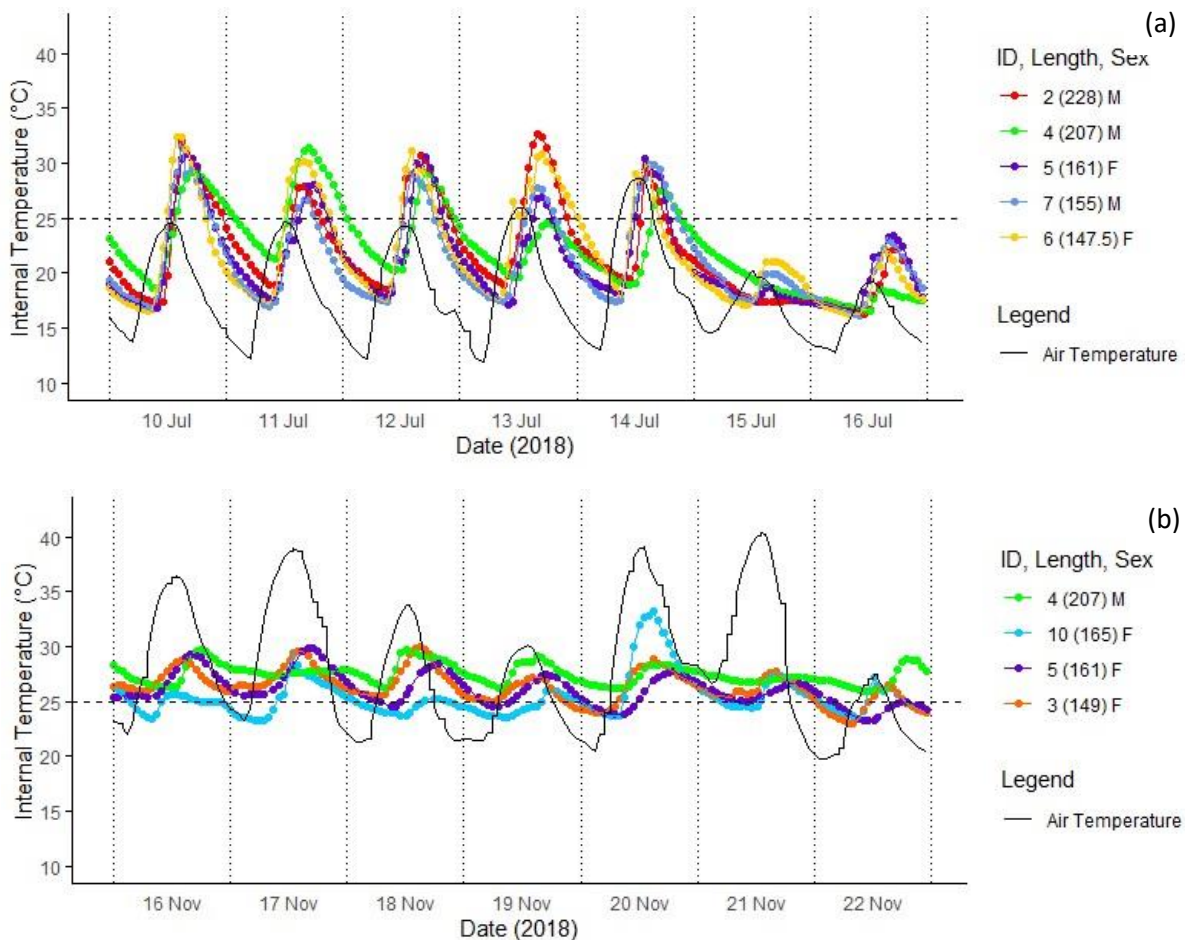


**Figure 30.** (a) Depicts the internal temperatures of five Nile crocodiles of varying size over a week in July 2018, (b) depicts the internal temperatures of four Nile crocodiles of varying size over a week in November 2018. The length measure refers to the crocodiles SVLs and is organized in descending order.

Consecutive male and female  $T_{b_{internal}}$ 's for week-long periods in October 2018 and September 2020 are depicted in figure 31. In these plots the male crocodile  $T_{b_{internal}}$ 's were greater than those of the females for most of the weekdays presented. There is also the effect of size to consider, male crocodiles grow larger than females and the potential effects of thermal inertia may have played a role. When considering the former plots from figures 29 and 30, the noticeable trend of males outperforming females (with regards to  $T_{b_{internal}}$ ) occurred more frequently in warmer (based on air temperature) weeks, in cooler weeks female crocodiles regulated more similarly to males. Figures 30b and 31a fall within the breeding season (October–January as per Swanepoel<sup>2</sup> *et al.*, 2000), the first noticeable variation was still the difference between male and female temperatures in these plots.

The mean  $T_{b_{internal}}$ 's for the week in October (IDs 3, 4, and 5) averaged 25.37 °C (ranging from 24.26–27.00 °C) and for the week in September averaged 24.53 °C (ranged from 22.85–25.45 °C) in November. When reassessing the September weeks warm and cool (22–23 September) dates, mean  $T_{b_{internal}}$ 's for the cooler days averaged 22.62 °C (ranging from 21.03–23.58 °C) and the warmer days averaged 25.30 °C (ranging from 23.57–26.33 °C). Heating and cooling rates for the plotted week in October averaged 0.46 °C per hour and 0.34 °C per hour, respectively. Heating and cooling rates for the plotted week in September averaged 0.83 °C per hour and 0.38 °C per hour, respectively. The warmer days in September had the crocodiles heating at 0.82 °C per hour and cooling at 0.41 °C per

hour, whereas the cooler days heating and cooling rates were 0.87 °C per hour and 0.29 °C per hour, respectively.

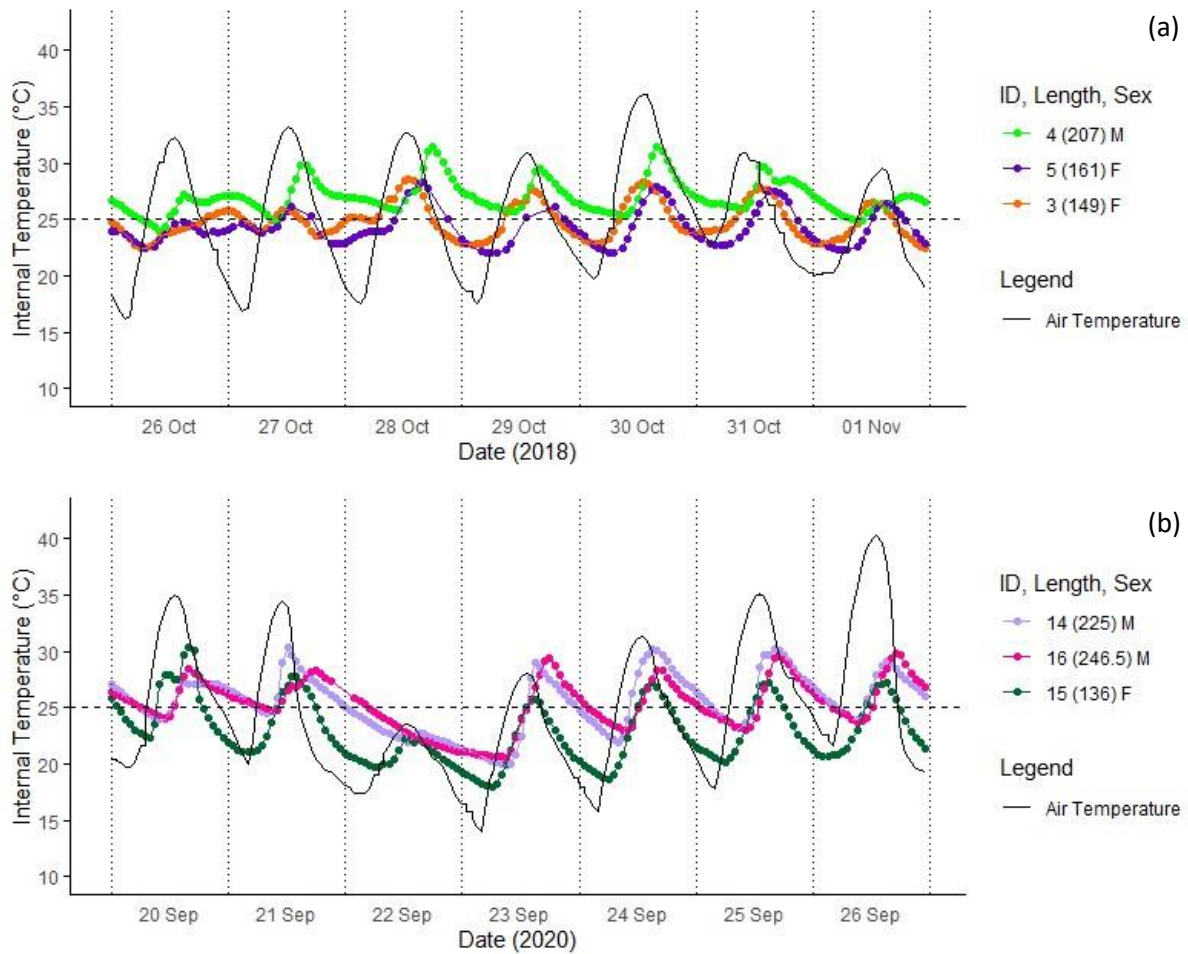


**Figure 31.** (a) Depicts the internal temperatures of one male and two female crocodiles over a week in October 2018, (b) depicts the internal temperatures of two males and one female crocodile over a week in September 2020. The length measure refers to the crocodiles SVLs and is organized in descending order.

#### 5.5.4. Cohort variability in temperatures

The results presented in this section are derived from pooled data for all crocodiles included in the study.  $T_{b_{internal}}$  and  $T_{b_{external}}$  varied with sex of the crocodiles ( $P < 0.001$ ,  $t = -14.36$ ,  $df = 21964$ ;  $P < 0.001$ ,  $t = 18.22$ ,  $df = 24875$ , respectively), with males achieving higher mean  $T_{b_{internal}}$ 's and lower  $T_{b_{external}}$ 's than females. Table 14 shows descriptive statistics for  $T_{b_{internal}}$  and  $T_{b_{external}}$  per sex.

**Table 14.** Descriptive statistics of Nile crocodile  $T_{b_{external}}$ 's ("EXT", in °C) and  $T_{b_{internal}}$ 's ("INT", in °C) per sex of the crocodiles.

Sex	Min		Max		Mean		SD		SE	
	EXT	INT	EXT	INT	EXT	INT	EXT	INT	EXT	INT
Male	9.47	15.49	43.86	37.07	23.22	24.56	5.54	3.63	0.04	0.04
Female	7.88	14.53	46.58	36.99	24.08	23.87	5.07	4.10	0.02	0.03

**Table 15.** Descriptive statistics of Nile crocodile  $Tb_{\text{external}}$ 's ("EXT", in °C) and  $Tb_{\text{internal}}$ 's ("INT", in °C) per meteorological and climatic seasons.

Season	Min		Max		Mean		SD		SE	
	EXT	INT	EXT	INT	EXT	INT	EXT	INT	EXT	INT
Summer	15.90	21.59	46.09	36.99	26.62	28.32	3.48	2.75	0.02	0.06
Autumn	10.43	18.37	45.80	34.13	24.21	24.37	4.46	2.74	0.04	0.05
Winter	7.88	14.53	39.03	34.68	20.34	21.51	5.19	3.99	0.04	0.04
Spring	10.08	16.86	46.58	37.37	24.48	24.95	5.14	3.23	0.03	0.03
Rainy	12.30	18.47	46.09	36.99	26.06	26.26	3.88	2.94	0.02	0.03
Dry	7.88	14.53	46.53	37.07	21.79	23.14	5.45	3.98	0.03	0.03

$Tb_{\text{internal}}$ 's and  $Tb_{\text{external}}$ 's varied with hour of the day ( $P < 0.001$ ,  $F = 566.96$ ,  $df = 11$ ) and month of the year ( $P < 0.001$ ,  $F = 194.37$ ,  $df = 11$ ). Both  $Tb_{\text{internal}}$ 's and  $Tb_{\text{external}}$ 's were positively correlated with hour of the day ( $r = 0.28$ ,  $P < 0.001$  and  $r = 0.21$ ,  $P < 0.001$ , respectively) and month of the year ( $r = 0.04$ ,  $P < 0.001$  and  $r = 0.15$ ,  $P < 0.001$ , respectively).  $Tb_{\text{external}}$ 's ( $P < 0.001$ ,  $F = 1608.41$ ,  $df = 3$ ) and  $Tb_{\text{internal}}$ 's ( $P < 0.001$ ,  $F = 252.31$ ,  $df = 3$ ) varied with time of the day. Post hoc (Bonferroni) analyses showed that  $Tb_{\text{external}}$ 's varied between all time of the day comparisons, and  $Tb_{\text{internal}}$ 's between all time-of-day comparisons except afternoon and evening periods. Meteorological ( $P < 0.001$ ,  $F = 775.50$ ,  $df = 3$ ;  $P < 0.001$ ,  $F = 725.41$ ,  $df = 3$ ) and climatic seasons ( $P < 0.001$ ,  $F = 1802.23$ ,  $df = 1$ ;  $P < 0.001$ ,  $F = 1392.62$ ,  $df = 1$ ) both influenced the time-of-day comparisons of  $Tb_{\text{external}}$ 's and  $Tb_{\text{internal}}$ 's. Figure 32 depicts the mean hourly and monthly  $Tb_{\text{internal}}$ 's,  $Tb_{\text{external}}$ 's, and air temperatures for the full cohort of crocodiles.

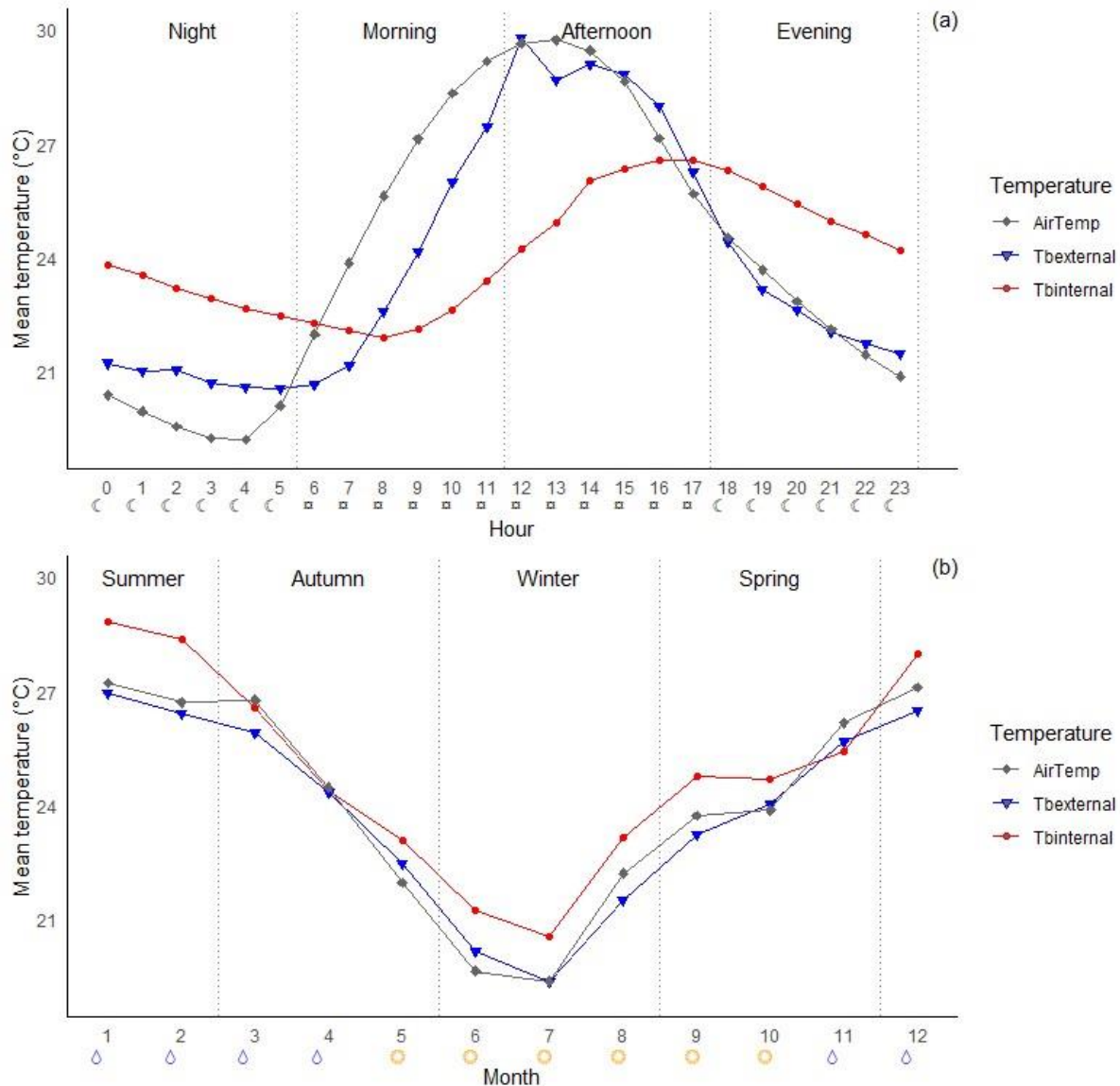


**Figure 32.** Mean hourly (a) and monthly (b) internal (“T<sub>internal</sub>”), external (“T<sub>external</sub>”), and air (“AirTemp”) temperatures. Time of day categories and day and night categories are shown in plot “a” with dotted lines on the plot and sun and moon symbols below the hours on the x-axis. Meteorological and climatic seasons are shown in plot “b” with dotted lines on the plot and colourful droplet (rainy) and sun (dry) symbols below the months on the x-axis, respectively.

T<sub>external</sub>’s varied with sex ( $P < 0.001$ ,  $F = 459.53$ ,  $df = 1$ ), and this variation exhibited meteorological seasonal trends ( $P < 0.001$ ,  $F = 6374.85$ ,  $df = 3$ ). Most sex-season post hoc (Bonferroni) comparisons were highly significant ( $P < 0.001$ ). The exceptions observed were male and female T<sub>external</sub>’s were similar (within sex) in both summer and autumn seasons, and male T<sub>external</sub>’s in autumn did not differ from female T<sub>external</sub>’s in spring ( $P > 0.05$ ). The effects of climatic (rainy versus dry) season on T<sub>external</sub>’s were also significant ( $P < 0.001$ ,  $F = 15709.70$ ,  $df = 1$ ), all pairwise comparisons were significant ( $P < 0.001$ ) except between females and males during the dry season ( $P > 0.05$ ). T<sub>internal</sub>’s varied with sex ( $P < 0.001$ ,  $F = 263.52$ ,  $df = 1$ ), and this variation exhibited meteorological seasonal trends ( $P < 0.001$ ,  $F = 3478.67$ ,  $df = 3$ ). All sex-meteorological season post hoc comparisons were significant (all  $P < 0.05$ ) except between males in autumn and males in spring ( $P > 0.05$ ). The effects of climatic (rainy versus dry) season on T<sub>internal</sub>’s were also significant ( $P < 0.001$ ,  $F = 5014.40$ ,  $df = 1$ ), all sex-climatic season

pairwise comparisons were significant ( $P < 0.001$ ). Figure 33 depicts the average  $T_{b_{\text{internal}}}$ 's and  $T_{b_{\text{external}}}$ 's of both sexes, per month.

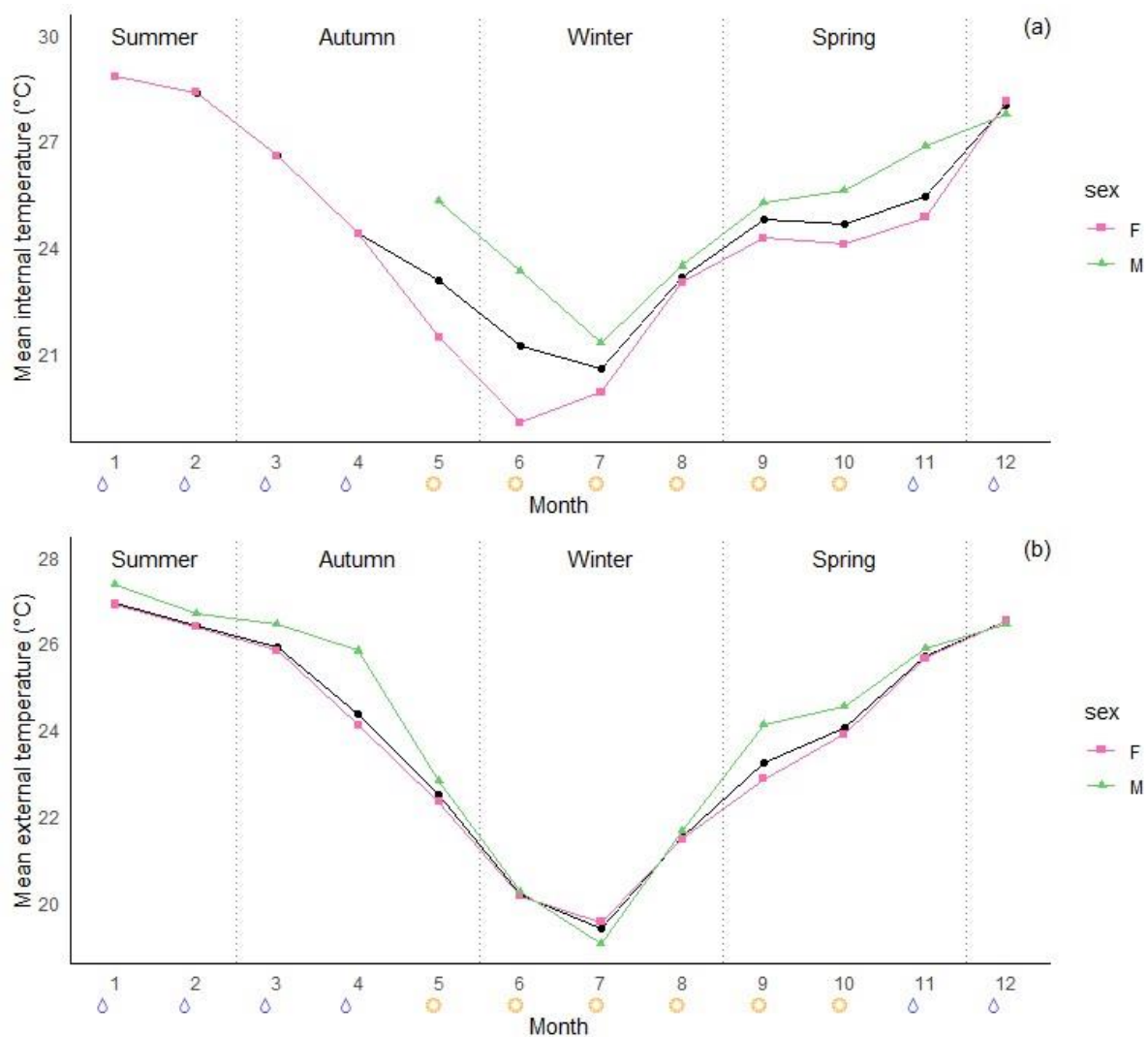


**Figure 33.** Mean monthly internal (a) and external (b) temperatures, for all crocodiles (black plot) and per sex (see legend). Meteorological and climatic seasons are shown with dotted lines on the plots and droplet (rainy) and sun (dry) symbols below the month numbers, respectively.

A GLMM analysis indicated that  $T_{b_{\text{internal}}}$ 's were significantly affected by  $T_{b_{\text{external}}}$ 's ( $P < 0.001$ ,  $F = 2305.36$ ,  $df = 1$ ), air temperatures ( $P < 0.001$ ,  $F = 1311.01$ ,  $df = 1$ ), crocodile total lengths ( $P < 0.005$ ,  $F = 9.55$ ,  $df = 1$ ), and activity levels ( $P < 0.001$ ,  $F = 81.24$ ,  $df = 1$ ). For every 1 °C increase in  $T_{b_{\text{external}}}$ ,  $T_{b_{\text{internal}}}$  increased by 0.28 °C. For every 1 °C increase in air temperatures,  $T_{b_{\text{internal}}}$  increased by 0.20 °C. Although the magnitude of the effects of  $T_{b_{\text{external}}}$  and air temperature on  $T_{b_{\text{internal}}}$  varied with each season, the direction of these effects remained consistent across all seasons. There was a weak positive correlation between  $T_{b_{\text{internal}}}$  and TL ( $r = 0.04$ ,  $P < 0.05$ ) and a weak positive correlation between  $T_{b_{\text{internal}}}$ 's and activity levels ( $r = 0.11$ ,  $P < 0.05$ ).

$T_{b_{\text{external}}}$ 's varied significantly with air temperatures ( $P < 0.001$ ,  $F = 18944.96$ ,  $df = 1$ ), TL of the crocodiles ( $P < 0.001$ ,  $F = 41.23$ ,  $df = 1$ ), and activity levels ( $P < 0.001$ ,  $F = 15.85$ ,  $df = 1$ ). Each 0.59 °C increase in air temperatures resulted in a 1 °C increase in  $T_{b_{\text{external}}}$ 's. The influence of air temperatures on  $T_{b_{\text{external}}}$ 's varied with season, but the direction of these effects was consistent across all seasons.

$T_{b_{\text{external}}}$ 's and total length were weakly and negatively correlated ( $r = -0.07$ ,  $P < 0.05$ ), and  $T_{b_{\text{external}}}$ 's and activity levels were weakly and positively correlated ( $r = 0.08$ ,  $P < 0.05$ ).

#### 5.5.5. Thermal behavioural inferences

The thermal behaviours (“heating” and “cooling”) exhibited varied significantly with air temperatures ( $P < 0.001$ ,  $F = 1833.19$ ,  $df = 3$ ), activity levels ( $P < 0.001$ ,  $F = 52.87$ ,  $df = 3$ ), and hour of the day ( $P < 0.001$ ,  $F = 38.76$ ,  $df = 3$ ). The mean air temperature when heating was  $26.20\text{ }^{\circ}\text{C}$  and when cooling was  $21.31\text{ }^{\circ}\text{C}$ . The mean crocodile activity levels when heating versus cooling were  $16040.81$  counts/hour and  $27696.41$  counts/hour, respectively. The proportion of each thermal behaviour exhibited per hour of the day also varied with crocodile sex ( $P < 0.001$ ,  $z = 27.38$ ,  $\beta = 0.90$ ,  $SE = 0.002$ ), meteorological seasons ( $P < 0.001$ ,  $z = 17.63$ ,  $\beta = 1.17$ ,  $SE = 0.07$  for summer compared to winter), and climatic seasons ( $P < 0.001$ ,  $z = 7.55$ ,  $\beta = 0.22$ ,  $SE = 0.03$ ). Figure 34 depicts the proportional thermal behaviours exhibited on an hourly basis, by crocodiles of both sexes. Proportional heating versus cooling behaviours varied between males and females between the hours of 18:00–09:00 (all  $P < 0.05$ ), but not between the hours of 10:00–17:00 ( $P > 0.05$ ). Specifically, female crocodiles had greater proportions of heating behaviours during the hours 18:00-09:00 than male crocodiles. The proportion of heating and cooling behaviours exhibited varied between all meteorological seasons (all  $P < 0.001$ , except between winter and autumn where  $P < 0.05$ ).

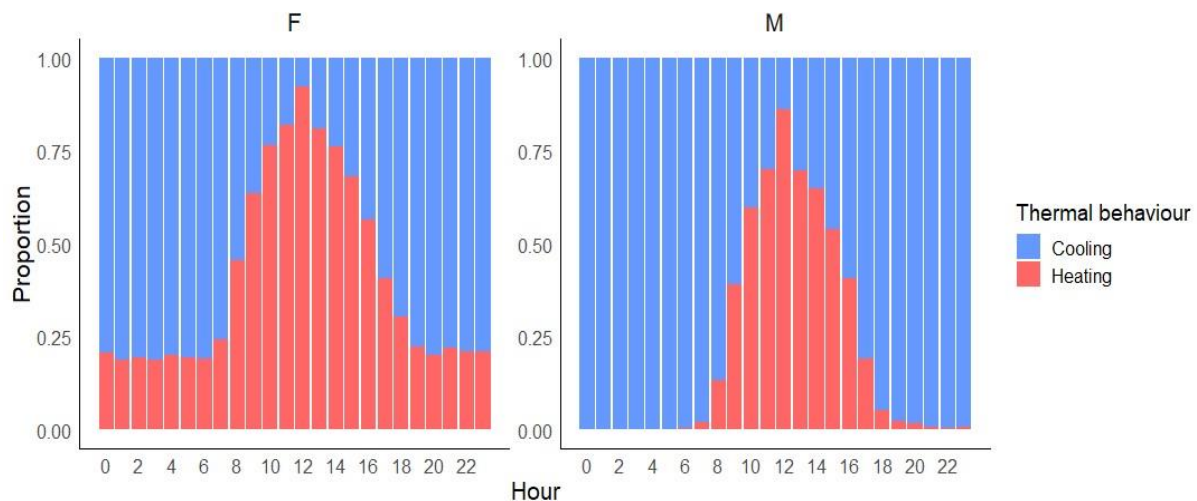


**Figure 34.** A proportional display of hourly inferred heating and cooling behaviours per sex of the crocodiles.

The hourly trends in the differences between body ( $T_{b_{\text{internal}}}$  and  $T_{b_{\text{external}}}$ ) and air temperatures, although similar in form, varied across meteorological seasons, sex, and hour of the day. The variable representing the difference between  $T_{b_{\text{external}}}$  and air temperatures (external body temperature – air temperature) was significantly affected by hour, sex, and meteorological season ( $P < 0.001$ ,  $F = 43.94$ ,  $df = 1$ ;  $P < 0.001$ ,  $F = 813.26$ ,  $df = 1$ ;  $P < 0.001$ ,  $F = 42.60$ ,  $df = 3$ , respectively). The variable representing the difference between  $T_{b_{\text{internal}}}$  and air temperatures ( $T_{b_{\text{internal}}} - \text{air temperature}$ ) was significantly affected by hour, sex, and meteorological season ( $P < 0.001$ ,  $F = 28.48$ ,  $df = 1$ ;  $P < 0.001$ ,  $F = 754.42$ ,  $df = 1$ ;  $P < 0.001$ ,  $F = 76.73$ ,  $df = 3$ , respectively). The variable representing the difference between  $T_{b_{\text{internal}}}$  and  $T_{b_{\text{external}}}$  (internal body temperature - external body temperature) was significantly affected by sex and meteorological season ( $P < 0.001$ ,  $F = 615.91$ ,  $df = 1$ ;  $P < 0.001$ ,  $F = 79.82$ ,  $df = 3$ ), but not hour of the day ( $P > 0.05$ ). Seasonal variations in these behavioural inference plots are depicted in figure 35. The general trends did not vary for the  $T_{b_{\text{internal}}}$  comparisons, nevertheless, slight seasonal variations were present. The  $T_{b_{\text{external}}}$  to air temperature comparisons, however, showed variable trends depending on season, these were particularly evident when comparing the near single-modal summer

trend against the double-modal winter trend. Interestingly, the spring and autumn comparisons were similar.

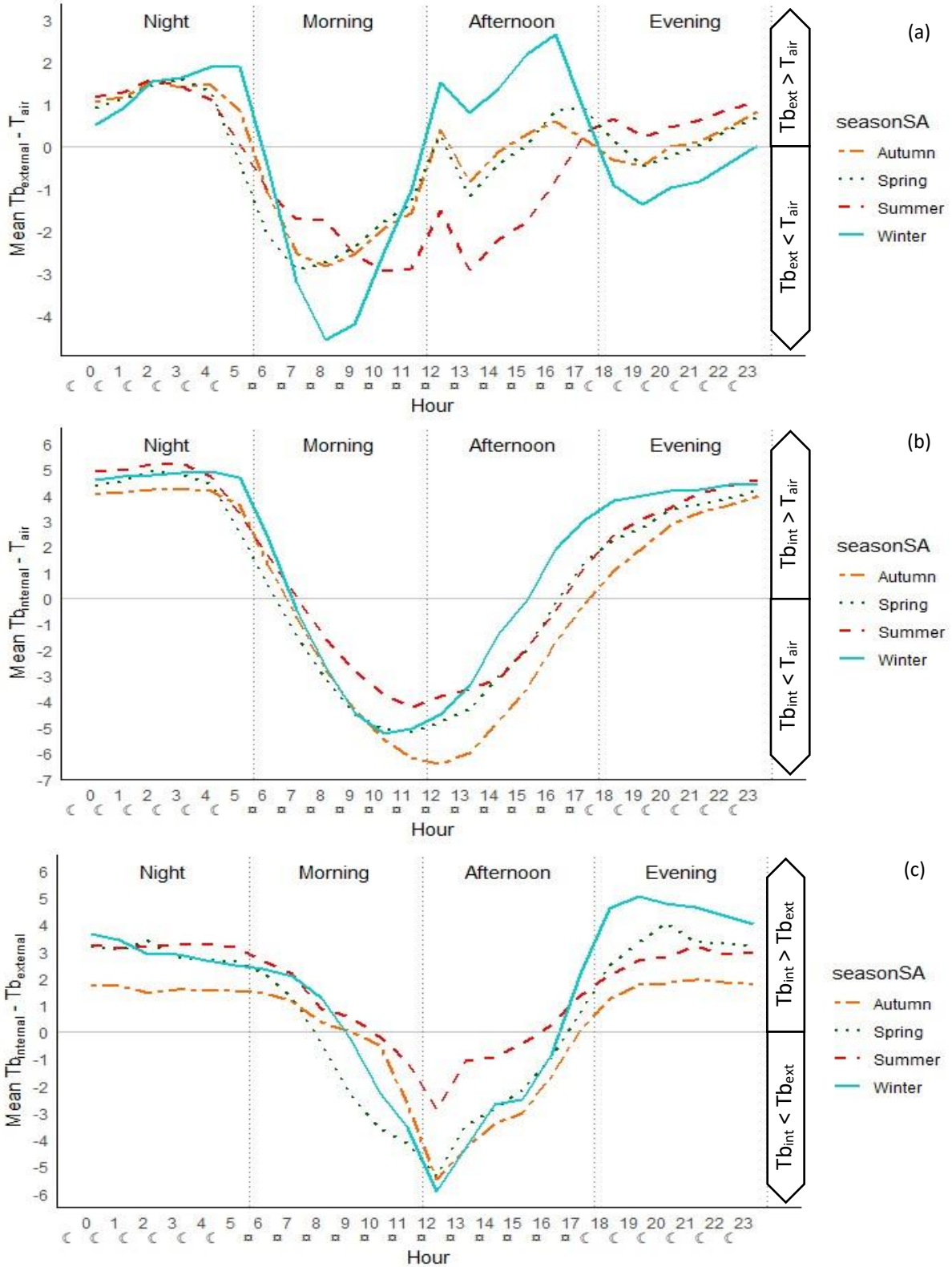


**Figure 35.** Mean hourly variations in temperature differences between internal (“ $Tb_{\text{int}}$ ”), external (“ $Tb_{\text{ext}}$ ”), and air temperature (“ $T_{\text{air}}$ ”) measurements across meteorological seasons. Time of day categories and day and night categories are shown with dotted lines on the plot and sun and moon symbols below the hours on the x-axis. Each season is represented by a unique colour and line texture

for clarity. A horizontal line at  $y = 0$  indicates the baseline where there is no difference, facilitating the comparison of temperatures above and below this threshold.

Regression analyses between  $T_{b_{\text{internal}}}$ ,  $T_{b_{\text{external}}}$ , and air temperature were all significant (all  $P < 0.001$ ) positive S-curve relationships (figure 36). There was a moderate relationship between  $T_{b_{\text{internal}}}$  and  $T_{b_{\text{external}}}$  ( $R^2 = 0.35$ ), a weak relationship between  $T_{b_{\text{internal}}}$  and air temperature ( $R^2 = 0.26$ ), and a strong relationship between air temperature and  $T_{b_{\text{external}}}$  ( $R^2 = 0.63$ ). These regression relationships can be visualized in equations 14–16.

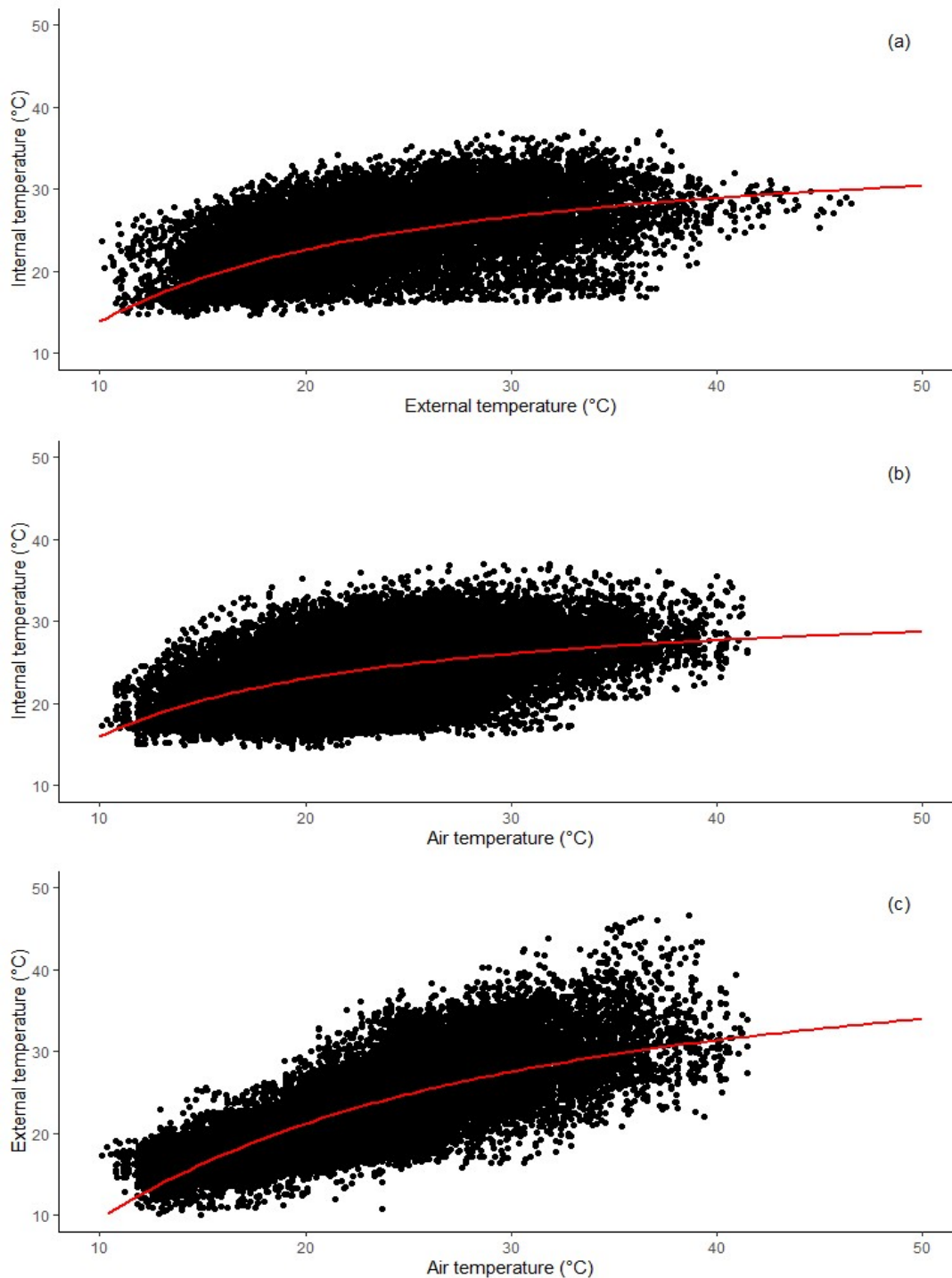


**Figure 36.** Scatterplots of internal versus external temperatures (a), internal versus air temperatures (b), and external versus air temperatures (c).

$$Tb_{\text{internal}} = e^{(3.610 + (-9.806)/Tb_{\text{external}})}, (R^2 = 0.35; P < 0.001) \quad \text{Equation 14}$$

$$Tb_{\text{internal}} = e^{(3.506 + (-7.366)/T_{\text{air}})}, (R^2 = 0.26; P < 0.001) \quad \text{Equation 15}$$

$$Tb_{\text{external}} = e^{(3.839 + (-15.706)/T_{\text{air}})}, (R^2 = 0.63; P < 0.001) \quad \text{Equation 16}$$

### 5.5.6. Crocodile activity

Male and female crocodile riverine habitat use for the current study are depicted in figure 37. Plotting each crocodile's longitudes and latitudes allowed a measure of visualization of the (linear) extent of river utilization. The extent of river use was similar between the sexes; however, the dam use differed noticeably. The deeper waters of the dam were primarily utilized during the winter, followed by intermediate dam use in spring and autumn, and minimal use during summer.

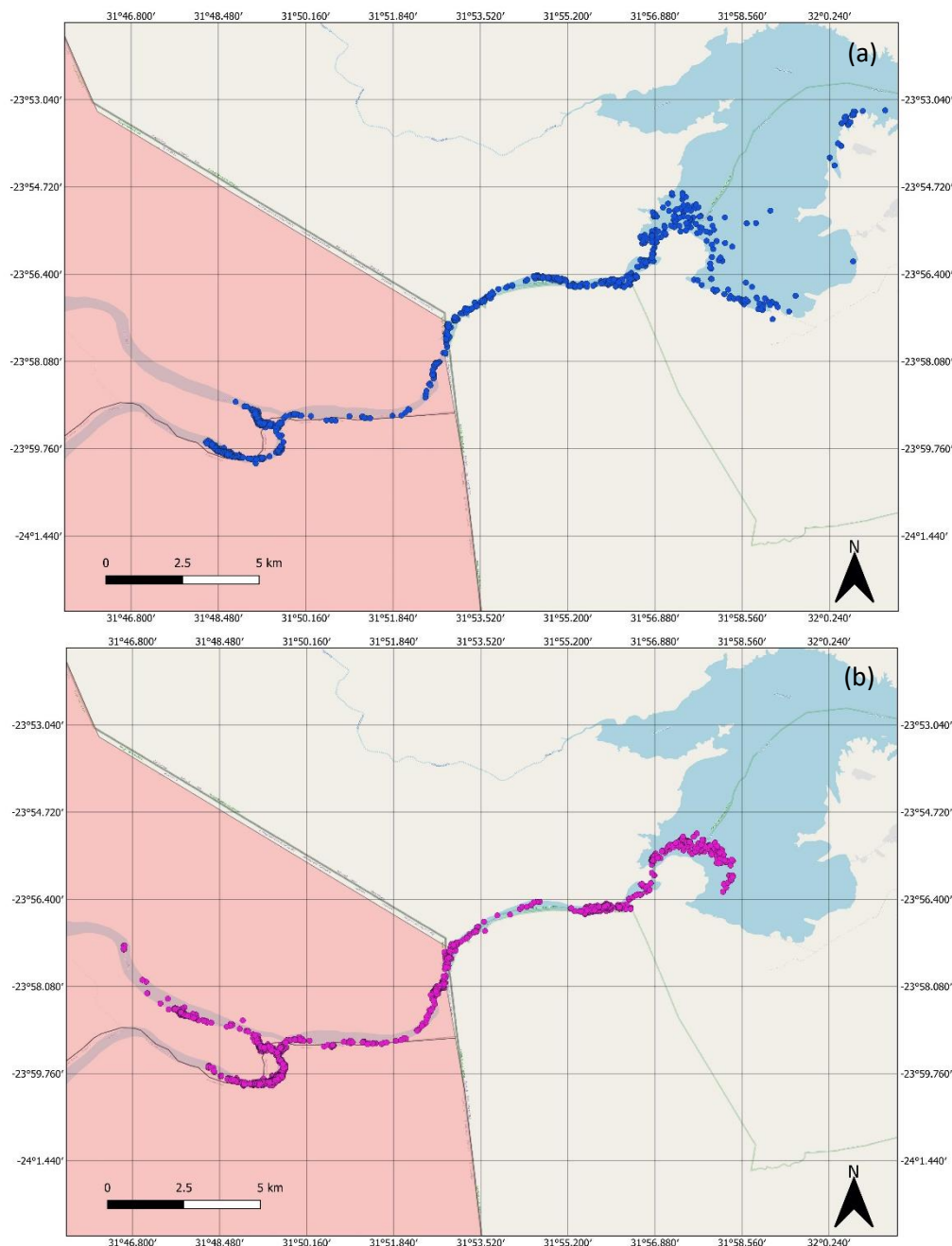
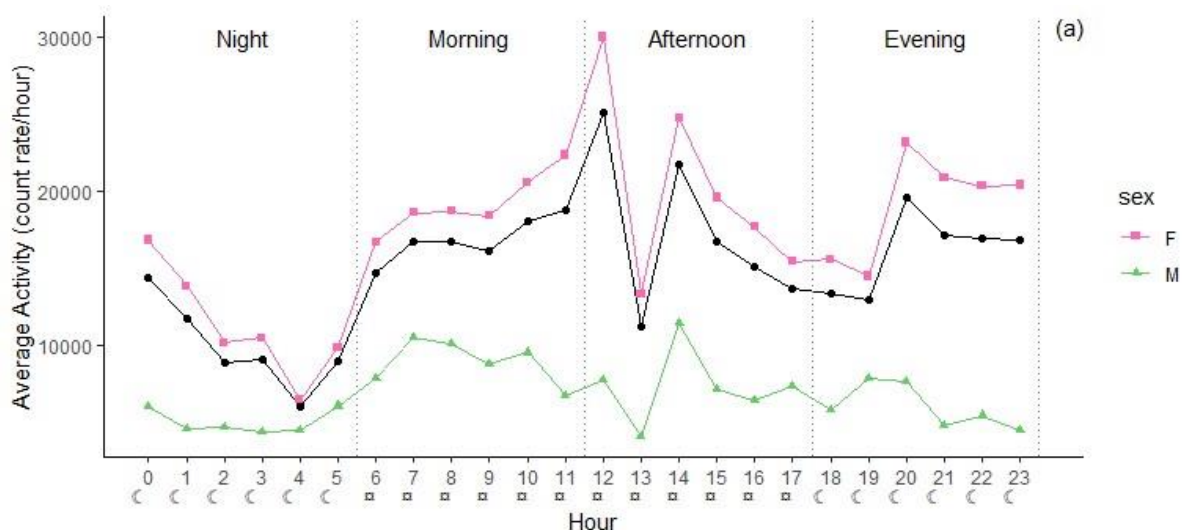


**Figure 37.** The extent of riverine habitat-use by all male (a) and all female (b) Nile crocodiles from 2018–2020.

Activity was assessed for the full cohort of crocodiles in this study. Activity levels, which are presented as the count rates per hour of the tilt/vibration sensor, ranged from 0–10589565 counts ( $\bar{x}$  = 15055 counts, SE = 483.66 counts) for all crocodiles. Both males and females had counts beginning at zero, the highest count rate for males was 3480883. Day and nighttime activity levels varied significantly ( $P < 0.001$ ,  $F = 17.63$ ,  $df = 1$ ). When comparing across sex, female crocodile day and nighttime activities varied significantly from one another ( $P < 0.001$ ,  $t = 4.08$ ,  $df = 86435$ ), this did not hold true for males ( $P > 0.05$ ).

A GLMM analysis indicated that activity varied significantly with  $Tb_{\text{internal}}$ 's ( $P < 0.001$ ,  $F = 85.32$ ,  $df = 1$ ),  $Tb_{\text{external}}$ 's ( $P < 0.001$ ,  $F = 20.31$ ,  $df = 1$ ), air temperatures ( $P < 0.001$ ,  $F = 28.79$ ,  $df = 1$ ), and total length of the crocodiles ( $P < 0.001$ ,  $F = 76.64$ ,  $df = 1$ ). For every 1 °C increase in air temperatures, the activity readings increased by 2262.87 counts. For every 1 °C increase in  $Tb_{\text{external}}$ 's, the activity readings decreased by 2063.32 counts. For every 1 °C increase in  $Tb_{\text{internal}}$ 's, the activity readings increased by 4494.83 counts. Overall, the effects of air temperatures,  $Tb_{\text{external}}$ 's, and  $Tb_{\text{internal}}$ 's on activity varied in both magnitude and direction across seasons, with their significance also differing. There was a weak positive correlation between activity and air temperature ( $r = 0.1$ ,  $P < 0.05$ ) and a weak negative correlation between activity levels and total lengths ( $r = -0.05$ ,  $P < 0.05$ ).

Activity levels varied with hour of the day ( $P < 0.001$ ,  $F = 3.38$ ,  $df = 23$ ) and month of the year ( $P < 0.001$ ,  $F = 76.63$ ,  $df = 11$ ), sex also impacted these findings ( $P < 0.001$ ,  $F = 84.32$ ,  $df = 1$ ;  $P < 0.001$ ,  $F = 27.16$ ,  $df = 1$ , respectively) (figure 38). A Bonferroni post hoc analysis of the full dataset indicated that there were activity level variations between the following hours only ( $P < 0.05$ ): 12:00 varied from 01:00–05:00 and 13:00, and 04:00 varied from 11:00, 14:00, and 20:00. The following hours did not vary from any other hours in terms of mean activity levels: 06:00–10:00, 15:00–19:00, and 21:00–00:00 ( $P > 0.05$ ). A post hoc analysis of the full dataset revealed that monthly activity levels varied erratically. Activity levels in December varied from all months except January, which similarly varied from all months except December (all  $P < 0.001$ ). February activity levels varied from those of all other months ( $P > 0.001$ ). Activity levels in March varied from those in May, July, and August; May activity levels also varied from those in April, which also varied from those in August ( $P < 0.001$ ). No other significant differences in monthly activity levels were identified ( $P > 0.05$ ).



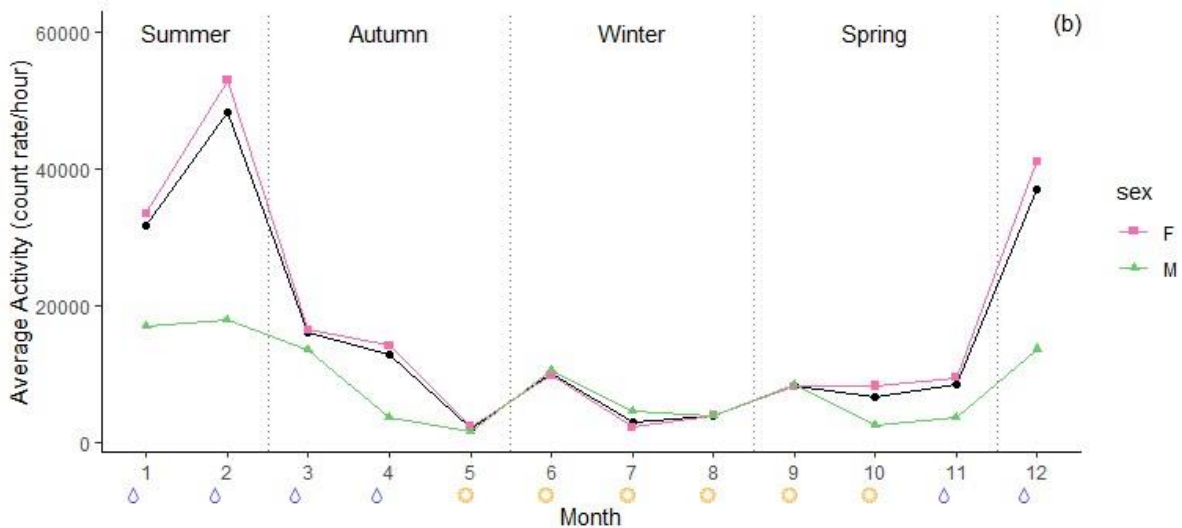


**Figure 38.** Mean hourly (a) and monthly (b) activity per season of the year. Male (M) and female (F) activities have been illustrated separately. Time of day categories and day and night categories are shown in plot “a” with dotted lines on the plot and sun and moon symbols below the hours on the x-axis. Meteorological and climatic seasons are shown in plot “b” with dotted lines on the plot and droplet (rainy) and sun (dry) symbols below the month numbers, respectively.

Activity levels varied between both meteorological and climatic seasons ( $P < 0.001$ ,  $F = 252.19$ ,  $df = 3$ ;  $P < 0.001$ ,  $F = 386.25$ ,  $df = 1$ , respectively). Activity levels in summer were significantly higher than those of all other seasons (all  $P < 0.001$ ) and autumn activity levels were also higher than winter activity levels ( $P < 0.05$ ). These seasonal comparisons held true for females, however, when assessing male activity levels, the variations between winter and autumn fell away. When it came to the climatic season comparisons, activity levels in the rainy season were consistently higher than those of the dry season, over all hours of the day ( $P < 0.05$ ). When further assessing this finding sex influenced rainy versus dry season activity ( $P < 0.001$ ,  $F = 29.69$ ,  $df = 1$ ), both male and female crocodiles were more active in the rainy than the dry season ( $P > 0.05$ ;  $P > 0.001$ , respectively). Male and female activity levels varied from one another in the rainy season ( $P < 0.001$ ), but not in the dry season ( $P > 0.05$ ).

Activity levels varied with the pre-defined time of the day categories of morning, afternoon, evening, and night ( $P < 0.001$ ,  $F = 12.76$ ,  $df = 3$ ). Specifically, night observations varied from all other times of the day (all  $P < 0.001$ ), no other variations were seen in activity levels ( $P > 0.05$ ). When compared between sexes this finding only held true for female crocodiles, male crocodile activity levels did not vary between any time of the day comparisons. Meteorological season had a significant impact on the activity levels expressed per time of day ( $P < 0.001$ ,  $F = 252.34$ ,  $df = 3$ ). In the autumn months, evening activity levels varied from morning and night activity levels ( $P < 0.05$ ;  $P < 0.001$ , respectively). In summer, the activity outputs of the crocodiles varied between most times of the day (all  $P < 0.001$ ), except between afternoon and morning, and evening and night ( $P > 0.05$ ). There were no significant differences found between crocodile activity levels between any time of the day comparisons for the seasons of spring or winter ( $P > 0.05$ ). These findings coincided, statistically, with the climatic (rainy and dry) season ( $P < 0.001$ ,  $F = 260.57$ ,  $df = 1$ ) and the day and nighttime (sun presence or absence) classifications ( $P < 0.001$ ,  $F = 17.67$ ,  $df = 1$ ) of activity levels. Crocodile activity levels in the dry season did not vary between day and nighttime ( $P > 0.05$ ), whereas in the rainy season the day and night activity levels varied significantly ( $P < 0.001$ ). Day and nighttime activity levels varied with sex of the crocodiles ( $P < 0.001$ ,  $F = 84.38$ ,  $df = 1$ ), but only for females ( $P < 0.001$ ) and not males ( $P > 0.05$ ). Female day and nighttime activity means were 19702.86 counts/hour and 15215.19 counts/hour,

respectively. Male day and nighttime activity counts were 8166.78 counts/hour and 5575.75 counts/hour, respectively. Figure 39 depicts the mean hourly activity over the meteorological and climatic seasons, as well as the impact of sex on these results.

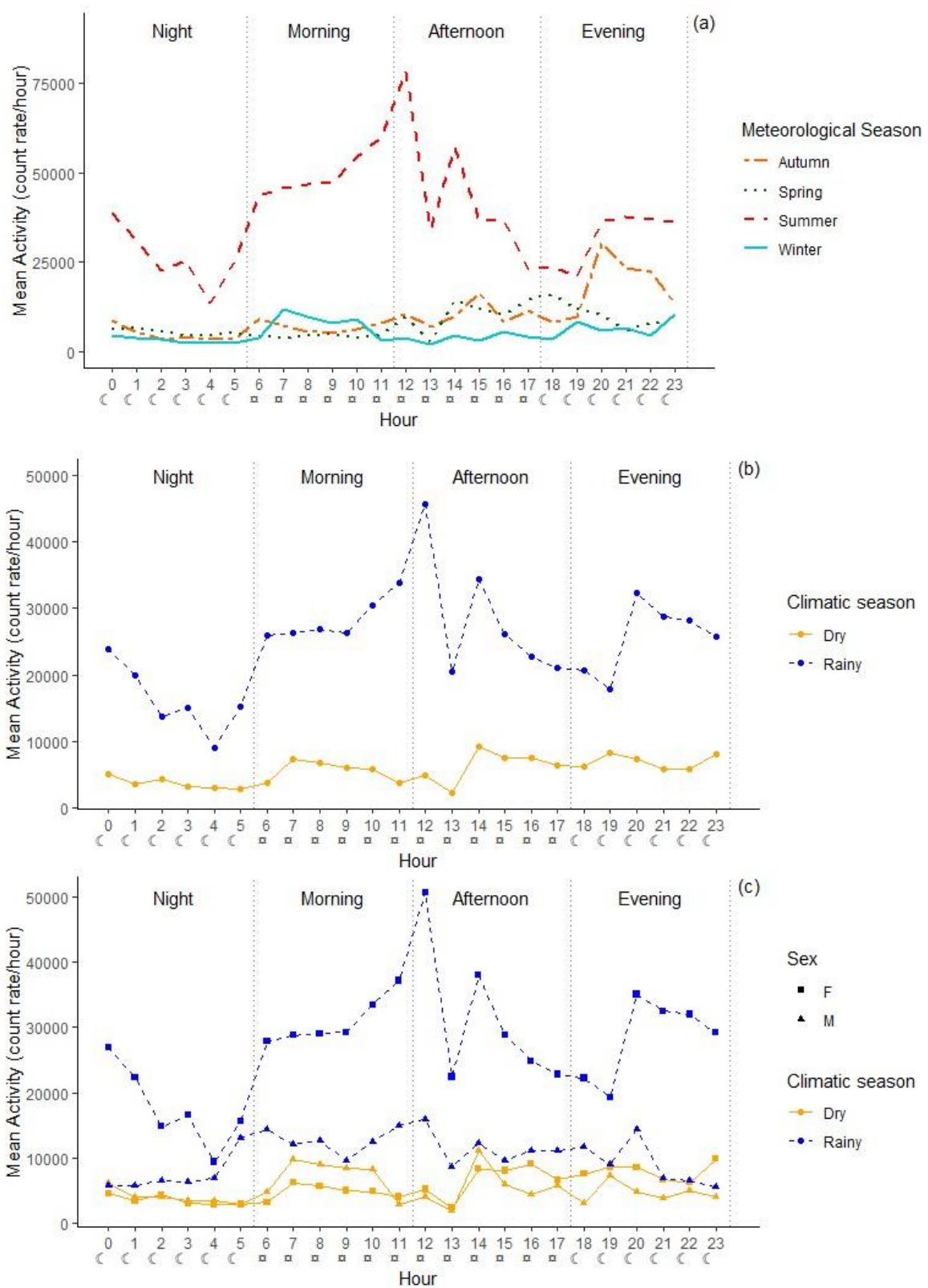


**Figure 39.** Mean hourly activity per meteorological (a) and climatic (b) seasons of the year. (c) Depicts the mean hourly activity over the climatic seasons, with sex as an added element. Time of day

categories and day and nighttime categories are shown with dotted lines on the plot and sun and moon symbols below the hours on the x-axis, respectively.

## 5.6. DISCUSSION

### 5.6.1. Crocodile temperatures

Data loggers deployed on female crocodiles exhibited longer functional durations compared to those deployed on males, this applied to both internally and externally attached devices between 2018 and 2020. For internal loggers, the disparity may have been related to the relative size of the logger in proportion to the crocodiles' body size. Given that the loggers were uniform in size, but the crocodiles varied in size (sex dependent), it is plausible that the dimensions of the male crocodiles' pyloric sphincters expedited the passage of the loggers, reducing the retention time. Regarding the external loggers, female crocodiles maintained functioning loggers for four times as long as males on average. This variation suggests a sex-specific interaction with the externally attached devices, which could be influenced by behavioural factors such as increased male aggression or territorial disputes during breeding seasons. Previous Nile crocodile studies have similarly noted that size and reproductive status (in females) impacted transmitter lifespans (Strauss *et al.*, 2008; Calverley & Downs, 2015).

A selection of individual crocodile  $Tb_{\text{internal}}$ 's was compared across seasons, size, and sex to identify and acknowledge individual variations and similarities. As the study site was a natural stretch of river, and there were no limitations on the crocodiles' movements, no crocodile would have experienced precisely the same thermal microclimates from day-to-day (Gertenbach, 1983; Venter & Gertenbach, 1986). There are also other variables at play when considering body temperature variations, ranging from crocodile size and thermal inertia effects to nutritional state or breeding status. In the plots presented in figures 29–31, the  $Tb_{\text{internal}}$  maximums and minimums lagged the daily air temperatures. The diurnal  $Tb_{\text{internal}}$  patterns exhibited by the crocodiles were present across all plots. Cooler air temperatures seemed to allow wider daily body temperature ranges for the crocodiles. On the occasion where one crocodile's  $Tb_{\text{internal}}$ 's varied substantially from those of the other crocodiles (see 20 November 2018 on figure 30b) the following possible explanations were considered: the crocodile may have recently fed, or the female may have been scouting a nesting site that day as this plot falls within the breeding season (October–January, as per Swanepoel<sup>2</sup> *et al.*, 2000).

Regardless of the time of year plotted, the crocodiles managed to successfully maintain maximum  $Tb_{\text{internal}}$ 's in the low 30s and minimums nearing 15 °C only on the very coldest of days. Thermoconforming ( $Tb_{\text{internal}}$  closely tracking ambient/air temperatures) and thermoregulating ( $Tb_{\text{internal}}$  remain constant regardless of air temperatures) occurrences were both encountered. Speculations regarding these two thermal behaviours were made with the other plotted crocodiles in mind. When plotting a single crocodile there were instances where it appeared that crocodile was thermoconforming; however, when another crocodile was plotted alongside it this outlook sometimes changed as the new individual's thermal experiences altered the perception of which animals were conforming versus regulating. Specifically, it seemed that the crocodiles in this study had greater need to thermoregulate during the hotter weeks depicted. These two thermal regulation mechanisms were interchangeable options, likely immediate-environment dependent. This is suggestive of the cooler air temperatures being closer to preferred body temperatures. In winter, crocodiles were able to allow their body temperatures to be dictated by ambient temperatures to a greater extent (even accumulating heat and raising body temperatures above those of air temperatures) than in warmer weeks (spring) when heat avoidance appeared more necessary. This correlates with the relatively lower activity levels for males and females during winter and spring when compared to summer, indicative of the many "inactive" hours spent accumulating heat via basking.

When a cool day followed a relatively warm day, the crocodiles  $T_{b_{\text{internal}}}$ 's dropped and achieving the daily peak the following day was hindered for most crocodiles, this was seen twice: 15 July 2018 (winter) and 22 September 2020 (spring). This was of interest as there were similarly cool days in winter where the crocodiles  $T_{b_{\text{internal}}}$ 's peaked, and in both cases the larger (SVL) crocodiles daily  $T_{b_{\text{internal}}}$  peaks were not as high as those of the smaller crocodiles. Due to the ectothermic nature of crocodiles this might be explained as a delayed physiological response resulting in inadequate heating when ambient temperatures suddenly drop. Another explanation is that these days were potentially not only cold but also cloudy or rainy, without the opportunity to bask out in the sun the animals may not have been able to behaviourally thermoregulate effectively. In both cases the crocodiles  $T_{b_{\text{internal}}}$ 's resumed the diurnal thermal regimes in the days that followed, ruling out illness as a potential cause. These individual variations and thermal regime comparisons align with the adjustable reptilian thermostat theory (Lang, 1977).

The  $T_{b_{\text{internal}}}$ 's of the KNP Nile crocodiles ranged from 14.53–37.07 °C across all seasons. Hocutt (2022) presented data from a nine-month period during 1986–1987 detailing  $T_{b_{\text{internal}}}$ 's of Nile crocodiles (1.94–3.48 m TL) in Lake Ngezi in Zimbabwe, these crocodiles exhibited maximum  $T_{b_{\text{internal}}}$ 's of 36.4 °C. The crocodiles in the current study exhibited very similar  $T_{b_{\text{internal}}}$  maximums. Downs *et al.* (2008) found  $T_{b_{\text{internal}}}$ 's of Nile crocodiles in lake St. Lucia (South Africa), ranging in total length from 1.14–2.62 m, ranged from 13.0–36.5 °C in winter. For comparative purposes the winter  $T_{b_{\text{internal}}}$ 's in the present study ranged from 14.53–34.68 °C, revealing a similar but slightly narrower range of internal body temperature regulation. In the St. Lucia study, it was noted that the crocodiles  $T_{b_{\text{internal}}}$ 's did not plateau but rather oscillated within mean ranges of 18.8–19.6 °C minimums and 26.9–29.2 °C maximums which were attained at approximately 07:00–08:00 and 14:00–15:00, respectively (Downs *et al.*, 2008). Examining the mean hourly winter data for the current study showed daily  $T_{b_{\text{internal}}}$  minima of 18.82 °C and maxima of 24.79 °C, which were achieved at approximately 03:00–07:00 and 12:00–15:00 within that meteorological season. Grigg *et al.* (1998) studied saltwater crocodiles and similarly recorded no daily plateaus in  $T_{b_{\text{internal}}}$ 's, as had been found in smaller crocodiles. Although the study locations, crocodile sizes, logger types, and logger placement/implantation methods varied for these studies, they all build toward our knowledge and understanding of the thermal experiences of Nile crocodiles.

Mean hourly  $T_{b_{\text{external}}}$ 's ranged between 21–30 °C throughout the day and followed a diurnal pattern of increasing following sunrise and decreasing during and after sunset. Mean  $T_{b_{\text{external}}}$ 's lagged air temperatures during the morning hours, peaking in the early afternoon and then, catching up, remained consistent with air temperatures into the evening. When nighttime air temperatures dipped below 20 °C the  $T_{b_{\text{external}}}$ 's levelled off at approximately 21 °C and remained there until morning. Mean  $T_{b_{\text{internal}}}$ 's lagged air and  $T_{b_{\text{external}}}$ 's and were maintained within a narrower range of approximately 22–26 °C, peaking in the late afternoons and slowly decreasing during the night reaching a minimum at around 08:00. This diurnal pattern of  $T_{b_{\text{external}}}$ 's remained consistent over meteorological seasons, except that the temperature ranges exhibited shifted seasonally, highlighting the active thermoregulatory behaviour of the crocodiles in this study.

Monthly mean  $T_{b_{\text{internal}}}$ 's and  $T_{b_{\text{external}}}$ 's of the Nile crocodiles in this study followed a similar pattern throughout the year mimicking, but lagging, seasonal air temperatures. Body temperatures ( $T_{b_{\text{internal}}}$  and  $T_{b_{\text{external}}}$ ) increased between August to January and then decreased from February to July. The lead up to the winter months showed sudden decreases from April to May, with June and July mean  $T_{b_{\text{internal}}}$ 's and  $T_{b_{\text{external}}}$ 's in the 19–21 °C range. Mean ambient and body temperatures in the summer months were the highest. Males maintained  $T_{b_{\text{internal}}}$ 's above those of the female crocodiles for all months except the first month of summer (December). Although mean male  $T_{b_{\text{internal}}}$ 's were not

available between January and April, the plotted results suggest that the male crocodiles began selecting slightly higher  $T_{b_{\text{internal}}}$ 's at this time. This was likely related not only to seasonal air temperature variations but to a reproductive component as well. Previous studies have found that crocodilian body temperatures (both male and female) increase as ambient temperatures do and this is associated with the initiation of reproductive cycles (Grigg & Gans, 1993; Lance, 1989). Higher body temperatures both expediate and contribute to successful spermatogenesis, ovarian cycle initiation, and vitellogenesis (Grigg & Gans, 1993; Lance, 1989). Larger (TL) crocodiles had statistically higher  $T_{b_{\text{internal}}}$ 's than smaller crocodiles. From the monthly temperature plots delineated by sex, and the individual  $T_{b_{\text{internal}}}$  plots, this was more pronounced in the warmer months of the year. Based on previous studies, some explanations for this observation include surface area to volume variations between larger and smaller individuals (males were generally larger), the greater thermal inertia of larger crocodiles enabling them to maintain body temperatures for longer periods than smaller individuals, reproductive requirements, or behavioural and physiological variations in thermoregulatory activities between larger and smaller crocodiles (Colbert *et al.*, 1946; Lance, 1989; Grigg & Gans, 1993; Lang, 1997; Grigg *et al.*, 1998; Seebacher *et al.*, 1999; Downs *et al.*, 2008).

A Pearson correlation analysis indicated a strong, and statistically significant, positive relationship between  $T_{b_{\text{internal}}}$ 's and  $T_{b_{\text{external}}}$ 's. However, independent t-tests and a GLMM analysis found significant differences in the temperatures recorded internally versus externally. Furthermore, regression analysis yielded a modest but statistically significant coefficient of determination ( $R^2 = 0.35$ ). Meteorological season comparisons of the data maintained these general findings, with variations in the strength of the relationship observed across different seasons.  $T_b$ 's of crocodilians are dependent, to an extent, on temperatures available in their immediate environments. These findings come together to highlight a moderate portion of  $T_{b_{\text{internal}}}$  dependence on  $T_{b_{\text{external}}}$ 's. Factors such as individual variations in thermoregulatory behaviours and physiologies, nutritional and reproductive status, and microclimate variations (dependent on each crocodiles' locational preferences) are assumed to have accounted for the rest.

#### 5.6.2. Thermal behaviour inferences

Heating (or heat seeking) and cooling (or heat avoidance) behaviours followed diurnal trends for all crocodiles in the study. These trends are synonymous with thermoregulatory behaviours which are well documented in large crocodiles (Grigg *et al.*, 1998; Downs *et al.*, 2008; Hocutt, 2022). When the impact of sex was assessed, the proportion of male crocodiles exhibiting heating versus cooling behaviours during the evening and nights varied from that of females. A small proportion of female crocodiles exhibited heating behaviours throughout the evening and night, whereas the majority if not all male crocodiles exhibited cooling behaviours during these times. This held true across both meteorological and climatic seasons; the proportion of females heating at night was greater in the dry season, and lowest in summer when compared to the other meteorological seasons. Thermal inertia is proposed as a contributor to this finding (Colbert *et al.*, 1946; Lang, 1977). Males were generally larger (TL) than females and due to thermal inertia would have lost their cumulated body heat from the day slower than smaller individuals, meaning they remained warmer than their surroundings for much of the evening and night. Most females experienced cooling behaviour in the evening and night as well; however, a small proportion of females were able to heat throughout the evening and night. This could be due to several factors such as physiological and nutritional states, breeding/nesting behaviours, seasonal air and water temperature variations, or individual microclimate selections. This intriguing finding warrants further investigation.

The comparative plots of the differences between the body ( $T_{b_{\text{internal}}}$  and  $T_{b_{\text{external}}}$ ) and air temperature data illustrated distinct diurnal and seasonal thermal patterns, emphasizing the influence of seasonal

changes on crocodile temperature dynamics. The erratic morning trend of the difference between air and  $T_{b_{\text{external}}}$ 's temperatures in summer was likely due to either intense shuttling activities required early in the day to haul out and begin selecting basking spots or attempts to avoid overheating in the late morning hours. Regardless of season, the crocodiles maintained higher average  $T_{b_{\text{internal}}}$ 's than that of the air or the  $T_{b_{\text{external}}}$ 's during the evening-nights. The  $T_{b_{\text{external}}}$  to air temperature comparison was more variable, reflecting the microhabitat selections (shuttling behaviours) of the crocodiles, which for the most part was continuous over meteorological season, with the widest differences seen in winter. Throughout winter, the  $T_{b_{\text{external}}}$ 's were maintained above the ambient air temperatures during the night, decreasing thereafter during the first half of the morning then gradually increasing and peaking in the early and late afternoons. This was followed by a decline in  $T_{b_{\text{external}}}$ 's during the early evening and a slow increase again into the night. The other seasons assessed showed the  $T_{b_{\text{external}}}$ 's overtaking that of air in the evenings and nights only. This is likely representative of winter-season daytime basking and nighttime return to the water, which concurs with the findings of Downs *et al.* (2008). The  $T_{b_{\text{internal}}}$  comparisons remained more stable across the meteorological seasons highlighting effective thermoregulation. There were significant differences in these variables when assessing for sex of the crocodiles; however, the general trends remained the same for both sexes. These statistical variations were likely due to a combination of season, breeding, and nesting requirements during the warmer months and size differentials during the cooler months.

Regression equations 14–16 highlighted the relationships between the various body and air temperature measurements. The relationships between  $T_{b_{\text{internal}}}$ 's and  $T_{b_{\text{external}}}$ 's ( $R^2 = 0.35$ ) and  $T_{b_{\text{internal}}}$ 's and air temperatures ( $R^2 = 0.26$ ) indicate a moderate proportion of the variance in  $T_{b_{\text{internal}}}$ 's could be explained by the crocodile's immediate environment and a less moderate proportion by the air temperatures in the region. The stronger relationship between external body and air temperatures ( $R^2 = 0.63$ ) indicates that ambient temperature has a significant impact on the temperature of the crocodiles immediate  $T_{b_{\text{external}}}$ . Crocodiles are known to bask in the sun or seek shade/water to regulate  $T_{b_{\text{internal}}}$ 's (Lang, 1987; Downs *et al.*, 2008). The low to moderate relationships involving  $T_{b_{\text{internal}}}$  confirm that while ambient temperatures influence a reptile's  $T_{b_{\text{internal}}}$ 's, there are other factors at play (e.g., behaviour, physiology, colouration) and various thermoregulatory strategies are likely employed by these animals to maintain preferred body temperatures.

### 5.6.3. Crocodile activity

Visualizing the extent of the male versus female river usage saw relatively fewer females utilizing the deeper waters of Massingir Dam. This is like a finding of Combrink (2014) where subadult/smaller Nile crocodiles in Lake St. Lucia avoided deeper waters, possibly due to predation risks from larger crocodiles. This indicates a size-related use of riverine environment; females may also have had less need to enter these deeper waters during breeding and nesting seasons as there would be less shoreline for nest site selection opportunities. The seasonal utilization of the river and dam areas likely reflects the seasonal water level fluctuations. Activity levels exhibited significant relationships with  $T_{b_{\text{internal}}}$ 's as well as air temperatures. Crocodiles were more active when their  $T_{b_{\text{internal}}}$ 's and air temperatures increased, this is synonymous with a previous wild Nile crocodile study in Lake St. Lucia (Combrink, 2014). This is an important distinction as the relationship between  $T_{b_{\text{external}}}$ 's and activity levels showed the opposite effect, indicating periods of high  $T_{b_{\text{external}}}$ 's (the likely result of basking) resulted in lowered activity levels, which suits the behavioural tendencies noted for crocodiles when they are warming up (Lang, 1977; Downs *et al.*, 2008). Larger (TL) crocodiles in this study were less active than smaller ones. One possible explanation, given that the male crocodiles were generally larger than the females, might be home range extents of male Nile crocodiles reducing in size as the crocodiles increase in size (Combrink, 2014).

The mean monthly activity levels during the dry season were comparable across sexes, with the biggest discrepancies occurring in summer. Although both male and female activity levels were significantly higher in summer compared to the other meteorological seasons, the mean female activity levels notably surpassed those of male crocodiles during this time. The increased activity in the rainy season compared to the dry season for both male and female crocodiles likely resulted from the increasing climatic temperatures and the concurrence of breeding season activities. Combrink (2014) noted an anomalous activity increase for nesting Nile crocodile females in Lake St. Lucia during the nesting season, this correlates with the sudden increase in the female's activity levels during the warmest months of the current study. Although identifying which females were definitively breeding and nesting was not possible, all crocodiles in the current study were adults and presumably could have bred. The activities of the female Nile crocodiles in KNP peaked during the summer months and began decreasing during autumn, whereas Lake St. Lucia female Nile crocodile activity peaked in autumn and summer for non-nesting females and in autumn for nesting females (Combrink, 2014). The activities of breeding, nest building, and nest guarding are all potential contributors to the activity increases observed (Hocutt *et al.*, 1992; Combrink, 2014; Calverley & Downs *et al.*, 2015).

Territory maintenance during the breeding season, courtship behaviours, and participating in breeding activities likely caused the activity increases for males during the rainy season (Pooley, 1982; Combrink, 2014). Increasing activity levels in summer were ambient temperature dependent, with an increased need for thermoregulation activities (e.g., shuttling between cooler and warmer gradients within their immediate environments) during the daylight hours to maintain comfortable  $T_{b\text{internal}}$  ranges (Cloudsley-Thompson, 1964; Hocutt *et al.*, 1992; Grigg *et al.*, 1998). Mean hourly activity levels varied between day and night classifications for female crocodiles, but not for males. Daytime activity was higher than nighttime activity for the KNP females, this contrasts with the findings of Combrink (2014) where adult Nile crocodile activity levels of both sexes peaked early in the evening.

## 5.7. CONCLUSIONS

The Nile crocodile population monitored was presumably healthy throughout the course of this study, no illness or deaths of study animals were recorded during 2018–2020. Thus, the range of  $T_{b\text{internal}}$ 's presented depicts the naturally selected and maintained  $T_{b\text{internal}}$ 's for a healthy sample of KNP crocodiles. It is doubtful that the crocodiles thermoregulated perfectly every day and this is evidenced in the individual plots where causations of variation were theorized, and instances of both thermoregulation and thermoconforming seemed interchangeable options. The daily  $T_{b\text{internal}}$  oscillations documented in the current study align with the findings of some crocodilian thermoregulation studies and deviate from others. Within some studies, individual  $T_{b\text{internal}}$ 's even varied between plateaus and oscillations, showing flexibility in crocodilian thermoregulatory capabilities (Lang, 1977; Grigg *et al.*, 1998; Downs *et al.*, 2008; Hocutt, 2022). The variation in these two thermal regimes has been proposed to be related to size of the crocodiles (Grigg *et al.*, 1998), longer term studies of a range of sizes are needed to confirm this, and potentially other contributors, for Nile crocodiles. Comparison of  $T_{b\text{internal}}$ 's and activity levels with other Nile crocodile populations in Africa showed several consistencies with what has been recorded in previous studies (Downs *et al.*, 2008; Combrink, 2014; Hocutt, 2022) despite the variable study locations, populations, and methodologies employed.

$T_{b\text{internal}}$  and activity level variations documented in the KNP Nile crocodiles were sex, size, season, and individual dependent. These influencing factors have been noted in other crocodilian studies; however, this is the first comprehensive look at a subset of KNPs adult Nile crocodile population.  $T_{b\text{internal}}$ 's increased for both males and females from November to December when ambient temperatures were highest. Although there were no  $T_{b\text{internal}}$ 's for males from January to February, if

the assumption that  $T_{b_{\text{internal}}}$ 's followed a similar pattern as that of  $T_{b_{\text{external}}}$ 's is made, then both  $T_{b_{\text{internal}}}$ 's and activity levels increased during the breeding season. Combrink (2014) also noted a breeding-season related activity spike in both male and female crocodiles. Although the causations of variation in individual  $T_{b_{\text{internal}}}$ 's for the current study are speculated, the lack of more in-depth behavioural data is one caveat of this study. Nile crocodile activity levels,  $T_{b_{\text{external}}}$ 's, and  $T_{b_{\text{internal}}}$ 's all decreased in the autumn months when mean air temperatures were decreasing, and troughed in the winter months when air temperatures were lowest.

#### 5.8. CRITICAL EVALUATION AND RECOMMENDATIONS

Future studies assessing long term body temperatures ( $T_{b_{\text{internal}}}$  and  $T_{b_{\text{external}}}$ ) and activity levels of crocodile populations might consider adding more extensive behavioural and environmental condition monitoring methods. The lack of more extensive environmental or climate data for the study period limits our understanding of the available thermal gradients and how these were utilized. Although the cohort variability gives a good idea of what the general population monitored was experiencing, there is clear individual variation when visualizing individual internal temperature comparisons. Paralleled climate and behavioural assessments will add a further dimension of understanding to similar studies.

## 6. Thermal profiles associated with nest site selection of Nile crocodiles (*Crocodylus niloticus*) on a commercial crocodile farm in South Africa

### 6.1. INTRODUCTION

The investigation of crocodile nest site selection and nest site characteristics is important in the context of climate change and related habitat alterations (Refsnider, 2012; Mainwaring *et al.*, 2017; Fukuda *et al.*, 2022). The direct and indirect effects of climate change on nest-building animals have been studied (McGaugh & Jansen, 2011; Refsnider, 2012; Telemeco *et al.*, 2013; Mainwaring *et al.*, 2017), and quantification of reptilian/crocodilian thermal regimes regarding nesting strategies is important for the future of these populations (Morjan, 2003; Murray *et al.*, 2016; Sullivan *et al.*, 2022; Fukuda *et al.*, 2022). Understanding the interrelationship between nest site selection and changing environmental conditions can assist in the development of strategies to protect crocodiles, their nesting habitats, and the ecosystem (Mainwaring *et al.*, 2017). The identification and study of crocodile nest sites in the wild can be problematic and logistically challenging. Studying farmed/captive crocodile nesting presents an opportunity to explore nest site selection and thermal preferences in a controlled setting.

Nesting activities have been documented for a variety of reptilian species, including the Nile crocodile (*Crocodylus niloticus*) (Swanepoel<sup>2</sup> *et al.*, 2000; Telemeco *et al.*, 2013; Murray *et al.*, 2020). Nest site selection and nesting success are influenced by temperature, soil composition, water proximity, height above water, vegetation cover, accessibility, human disturbance, and nesting site history (Pooley & Gans, 1976; Kofron, 1989; Hartley, 1990; Swanepoel<sup>2</sup> *et al.*, 2000; Botha, 2005; Maciejewski, 2006; Grigg, 2015). Nest site selection and maternal behaviours vary with species, location, female experience, and the presence of competing nesting females in the area (Murray *et al.*, 2020). Female egg-laying behaviours can depend on environmental cues associated with season, such as rainfall, temperature and day length (Kofron, 1989; Swanepoel<sup>2</sup> *et al.*, 2000; Refsnider, 2012; Murray *et al.*, 2020). The success of breeding, nesting, incubation, and hatching are influenced by environmental temperatures, population genetic variability, the general health of the breeding population, as well as husbandry practices for captive populations (Huchzermeyer, 2003; Bothma & Van Rooyen, 2005; Maciejewski, 2006; Bassetti *et al.*, 2014; López-Luna *et al.*, 2015; Manolis & Webb, 2016). Temperature-dependent sex determination (TSD) is well documented in crocodilians, where incubation temperatures determine the sex of the hatchlings (Deeming, 2004; Bothma & Van Rooyen, 2005; López-Luna *et al.*, 2015). Consistently high (> 34 °C) and low (< 31 °C) temperatures yield predominantly female hatchlings whilst intermediate temperatures yield predominantly males (Hutton<sup>2</sup>, 1987; Deeming, 2004; Bothma & Van Rooyen, 2005). There are concerns that climate change may negatively influence reptiles sex ratios and increase egg mortality, which could jeopardize the future stability of some populations (Maciejewski, 2006; Refsnider, 2012; Telemeco *et al.*, 2013; Hill *et al.*, 2015). Commercially farmed crocodile eggs are incubated artificially under strict temperature (29–33 °C) and humidity (90–99 % relative humidity) regimes to maximize hatching success (Bolton, 1989; Bothma & Van Rooyen, 2005; Tosun, 2013; Manolis & Webb, 2016). Incubation temperatures play a role in hatchling fertility and the pre-determination of preferred temperature ranges later in life (Lang<sup>2</sup>, 1987; Tosun, 2013; Manolis & Webb, 2016; Murray *et al.*, 2020). Egg sizes (which correlate with the size of the breeding female) and extent of sun exposure at nesting sites affect incubation temperatures (Swanepoel<sup>2</sup> *et al.*, 2000; Murray *et al.*, 2016; López-Luna *et al.*, 2020). Shading can significantly affect the temperatures within nests and possibly even egg sex ratios (Lang *et al.*, 1989; Leslie & Spotila, 2001; Botha, 2005; López-Luna *et al.*, 2015). Although most crocodiles will nest in a similar location each year, the selection of sunny versus shaded nesting sites can vary locationally and

seasonally (Lang *et al.*, 1989; López-Luna *et al.*, 2015; Combrink *et al.*, 2016). Shading adjacent to nesting sites allows female crocodiles to guard from nearby even when ambient temperatures are high (Kofron, 1989; Combrink *et al.*, 2016).

The depth at which crocodiles lay eggs varies with species and environmental conditions, including habitat quality and available nesting materials. Female crocodiles lay their eggs at depths providing stable temperatures and adequate moisture for embryo development and survival, exercising a degree of control over incubation success and sex ratios (Bolton, 1989; Bothma & Van Rooyen, 2005; Grigg, 2015; Mainwaring *et al.*, 2017; López-Luna *et al.*, 2020). Nile crocodiles typically lay eggs in holes dug into sandy or loamy soils, with nest depths of 10–45 centimetres (cm) below the soil surface, and nest widths of 18–76 cm in diameter (Pooley & Gans, 1976; Kofron, 1989; Hartley, 1990; Swanepoel<sup>2</sup> *et al.*, 2000). Female crocodiles exhibit maternal behaviour before laying, by exercising circuitous visitations to determine nest-site suitability, sometimes even digging practise nests, and after laying eggs, to defend the nesting site from predation, thermal exposure, or when it rains to keep the area directly over the nest dry (Kofron, 1989; Messel & Vorlicek, 1989; Van Weerd, 2010; Combrink *et al.*, 2016). Nesting areas available to captive/farmed crocodiles vary substantially from those of wild crocodiles. Farmed crocodile pen structures require nesting sites that are in proximity to the water for easy crocodile access, while maintaining a safe enough distance for worker safety during egg collections (Bothma & Van Rooyen, 2005; Brien *et al.*, 2007). Farm nesting sites are more controlled and closely spaced than in the wild, with flat topography, river sand substrate, and more homogeneous site conditions. Farmed crocodiles endure more frequent exposure to human disturbances than those in the wild, and the extent of shade cover over nesting sites differs between farms (Bothma & Van Rooyen, 2005; Brien *et al.*, 2007).

Nest microclimates, in and around nesting sites, have been investigated for several crocodylian species in the wild, including the Nile crocodile, using various temperature recording devices (Hutton<sup>2</sup>, 1987; Murray *et al.*, 2016; López-Luna *et al.*, 2020). iButtons are small, sturdy, steel encased temperature loggers that have been extensively applied to habitat, plant, and animal thermal studies, including crocodiles (Seebacher *et al.*, 2003; Downs *et al.*, 2008; López-Luna *et al.*, 2015; Smith *et al.*, 2015; Murray *et al.*, 2016; Fawcett *et al.*, 2019). Uncrewed aerial vehicles (UAVs), or drones, have proven useful for monitoring wild and captive animal populations (Aubert *et al.*, 2021; Viljoen<sup>1,3</sup> *et al.*, 2023). The plethora of sensor options enable animal health/condition, behaviour, temperature, population/spatial distribution, habitat use, welfare, and productivity assessments (Ezat *et al.*, 2018; Zhang *et al.*, 2020; de Kock *et al.*, 2021; Aubert *et al.*, 2021; Ramos *et al.*, 2022; Viljoen<sup>1,3</sup> *et al.*, 2023). The advantages associated with drone surveys are numerous, and include access to inaccessible areas, non-invasive surveying of shy/dangerous/skittish species, large area coverage, and fast-paced data capture (Aubert *et al.*, 2021; Viljoen<sup>1,3</sup> *et al.*, 2023). Surveying animals appropriately with drones has been assessed at length and should be considered whenever applying this technology for ethical reasons and to avoid biases introduced by vigilance reactions elicited by drone presence (Hodgson & Koh, 2016; Bevan *et al.*, 2018; Raoult *et al.*, 2020; Viljoen<sup>2</sup> *et al.*, 2023).

The thermal and locational characteristics of preferred nesting sites and nest occupancy on commercial crocodile farms has yet to be assessed to our knowledge. Thermal data for the pen, the crocodiles within the pen, and the various pen surface/substrates were collected using a thermal drone and iButtons. This allowed the combining of surface thermal data with sand (within nest sites) thermal data.

## 6.2. AIMS AND HYPOTHESES

The present study aimed to assess the current nesting environment on a crocodile farm in South Africa, examining the associations between various nest site selection parameters, with a particular

emphasis on the role of temperature. The following parameters were studied: pen area/substrate utilization, nest site occupancy versus active nesting, nesting female size and distribution over nesting sites, nest locations and orientation, nest thermal profiles, shading and grassy cover effects over different nesting areas, distances from the water bodies, and potential human disruptions.

It was hypothesized that the thermal profiles within nests and the factors affecting nest temperatures (orientation, shading, and grassy cover) would directly impact nest site and depth selections, larger and presumably more dominant females would dictate nesting area use, nests closer to waterbodies would be more frequently utilized, and that human presence would not impact nesting behaviours as these crocodiles were habituated to the environment and the frequent presence of humans (personnel and tourists).

### 6.3. MATERIALS AND METHODS

#### 6.3.1 Study site and animals

A single large breeder pen (5020 m<sup>2</sup>), on a crocodile farm in South Africa, was selected for the assessment of factors impacting nest site selection in commercial settings. The present study was conducted over a single breeding/nesting season (from October–December 2022), which spans autumn and summer in South Africa. The pen was an open-air enclosure and contained three water bodies with gradient depths, reaching a maximum of 2 m, each surrounded by concrete basking areas. Several large areas of grass and sand were interspersed between the water bodies. Nesting areas, cordoned off with short brick walls for nest separation, were dispersed throughout the pen. The only areas within the pen that possessed suitable nesting sand were those intentionally designed as nesting sites. Henceforth, the different areas of the pen will be referred to as “water” for the water bodies, “concrete” for the surrounding basking areas, “grass/sand” for the interspersed grassy areas, and “nests” for areas of the pen where bricked-off nesting areas were present.

There were 126 nest sites (exclusively fine sanded) spread throughout the pen, some nests were situated along the walls of the pen, and some were more centrally located within the pen. The nests were numbered and assigned into six “sections” by location within the pen and will be referred to as sections A–F henceforth (figure 40). Within these sections the nests varied in orientation, which was defined as the compass direction that each nest-opening faced. Four nest orientations were defined: Southeast (SE) facing, Northeast (NE) facing, Southwest (SW) facing, and Northwest (NW) facing. The neighbouring tourism building included a walkway which extended part way into the pen. This walkway was situated at ground level, flanked by brick walls and safety fencing, and included a sheet-metal roof. Shading (dependent on the time of day) was provided by the tall brick perimeter walls of the pen, trees external to and within the pen, shade netting, and the roof over the tourist walkway.

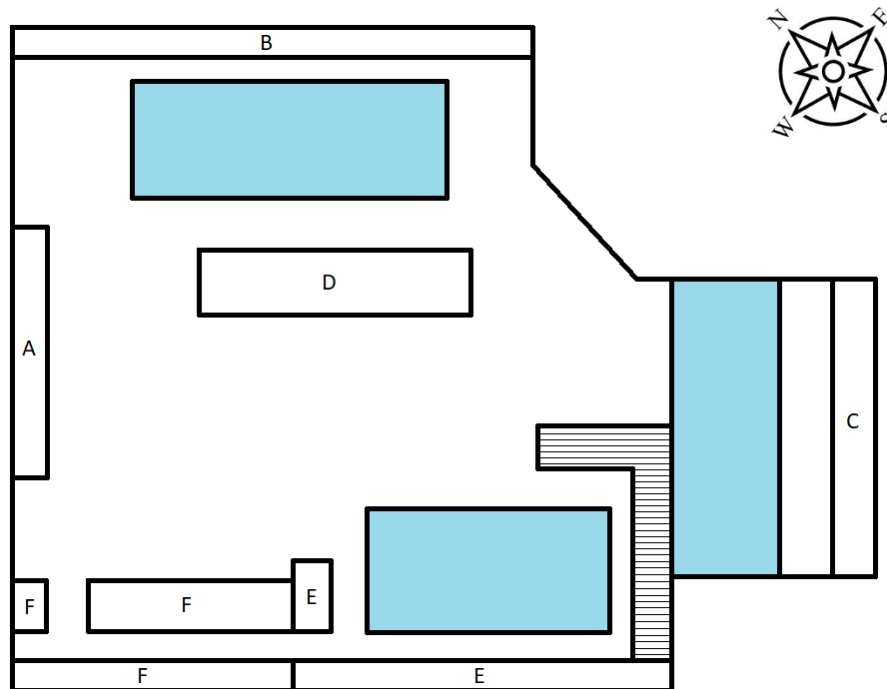


**Figure 40.** A not-to-scale diagram of the study site, showing the placements of nesting sections A–F. The walkway is represented with horizontal-lines, and the waterbodies are coloured blue.

Two hundred and thirty-three breeder Nile crocodiles, ranging in snout-hindlimb length (SHL) from 1.2–2.4 m, were counted within the pen, the exact male to female ratio was unknown. SHL is a measure like that of snout-vent length, which was adapted for drone-based length measurements (Myburgh, 2021; Viljoen<sup>1</sup> *et al.*, 2023). SHL is measured from the tip of the snout to the circumcircle scute layer immediately posterior to the back legs. If these features were not identifiable for a crocodile, the morphometric was skipped for that animal. This occurred in instances where the crocodiles were partially submerged in water, laying with body parts crossing over one another, or laying very close to a nest wall. No alterations were made to the pen setup or substrates for this study. The personnel assigned to the pen, specifically those responsible for egg collection, remained consistent throughout the nesting season. Climate data were obtained from South African Weather Services (SAWS) and Weather Underground (<https://www.wunderground.com/>) weather stations nearest the farm, 11.29 km and 8.15 km away, respectively. Hourly air temperatures (°C), relative humidity (% RH), rainfall (mm), wind speed (m/s), and solar radiation (W/m<sup>2</sup>) data were incorporated into this study. The term “solar radiation” refers to solar irradiance, the total radiation received at the Earth’s surface. Unfortunately, data on cloud-cover was not available, which precluded the quantification of its effect on the study findings.

### 6.3.2. Nest depth evaluation

Nest depths were evaluated early in the nesting season to identify the most appropriate depths for the assessment of the thermal profiles within nests in the pen that was eventually selected. Various depths within 32 nests, across three pens, were measured upon egg extraction. Egg extractions occurred daily in the early hours of the morning (05:00–07:00), when the crocodiles were least active, throughout the nesting season. A team of three experienced farm personnel identified nesting sites where digging/nesting by a crocodile had occurred. The procedures for egg collection were conducted in accordance with Section 7 of the South African National Standard for Crocodiles in Captivity (SANS, 2009). Following egg collections, the nests were raked flat, ensuring any new nest digging activity would be spotted the following day. Breeder pens on the farm were built between 1990–1996 and

although river sand was used to fill all nesting sites, sand consistency variations were noticed during excavations. Of the 32 nests, 16 were from nests with coarse and loosely packed sand, and 16 were from nests with densely packed fine sand. The first measure was the depth of the last egg deposited (most shallow) by the nesting female, from the top of the egg to ground surface level. The second measure was the depth at which the first egg was deposited (deepest) by the nesting female, measured from the top of the egg to the ground surface level. These two measures were then used to determine the overall nest depth of the full nest (the difference between the deepest and shallowest egg depths). Two of the 32 nests had a single egg sitting at or just below ground level, > 10 cm from the rest of the nest's eggs, these eggs were omitted.

### 6.3.3. Thermal profiles within nests

The subsurface thermal properties of a selection of nests were assessed using Liquid Armour (<https://liquidarmour.co.za/>) coated iButtons (DS1921G-F50 Thermocron), secured in 3D printed iButton holders (figure 41a), and refurbished iButtons (chapter 2's MD 2.4). Liquid Armour was used as a waterproofing agent for the iButtons. The iButton holders were printed with a Creality Ender-3 V2 3D printer, with PLA+ plastic; the holder design was publicly accessible on Thingiverse (design reference number: 2895204).

Twenty-four iButtons were placed in various nests, differing in location and orientation within the pen, to assess the thermal properties at multiple depths within those nests. Based on the findings of the preliminary nest depth study, six nests were fitted with four iButtons each, at predetermined depths suited to fine sanded nests. These iButtons were tied (via their 3D printed holders) onto brightly coloured (spray painted) wooden dowels and inserted vertically into the selected nests so that the shallowest iButton was 10 cm below ground surface level, and each following iButton another 10 cm below the previous, up until 40 cm below ground surface level (figure 41b). The brightly coloured dowels ensured that the iButtons remained in place, and should the dowel be exposed due to crocodiles digging in the vicinity they would be easily noticed by the farms nest attendees. The nests were checked daily, no dowels were dug up during the study. Nests containing these evenly spaced iButtons, from 10–40 cm, will be referred to as “dowel” nests.

Nine refurbished iButtons (chapter 2's MD 2.4) were used to measure single-depth temperatures in randomly selected, confirmed nests, as they were being harvested. These single refurbished iButtons were tied (taped onto a 3D printed holder) onto a length of brightly coloured rope and tagged using key tags (figure 41c). The single iButtons were inserted into confirmed nests during excavations. In each case, the depth of the deepest egg was measured and as the egg was removed, the iButton was placed into those eggs previous positions (with the colourful rope angled upward), and the nest was covered. The brightly coloured ropes facilitated easier extraction after the study owing to their visibility. The nests with these single loggers will be referred to as “single” harvested nests.

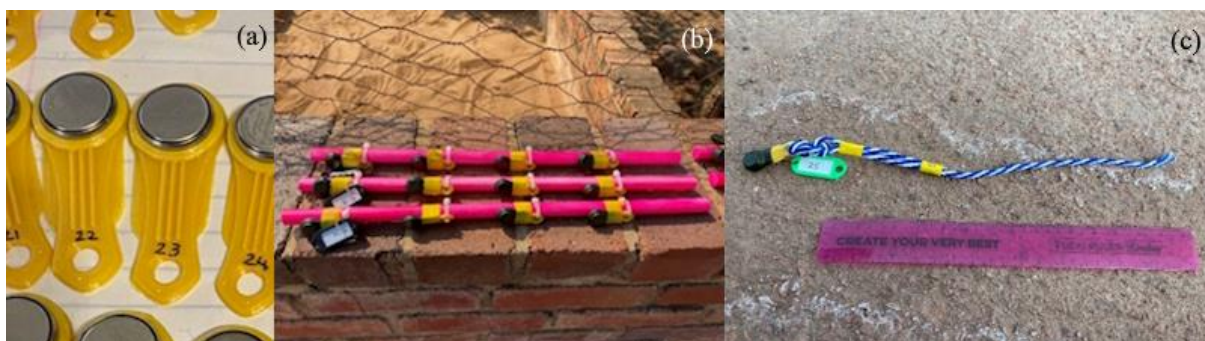


**Figure 41.** Images of (a) the 3D printer holders, (b) dowel iButtons, and (c) single iButtons.

Due to the farms daily egg collection policy, eggs were not left in the nesting sites long enough for logger placements among them. Instead, this study evaluated the nesting environment and identified potential factors that influence nest site and nest depth selections by the nesting crocodiles.

#### 6.3.4. Surface and faunal temperature variations

A single day of hourly flights from 07:00–15:00 was conducted with a Mavic 2 Enterprise Dual drone (899 grams) in early December (1 December 2022). The flights occurred at an altitude of 35 m above ground level, relative to the take-off point, and were initiated out of sight of the pen so as not to alert/stress the crocodiles. The flight path was programmed in a third-party flight software package ([Dronelink](#)) and was consistent throughout all flights. Ground control points, modelled after those used in Messina & Modica (2020), were arranged around the perimeter of the pen. The location of each ground control point was recorded with an Emlid Reach RS+ differential GPS, ensuring the precise alignment of the resulting imagery after photogrammetric processing. The thermal drone used in this study does not output precise temperature readings but distinguishes the temperature variation within a study site. See the method described in Viljoen<sup>3</sup> *et al.* (2023) for more information on temperature extraction from thermal maps. The method allows the derivation of temperatures from maps produced by the Mavic 2 Enterprise Dual drone to within 2.6 °C (root mean squared error).

Once the resulting imagery was processed in OpenDroneMap (ODM, version 1.9.3 build 30) and imported into QGIS (version 3.16-Hannover) (QGIS Development Team, 2021), thermal data for the pen (all substrates), nesting sites (surface temperatures, area shading ratio, and grass growth effects) and crocodiles (“back temperatures”), were determined using point layers and zonal statistic extractions from polygon layers. To record back temperatures, a “point” marker was placed on the centre of the back or the head (if that was all that was visible, i.e., in a water body) of each crocodile within view. A second marker was placed next to each crocodile on the substrate type it was selecting, these markers recorded the “positional temperatures” selected by each individual crocodile (figure A17, A18). The area, and therefore substrate type, of the pen being selected by each crocodile was delineated using a polygon layer to outline the distinct surface substrates visible (i.e., water, concrete, grass/sand, and nests). The “join attributes” function was used to combine the substrates-polygon and point layer indicating the crocodiles’ positions. A second polygon layer distinguished the nesting sites by number, allowing the extraction of specific nest information whenever a crocodile was occupying a nesting site.

Proportional shading over nesting sites was quantified using zonal statistic layers. The hourly percentage of shading over each nesting site was calculated and then classified into five categories, each representing bins of 20 percent (i.e., 0–19%, 20–39%, 40–59%, 60–79%, and 80–100%). Instead of quantification as a percentage (like that of the shading evaluation), nests were simply categorized based on the presence or absence of grass during the assessment. This was due to the heterogeneous nature of the grass dispersion across different nesting sites. Crocodile SHL measures were recorded with a line-string layer.

#### 6.3.5. Crocodile pen and nest utilization

A DJI Mini 2 SE drone (249 grams) was flown once per week, on a randomly selected day of the week, in the morning (between 06:00 and 07:00) and afternoon (between 15:00 and 17:00) for seven weeks during the breeding/nesting season (October–December 2022). A midday flight (12:00–12:30) was included on three of these occasions. All flights occurred at an altitude of 35 m above ground level, with 85% side and frontal image overlap, and were initiated out of sight of the pen. The same flight path was used as for the Mavic 2 Enterprise Dual drone flights.

Behavioural data (pen area utilization, nest occupancy, nest utilization, and nesting section/orientation preferences) were recorded with a combination of drone imagery and the farms nest records for the breeding/nesting season. “Nest occupancy” refers to the crocodiles occupying a nesting site during the observation periods, whereas nest “utilization” or “preference” refers to the committed use (i.e., confirmation of eggs being deposited, which were reflected by the farms nest records for the season) of a nesting site. Due to the unequal distribution of nests across sections, directly comparing nest occupancy and nest preferences would introduce bias, proportional comparisons were employed when comparing these two variables. The total number of nesting sites occupied and utilized per section were normalized by the total nest count within each section. This controlled for potential biases favouring sections with a greater number of nesting sites.

The distances from each nest (measured from the nests entrance) to the closest water body and the tourist walkway were extracted from the drone imagery using line-string layers. Crocodile positions and SHLs were recorded for each timeslot where possible using the layer types described in 6.3.4. Observations of urination directly over nesting sites by the attending crocodiles was made; however, there were not enough instances of this behaviour for statistical analyses. Some suggested purposes of this behaviour are to aid in nest material decomposition, to add moisture to the nest during dry periods, to cool the nests, or to ensure hatchlings recognize the mother upon emergence (McIlhenny, 1934; Yangprapakorn *et al.*, 1971; Honegger, 1971; Huchzermeyer, 2003; López-Luna *et al.*, 2015).

#### 6.4. DATA ANALYSIS

The data were analysed in R (2022.12.0 Build 353) and IBM SPSS Statistics (version 28). Summary statistics were the starting point to all analyses to view the data distribution, identify potential outliers, and assess the fundamental characteristics of the data. In instances where categorical variables needed comparison, Chi-square analyses were employed. This was followed by normality determinations to ensure the assumptions for subsequent tests were met. Multivariate Analyses of Variance (MANOVA) were used to assess the effects of multiple factors on the dependent variables. Where these resulted in significant outcomes, post hocs (Bonferroni) were conducted to determine specific pairwise group differences. Mixed model analyses were then employed to ascertain if there was an enhancement in sensitivity when accounting for both fixed and random effects. Pearson product moment correlations and regression analyses were used to determine linear relationships between variables. All data were analysed for the determination of significant differences at  $P < 0.05$ , highly significant differences were noted if  $P < 0.001$ .

#### 6.5. RESULTS

##### 6.5.1. Study site and animals

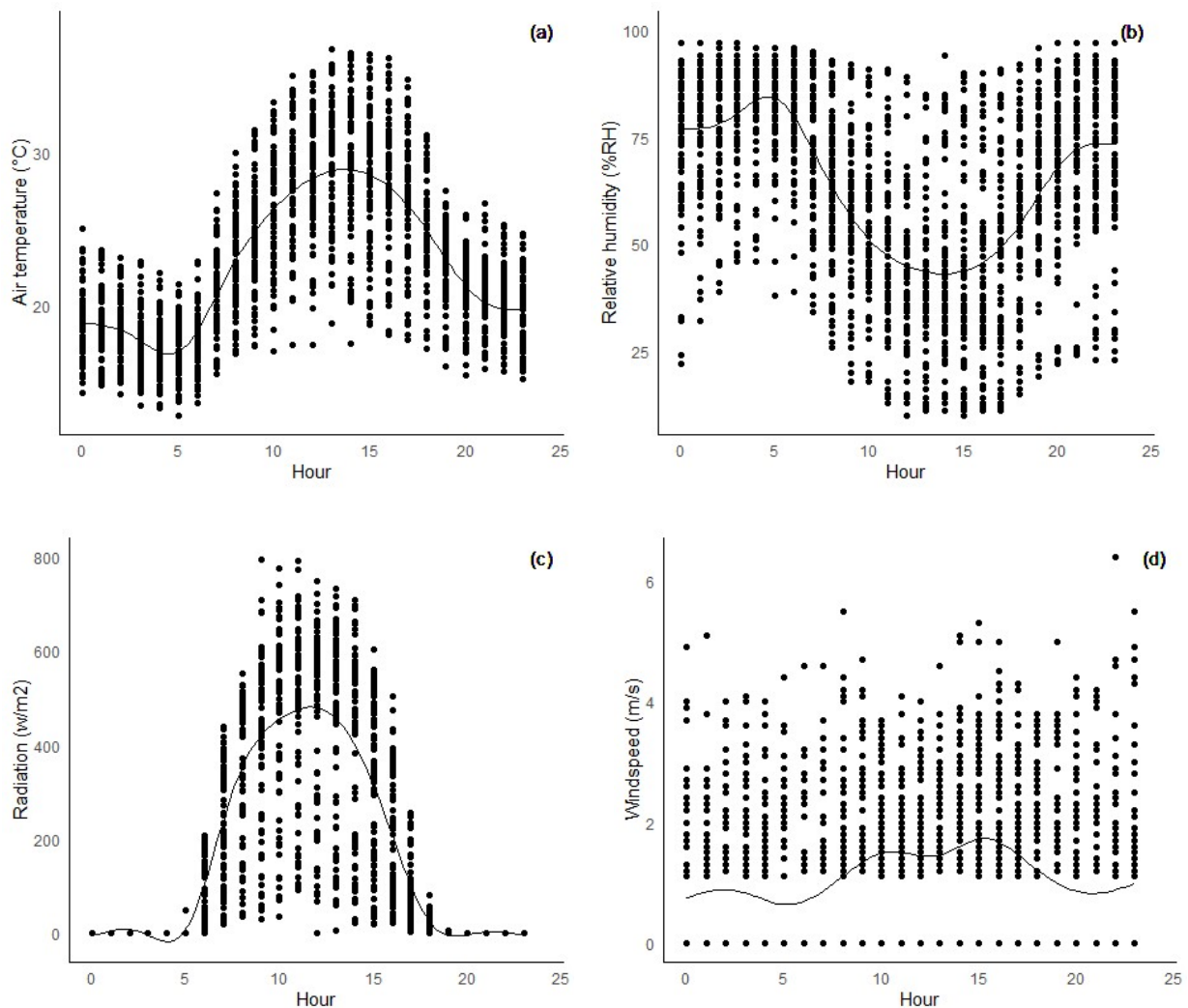
One hundred and thirty-eight nests were produced during the nesting season. The number of eggs collected ranged from 15–62 ( $\bar{x} = 35.5$ ,  $SD = 10.1$ ,  $SE = 0.9$ ), and the number of eggs hatched ranged from 0–49 ( $\bar{x} = 15.9$ ,  $SD = 14.3$ ,  $SE = 1.3$ ). Hatching success ranged from 0–100% ( $\bar{x} = 41.8\%$ ,  $SD = 39.7\%$ ,  $SE = 3.4\%$ ), 40% of the nests had a 0% hatching success rate.

Distance from the closest water body varied significantly between most nesting sections ( $P < 0.001$ ,  $F = 53.19$ ,  $df = 5$ ) (table 16). Sections A and F did not vary from one another regarding distances from the closest water body. Section B did not vary from sections C or E, nor did sections C and E vary from one another in terms of distances from the closest water body ( $P > 0.05$ ). The distances from the tourist walkway varied significantly between most nesting sections ( $P < 0.001$ ,  $F = 86.44$ ,  $df = 5$ ). Section A did not vary from sections B or F, nor did sections B and F vary from one another in terms of distances from the tourist walkway ( $P > 0.05$ ). Section C did not vary from sections D or E, nor did sections D and E vary from one another regarding distances from the tourist walkway ( $P > 0.05$ ).

**Table 16.** Nest site divisions by section, orientation, number of nests per section, mean distance from the closest water body, and mean distance from the tourist walkway.

Nest section	Orientations	Number of nesting sites	Mean distance from water (m)	Mean distance from walkway (m)
A	SE	17	22.3	47.9
B	SW	22	4.5	45.2
C	NW	11	7.3	16.8
D	NE & SW	14 & 14	14.3	19.6
E	NE & SE	11 & 4	4.3	23.2
F	NE, SE & SW	21, 3 & 9	20.4	46.1

During the study period, air temperatures ranged from 12.8–36.8 °C ( $\bar{x}$  = 22.8 °C, SD = 5.2 °C, SE = 0.1 °C), relative humidity ranged from 10–97 % RH ( $\bar{x}$  = 63.1 % RH, SD = 22.4 % RH, SE = 0.5 % RH), rainfall ranged from 0–17 mm ( $\bar{x}$  = 0.1 mm, SD = 0.9 mm, SE = 0.0 mm), windspeeds ranged from 0–6.4 m/s ( $\bar{x}$  = 1.1 m/s, SD = 1.3 m/s, SE = 0.0 m/s), and solar radiation ranged from 0–795.7 W/m<sup>2</sup> ( $\bar{x}$  = 160.5 W/m<sup>2</sup>, SD = 221.3 W/m<sup>2</sup>, SE = 5.1 W/m<sup>2</sup>) (figure 42).



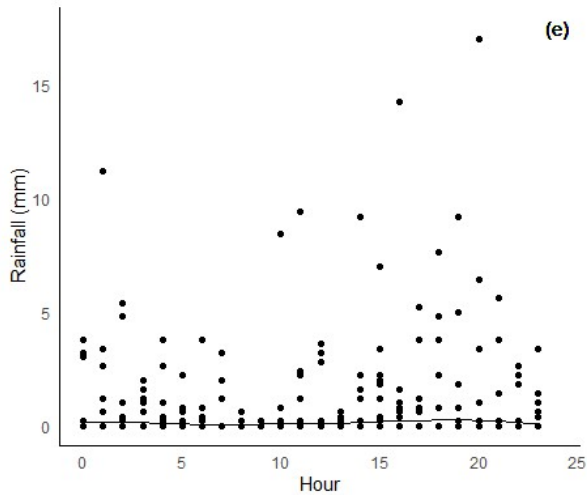


**Figure 42.** Hourly (a) air temperature ( $^{\circ}\text{C}$ ), (b) relative humidity (% RH), (c) solar radiation ( $\text{W}/\text{m}^2$ ), (d) wind speed ( $\text{m}/\text{s}$ ), and (e) rainfall ( $\text{mm}$ ) throughout the nesting period (October–December 2022). Solid lines represent the mean per hour.

#### 6.5.2. Nest depth evaluation

Shallowest egg depths ranged from 10.00–18.00 cm ( $\bar{x} = 13.47$  cm,  $\text{SD} = 2.29$  cm,  $\text{SE} = 0.57$  cm) for nests with coarse sand, and from 10.5–24.5 cm ( $\bar{x} = 17.03$  cm,  $\text{SD} = 4.18$  cm,  $\text{SE} = 1.04$  cm) for nests with fine sand. Deepest egg depths ranged from 27.00–33.50 cm ( $\bar{x} = 29.72$  cm,  $\text{SD} = 1.84$  cm,  $\text{SE} = 0.46$  cm) for coarse sanded nests, and from 18.00–39.00 cm ( $\bar{x} = 29.06$  cm,  $\text{SD} = 5.16$  cm,  $\text{SE} = 1.29$  cm) for fine sanded nests. Nest depths ranged from 11.00–20.50 cm ( $\bar{x} = 16.25$  cm,  $\text{SD} = 2.74$  cm,  $\text{SE} = 0.69$  cm) for coarse sanded nests, and from 3.00–17.00 cm ( $\bar{x} = 12.03$  cm,  $\text{SD} = 3.56$  cm,  $\text{SE} = 0.89$  cm) for fine sanded nests. Four out of 32 nests had nest depths  $< 10$  cm where the eggs were spread over a larger diameter than in other measured nests. The shallowest egg depth and total nest depths measured varied significantly ( $P < 0.05$ ,  $t = -2.991$ ,  $\text{df} = 23.276$ ;  $P < 0.001$ ,  $t = 3.753$ ,  $\text{df} = 28.172$ , respectively) between the different sand types. The fine sanded nests had more compact nest depths, with the first eggs buried deeper than those of the coarse sanded nests. The deepest egg depths did not vary significantly between sand types (figure 43).

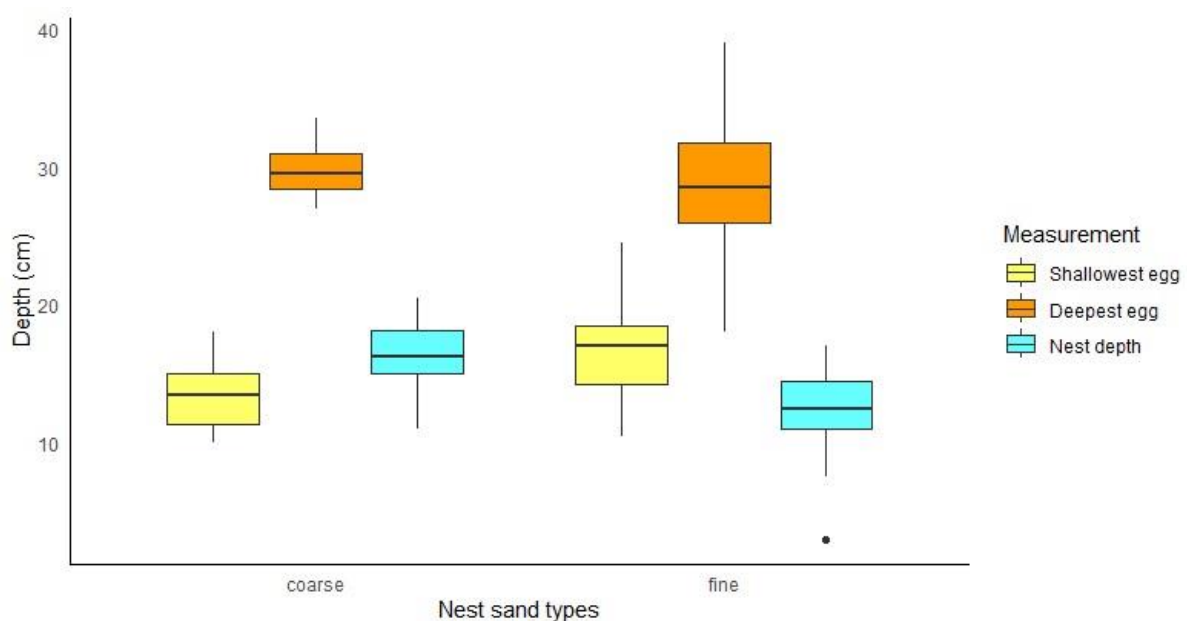


**Figure 43.** Nest depth variables (shallowest egg, deepest egg, and nest depth) between coarse and

fine sanded nests on a commercial Nile crocodile farm in South Africa. Each boxplot displays the median (centre line), interquartile range (box edges), and 1.5 \* IQR (whiskers). Points beyond the whiskers represent outliers.

### 6.5.3. Thermal profiles within nests

Of the thirty-three iButtons deployed throughout various nesting sites on the farm, a single iButton was not recovered from a section F dowel. Subsurface nest temperatures were significantly affected by nest orientation ( $P < 0.001$ ,  $F = 43.359$ ,  $df = 1$ ), nest section ( $P < 0.001$ ,  $F = 186.405$ ,  $df = 2$ ), depth ( $P < 0.001$ ,  $F = 457.510$ ,  $df = 1$ ), grassy growth over the top of nests ( $P < 0.001$ ,  $F = 1062.174$ ,  $df = 1$ ), and hour of the day ( $P < 0.001$ ,  $F = 227.242$ ,  $df = 1$ ). Nest temperatures were significantly affected by air temperature ( $P < 0.001$ ,  $F = 258.902$ ,  $df = 1$ ), relative humidity ( $P < 0.001$ ,  $F = 5129.134$ ,  $df = 1$ ), solar radiation ( $P < 0.001$ ,  $F = 7164.951$ ,  $df = 1$ ), wind speed ( $P < 0.001$ ,  $F = 91.122$ ,  $df = 1$ ), and rainfall ( $P < 0.001$ ,  $F = 673.969$ ,  $df = 1$ ).

Air temperatures, windspeed, and radiation were significantly and positively correlated with nest temperatures ( $r = 0.43$ ,  $P < 0.001$ ;  $r = 0.12$ ,  $P < 0.001$ ;  $r = 0.05$ ,  $P < 0.001$ , respectively). Relative humidity was negatively correlated to nest temperatures ( $r = -0.52$ ,  $P < 0.001$ ). Rainfall was not significantly correlated to nest temperatures ( $P > 0.05$ ). When assessing the correlations for the dowel-containing nests only, the strength of the correlations between nest temperatures and all climate variables decreased with increasing depth. At a depth of 10 cm below ground level, rainfall was weakly but significantly correlated with sand temperatures ( $r = -0.06$ ,  $P < 0.001$ ), none of the deeper depths' temperatures were correlated to rainfall ( $P > 0.05$ ). Single harvested nests did not have a significant correlation between sand temperatures and rainfall ( $P > 0.05$ ). Nest temperatures were positively correlated to hour of the day ( $r = 0.27$ ,  $P < 0.001$ ).

**Table 17.** Descriptive statistics for the temperatures (°C) recorded by iButtons deployed on dowels, ordered by section and depth (cm).

iButtons	Section	Depth	Min	Max	Mean	SD	SE
1, 5, 9	A	10	15.5	49.5	24.9	5.0	0.06
2, 6, 10		20	16.5	35.5	24.4	3.4	0.04
3, 7, 11		30	18	35	24.4	2.6	0.03
4, 8, 12		40	19	32.5	24.2	2.1	0.03
13, 17, 21	F	10	15	46.5	26.1	5.5	0.07
14, 18, 22		20	17.5	37	25.8	3.7	0.05
15, 19		30	19.5	36	25.9	2.7	0.04
16, 20, 24		40	20	30.5	25.4	2.1	0.03

**Table 18.** Descriptive statistics for the temperatures (°C) recorded by iButtons deployed as singles, ordered by depth (cm).

iButtons	Section	Orientation	Depth	Min	Max	Mean	SD	SE
32	B	SW	19	19.5	32.5	25.0	2.3	0.05
27	C	NW	19.5	22	38	28.7	2.9	0.06
34	D	SW	23	20.5	32	25.4	2.4	0.06
38	F	NE	24	20	30.5	25.7	2.3	0.05
30	F	NE	27.5	21	31	25.7	2.1	0.05
28	D	NE	30.5	20	30.5	26.2	2.1	0.05
31	A	SE	34	19.5	30.5	24.6	2.4	0.06
44	F	SW	34	21	30.5	25.9	1.9	0.04
33	C	NW	35	22	29	25.5	1.8	0.04

The only nesting section not represented by a single iButton was section E. A single iButton in section C, buried at a depth of 19.5 cm below ground level, malfunctioned, and the outputs of that logger are not included in the analyses that follow.

Based on descriptive trends (table 17), as depths within the nests with dowels progressed from 10–40 cm, the minimum temperatures recorded increased, the maximum temperatures declined, the range of temperatures (maximum–minimum) decreased, and the mean temperatures remained comparable. Section A dowel-nest temperatures ranged from 15.5 °C to 49.5 °C, whereas section F dowel-nest temperatures ranged from 15 °C to 46.5 °C. Temperatures recorded by the dowel iButtons at varying depths differed significantly ( $P < 0.001$ ,  $F = 78.97$ ,  $df = 3$ ) from one another, except for measurements at 20 cm and 30 cm depths (figure 44a). The depths monitored by single iButtons, at the depth of the deepest egg from harvested nests, ranged from 19 cm to 35 cm deep. The minimum sand temperatures recorded in the harvested nests ranged from 19.5 °C to 22 °C, maximums ranged from 30.5 °C to 32.5 °C and means ranged between 24.6 °C and 26.2 °C (table 18). Temperatures recorded by the single iButtons differed significantly with depth ( $P < 0.001$ ,  $F = 60.89$ ,  $df = 6$ ), and therefore from one another, for the most part ( $P < 0.05$ ). The exceptions to this finding were that nest temperatures did not vary ( $P > 0.05$ ) between the depths of 23 cm to 34 cm and 35 cm, and 24 cm to 27.5 cm and 35 cm (figure 44b).

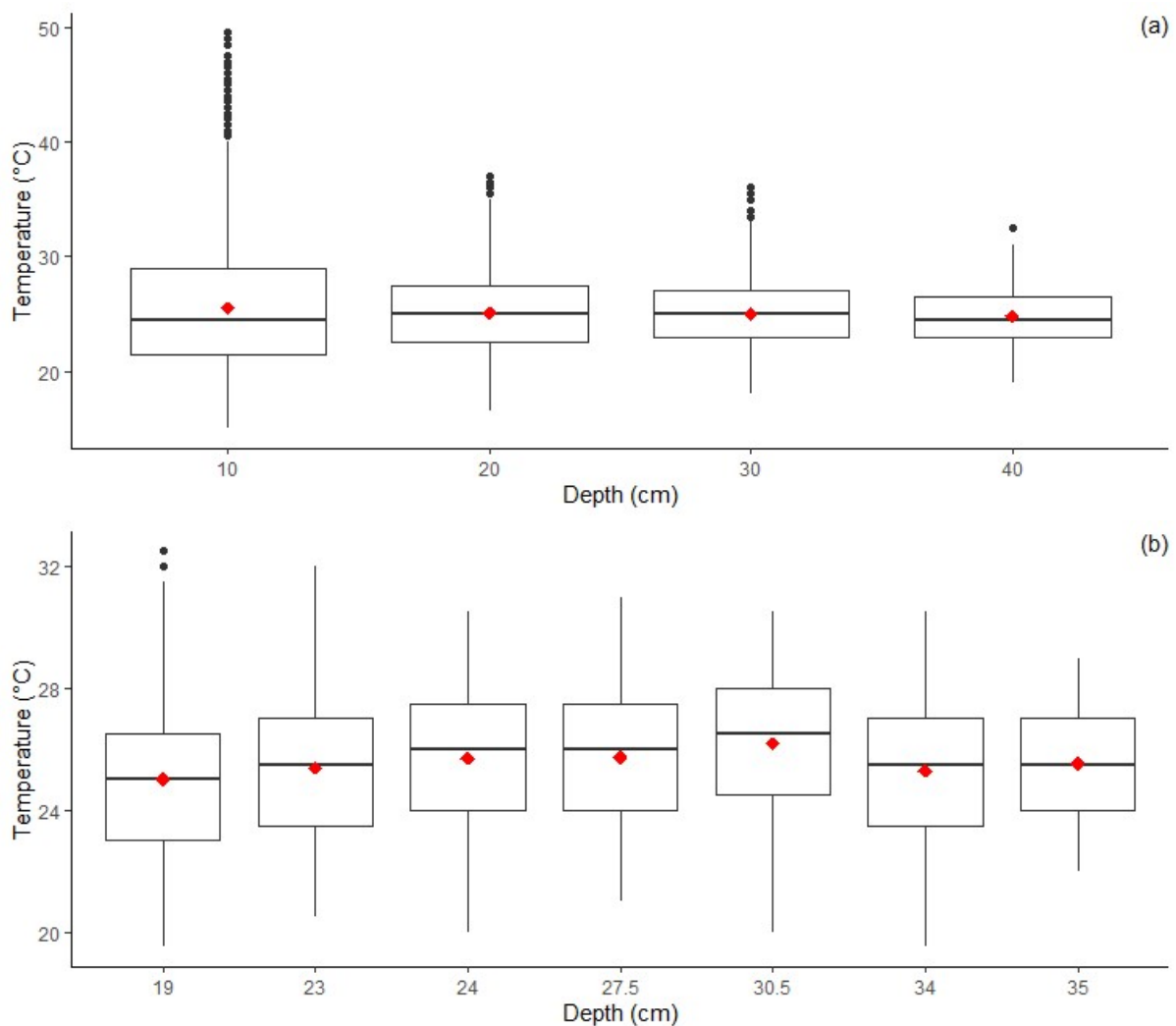


**Figure 44.** Sand temperatures recorded at varying depths below ground level. Plot (a) depicts measurements from dowel iButtons placed at 10, 20, 30, and 40 cm below the surface, and (b) depicts

temperatures from harvested nest sites, specifically at the depth of the deepest egg, using single iButtons. Each boxplot displays the median (centre line), interquartile range (box edges), and 1.5 \* IQR (whiskers). Points beyond the whiskers represent outliers and means are represented by red rhombuses.

Nesting section and orientation had variable effects on minimum, maximum, and mean daily nest temperatures. Minimum daily nest temperatures varied significantly between all nest sections ( $P < 0.001$ ,  $F = 624.8$ ,  $df = 4$ ), except sections C and F ( $P > 0.05$ ). Minimum daily nest temperatures also varied with nest orientation ( $P < 0.001$ ,  $F = 791.4$ ,  $df = 3$ ), where SE facing nests varied from all other orientations (all  $P < 0.001$ ). Maximum daily nest temperatures varied significantly between all nest sections ( $P < 0.001$ ,  $F = 208.7$ ,  $df = 4$ ), except sections A and B ( $P > 0.05$ ). Maximum daily sand temperatures varied between all nest orientations ( $P < 0.001$ ,  $F = 270.6$ ,  $df = 3$ ), except SW and NW facing nests which did not vary from one another ( $P > 0.05$ ). Mean daily nest temperatures varied significantly with nesting section ( $P < 0.001$ ,  $F = 345.9$ ,  $df = 4$ ), except in sections D and F ( $P > 0.05$ ). Mean daily nest temperatures varied significantly with nest orientation ( $P < 0.001$ ,  $F = 436.6$ ,  $df = 3$ ), except in SW and NW facing nests ( $P > 0.05$ ).

Nest temperatures recorded in dowel-fitted nests only were significantly ( $P < 0.001$ ,  $F = 1492$ ,  $df = 1$ ) affected by orientation (and therefore section, as only one orientation within each section was assessed). NE facing nests (section F dowels) recorded higher mean temperatures than SE facing nests (section A dowels). The effects of orientation and section on nest temperatures were assessed separately for single iButtons, as these represented crocodile-selected sections and orientations. NE facing nests had the highest mean temperatures ( $\bar{x} = 25.86$  °C), followed by NW ( $\bar{x} = 25.52$  °C), SW ( $\bar{x} = 25.46$  °C), and SE facing nests ( $\bar{x} = 24.55$  °C) (figure 45). Among single iButton loggers, nest temperatures varied significantly with nest orientation ( $P < 0.001$ ,  $F = 171.8$ ,  $df = 3$ ), between all orientations (all  $P < 0.001$ ) except SW and NW facing nests ( $P > 0.05$ ). Single-iButton nest depths per orientation were tentatively assessed, dowel-iButton nests were excluded as these depths were not selected by the crocodiles. NW facing nests had the highest mean nest depths ( $\bar{x} = 35$  cm) followed by SE ( $\bar{x} = 34$  cm), NE ( $\bar{x} = 27.3$  cm) and SW facing nests ( $\bar{x} = 25.6$  cm). Nest depths varied significantly with orientation ( $P < 0.001$ ,  $F = 3508$ ,  $df = 3$ ), all orientations varied from one another in this way (all  $P < 0.001$ ). Mean subsurface temperatures per nesting sections A–D and F were 24.55 °C, 25.03 °C, 25.52 °C, 25.85 °C, and 25.79 °C, respectively. Nest temperatures varied significantly with nest section ( $P < 0.001$ ,  $F = 160$ ,  $df = 4$ ), between all sections (all  $P < 0.001$ ), except sections D and F ( $P > 0.05$ ).

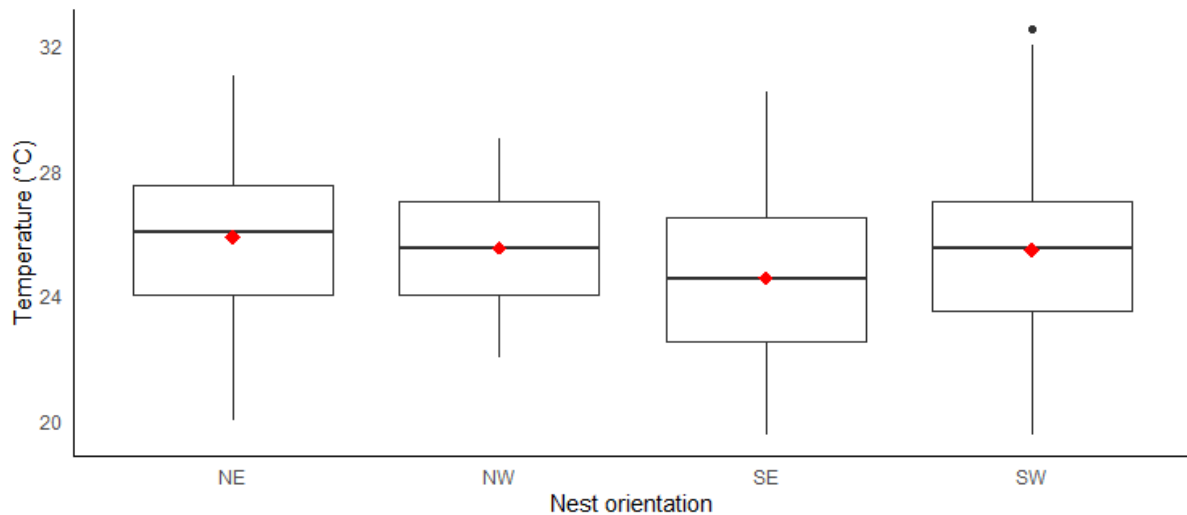


**Figure 45.** Single iButton sand temperatures recorded in each nest orientation. Each boxplot displays the median (centre line), interquartile range (box edges), and 1.5 \* IQR (whiskers). Points beyond the whiskers represent outliers and means are represented by red rhombuses.

Daily nest temperature ranges varied significantly with depth ( $P < 0.001$ ,  $F = 72.852$ ,  $df = 10$ ) and orientation ( $P < 0.001$ ,  $F = 37.062$ ,  $df = 3$ ). Specifically, as depths increased, the recorded temperature ranges decreased (figure 46). When assessing the dowel-fitted nests exclusively, SE facing nests (section A dowels) exhibited a mean daily temperature range of 7.49 °C, while those facing NE (section F dowels) exhibited a mean daily temperature range of 8.21 °C. Post hoc (Bonferroni) comparisons revealed significant differences between daily temperature range means between all dowel depth categories (all  $P < 0.001$ ). The interaction of depth and orientation effects on the dowel temperatures were complex (figure 46a). At 10 cm, temperatures differed from all other depth and orientation combinations (all  $P < 0.001$ ). At 20 cm, temperatures varied from all other combinations (all  $P < 0.001$ ), except between SE and NE orientations at this same depth ( $P > 0.05$ ). At 30 cm, temperatures differed from all other combinations, except between SE and NE orientations at this same depth, between 30 cm deep NE nests versus 40 cm deep SE nests, and between 30 cm and 40 cm deep SE nests ( $P > 0.05$ ). At 40 cm, temperatures differed from all other combinations (all  $P < 0.001$ ), except between SE and NE orientations at this same depth ( $P > 0.05$ ).

When assessing the single iButton-fitted nests exclusively (figure 46b), mean daily nest temperature ranges varied from 1.05–3.99 °C. Mean ranges differed significantly between the depth of 19 cm and those  $\geq 27.5$  cm (all  $P < 0.001$ ). Mean daily temperature ranges recorded at depths of 23 cm and 24 cm did not differ from those recorded at 19 cm below ground level ( $P > 0.05$ ). Mean daily nest temperature ranges at 23 cm deep varied significantly from those  $\geq 24$  cm deep (all  $P < 0.001$ ), and those at 24 cm deep varied from depths  $\geq 30.5$  cm (all  $P \leq 0.001$ ). Mean ranges differed significantly ( $P < 0.05$ ) between 35 cm below ground surface level and all other depths (all  $P < 0.001$ ). Mean daily nest temperature ranges varied significantly between all orientations when assessing the single iButton-fitted nests (all  $P < 0.001$ ). Ranked by their daily temperature ranges, SW facing nests had the highest mean range ( $\bar{x} = 3.328$  °C), followed by NE ( $\bar{x} = 2.701$  °C), SE ( $\bar{x} = 2.020$  °C), and NW ( $\bar{x} = 1.052$  °C) facing nests (figure 46c).

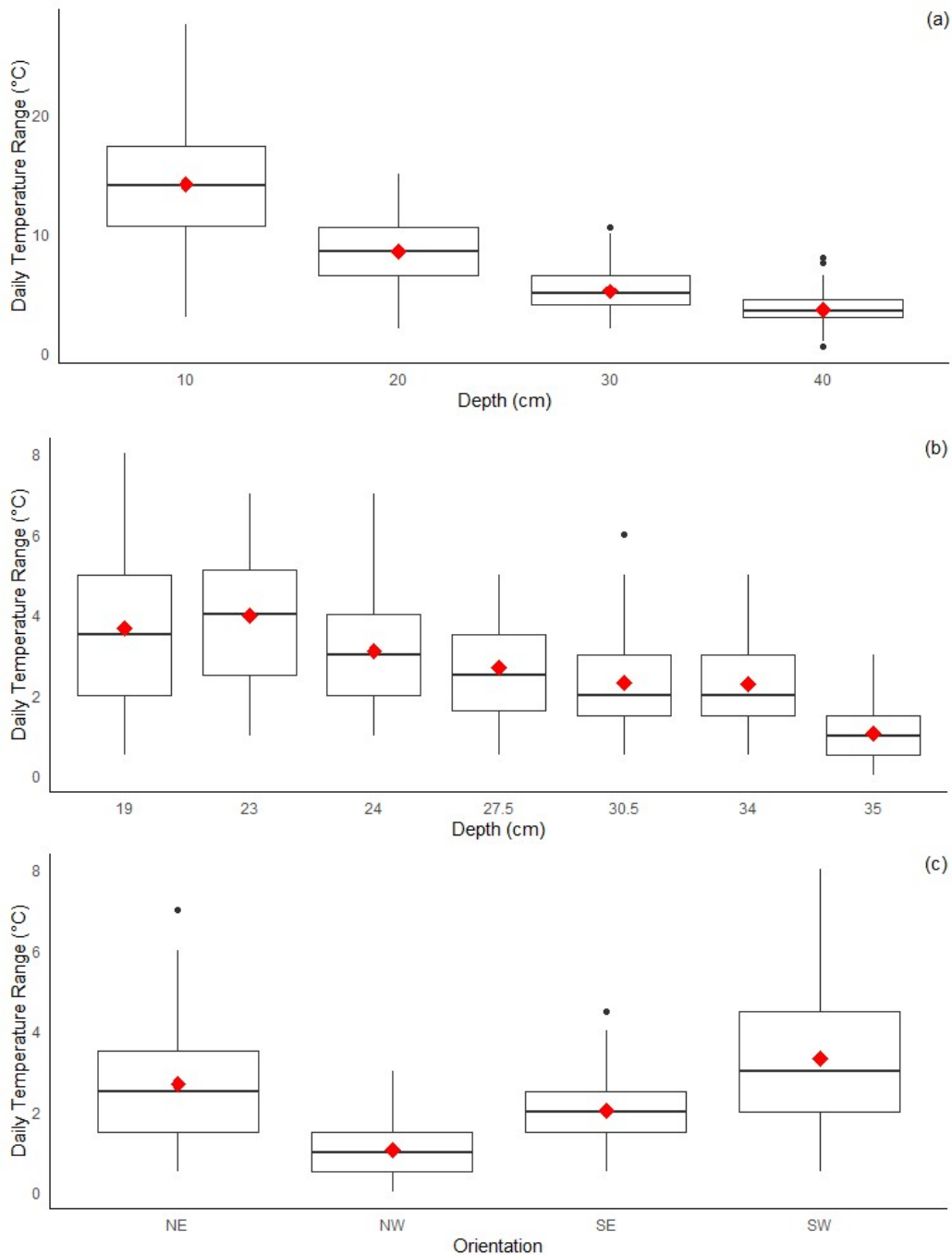


**Figure 46.** Daily sand temperature ranges of the dowel iButtons arranged by depth (a), single iButtons arranged by depth (b), and single iButtons arranged by orientation (c). Each boxplot displays the median (centre line), interquartile range (box edges), and 1.5 \* IQR (whiskers). Points beyond the whiskers represent outliers and means are represented by red rhombuses.

No nests with dowel iButtons had any grassy growth, whereas four of the nine nests with single iButtons did endure grassy growth. The four affected depths were as follows: 19 cm, 30.5 cm, 34 cm, and 35cm (iButtons 32, 28, 31, and 33, respectively). Of the four nests, the 30.5 cm deep nests temperature readings were not significantly affected by grassy growth over the top of the nest ( $P > 0.05$ ). The 19 cm, 34 cm, and 35 cm depth nest temperatures were significantly affected by grassy cover ( $P < 0.001$ ,  $t = 6.130$ ,  $df = 1380.4$ ;  $P < 0.001$ ,  $t = 14.725$ ,  $df = 1198.6$ ;  $P < 0.001$ ,  $t = 15.932$ ,  $df = 971.0$ , respectively). According to the t-values, the mean temperatures of nests with grassy cover were lower than those of nests without grass. The nests where grassy growth occurred were each located

in unique sections and orientations; therefore, no orientation/section interaction effects were assessed to avoid biases.

#### 6.5.4. Surface and faunal temperature variations

Crocodile back temperatures were significantly influenced by positional temperatures ( $P < 0.001$ ,  $t = 38.02$ ,  $\beta = -0.21$ ,  $SE = 0.01$ ); the back temperatures of the crocodiles fell within the range of the positional temperatures throughout the observation period (table 19). Crocodile back temperatures were significantly affected by air temperatures ( $P < 0.05$ ,  $t = 2.98$ ,  $\beta = 0.44$ ,  $SE = 0.14$ ), relative humidity ( $P < 0.05$ ,  $t = 3.14$ ,  $\beta = 0.13$ ,  $SE = 0.04$ ), and wind speed ( $P < 0.001$ ,  $t = -4.07$ ,  $\beta = -0.70$ ,  $SE = 0.17$ ), but not solar radiation ( $P > 0.05$ ). Crocodile back temperatures varied with the selected pen substrates ( $P < 0.001$ ,  $F = 112.99$ ,  $df = 3$ ). Specifically, crocodiles within the waterbodies of the pen had significantly lower back temperatures than other substrates (all  $P < 0.001$ ), no other substrates differed significantly in terms of back temperatures ( $P > 0.05$ ). Back temperatures of crocodiles occupying nesting areas did not vary with nest orientation or section ( $P > 0.05$ ).

**Table 19.** Descriptive statistics of drone-derived crocodile back temperatures, positional temperatures, surface temperatures of crocodile-occupied nests, crocodile SHLs, and climate variables on the day of the thermal flights (1 December 2022).

Variable	Min	Max	Mean	SD	SE
Crocodile back temperatures (°C)	17.4	50.6	30.6	4.8	0.1
Crocodile positional temperatures (°C)	15.1	56.3	29	8	0.2
Nest surface temperatures (°C)	19.3	31.1	23.6	2.7	0.2
Snout-hindlimb lengths (m)	1.2	2.3	1.6	0.2	0.0
Air temperature (°C)	22.8	32.6	28.1	3.3	0.0
Relative humidity (% RH)	29	61	42	11.5	0.3
Wind speed (m/s)	0	1.5	0.3	0.5	0.0
Solar radiation (W/m <sup>2</sup> )	364.1	610.9	523.7	94.4	2.3

Proportional area/substrate occupancy per flight was assessed by identifying the substrate selections of all crocodiles within view (figure 47), allowing nest site occupancy comparisons over time of the day. As the morning progressed, the proportional use of the nesting areas within the pen decreased, reaching 0% of crocodiles in view occupying nesting areas between the hours of 11:00 and 12:00. Proportional nesting area use increased again from 14:00–15:00, following a drop in air temperatures, when relative humidity was low. Although there was a peak in the wind speeds at 11:00, there were no crocodiles occupying nesting sites at this time. The second peak in wind speeds at 14:00 did seem to align with increasing nest occupancies (figure 48). Air temperature and relative humidity had small but significant negative correlations with proportional nest occupancy ( $r = -0.18$ ,  $P < 0.001$ ;  $r = -0.11$ ,  $P < 0.001$ , respectively). Radiation was strongly and negatively correlated with proportional nest occupancy ( $r = -0.96$ ,  $P < 0.001$ ). Wind speed showed a strong positive correlation with the occupancy of nests within the pen ( $r = 0.87$ ,  $P < 0.001$ ).

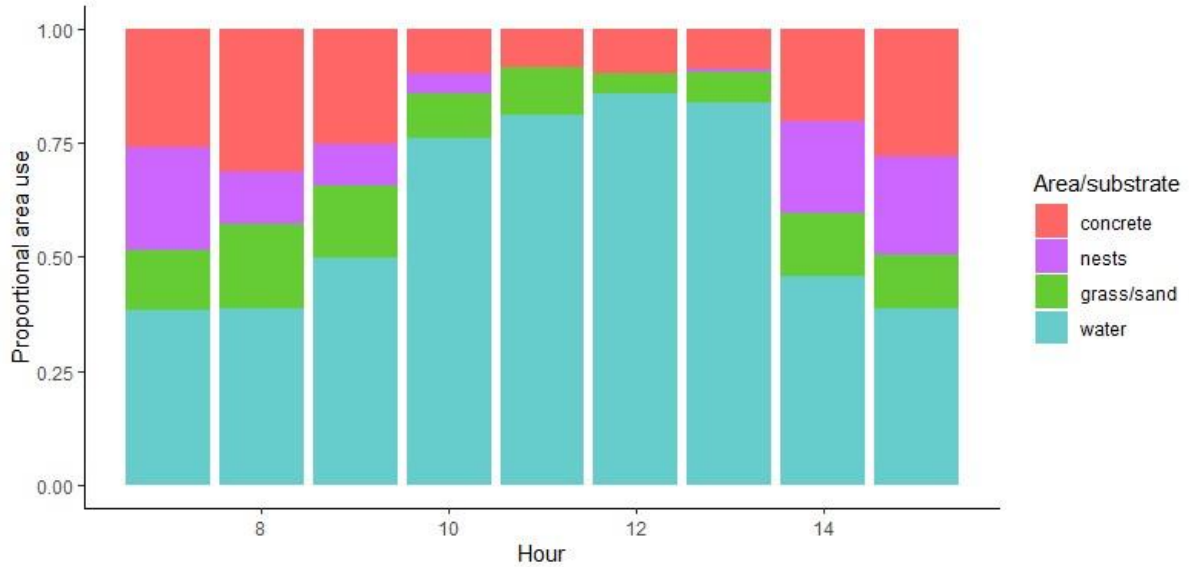


**Figure 47.** A stacked bar plot depicting the proportional pen area/substrate occupancy per hour on 1 December 2022, from the DJI Mavic 2 Enterprise Dual drone-produced imagery.

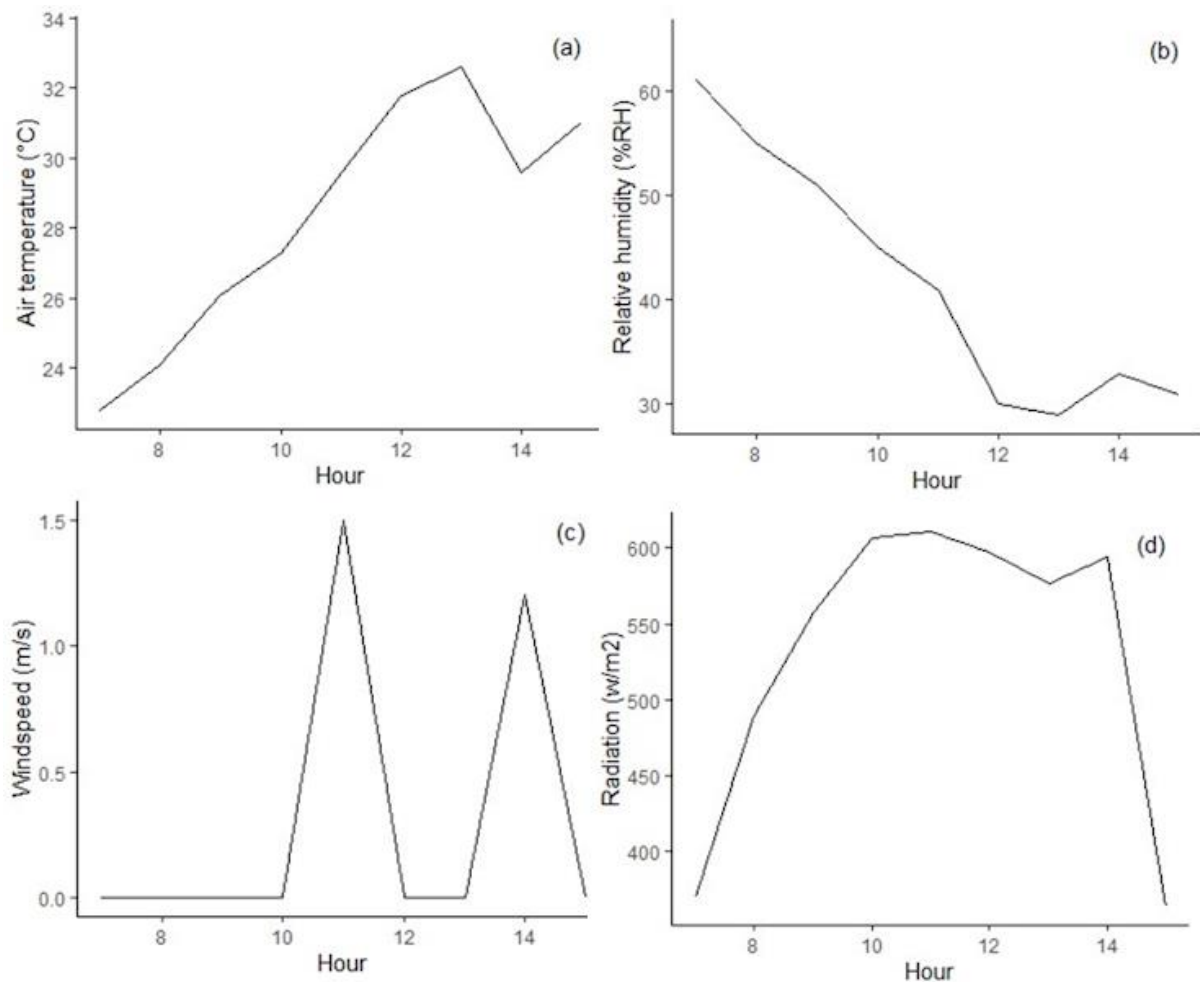


**Figure 48.** Depicts the hourly (a) air temperature (°C), (b) relative humidity (% RH), (c) wind speed (m/s), and (d) radiation (W/m<sup>2</sup>) on 1 December 2022.

Nest surface temperatures varied significantly with shading ( $P < 0.001$ ,  $F = 140.048$ ,  $df = 1$ ), section ( $P < 0.001$ ,  $F = 22.468$ ,  $df = 4$ ), presence of grass over the nest ( $P < 0.001$ ,  $F = 301.345$ ,  $df = 1$ ), and hour

of the day ( $P < 0.001$ ,  $F = 288.891$ ,  $df = 8$ ). As proportional shading over nesting sites increased, nest surface temperatures decreased. The mean nest surface temperatures for increasing shading bins were: 44.53 °C (0–19% shading), 37.71 °C (20–39% shading), 28.10 °C (40–59% shading), 22.98 °C (60–79% shading), and 21.34 °C (80–100% shading). Nest surface temperatures between all shading bins differed significantly (all  $P < 0.05$ ) from one another, except the fourth and fifth (representing shading percentages from 60–100% of the nests area). Sections D and Fs nest surface temperatures varied significantly from those of all other nesting sections (all  $P < 0.001$ ), as well as from one another ( $P < 0.001$ ). Specifically, nesting section F ( $\bar{x} = 46.76$  °C) had the highest nest surface temperatures, followed by section D ( $\bar{x} = 42.63$  °C), all other section means were between 34.75–36.92 °C (figure 49a). The remaining nesting sections did not vary significantly ( $P > 0.05$ ) from one another in terms of surface temperatures (table 20). Nests with grass growth ( $\bar{x} = 36.24$  °C) had significantly lower surface temperatures than those without ( $\bar{x} = 46.10$  °C) (figure 49c). Mean nest surface temperatures varied significantly ( $P \leq 0.05$ ) between all hours of the day except 09:00 and 14:00, 10:00 and 15:00, 12:00 and 13:00, and 14:00 and 15:00. Nest surface temperatures did not significantly vary with nest orientation (all  $P > 0.05$ ) (figure 49b).

**Table 20.** Nest surface temperature (°C) descriptive statistics per nesting section between 07:00 and 15:00, on 1 December 2022.

Section	Min	Max	Mean	SD	SE
A	23.1	50.0	36.8	6.5	0.5
B	20.3	66.4	36.9	10.8	0.8
C	19.3	53.7	36.6	9.5	1.0
D	20.8	67.3	42.6	12.1	0.8
E	20.2	50.0	34.8	6.1	0.5
F	20.8	66.7	46.8	12.3	0.7

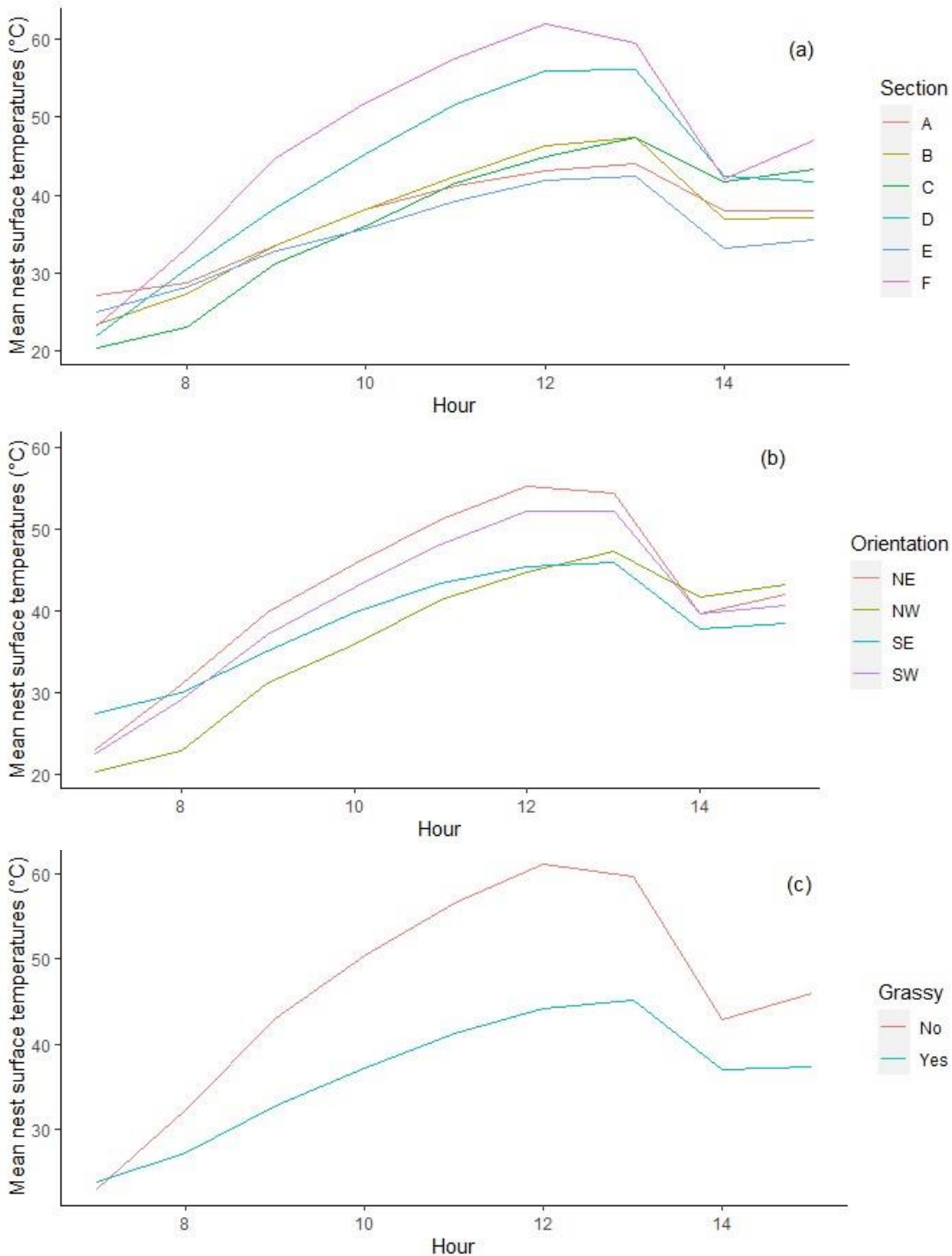


**Figure 49.** Mean hourly nest surface temperatures by (a) nesting section, (b) nesting orientation, and (c) grass-cover status of the nesting sites.

Shading over the nesting sites varied significantly with section ( $P < 0.001$ ,  $F = 9.89$ ,  $df = 4$ ), orientation ( $P < 0.001$ ,  $F = 26.52$ ,  $df = 2$ ), and hour of the day ( $P < 0.001$ ,  $F = 288.89$ ,  $df = 8$ ). The mean shading percentages for the nest sections A–F were 11.67%, 22.03%, 21.13%, 16.87%, 16.77%, and 22.08%, respectively. Section A varied significantly from sections B ( $P < 0.001$ ), C ( $P < 0.05$ ), and F ( $P < 0.001$ ) with regards to shading, as did section F from section D ( $P < 0.05$ ) (figure 50a). The mean shading percentages for the nest orientations NE, NW, SE, and SW were 20.02%, 21.13%, 11.20%, and 21.02%, respectively. The shade cover of SE facing pens was significantly lower than all other orientations (all

$P < 0.001$ ). The shade cover of the other nest orientations did not significantly differ ( $P > 0.05$ ) from one another (figure 50b).

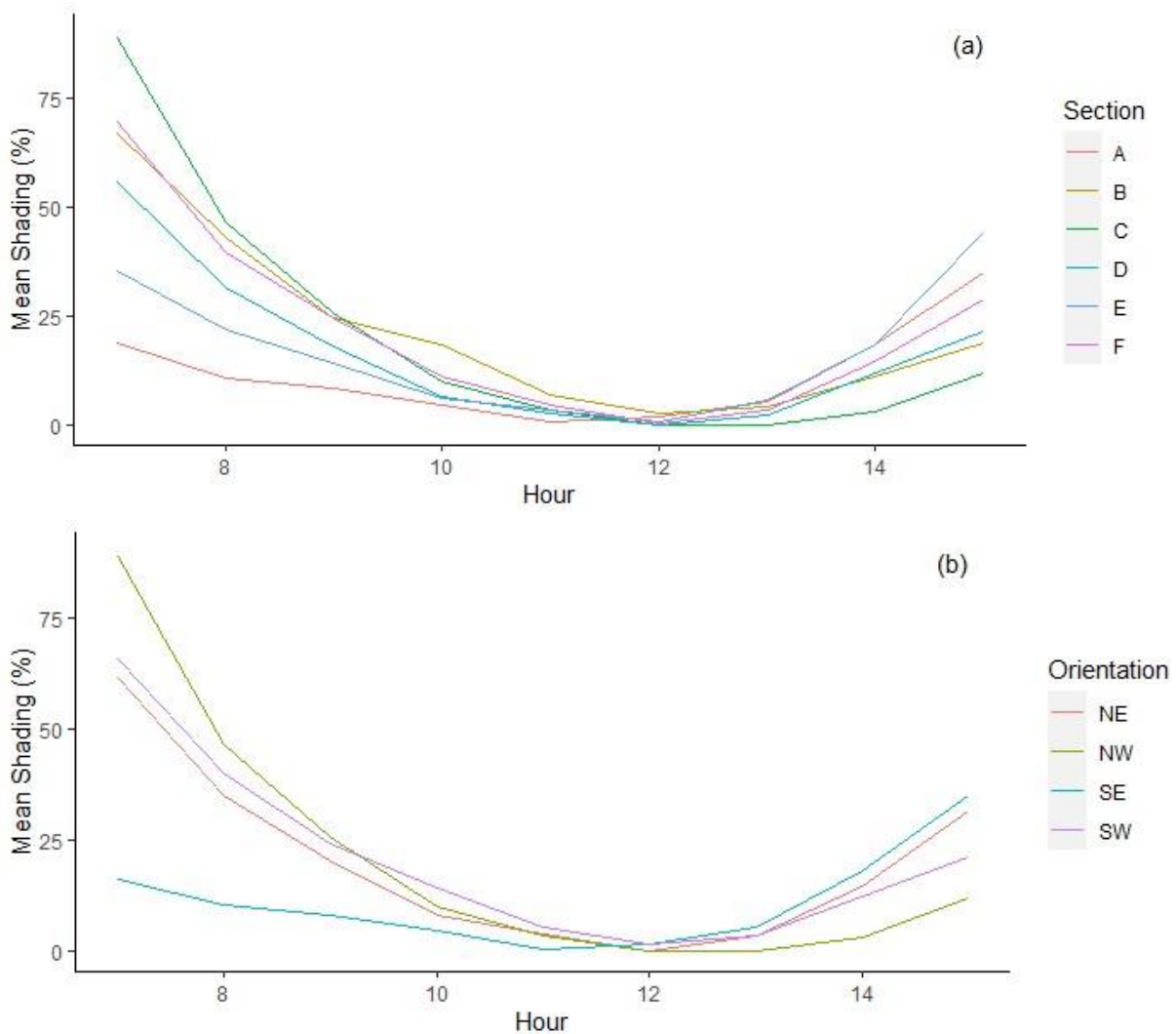


**Figure 50.** Mean hourly shading percentage over nesting sites per (a) nesting section and (b) nesting orientation.

#### 6.5.5. Crocodile pen and nest utilization

Proportional pen area/substrate occupancy varied significantly over the seven monitored weeks ( $P < 0.001$ ,  $\chi^2 = 790.76$ ,  $df = 48$ ) and between all time-of-day categories ( $P < 0.001$ ,  $\chi^2 = 561.80$ ,  $df = 6$ ) (figure 51). The proportional occupancy of nesting sites was greatest in the afternoon (30% of the crocodiles within view), followed by the morning, and finally midday. The proportional occupancy of waterbodies showed the opposite pattern, where 73% of the crocodiles within view during midday flights were occupying waterbodies. The grass/sand substrate was the least frequently occupied at all times of the day.

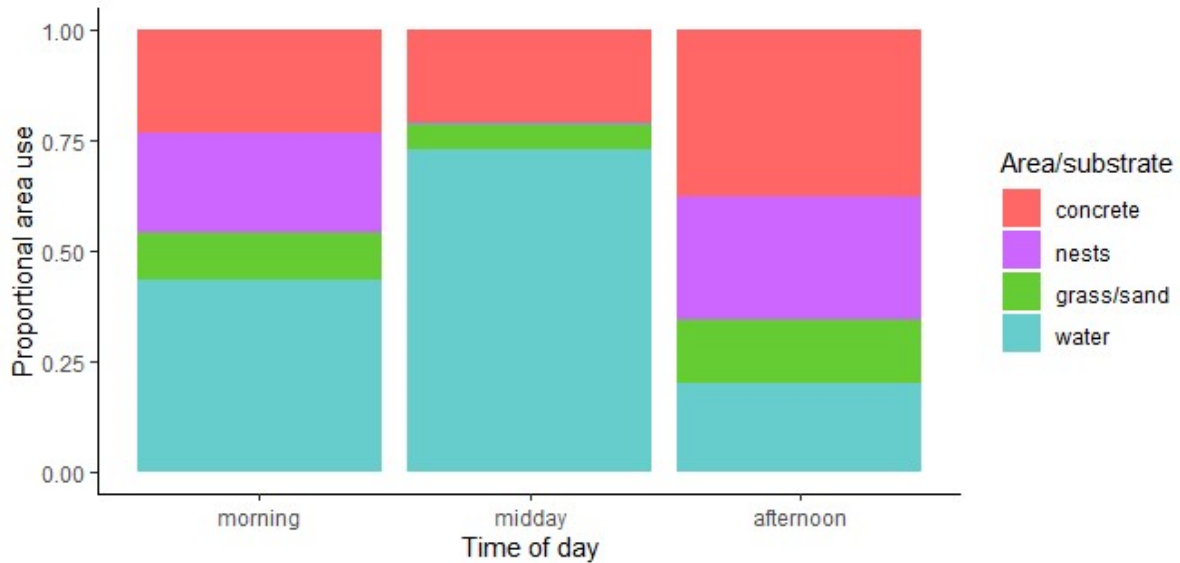


**Figure 51.** Proportional pen area/substrate use per time of the day, categorized into morning (before 11:00), midday (12:00–13:00), and afternoon (after 15:00).

Nest site occupancy varied significantly with air temperatures ( $P < 0.001$ ,  $z = 5.001$ ,  $\beta = -0.055$ ,  $SE = 0.002$ ) and solar radiation levels ( $P < 0.001$ ,  $z = -11.722$ ,  $\beta = -0.007$ ,  $SE = 0.001$ ), but was not impacted by grassy cover over the nesting sites ( $P > 0.05$ ). The frequency of nest occupancy was found to vary significantly with both the distance of the nests from the closest water bodies ( $P < 0.05$ ,  $t = -2.091$ ,  $\beta = -0.129$ ,  $df = 89.18$ ) and from the tourist walkway ( $P < 0.05$ ,  $t = -3.259$ ,  $\beta = -0.127$ ,  $df = 69.39$ ). Specifically, nests closer to waterbodies and the walkway were occupied more often. Nesting section confirmations (i.e., eggs recovered) were significantly ( $P < 0.05$ ,  $t = 3.616$ ,  $\beta = 0.089$ ,  $df = 17.19$ ) affected by distance from the walkway, but no effect was found for distance from the closest water body ( $P > 0.05$ ). Specifically, confirmed nests were more frequent at nesting sites further from the walkway.

A Chi square test indicated that there was an association between the nests occupied (“occupancy”) in the drone imagery and the confirmed successful nests (“utilization”) excavated across different nesting sections ( $P < 0.001$ ,  $\chi^2 = 5878.8$ ,  $df = 1$ ). However, the limited overlap between the drone and farm datasets precluded a statistical confirmation of this association per nesting section. Both nest occupancy ( $P < 0.001$ ,  $\chi^2 = 99.886$ ,  $df = 5$ ) and confirmed nesting ( $P < 0.001$ ,  $\chi^2 = 49.195$ ,  $df = 5$ ) showed significant variation across different sections when assessed separately (figure 52).

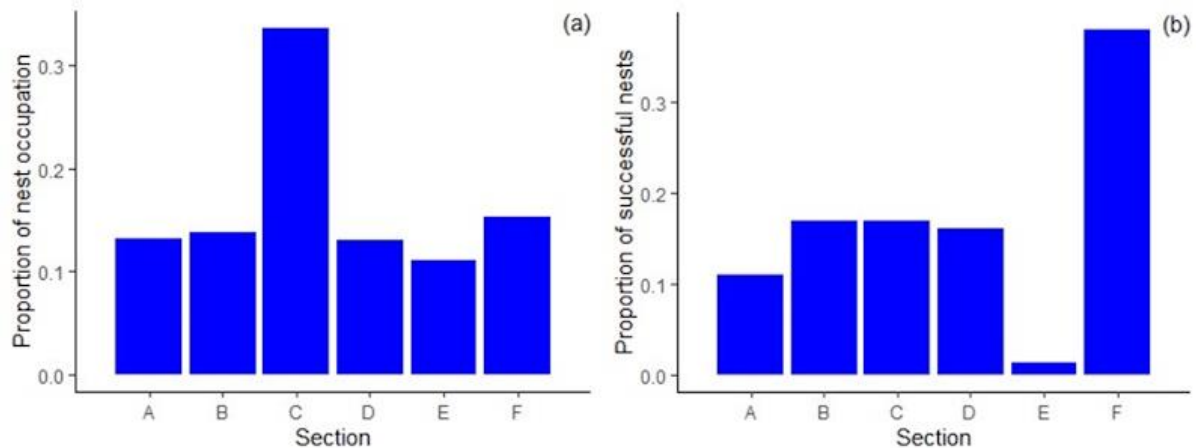


**Figure 52.** The proportional nest site occupancy (a) and confirmed nesting successes (b) per nesting section.

Proportions from figure 52 were converted to percentages for ease of discussion and interpretation. Nesting section C was the most frequently occupied (34%), and Section F was the most frequently nested in (38%). Nesting section E was the least frequently occupied (11%) and nested in (0% - this value is rounded, there was a single nest confirmed in section E throughout the full nesting period). Sections A, B, D, and F had intermediate occupancy with proportions of 13%, 14%, 13%, and 15%, respectively. Sections A–D had varying levels of nest utilization with proportions of 11%, 17%, 17%, and 16%, respectively. Nesting sections were preferentially occupied and utilized in the following orders:  $C > F > B > A \text{ \& } D > E$  and  $F > B \text{ \& } C > D > A > E$ , respectively. Both nest occupancy ( $P < 0.001$ ,  $\chi^2 = 113.3$ ,  $df = 3$ ) and nest utilization ( $P < 0.05$ ,  $\chi^2 = 9.784$ ,  $df = 3$ ) showed significant variation across different orientations as well. Nest facing NW were the most frequently occupied (46%), NE facing nests had intermediate occupancy (23%), and SE and SW facing nests had the lowest occupancies (both 16%). Orientation NE was nested in most frequently (36%), followed by orientations NW and SW (both 23%), and finally SE (18%). As the nesting season progressed, grass began growing into some of the nesting sites. Once this grassy growth began, nests with grassy cover produced significantly less in terms of nesting success (i.e., eggs deposited) than those without ( $P < 0.001$ ,  $\chi^2 = 28.571$ ,  $df = 1$ ).

The mean SHLs of crocodiles per pen area/substrate, nesting section, and nesting orientation were ranked as follows: concrete > water > grass/sand > nests,  $C > B > D > F > A > E$ , and  $NW > NE > SW > SE$ , respectively (figure 53). SHLs of crocodiles occupying the different areas/substrates of the pen varied significantly ( $P < 0.001$ ,  $F = 63.84$ ,  $df = 3$ ). Specifically, crocodiles occupying nests were shorter than those occupying all other substrates (all  $P < 0.001$ ). Crocodiles occupying concrete areas also varied in length (longer SHLs) when compared to those occupying grass/sand areas ( $P < 0.001$ ). SHLs of crocodiles within the nesting areas of the pen varied significantly with section ( $P < 0.001$ ,  $F = 14.970$ ,  $df = 5$ ) and orientation ( $P < 0.001$ ,  $F = 8.667$ ,  $df = 2$ ). The mean SHLs recorded within nesting section C were significantly greater than those for all other sections (all  $P < 0.001$ ), no other sections varied from one another regarding this morphometric ( $P > 0.05$ ). The mean SHLs recorded within nests facing the NW significantly varied from other all other orientations (all  $P < 0.001$ ).

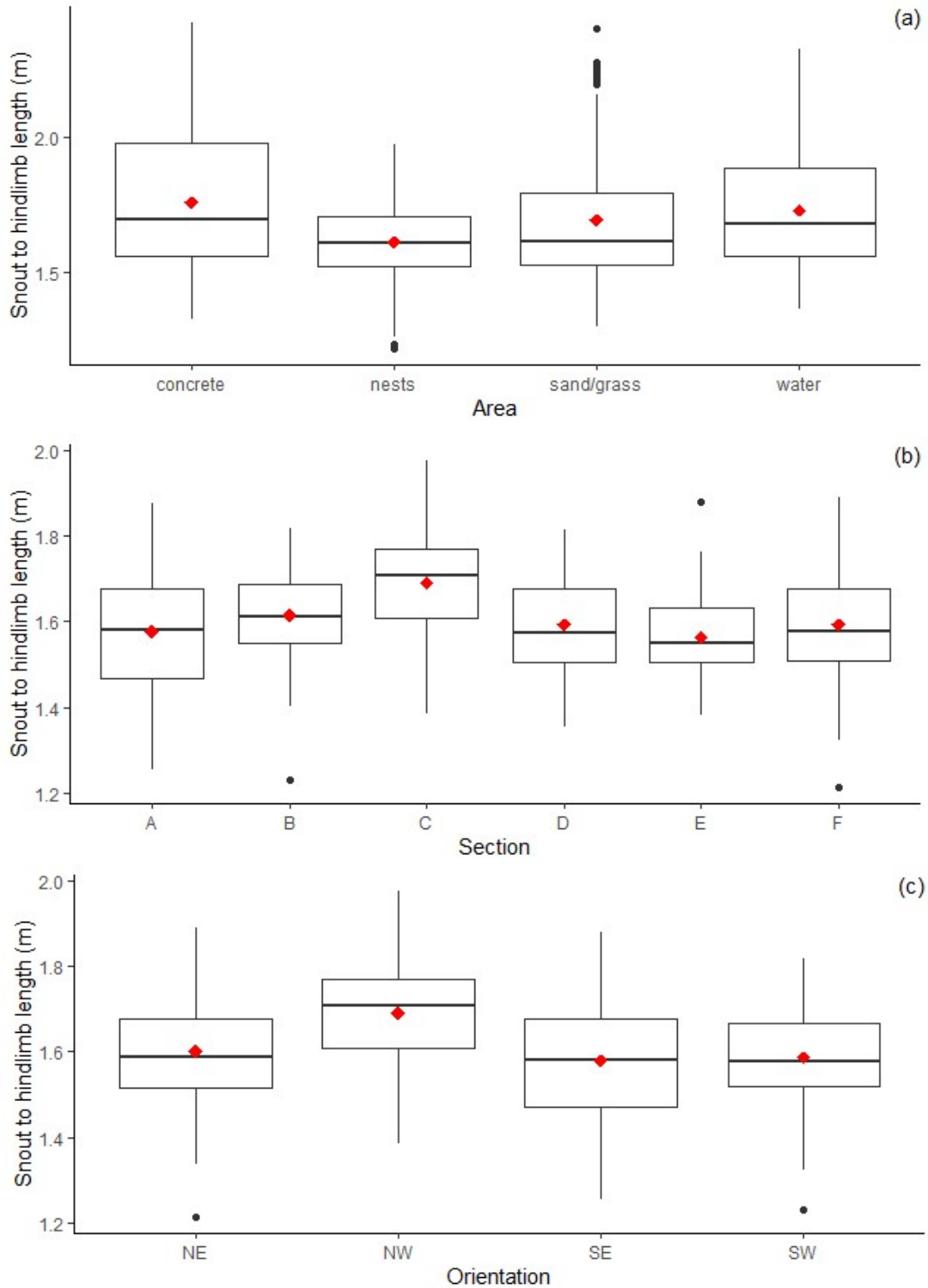


**Figure 53.** SHL of the crocodiles occupying the various pen areas (a), nesting sections (b), and nesting orientations (c). Each boxplot displays the median (centre line), interquartile range (box edges), and 1.5 \* IQR (whiskers). Points beyond the whiskers represent outliers and means are represented by red rhombuses.

## 6.6. DISCUSSION

### 6.6.1. Nest depth evaluation

Crocodile nest depths in this study were consistent with previous wild Nile crocodile nest studies (Pooley & Gans, 1976; Kofron, 1989; Hartley, 1990; Swanepoel<sup>2</sup> *et al.*, 2000). Nest depth varied between sand types (coarse versus fine), which may have impacted the ease of nest construction. Nests dug in densely packed fine sand were shallower, with the first eggs laid at deeper depths than in coarse sand nests. The looser consistency of coarse-sand nests likely impacted the stability/uniformity of the nests. If the sand constantly fell back inward during digging, the result would be a narrower nesting space, potentially explaining why the deepest eggs were comparably deep with fine sanded nests but the final eggs laid were shallower, increasing overall nest depths. Not all assessed nests were spherical, some were tightly packed, whilst others were spread out in a flatter topography. These findings concur with Kofron (1989), where soil type affected Nile crocodile nest cavity structure/shape as follows: bowl-shaped nests were produced in loose sand, funnel-shaped nests in loose sands with firm substrate, and “roofed” downward slanting nests in firm soils. Soil particle size has also been implicated in the thermal regimes of crocodile nests (Somaweera & Shine, 2013). In the current study, the deepest egg depths recorded between nests with the two sand-types did not differ. This could be attributed to the comparable size of the breeding females (similar digging capabilities) or to instinctual behaviour, such as a preferred 'default' depth for nesting. The preferred depth for the deepest egg, whether chosen for nest stability, optimal incubation conditions, protective measures against predators or adverse weather, or some unknown factor(s) remained consistent regardless of the sand type.

### 6.6.2. Thermal profiles within nests

Subsurface nest temperatures were influenced by climatic conditions, nest site location/orientation, nest depth, and grass cover. Thermal inertia slowed heating from ambient temperatures and radiation at deeper depths. As relative humidity increased, nest temperatures decreased. The strength of this correlation diminished as soil depths increased, supporting the established relationship between relative humidity and soil moisture content, and subsequently, soil thermal inertia. Although there was relatively little rainfall during the study, the effect on shallower nest temperatures was intuitive, the cooling effect lessened with increasing depths.

Section F dowel iButtons recorded higher temperatures and greater daily temperature ranges than in section A. These sections differed in daily shade percentages (orientation based) and nest surface temperatures. Differential sunlight, wind, and shade exposure likely contributed to observed variations in nest surface temperatures between the sections. Single nest depths ranged from 19–35 cm, and although mean temperatures fell within 1.15 °C of one another and mean daily temperature ranges varied between 1.05 °C and 3.99 °C, recorded temperatures varied significantly. Nest depths varied between all orientations, whereas subsurface temperatures varied between all orientations except SW and NW facing nests. Nest surface temperatures did not vary with orientation, but shading proportions varied between SE facing nests and other orientations. These findings suggest female crocodiles may select nest depths, and therefore temperatures, based on orientation, independent of shading and nest surface temperatures; the rationale is unclear. Only sections D and F did not vary from one another regarding mean nest temperatures, these sections had the highest surface and subsurface nest temperatures. Grass growth over nests, likely enhancing the boundary layer effect, acted as a thermal buffer and reduced the direct impact of solar radiation on the sand below.

Mean temperatures at various depths (single and dowel nests) tended to fit into the narrow range of 25–26 °C, highlighting a measure of stability within the nesting environment. Shallower depths had greater daily temperature variations, this necessitates further exploration of whether crocodiles select

nest depths based on daily temperature ranges or averages. This is like western painted turtle (*Chrysemys picta bellii*) mean nest temperatures not varying with nest depth, but the daily range in nest temperatures did vary (Refsnider, 2012). The effects of orientation (interpreted with caution) on daily temperature ranges were significant for all comparisons, suggesting orientation affected subsurface temperature ranges at various depths. A soil temperature study in China (1962-2011) found global warming effects occurred as deep as 3.2 m, with soil surface temperatures having increased 31% more than air temperatures (Zhang *et al.*, 2016). Although there are distinct climatic, geographical, and environmental differences between regions, the broader insights remain valuable. Nile crocodile nest depths fall well within 3.2 m of the ground surface, such temperature changes could pose challenges for incubation success, sex determination, and hatchling survival. Lizards (*Bassiana duperreyi*) changed nesting depths and timing in response to rising ambient temperatures, but the seasonal progression of soil temperatures had also shifted due to climate change. Unfortunately, their attempts at nest temperature remediation were unsuccessful and offspring sex ratios were affected (Telemeco *et al.*, 2009).

Although incubation and hatching are artificially managed on farms, nesting activities and behaviours of breeding males and nesting females might be impacted by climate change. Habitat and nest quality alterations due to climate change necessitate adaptations by wild crocodile populations (Refsnider, 2012; Mainwaring *et al.*, 2017; Fukuda *et al.*, 2022). Farmed crocodiles do not have the same opportunity to adapt to changing environments by relocating, modifying nesting sites, or altering nesting materials. Consequently, there is concern regarding unmonitored changes in the immediate environment/habitats of commercially farmed crocodiles. From a nesting perspective this involves understanding and controlling for thermal and behavioural factors which influence nest site selections.

#### 6.6.3. Surface and faunal temperature variations

Crocodile back temperatures were affected by positional temperature, air temperature, relative humidity, radiation, and wind speeds. These findings, alongside the proportional hourly area/substrate use results, are consistent with ectothermy, supporting the idea that farmed crocodiles relinquish nesting behaviours during the warmest parts of the day to seek out more thermally comfortable areas within the pen. This is like the finding of Combrink *et al.* (2016) where wild female Nile crocodiles were rarely seen guarding nests diurnally unless there was nearby shade cover or during cooler/cloudy/rainy weather. Although nearby shading is beneficial for the guarding behaviours of wild female crocodiles, nesting sites are predominantly located in less-shaded areas (Kofron, 1989, López-Luna *et al.*, 2015; Combrink *et al.*, 2016). Shade implementations close to nesting sites might benefit the farmed nesting females in terms of nest site guarding behaviours. Shading over nests was shown as an effective mitigation strategy buffering increases in sand temperatures for sea turtle nests (Hill *et al.*, 2015), and this may be applicable for crocodile nests as well.

The correlations of radiation and wind speed with nest occupancy in the current study were stronger than those of air temperature and relative humidity, indicating a more impactful influence over crocodile nesting behaviours. Nest occupancy decreased as radiation levels increased and increased as wind speeds increased. Higher radiation levels, increasing temperatures, and increasing relative humidity decreased the appeal of occupying nesting sites, suggesting a thermal threshold for crocodile comfort in nest sites. Increased wind speeds may have altered the atmospheric boundary layer directly over the nesting sites, making the nesting sites more thermally tolerable. Nest orientation, section, shading, and grassy cover all impacted nest surface temperatures. Nests with grassy cover growing over the surface had lower surface temperatures.

#### 6.6.4. Crocodile pen and nest utilization

Nest occupancy was linked to increasing air temperatures and radiation levels nearing midday, with crocodiles retreating to the waterbodies or concrete. Nest defence and/or thermal protection would not have been prioritized if thermoregulatory requirements took precedence (Kofron, 1989; Swanepoel *et al.*, 2000; Bourquin, 2008). Grass growth did not affect nest occupancy behaviours. More frequent occupation of nests closer to the walkway confirmed that crocodiles were not behaviourally impacted by human presence. However, confirmed nests were more frequent further from the walkway, countering the hypothesis that human presence would not impact nesting. This might be attributed to visitor activity/disturbance, a perceived predation risk, practise/decoy nesting (Lang *et al.*, 1989; Van Weerd, 2010), or other factors impacting nest-habitat quality. Nests closer to water were occupied more frequently, likely due to easier access. Distance from water had no significant effect on successful nesting (i.e., egg deposition), contradicting that hypothesis. For wild Nile crocodiles, distance from water does not independently impact nest site selections, rather the relationship between this parameter and height above water (Swanepoel, 2000; Botha, 2005). These natural nests were dug on inclines, this is dissimilar to farmed crocodile experiences where nests are built with relatively flat topographies and height above water is set by the pen design.

Section F was frequented comparably with most other sections, was second highest in distance from the water and walkway, and had the greatest confirmed nesting frequency. Section C had the highest occupancy frequency, but comparable confirmed nesting frequency with most other sections. Section E was interesting, it had a comparatively low distance from the walkway, the shortest average distance from water, and was frequented comparably with most other sections; however, it was least preferred for nesting. All sites within section E were grassy by the end of the nesting season; however, this section was least favoured for active nesting both before (one nest produced) and after (no nests produced) grassy growth. Section A had the greatest mean distances from water and the walkway and was the second least preferred for nesting.

Shorter (SHL) individuals occupied nests; these were most likely breeding females. Larger females did not dominate preferred nesting sections within the pen, only section C had comparatively higher SHLs. It is possible that smaller females may not have approached nesting sites as readily, or that size is not an entirely reliable indicator of dominance. This study captured only a snapshot of nesting behaviours; further research would be needed to confirm these findings.

#### 6.7. CONCLUSIONS

Subsurface nest temperature data revealed intricate thermal variations influenced by climatic conditions, nest site location and orientation, nest depth, and grass cover. Although farmed crocodiles' choices for nesting sites and sand types are more limited than in the wild, crocodiles in the current study dug nests of comparable depth to those dug by wild Nile crocodiles. Whilst mean temperatures and daily temperature ranges within nests varied statistically, the real-world impact of these fluctuations requires further evaluation. Nest temperatures decreased with increasing sand depths, and temperatures recorded at deeper depths were less influenced by surface conditions. Grassy cover significantly affected nest surface and subsurface temperatures; these nests were selected against for egg laying purposes.

Circuitous nest visitations likely contributed to the occupancy versus successful nesting findings, demonstrating the female crocodile's ability to recognize human presence as a potential predation risk to their clutches. Nesting section F was preferred for confirmed nests but had comparable occupancy rates with most other sections. This section had the highest mean nest surface temperatures, second highest subsurface temperatures, second highest mean proportional shading, and second highest distances from both the walkway and nearest water body. The findings herein

showed a hierarchical preference for nesting sections within the pen, based upon a combination of influencing factors. Larger, presumably more dominant, females did not impact the nesting behaviours/capabilities of smaller, presumably less dominant, females.

Wild crocodile populations have demonstrated resilience by adapting to multiple climate changes over many years. Current changes in climate are largely driven by human activities and are occurring faster than in the past, with largely unpredictable outcomes. If climatic changes in nesting environments occur, female crocodiles might reduce their nesting activities, purposefully alter the timing and/or depths of their nests or be forced to compete for desirable or thermally optimal nesting sites. These compensations may not be sufficient, as has been shown in nesting lizards and sea turtles (Telemeco *et al.*, 2009; Hill *et al.*, 2015). Crocodile nest site preferences, as shown by the current study, are complex but quantifiable, and therefore manageable on farms. Identifying the features making nesting sites “preferable” to farmed crocodiles (considering both thermal and behavioural effects) will inform future pen layout/alteration requirements, ensuring welfare requirements are met. Manipulation of shading and cover near nest sites in farmed environments could delay the potential negative effects of climate change on nest temperatures and nest site selections.

#### 6.8. CRITICAL EVALUATION AND RECOMMENDATIONS

The roles that section, orientation, human presence, ambient/environmental temperatures, and subsurface sand temperatures play in determining nest site selection and nest depths on farms, require further evaluation. Assessing multiple nesting groups, over multiple breeding seasons, including further climate variables, and adding nighttime recordings will benefit future studies.

## 7. Concluding summary

In conclusion, the method development and application of multiple frontier technologies in this research has yielded significant insights into the thermal and behavioural patterns of Nile crocodiles, both in captive and wild environments. A central theme across all chapters has been the welfare of Nile crocodiles, providing valuable perspectives on the ethical implications of commercial farming and the natural behaviours and thermal experiences of these animals in the wild, specifically within Kruger National Park. Parallels between some chapters in this thesis are noted in this conclusion. Statistical comparisons were ruled out due to the vast variations in the methods and technologies employed, locations and times of year that were assessed, and the different populations studied (e.g., size class variations and/or wild versus captive conditions). Internal body temperature ( $T_{b_{\text{internal}}}$ ) outcomes between chapters 2.5 and 5, as well as external body temperature ( $T_{b_{\text{external}}}$ ) comparisons between chapters 4, 5, and 6 are considered. Farmed breeder Nile crocodile thermoregulatory behaviours were assessed in chapters 4 and 6, which correspond to non-breeding and breeding seasons, qualitative behavioural comparisons are made between these seasons. The NSPCAs hyperthermia concerns, and recommendations for more effective cooling strategies, on commercial crocodile farms in South Africa are validated in chapters 2.5, 4, and 6, and management recommendations are made.

Mean internal body temperatures ( $T_{b_{\text{internal}}}$ ) of farmed and wild Nile crocodiles during summer months were within  $\leq 2$  °C of each other (chapters 2.5 and 5), regardless of variations in logger types, crocodile size classes and sex, and locations and years of the two assessments. Mean daytime external body temperatures ( $T_{b_{\text{external}}}$ ) of farmed and wild Nile crocodiles during summer and winter months were within 3.2 °C and 6.4 °C of each other (chapters 4 and 5), respectively. This was regardless of variations in logger types, potential sex effects, study locations, and the years of the two assessments. Although these comparisons are drawn without statistical analyses, they suggest a measure of  $T_b$  consistency, more so for internal than for external temperatures, highlighting thermoregulatory efficiencies across size classes and wild and captive populations. A further comment on long-term internal temperature monitoring in crocodiles is the recommendation of dental acrylic as the more robust encapsulation material when using force-fed loggers (chapters 2.5, 2.6, and 5).

Pen substrate utilizations were captured in drone imagery in chapters 4 and 6 of this thesis, one chapter assessed summer and winter substrate selections and the other looked at the same substrate selections over a breeding season. Substrate utilization during the breeding season (which includes autumn and summer months) was more like the summer than the winter substrate utilizations, which was expected due to seasonal similarities. The breeding season to summer comparison saw similarity in the proportional waterbody utilizations, which were greater than in winter; waterbody use peaked during the warmest (air temperature) hours of the day. Nest utilization markedly increased during the breeding season compared to the summer and winter comparisons, especially in the early mornings and afternoons, while water utilization concurrently decreased at these times, suggesting an inverse relationship in the usage patterns. Where concrete utilization was favoured in winter, this substrates utilization decreased comparatively in breeding and summer seasons. These patterns suggest that monitoring nesting activities at different times, possibly outside of daytime hours, could potentially yield more effective results. Similar future studies should consider adding nighttime substrate utilization assessments.

Effective shade provision and regular waterbody replenishment have been recommended by the NSPCA for commercial crocodile farms in South Africa; the goal of which is the prevention of summertime hyperthermia in concrete-dominated pens. Considering affordability, regularly replenishing waterbodies more often than what is required for hygiene purposes, or implementing water-cooling systems, is likely the more costly and drought-dependent approach to providing a wider

range of cooling options in summer. Colourful concretes were not as variable as imagined in terms of their thermal properties, and even seasonal spray-on solutions are likely laborious and costly, potentially outweighing the benefits of such an approach. Shade provision over concrete areas of pens has been identified, in multiple chapters of this work (chapters 2.5 and 4), as an effective daytime concrete-coolant. Although the extent and efficiency of shading were not tackled in this thesis, both instances of shade provision over concrete areas (one via a shade net and another via a tree) showed cooling results that rivalled daytime water temperatures during the warmest part of the day. In both cases, the shading provided covered  $\leq 20\%$  of the available concrete area. Due to space restrictions imposed by high stocking densities, as well as the resulting dominance-related behaviours, it stands to reason that many of the crocodiles in the pens would not have had the opportunity to make use of these shaded concrete areas when needed. Summertime shade provision over larger portions of pens would create more cooling opportunities for the housed populations. Removeable shade netting would be ideal, meeting the seasonal requirements specific to the current hyperthermia concerns.

With the recent high-temperature concerns for farmed crocodiles and the potential contribution of cold temperatures toward the pansteatitis events affecting wild crocodiles, many of the hypotheses were centred around how Nile crocodiles are currently affected by, experiencing, and managing local environmental temperatures. The hypotheses that drones could be used to effectively record welfare via the reliable and non-invasive capture of morphometric measurements, as well as thermoregulatory and reproductive behaviours via seasonal monitoring of farmed crocodile pens and the inhabitants, were confirmed in the current research. Drone assessments were carried out on both grower and breeder sized Nile crocodiles. Recommended drone models and flight altitudes varied between the size classes, and the recommended time of day for conducting flights was comparable among size classes but varied with season (early mornings for summer and late mornings for winter). Merging drone data with those of crocodile-proofed ground-level abiotic recording devices and local weather stations yielded fast-paced, cost-effective, non-invasive, and comprehensive assessments of farmed Nile crocodile habitat experiences, nest site selections, health, and behaviour. The assessment of wild crocodile thermal experiences and activity furthers our understanding of the hypothesized cool-weather effects which have been suggested as linked to the health of the Nile crocodile population within Kruger National Park. Incorporating modern, cutting-edge technologies alongside the well-established, more traditional monitoring devices and techniques has advanced our understanding of the thermal responses and behaviours of captive and wild Nile crocodiles in South Africa.

While this work has answered key questions, it has also opened new avenues of inquiry, underscoring the dynamic and evolving nature of Nile crocodile research and conservation. Several limitations encountered during the conduction of studies within this thesis are acknowledged. There are multiple climatic/abiotic factors that were not included in this collection of studies, future assessments should aim to capture as much of the immediate and regional climatic factors as possible for proactive and predictive management strategies. Resource constraints impacted the length of data collection and the quality and quantity of tools/materials available to this research. Sample sizes were occasionally smaller than ideal due to failure of the technologies deployed, affecting the generalizability of some findings. Time limitations prevented the repetition of experiments or extension of the research period, which could have strengthened some outcomes.

## 8. References

- Allan, B.M., Lerodiconou, D., Hoskins, A.J. and Arnould, J.P. (2019). A rapid UAV method for assessing body condition in fur seals. *Drones*, 3(1), 24. DOI: [10.3390/drones3010024](https://doi.org/10.3390/drones3010024)
- American Society of Heating, Refrigerating and Air-Conditioning Engineers (2009). 2009 ASHRAE Handbook: Fundamentals (Inch pound edition). ASHRAE Inc. Atlanta, GA.
- Andrew, W., Greatwood, C., and Burghardt, T. (2020). Fusing animal biometrics with autonomous robotics: Drone-based search and individual ID of Friesian cattle. In Proceedings of the IEEE/CVF Winter Conference on Applications of Computer Vision Workshops, 38–43. DOI: [10.1109/WACVW50321.2020.9096949](https://doi.org/10.1109/WACVW50321.2020.9096949)
- Ashton, P. J. (2010). Demise of the Nile crocodile (*Crocodylus niloticus*) as a keystone species for aquatic ecosystem conservation in South Africa: the case of the Olifants River. *Aquatic Conservation: Marine and Freshwater Ecosystems*, 20(5), 489–493. DOI: [10.1002/aqc.1132](https://doi.org/10.1002/aqc.1132)
- Ashton, P. J. (2007). Riverine biodiversity conservation in South Africa: current situation and future prospects. *Aquatic Conservation: Marine and Freshwater Ecosystems*, 17(5), 41-445. DOI: [10.1002/aqc.886](https://doi.org/10.1002/aqc.886)
- Ashton, P. J., Love, D., Mahachi, H., and Dirks, P. H. G. M. (2001). An overview of the impact of mining and mineral processing activities on water resources and water quality in the Zambezi, Limpopo and Olifants basins in southern Africa. *Mining, Minerals and Sustainable Development Project Report*. CSIR-Environmentek, Pretoria, South Africa and Geology Department, University of Zimbabwe, Harare, Zimbabwe.
- Aubert, C., Le Moguédec, G., Assio, C., Blatrix, R., Ahizi, M.N.D., Hedegbetan, G.C., Kpera, N.G., Lapeyre, V., Martin, D., Labbé, P. and Shirley, M.H. (2021). Evaluation of the use of drones to monitor a diverse crocodylian assemblage in West Africa. *Wildlife Research*, 49(1), 11-23. DOI: [10.1071/WR20170](https://doi.org/10.1071/WR20170)
- Bassetti, L. A., Marques, T. S., Malvásio, A., Piña, C. I., and Verdade, L. M. (2014). Thermoregulation in captive broad-snouted caiman (*Caiman latirostris*). *Zoological Studies*, 53(1), 9. DOI: [10.1186/1810-522X-53-9](https://doi.org/10.1186/1810-522X-53-9)
- Bayliss, P. (1987). Survey methods and monitoring within crocodile management programmes. *Wildlife management: crocodiles and alligators*, 157-175.
- Behangana, M., Wilber, L., Dendi, D., Luiselli, L. and Ochanda, D. (2017). Population surveys of Nile crocodiles (*Crocodylus niloticus*) in the Murchison Falls National Park, Victoria Nile, Uganda. *European Journal of Ecology*, 3(2), 67-76. DOI: [10.1515/eje-2017-0015](https://doi.org/10.1515/eje-2017-0015)
- Bevan, E., Whiting, S., Tucker, T., Guinea, M., Raith, A. and Douglas, R. (2018). Measuring behavioral responses of sea turtles, saltwater crocodiles, and crested terns to drone disturbance to define ethical operating thresholds. *PLoS One*, 13(3), e0194460. DOI: [10.1371/journal.pone.0194460](https://doi.org/10.1371/journal.pone.0194460)
- Beyeler, P. M. (2011). Protein requirements of juvenile Nile crocodiles (*Crocodylus niloticus*) in an intensive production system (Doctoral dissertation, University of Pretoria).
- Blessing, M., Tendayi, N., Wilson, M., Lesley, M., Evermess, S., Chiedza, M., and Zacharia, I. (2014). Effect of feeding different graded dietary protein levels on growth rate of Nile crocodile

- (*Crocodylus niloticus*) hatchlings. *International Journal of Science, Technology & Management*, 3 (12), 123-128.
- Bolton, M. (1989). The management of crocodiles in captivity. FAO conservation guide 22. Rome: *Food and Agricultural Organization of the United Nations*.
- Booyens, P. L., Bouwman, H., Pieters, R., Pienaar, D., and Govender, D. (2013). Mass mortalities of Nile crocodiles (*Crocodylus niloticus*) in the Kruger National Park, South Africa. *Suid-Afrikaanse Tydskrif vir Natuurwetenskap en Tegnologie*, 32(1), 1. DOI: [10.4102/satnt.v32i1.787](https://doi.org/10.4102/satnt.v32i1.787)
- Botha, P. J. (2005). The ecology and population dynamics of the Nile crocodile *Crocodylus niloticus* in the Flag Boshielo Dam, Mpumalanga province, South Africa (Masters dissertation, University of Pretoria).
- Bothma, J. D. P., and Van Rooyen, N. (2005). Intensive wildlife production in Southern Africa. Van Schaik Publishers, 16, 268-300. ISBN 0627025498.
- Bourquin, S. L. (2008). The population ecology of the Nile crocodile (*Crocodylus niloticus*) in the panhandle region of the Okavango Delta, Botswana (Doctoral dissertation, Stellenbosch University).
- Brandt, L.A., Nestler, J.H., Brunell, A.M., Beauchamp, J.S. and Mazzotti, F.J. (2016). Variation in body condition of *Alligator mississippiensis* in Florida. *Bulletin of the Florida Museum of Natural History*, 54, 1-12.
- Brien, M. L., Cherkiss, M. S., Parry, M. W., and Mazzotti, F. J. (2007). Housing Crocodilians in Captivity: Considerations for Central America and Caribbean. Gainesville: University of Florida Institute of Food and Agricultural Sciences. DOI: [10.32473/edis-uw255-2007](https://doi.org/10.32473/edis-uw255-2007)
- Brien, M., Webb, G., Manolis, C., Lindner, G., and Ottway, D. (2010). A method for attaching tracking devices to crocodilians. *Herpetological Review*, 41(3), 305–308. <https://www.researchgate.net/publication/283498972>
- Brien, M. L., Webb, G. J., Gienger, C. M., Lang, J. W., and Christian, K. A. (2012). Thermal preferences of hatchling saltwater crocodiles (*Crocodylus porosus*) in response to time of day, social aggregation and feeding. *Journal of Thermal Biology*, 37(8), 625-630. DOI: [10.1016/j.jtherbio.2012.08.003](https://doi.org/10.1016/j.jtherbio.2012.08.003)
- <sup>1</sup>Brien, M. L., Webb, G. J., Lang, J. W., McGuinness, K. A., and Christian, K. A. (2013). Born to be bad: agonistic behaviour in hatchling saltwater crocodiles (*Crocodylus porosus*). *Behaviour*, 150(7), 737-762. DOI: [10.1163/1568539X-00003078](https://doi.org/10.1163/1568539X-00003078)
- <sup>2</sup>Brien, M. L., Webb, G. J., Lang, J. W., and Christian, K. A. (2013). Intra-and interspecific agonistic behaviour in hatchling Australian freshwater crocodiles (*Crocodylus johnstoni*) and saltwater crocodiles (*Crocodylus porosus*). *Australian Journal of Zoology*, 61(3), 196-205. DOI: [10.1071/ZO13035](https://doi.org/10.1071/ZO13035)
- <sup>3</sup>Brien, M. L., Lang, J. W., Webb, G. J., Stevenson, C., and Christian, K. A. (2013). The good, the bad, and the ugly: agonistic behaviour in juvenile crocodilians. *PloS one*, 8(12), e80872. DOI: [10.1371/journal.pone.0080872](https://doi.org/10.1371/journal.pone.0080872)
- Calverley, P. M., and Downs, C. T. (2015). Movement and home range of Nile crocodiles in Ndumo game reserve, South Africa. *Koedoe: African Protected Area Conservation and Science*, 57(1), 1-13. DOI: [10.4102/koedoe.v57i1.1234](https://doi.org/10.4102/koedoe.v57i1.1234)

- Casas, R., Hermosa, A., Marco, Á., Blanco, T., and Zarazaga-Soria, F. J. (2021). Real-time extensive livestock monitoring using LPWAN smart wearable and infrastructure. *Applied Sciences*, 11(3), 1240. DOI: [10.3390/app11031240](https://doi.org/10.3390/app11031240)
- Chabert, T., Colin, A., Aubin, T., Shacks, V., Bourquin, S.L., Eelsey, R.M., Acosta, J.G. and Mathevon, N. (2015). Size does matter: crocodile mothers react more to the voice of smaller offspring. *Scientific reports*, 5(1), p.15547. DOI: [10.1038/srep15547](https://doi.org/10.1038/srep15547)
- Cloudsley-Thompson, J. L. (1964). Diurnal rhythm of activity in the Nile crocodile. *Animal Behaviour*, 12(1), 98-100. DOI: [10.1016/0003-3472\(64\)90109-5](https://doi.org/10.1016/0003-3472(64)90109-5)
- Colbert, E. H., Cowles, R. B., and Bogert, C. M. (1946). Temperature tolerances in the American alligator and their bearing on the habits, evolution, and extinction of the dinosaurs. *Bulletin of the American Museum of Natural History*, 86(7).
- Combrink, X., Warner, J. K., and Downs, C. T. (2016). Nest predation and maternal care in the Nile crocodile (*Crocodylus niloticus*) at Lake St Lucia, South Africa. *Behavioural Processes*, 133, 31-36. DOI: [10.1016/j.beproc.2016.10.014](https://doi.org/10.1016/j.beproc.2016.10.014)
- Combrink, A. S. (2014). Spatial and reproductive ecology and population status of the Nile Crocodile (*Crocodylus niloticus*) in the Lake St Lucia estuarine system (Doctoral dissertation, University of KwaZulu Natal).
- Combrink, X., Warner, J. K., Hofmeyr, M., Govender, D., and Ferreira, S. M. (2012). Standard operating procedure for the monitoring, capture and sampling of Nile Crocodiles (*Crocodylus niloticus*). *South African National Parks, Skukuza, South Africa, unpublished report*, 1-14. DOI: [10.13140/RG.2.2.17129.08800](https://doi.org/10.13140/RG.2.2.17129.08800)
- Combrink, A.S. (2004). Population Survey of *Crocodylus niloticus* (Nile crocodile) at Lake Sibaya, Republic of South Africa (Masters dissertation, University of KwaZulu Natal).
- Cremieux, J., Vázquez, T., Alpizar, E., and Melo, V. (2005). Management of *Crocodylus moreletii* in captivity conditions. *International Society for Animal Hygiene*, 2, 415-417.
- Crocodile Farmers Association of Zimbabwe (CFAZ): Codes of Practice (2012). Prepared in consultation with: Wildlife Veterinary Unit, Dept. of Veterinary Services, Ministry of Agriculture Zimbabwe Parks & Wildlife Management Authority, Ministry of Environment Veterinarians for Animal Welfare Zimbabwe.
- Cuijk, Y. V. (2011). Feeding behavior of captive juvenile *Crocodylus porosus* (Doctoral dissertation, Utrecht University).
- Dabrowski, J. M., and De Klerk, L. P. (2013). An assessment of the impact of different land use activities on water quality in the upper Olifants River catchment. *Water SA*, 39(2), 231-244. DOI: [10.4314/wsa.v39i2.6](https://doi.org/10.4314/wsa.v39i2.6)
- Davies, C. L. (2005). Thermoregulation, activity and energetics of the pig-nosed turtle (*Carettochelys insculpta*) in the Daly River, Northern Territory (Doctoral dissertation, University of Canberra).
- Davis, B. M. (2001). Improved nutrition and management of farmed crocodiles—hatchling to harvest. Australian Government Rural Industries Research and Development Corporation. *RIRDC Project*, 01/123.

- de Kock, M. E., O'Donovan, D., Khafaga, T., and Hejzmanová, P. (2021). Zoometric data extraction from drone imagery: the Arabian oryx (*Oryx leucoryx*). *Environmental Conservation*, 48(4), 295-300. DOI: [10.1017/S0376892921000242](https://doi.org/10.1017/S0376892921000242)
- Deeming, D. C. (2004). Temperature-dependent sex determination in vertebrates. Smithsonian books, ISBN 1-58834-203-4, 33-41.
- Desai, B., Patel, A., Patel, V., Shah, S., Raval, M. S., and Ghosal, R. (2022). Identification of free-ranging mugger crocodiles by applying deep learning methods on UAV imagery. *Ecological Informatics*, 72, 101874. DOI: [10.1016/j.ecoinf.2022.101874](https://doi.org/10.1016/j.ecoinf.2022.101874)
- De Villiers, S., and Mkwelo, S. T. (2009). Has monitoring failed the Olifants River, Mpumalanga? *Water SA*, 35(5), 671-676. DOI: [10.4314/wsa.v35i5.49193](https://doi.org/10.4314/wsa.v35i5.49193)
- Diefenbach, C. O. D. C. (1975). Gastric function in *Caiman crocodilus* (Crocodylia: Reptilia)—II. Effects of temperature on pH and proteolysis. *Comparative Biochemistry and Physiology Part A: Physiology*, 51(2), 267-274. DOI: [10.1016/0300-9629\(75\)90370-9](https://doi.org/10.1016/0300-9629(75)90370-9)
- Domone, P., and Illston, J. (2010). Construction materials: their nature and behaviour. Fourth edition, CRC press.
- Downs, C.T., Greaver, C. and Taylor, R. (2008). Body temperature and basking behaviour of Nile crocodiles (*Crocodylus niloticus*) during winter. *Journal of Thermal Biology*, 33(3), 185-192. DOI: [10.1016/j.jtherbio.2008.02.001](https://doi.org/10.1016/j.jtherbio.2008.02.001)
- Edwards, G.P., Webb, G.J., Manolis, S.C. and Mazanov, A. (2017). Morphometric analysis of the Australian freshwater crocodile (*Crocodylus johnstoni*). *Australian Journal of Zoology*, 65(2), 97-111. DOI: [10.1071/ZO16079](https://doi.org/10.1071/ZO16079)
- Elijah, O., Rahman, T. A., Orikumhi, I., Leow, C. Y., and Hindia, M. N. (2018). An overview of Internet of Things (IoT) and data analytics in agriculture: Benefits and challenges. *IEEE Internet of things Journal*, 5(5), 3758-3773. DOI: [10.1109/JIOT.2018.2844296](https://doi.org/10.1109/JIOT.2018.2844296)
- Elsley, R. M., Joanen, T., McNease, L., and Lance, V. (1990). Stress and plasma corticosterone levels in the American alligator—relationships with stocking density and nesting success. *Comparative Biochemistry and Physiology Part A: Physiology*, 95(1), 55-63. DOI: [10.1016/0300-9629\(90\)90009-H](https://doi.org/10.1016/0300-9629(90)90009-H)
- Elsley, R.M. and Trosclair, P.L. (2016). The use of an unmanned aerial vehicle to locate alligator nests. *Southeastern Naturalist*, 15(1), 76-82. DOI: [10.1656/058.015.0106](https://doi.org/10.1656/058.015.0106)
- Ezat, M.A., Fritsch, C.J. and Downs, C.T. (2018). Use of an unmanned aerial vehicle (drone) to survey Nile crocodile populations: A case study at Lake Nyamithi, Ndumo game reserve, South Africa. *Biological Conservation*, 223, 76-81. DOI: [10.1016/j.biocon.2018.04.032](https://doi.org/10.1016/j.biocon.2018.04.032)
- Fawcett, S., Sistla, S., Dacosta-Calheiros, M., Kahraman, A., Reznicek, A. A., Rosenberg, R., and von Wettberg, E. J. (2019). Tracking microhabitat temperature variation with iButton data loggers. *Applications in Plant Sciences*, 7(4), e01237. DOI: [10.1002/aps3.1237](https://doi.org/10.1002/aps3.1237)
- Ferreira, S.M. and Pienaar, D. (2011). Degradation of the crocodile population in the Olifants River gorge of Kruger National Park, South Africa. *Aquatic Conservation: Marine and Freshwater Ecosystems*, 21(2), 155-164. DOI: [10.1002/aqc.1175](https://doi.org/10.1002/aqc.1175)

- Flint, N. S., Van der Bank, F. H., and Grobler, J. P. (2000). A lack of genetic variation in commercially bred Nile crocodiles (*Crocodylus niloticus*) in the North-West Province of South Africa. *Water SA-Pretoria*, 26(1), 105-110. CABI 20000106191.
- Franklin, C. E., and Seebacher, F. (2003). The effect of heat transfer mode on heart rate responses and hysteresis during heating and cooling in the estuarine crocodile *Crocodylus porosus*. *Journal of Experimental Biology*, 206(7), 1143-1151. DOI: [10.1242/jeb.00222](https://doi.org/10.1242/jeb.00222)
- Fukuda, Y., McDonald, P. J., and Crase, B. (2022). Lost to the Sea: Predicted Climate Change Threats to Saltwater Crocodile Nesting Habitat. *Frontiers in Ecology and Evolution*, 10, 839423. DOI: [10.3389/fevo.2022.839423](https://doi.org/10.3389/fevo.2022.839423)
- Ganswindt, S. B., Myburgh, J. G., Cameron, E. Z., and Ganswindt, A. (2014). Non-invasive assessment of adrenocortical function in captive Nile crocodiles (*Crocodylus niloticus*). *Comparative Biochemistry and Physiology Part A: Molecular & Integrative Physiology*, 177, 11-17. DOI: [10.1016/j.cbpa.2014.07.013](https://doi.org/10.1016/j.cbpa.2014.07.013)
- Gertenbach, W. D. (1983). Landscapes of the Kruger national park. *Koedoe*, 26(1), 9-121. DOI: [10.4102/koedoe.v26i1.591](https://doi.org/10.4102/koedoe.v26i1.591)
- Glanville, E. J., and Seebacher, F. (2006). Compensation for environmental change by complementary shifts of thermal sensitivity and thermoregulatory behaviour in an ectotherm. *Journal of Experimental Biology*, 209(24), 4869-4877. DOI: [10.1242/jeb.02585](https://doi.org/10.1242/jeb.02585)
- Grigg, G., and Gans, C. (1993). Morphology and physiology of the Crocodylia. Fauna of Australia Vol 2A Amphibia and Reptilia. *Australian Government Publishing Service, Canberra*, 326-336.
- Grigg, G. C., and Alchin, J. (1976). The role of the cardiovascular system in thermoregulation of *Crocodylus johnstoni*. *Physiological Zoology*, 49(1), 24-36.
- Grigg, G. C., Seebacher, F., Beard, L. A., and Morris, D. (1998). Thermal relations of large crocodiles, *Crocodylus porosus*, free-ranging in a naturalistic situation. Proceedings of the Royal Society of London. *Series B: Biological Sciences*, 265(1407), 1793-1799. DOI: [10.1098/rspb.1998.0504](https://doi.org/10.1098/rspb.1998.0504)
- Grigg, G. (2015). Biology and evolution of crocodylians. Ithaca, NY: Comstock Publishing Associates (Cornell University Press). DOI: [10.1071/9781486300679](https://doi.org/10.1071/9781486300679)
- Groffen, J., Parmentier, H. K., Van de Ven, W. A. C., and Van Weerd, M. (2013). Effects of different rearing strategies and ages on levels of natural antibodies in saliva of the Philippine crocodile. *Health*, 84, 13-25. DOI: [10.3724/SP.J.1245.2013.00022](https://doi.org/10.3724/SP.J.1245.2013.00022)
- Hartley, D. D. R. (1990). A survey of crocodile nests in Umfolozi Game Reserve. *Lammergeyer. Pietermaritzburg*, 41, 1-12.
- Hicks, J. W. (2002). The physiological and evolutionary significance of cardiovascular shunting patterns in reptiles. *Physiology*, 17(6), 241-245. DOI: [10.1152/nips.01397.2002](https://doi.org/10.1152/nips.01397.2002)
- Hill, J. E., Paladino, F. V., Spotila, J. R., and Tomillo, P. S. (2015). Shading and watering as a tool to mitigate the impacts of climate change in sea turtle nests. *PloS one*, 10(6), e0129528. DOI: [10.1371/journal.pone.0129528](https://doi.org/10.1371/journal.pone.0129528)
- Hobbs, P., Oelofse, S. H., and Rascher, J. (2008). Management of environmental impacts from coal mining in the upper Olifants River catchment as a function of age and scale. *International Journal of Water Resources Development*, 24(3), 417-431. DOI: [10.1080/07900620802127366](https://doi.org/10.1080/07900620802127366)

- Hocutt, C. H. (2022). Seasonal Variation in Thermoregulation of Wild Free-Ranging Nile Crocodiles: Recovery of a 36-Year-Old Data Set. *International Journal of Current Microbiology and Applied Sciences*, 11(10), 101-114. DOI: [10.20546/ijcmas.2022.1110.013](https://doi.org/10.20546/ijcmas.2022.1110.013)
- Hocutt, C. H., Loveridge, J. P., and Hutton, J. M. (1992). Biotelemetry monitoring of translocated *Crocodylus niloticus* in Lake Ngezi, Zimbabwe. *Journal of Zoology*, 226(2), 231-242. DOI: [10.1111/j.1469-7998.1992.tb03836.x](https://doi.org/10.1111/j.1469-7998.1992.tb03836.x)
- Hodgson, J.C. and Koh, L.P. (2016). Best practice for minimising unmanned aerial vehicle disturbance to wildlife in biological field research. *Current Biology*, 26(10), 404-405. DOI: [10.1016/j.cub.2016.04.001](https://doi.org/10.1016/j.cub.2016.04.001)
- Hoffman, L. C., Fisher, P. P., and Sales, J. (2000). Carcass and meat characteristics of the Nile crocodile (*Crocodylus niloticus*). *Journal of the Science of Food and Agriculture*, 80(3), 390-396. DOI: [10.1002/1097-0010\(200002\)80:3<390::AID-JSFA540>3.0.CO;2-G](https://doi.org/10.1002/1097-0010(200002)80:3<390::AID-JSFA540>3.0.CO;2-G)
- Honegger, R. E. (1971). Zoo breeding and crocodile bank. Published with the financial assistance of UNESCO.
- Huchzermeyer, F. W. (2002). Diseases of farmed crocodiles and ostriches. *Scientific and technical journal-International Office of Epizootics*, 21(1), 265-276. DOI: [10.20506/rst.21.2.1334](https://doi.org/10.20506/rst.21.2.1334)
- Huchzermeyer, F. W. (2003). Diseases of farmed crocodiles and ostriches. *Scientific and technical journal-International Office of Epizootics*, 21(1), 265-276. DOI: [10.20506/rst.21.2.1334](https://doi.org/10.20506/rst.21.2.1334)
- Huchzermeyer, K. D. A., Woodborne, S., Osthoff, G., Hugo, A., Hoffman, A. C., Kaiser, H., Steyl, J. C. A., and Myburgh, J. G. (2017). Pansteatitis in polluted Olifants River impoundments: nutritional perspectives on fish in a eutrophic lake, Lake Loskop, South Africa. *Journal of Fish Diseases*, 40(11), 1665-1680. DOI: [10.1111/jfd.12633](https://doi.org/10.1111/jfd.12633)
- <sup>1</sup>Hutton, J.M. (1987). Morphometrics and field estimation of the size of the Nile crocodile. *African Journal of Ecology*, 25(4), 225-230. DOI: [10.1111/j.1365-2028.1987.tb01113.x](https://doi.org/10.1111/j.1365-2028.1987.tb01113.x)
- <sup>2</sup>Hutton, J. M. (1987). Incubation temperatures, sex ratios and sex determination in a population of Nile crocodiles (*Crocodylus niloticus*). *Journal of Zoology*, 211(1), 143-155. DOI: [10.1111/j.1469-7998.1987.tb07458.x](https://doi.org/10.1111/j.1469-7998.1987.tb07458.x)
- Isberg, S., Combrink, X., Lippai, C. & Balaguera-Reina, S.A. (2019). *Crocodylus niloticus*. The IUCN Red List of Threatened Species 2019: e.T45433088A3010181. DOI: [10.2305/IUCN.UK.2019-1.RLTS.T45433088A3010181.en](https://doi.org/10.2305/IUCN.UK.2019-1.RLTS.T45433088A3010181.en)
- Isberg, S. R. (2007). Nutrition of juvenile saltwater crocodiles (*Crocodylus porosus*) in commercial production systems. *Perspective in Agriculture, Veterinary Science, Nutrition and Natural Resources*, 2(91), 1-11. DOI: [10.1079/PAVSNNR20072091](https://doi.org/10.1079/PAVSNNR20072091)
- Janes, D., and Gutzke, W. H. (2002). Factors affecting retention time of turtle scutes in stomachs of American alligators, *Alligator mississippiensis*. *American Midland Naturalist*, 115-119. DOI: [10.1674/0003-0031\(2002\)148\[0115:FARTOT\]2.0.CO;2](https://doi.org/10.1674/0003-0031(2002)148[0115:FARTOT]2.0.CO;2)
- Jordaan, P.R. (2021). The establishment of a multifaceted *Crocodylus niloticus* Laurenti 1768 monitoring programme on Maputo Special Reserve (Maputo Province, Mozambique) with preliminary notes on the population (Reptilia: Crocodylidae). *Herpetology Notes*, 14, 1155-1162.

- Joubert, S. (2007). The Kruger National Park: A history volume 2. High Branching.
- Keenan, S. W., Engel, A. S., and Elsey, R. M. (2013). The alligator gut microbiome and implications for archosaur symbioses. *Scientific reports*, 3(1), 2877. DOI: [10.1038/srep02877](https://doi.org/10.1038/srep02877)
- Kofron, C. P. (1989). Nesting ecology of the Nile crocodile (*Crocodylus niloticus*). *African Journal of Ecology*, 27(4), 335-341. DOI: [10.1111/j.1365-2028.1989.tb01027.x](https://doi.org/10.1111/j.1365-2028.1989.tb01027.x)
- Kyalo, S. (2008). Non-detriment finding studies on Nile crocodile (*Crocodylus niloticus*): The status of and trade in the Nile crocodile in Kenya. In NDF Workshop Case Studies, *WG7-Reptiles and Amphibians*, 17-22.
- Lance, V. A. (1989). Reproductive cycle of the American alligator. *American Zoologist*, 29(3), 999-1018. DOI: [10.1093/icb/29.3.999](https://doi.org/10.1093/icb/29.3.999)
- Lane, E. P., Huchzermeyer, F. W., Govender, D., Bengis, R. G., Buss, P. E., Hofmeyr, M., Myburgh, J. G., Steyl, J. C. A., Pienaar, D. J., and Kotze, A. (2013). Pansteatitis of unknown etiology associated with large-scale Nile crocodile (*Crocodylus niloticus*) mortality in Kruger National Park, South Africa: Pathologic findings. *Journal of Zoo and Wildlife Medicine*, 44(4), 899-910. DOI: [10.1638/2012-0264R.1](https://doi.org/10.1638/2012-0264R.1)
- Lang, J. W. (1977). Studies of the thermal behavior and body temperature of crocodylians. University of Minnesota ProQuest Dissertations Publishing, 7809689 (Doctoral dissertation, University of Minnesota).
- <sup>1</sup>Lang, J. W. (1987). Crocodylian behaviour: implications for management. *Wildlife Management: Crocodiles and Alligators*, 273-294. Surrey Beatty, Sydney. ISBN 0949324094.
- <sup>2</sup>Lang, J. W. (1987). Crocodylian thermal selection. *Wildlife Management: Crocodiles and Alligators*, 301-317. Surrey Beatty, Sydney. ISBN 0949324094.
- Lang, J. W., Andrews, H., and Whitaker, R. (1989). Sex determination and sex ratios in *Crocodylus palustris*. *American Zoologist*, 29(3), 935-952. DOI: [10.1093/icb/29.3.935](https://doi.org/10.1093/icb/29.3.935)
- Leslie, A. J., and Spotila, J. R. (2001). Alien plant threatens Nile crocodile (*Crocodylus niloticus*) breeding in Lake St. Lucia, South Africa. *Biological Conservation*, 98(3), 347-355. DOI: [10.1016/S0006-3207\(00\)00177-4](https://doi.org/10.1016/S0006-3207(00)00177-4)
- López-Luna, M. A., González-Soberano, J., González-Jáuregui, M., Escobedo-Galván, A. H., Suárez-Domínguez, E. A., Rangel-Mendoza, J. A., and Morales-Mávil, J. E. (2020). Nest-site selection and nest size influence the incubation temperature of Morelet's crocodiles. *Journal of Thermal Biology*, 91, 102624. DOI: [10.1016/j.jtherbio.2020.102624](https://doi.org/10.1016/j.jtherbio.2020.102624)
- López-Luna, M. A., Hidalgo-Mihart, M. G., Aguirre-León, G., González-Ramón, M. D. C., and Rangel-Mendoza, J. A. (2015). Effect of nesting environment on incubation temperature and hatching success of Morelet's crocodile (*Crocodylus moreletii*) in an urban lake of Southeastern Mexico. *Journal of Thermal Biology*, 49, 66-73. DOI: [10.1016/j.jtherbio.2015.01.006](https://doi.org/10.1016/j.jtherbio.2015.01.006)
- Lovegrove, B. G. (2009). Modification and miniaturization of ThermoChron iButtons for surgical implantation into small animals. *Journal of Comparative Physiology B*, 179, 451-458. DOI: [10.1007/s00360-008-0329-x](https://doi.org/10.1007/s00360-008-0329-x)

- Loveridge, J. P. (1984). Thermoregulation in the Nile crocodile, *Crocodylus niloticus*. *Symposia of the Zoological Society of London*, 52, 443-467.
- MacGregor, J. (2006). Call of the Wild: Captive Crocodilian Production and the Shaping of Conservation Incentives. TRAFFIC International, Cambridge, UK. ISBN 1858502209.
- Maciejewski, K. (2006). Temperature-dependent sex determination in the Nile crocodile, *Crocodylus niloticus*, in the Okavango River, Botswana, and the effect of global climate change (Doctoral dissertation, Stellenbosch University).
- Magnino, S., Colin, P., Dei-Cas, E., Madsen, M., McLauchlin, J., Nöckler, K., Maradona, M.P., Tsigarida, E., Vanopdenbosch, E. and Van Peteghem, C. (2009). Biological risks associated with consumption of reptile products. *International journal of food microbiology*, 134(3), 163-175. DOI: [10.1016/j.ijfoodmicro.2009.07.001](https://doi.org/10.1016/j.ijfoodmicro.2009.07.001)
- Magnusson, W. E. (1979). Maintenance of temperature of crocodile nests (*Reptilia, Crocodylidae*). *Journal of Herpetology*, 13(4) 439-443. <https://www.jstor.org/stable/1563479>
- Mainwaring, M. C., Barber, I., Deeming, D. C., Pike, D. A., Roznik, E. A., and Hartley, I. R. (2017). Climate change and nesting behaviour in vertebrates: a review of the ecological threats and potential for adaptive responses. *Biological Reviews*, 92(4), 1991-2002. DOI: [10.1111/brv.12317](https://doi.org/10.1111/brv.12317)
- Manolis, S.C. and Webb, G. (2013). Assessment of saltwater crocodile (*Crocodylus porosus*) attacks in Australia (1971–2013): implications for management. In Proceedings of the 22nd Working Meeting of the IUCN–SSC Crocodile Specialist Group, 21, 97–104. IUCN, Gland, Switzerland.
- Manolis, S. C. and Webb, G. J. W. (2016). Best Management Practices for Crocodilian Farming. Version 1. IUCN-SSC Crocodile Specialist Group: Darwin, Australia.
- Mazzotti, F.J., Cherkiss, M.S., Brandt, L.A., Fujisaki, I., Hart, K., Jeffery, B., McMurry, S.T., Platt, S.G., Rainwater, T.R. and Vinci, J. (2012). Body condition of Morelet's crocodiles (*Crocodylus moreletii*) from Northern Belizea. *Journal of Herpetology*, 46(3), 356-362. DOI: [10.1670/11-188](https://doi.org/10.1670/11-188)
- McGaugh, S. E., and Janzen, F. J. (2011). Effective heritability of targets of sex-ratio selection under environmental sex determination. *Journal of Evolutionary Biology*, 24(4), 784-794. DOI: [10.1111/j.1420-9101.2010.02211.x](https://doi.org/10.1111/j.1420-9101.2010.02211.x)
- McIlhenny, E. A. (1934). Notes on incubation and growth of alligators. *Copeia*, 1934(2), 80-88. <https://www.jstor.org/stable/1435797>
- Mellor, D. J. (2017). Operational details of the Five Domains Model and its key applications to the assessment and management of animal welfare. *Animals*, 7(8), 60. DOI: [10.3390/ani7080060](https://doi.org/10.3390/ani7080060)
- Mellor, D. J. (2016). Updating animal welfare thinking: moving beyond the “five freedoms” towards “a life worth living”. *Animals*, 6(3), 21. DOI: [10.3390/ani6030021](https://doi.org/10.3390/ani6030021)
- Messel, H., & Vorlicek, G. C. (1989). Growth of *Crocodylus porosus* in the wild in northern Australia. *Crocodiles: Their Ecology, Management, and Conservation*, 110-137.
- Messina, G., and Modica, G. (2020). Applications of UAV thermal imagery in precision agriculture: State of the art and future research outlook. *Remote Sensing*, 12(9), 1491. DOI: [10.3390/rs12091491](https://doi.org/10.3390/rs12091491)

- Mlilwana, T. P., and Kearsley, E. P. (2022). Light-coloured concrete surfacing for urban heat-island mitigation in Southern Africa. *Journal of the South African institution of civil engineering*, 64(2), 2-12. DOI: [10.17159/2309-8775/2022/v64no2a1](https://doi.org/10.17159/2309-8775/2022/v64no2a1)
- Morjan, C. L. (2003). How rapidly can maternal behavior affecting primary sex ratio evolve in a reptile with environmental sex determination? *The American Naturalist*, 162(2), 205-219. DOI: [10.2307/3473211](https://doi.org/10.2307/3473211)
- Moon, K. E., Wang, S., Bryant, K., and Gohlke, J. M. (2021). Environmental heat exposure among pet dogs in rural and urban settings in the Southern United States. *Frontiers in veterinary science*, 1142. DOI: [10.3389/fvets.2021.742926](https://doi.org/10.3389/fvets.2021.742926)
- Morpurgo, B., Gvaryahu, G., and Robinzon, B. (1993). Aggressive behaviour in immature captive Nile crocodiles, *Crocodylus niloticus*, in relation to feeding. *Physiology & Behavior*, 53(6), 1157-1161. DOI: [10.1016/0031-9384\(93\)90373-N](https://doi.org/10.1016/0031-9384(93)90373-N)
- Mpofu, C. N. B., Mhlanga, M., and Moyo, N. (2015). Pond type and pre-tanning processes affects size and quality of captive Nile crocodile skins. *Agricultural Advances*, 4(4), 42-48. DOI: [10.14196/aa.v4i4.1858](https://doi.org/10.14196/aa.v4i4.1858)
- Murray, C. M., Crother, B. I., and Doody, J. S. (2020). The evolution of crocodylian nesting ecology and behavior. *Ecology and evolution*, 10(1), 131-149. DOI: [10.1002/ece3.5859](https://doi.org/10.1002/ece3.5859)
- Murray, C. M., Easter, M., Padilla, S., Marin, M. S., and Guyer, C. (2016). Regional warming and the thermal regimes of American crocodile nests in the Tempisque Basin, Costa Rica. *Journal of Thermal Biology*, 60, 49-59. DOI: [10.1016/j.jtherbio.2016.06.004](https://doi.org/10.1016/j.jtherbio.2016.06.004)
- Myburgh, H.A. (2021). Aspects of monitoring wild and captive Nile crocodile (*Crocodylus niloticus*) populations in southern Africa (Doctoral dissertation, University of KwaZulu Natal).
- Myburgh, A., Botha, H., Downs, C.T. and Woodborne, S. (2021). The application and limitations of a low-cost UAV platform and open-source software combination for ecological mapping and monitoring. *African Journal of Wildlife Research*, 51(1), 166-177. DOI: [10.3957/056.051.0166](https://doi.org/10.3957/056.051.0166)
- Nieuwoudt, C., Quinn, L., Pieters, R., Enge, E. K., Kylin, H., Pienaar, D., and Bouwman, H. (2009). Mass deaths of crocodiles in the Kruger National Park, South Africa: An investigation into possible causes. In Poster presented at: *19th Annual Meeting of the Society of Environmental Toxicology and Chemistry*.
- Ojeda-Adame, R.A., Hernández-Hurtado, H., Ramírez-Martínez, M.M. and Iñiguez-Davalos, L.I. (2020). A body condition score for crocodylians. *South American Journal of Herpetology*, 16(1), 10-15. DOI: [10.2994/SAJH-D-18-00074.1](https://doi.org/10.2994/SAJH-D-18-00074.1)
- Osthoff, G., Hugo, A., Govender, D., Huchzermeyer, F., & Bouwman, H. (2014). Comparison of the lipid composition of three adipose tissue types of male and female wild Nile crocodiles (*Crocodylus niloticus*). *Journal of Herpetology*, 48(4), 525-531. DOI: [10.1670/13-096](https://doi.org/10.1670/13-096)
- Osthoff, G., Hugo, A., Bouwman, H., Buss, P., Govender, D., Joubert, C. C., and Swarts, J. C. (2010). Comparison of the lipid properties of captive, healthy wild, and pansteatitis-affected wild Nile crocodiles (*Crocodylus niloticus*). *Comparative Biochemistry and Physiology Part A: Molecular & Integrative Physiology*, 155(1), 64-69. DOI: [10.1016/j.cbpa.2009.09.025](https://doi.org/10.1016/j.cbpa.2009.09.025)
- Pooley, A. C., and Gans, C. (1976). The Nile crocodile. *Scientific American*, 234(4), 114-125.

- Pooley, A. C. (1982). Further observations on the Nile crocodile *Crocodylus niloticus* in the St. Lucia Lake System. *St. Lucia research review*, 144-161.
- Pooley, S., Botha, H., Combrink, X., and Powell, G. (2019). Synthesizing Nile crocodile *Crocodylus niloticus* attack data and historical context to inform mitigation efforts in South Africa and eSwatini (Swaziland). *Oryx*, ISSN 0030-6053. DOI: [10.1017/S0030605318001102](https://doi.org/10.1017/S0030605318001102)
- Porter, W. R., Sedlmayr, J. C., and Witmer, L. M. (2016). Vascular patterns in the heads of crocodylians: blood vessels and sites of thermal exchange. *Journal of Anatomy*, 229(6), 800-824. DOI: [10.1111/joa.12539](https://doi.org/10.1111/joa.12539)
- Price, C., Ezat, M. A., Hanzen, C., and Downs, C. T. (2022). Never smile at a crocodile: Gaping behaviour in the Nile crocodile at Ndumo Game Reserve, South Africa. *Behavioural Processes*, 203, 104772. DOI: [10.1016/j.beproc.2022.104772](https://doi.org/10.1016/j.beproc.2022.104772)
- QGIS Development Team (2021). QGIS Geographic Information System. Open-Source Geospatial Foundation Project. <http://qgis.osgeo.org>
- Ramos, E.A., Landeo-Yauri, S., Castelblanco-Martínez, N., Arreola, M.R., Quade, A.H. and Rieucan, G. (2022). Drone-based photogrammetry assessments of body size and body condition of Antillean manatees. *Mammalian Biology*, 1-15. DOI: [10.1007/s42991-022-00228-4](https://doi.org/10.1007/s42991-022-00228-4)
- Raoult, V., Colefax, A.P., Allan, B.M., Cagnazzi, D., Castelblanco-Martínez, N., Ierodiaconou, D., Johnston, D.W., Landeo-Yauri, S., Lyons, M., Pirotta, V., Schofield, G., and Butcher, P.A. (2020). Operational protocols for the use of drones in marine animal research. *Drones*, 4(4), 64. DOI: [10.3390/drones4040064](https://doi.org/10.3390/drones4040064)
- Refsnider, J. M. (2012). Effects of climate change on reptiles with temperature-dependent sex determination and potential adaptation via maternal nest-site choice (Doctoral dissertation, Iowa State University). <https://lib.dr.iastate.edu/etd/12570>.
- Robert, K. A. and Thompson, M. B. (2003). Reconstructing Thermocron iButtons to reduce size and weight as a new technique in the study of small animal thermal biology. *Herpetological Review*, 34(2), 130-132.
- Salem, A. (2011). Morphometric measurement and field estimation of the size of *Crocodylus niloticus* in Lake Nasser (Egypt). *Transylv Rev Syst Ecol Res*, 12, 53-74.
- Seebacher, F. (2005). A review of thermoregulation and physiological performance in reptiles: what is the role of phenotypic flexibility? *Journal of Comparative Physiology B*, 175(7), 453-461. DOI: [10.1007/s00360-005-0010-6](https://doi.org/10.1007/s00360-005-0010-6)
- Seebacher, F., and Franklin, C. E. (2004). Cardiovascular mechanisms during thermoregulation in reptiles. Elsevier, *International Congress Series*, 1275, 242-249. DOI: [10.1016/j.ics.2004.08.050](https://doi.org/10.1016/j.ics.2004.08.050)
- Seebacher, F., and Franklin, C. E. (2007). Redistribution of blood within the body is important for thermoregulation in an ectothermic vertebrate (*Crocodylus porosus*). *Journal of Comparative Physiology B*, 177, 841-848. DOI: [10.1007/s00360-007-0181-4](https://doi.org/10.1007/s00360-007-0181-4)
- Seebacher, F., Guderley, H., Elsey, R. M. and Trosclair, P. L. (2003). Seasonal acclimatization of muscle enzymes in a reptile (*Alligator mississippiensis*). *Journal of Experimental Biology*, 206, 1193–1200. DOI: [10.3390/drones4040064](https://doi.org/10.3390/drones4040064)

- Seebacher, F., and Grigg, G. C. (1997). Patterns of body temperature in wild freshwater crocodiles, *Crocodylus johnstoni*: thermoregulation versus thermoconformity, seasonal acclimatization, and the effect of social interactions. *Copeia*, 549-557. DOI: [10.2307/1447558](https://doi.org/10.2307/1447558)
- Seebacher, F., Grigg, G. C., and Beard, L. A. (1999). Crocodiles as dinosaurs: behavioural thermoregulation in very large ectotherms leads to high and stable body temperatures. *Journal of Experimental Biology*, 202(1), 77-86. DOI: [10.1242/jeb.202.1.77](https://doi.org/10.1242/jeb.202.1.77)
- Seebacher, F., and Grigg, G. C. (2001). Social interactions compromise thermoregulation in crocodiles *Crocodylus johnstoni* and *Crocodylus porosus*. *Crocodylian Biology and Evolution*, 1, 310-316. Corpus ID: 82893822
- Seebacher, F. (1999). Behavioural postures and the rate of body temperature change in wild freshwater crocodiles, *Crocodylus johnstoni*. *Physiological and Biochemical Zoology*, 72(1), 57-63. DOI: [10.1086/316638](https://doi.org/10.1086/316638)
- Shilton, C., Brown, G. P., Chambers, L., Benedict, S., Davis, S., Aumann, S., and Isberg, S. R. (2014). Pathology of runting in farmed saltwater crocodiles (*Crocodylus porosus*) in Australia. *Veterinary Pathology Online*, 51(5), 1022-1034. DOI: [10.1177/0300985813516642](https://doi.org/10.1177/0300985813516642)
- Shirley, M.H., Burtner, B., Oslisly, R., Sebag, D. and Testa, O. (2017). Diet and body condition of cave-dwelling dwarf crocodiles (*Osteolaemus tetraspis*, Cope 1861) in Gabon. *African Journal of Ecology*, 55(4), 411-422. DOI: [10.1111/aje.12365](https://doi.org/10.1111/aje.12365)
- Singh, R. K., Aernouts, M., De Meyer, M., Weyn, M., and Berkvens, R. (2020). Leveraging LoRaWAN technology for precision agriculture in greenhouses. *Sensors*, 20(7), 1827. DOI: [10.3390/s20071827](https://doi.org/10.3390/s20071827)
- Smith, J. A., Cooper, C. B., Reynolds, S. J., and Deeming, D. C. (2015). Advances in techniques to study incubation. *Nests, eggs, and incubation: new ideas about avian reproduction*, 179-195. DOI: [10.1093/acprof:oso/9780198718666.003.0015](https://doi.org/10.1093/acprof:oso/9780198718666.003.0015)
- Soledade Lemos, L., Burnett, J.D., Chandler, T.E., Sumich, J.L. and Torres, L.G. (2020). Intra- and inter-annual variation in gray whale body condition on a foraging ground. *Ecosphere*, 11(4), e03094. DOI: [10.1002/ecs2.3094](https://doi.org/10.1002/ecs2.3094)
- Somaweera, R., and Shine, R. (2013). Nest-site selection by crocodiles at a rocky site in the Australian tropics: Making the best of a bad lot. *Austral Ecology*, 38(3), 313-325. DOI: [10.1111/j.1442-9993.2012.02406.x](https://doi.org/10.1111/j.1442-9993.2012.02406.x)
- South African Bureau of Standards. (2009). South African National Standard for Crocodiles in Captivity (SANS 631:2009, edition 1). SABS Standards Division, ISBN 978-0-626-22294-9
- Spotila, J. R., Terpin, K. M., and Dodson, P. (1977). Mouth gaping as an effective thermoregulatory device in alligators. *Nature*, 265(5591), 235-236. DOI: [10.1038/265235a0](https://doi.org/10.1038/265235a0)
- Strauss, M., Botha, H., and Van Hoven, W. (2008). Nile crocodile *Crocodylus niloticus* telemetry: observations on transmitter attachment and longevity. *South African Journal of Wildlife Research*, 38(2), 189-192. DOI: [10.3957/0379-4369-38.2.189](https://doi.org/10.3957/0379-4369-38.2.189)
- Sullivan, S., Heinrich, G. L., Mattheus, N. M., Cassill, D., and Doody, J. S. (2022). Can Reptiles Use Nest Site Choice Behavior to Counter Global Warming Effects on Developing Embryos? Potential Climate Responses in a Turtle. *Frontiers in Ecology and Evolution*, 10, 825110. DOI: [10.3389/fevo.2022.825110](https://doi.org/10.3389/fevo.2022.825110)

- Sutherland, K., Ndlovu, M., and Pérez-Rodríguez, A. (2018). Use of artificial waterholes by animals in the southern region of the Kruger National Park, South Africa. *African Journal of Wildlife Research*, 48(2), 1-14. DOI: [10.3957/056.048.023003](https://doi.org/10.3957/056.048.023003)
- <sup>1</sup>Swanepoel, D., Kriek, N.P.J. and Boomker, J.D.F., 2000. Selected chemical parameters in the blood and metals in the organs of the Nile crocodile, *Crocodylus niloticus*, in the Kruger National Park. *Onderstepoort Journal of Veterinary Research*, 67, 141-148. PMID: 11028751
- <sup>2</sup>Swanepoel, D. G. J., Ferguson, N. S., and Perrin, M. R. (2000). Nesting ecology of Nile crocodiles (*Crocodylus niloticus*) in the Olifants River, Kruger National Park. *Koedoe*, 43(2), 35-46. DOI: [10.4102/koedoe.v43i2.197](https://doi.org/10.4102/koedoe.v43i2.197)
- Telemeco, R. S., and Gangloff, E. J. (2021). Introduction to the special issue—Beyond CTMAX and CTMIN: Advances in studying the thermal limits of reptiles and amphibians. *Journal of Experimental Zoology Part A: Ecological and Integrative Physiology*, 335(1), 5-12. DOI: [10.1002/jez.2447](https://doi.org/10.1002/jez.2447)
- Telemeco, R. S., Gangloff, E. J., Cordero, G. A., Polich, R. L., Bronikowski, A. M., and Janzen, F. J. (2017). Physiology at near-critical temperatures, but not critical limits, varies between two lizard species that partition the thermal environment. *Journal of Animal Ecology*, 86(6), 1510-1522. DOI: [10.1111/1365-2656.12738](https://doi.org/10.1111/1365-2656.12738)
- Telemeco, R. S., Abbott, K. C., and Janzen, F. J. (2013). Modelling the effects of climate change–induced shifts in reproductive phenology on temperature-dependent traits. *The American Naturalist*, 181(5), 637-648. DOI: [10.1086/670051](https://doi.org/10.1086/670051)
- Telemeco, R. S., Elphick, M. J., and Shine, R. (2009). Nesting lizards (*Bassiana duperreyi*) compensate partly, but not completely, for climate change. *Ecology*, 90(1), 17-22. DOI: [10.1890/08-1452.1](https://doi.org/10.1890/08-1452.1)
- Terpin, K. M., Spotila, J. R., and Foley, R. E. (1979). Thermoregulatory adaptations and heat energy budget analyses of the American alligator, *Alligator mississippiensis*. *Physiological Zoology*, 52(3), 296-312. DOI: [10.1086/physzool.52.3.30155752](https://doi.org/10.1086/physzool.52.3.30155752)
- Toffanin, P. (2019). OpenDroneMap: The Missing Guide. UAV4GEO. <https://odmbook.com/>
- Tosun, D. D. (2013). Crocodile farming and its present state in global Aquaculture. *Journal of Fisheries Sciences*, 7(1), 43-57. DOI: [10.3153/jfscom.2013005](https://doi.org/10.3153/jfscom.2013005)
- Utete, B. (2021). A review of the conservation status of the Nile crocodile (*Crocodylus niloticus* Laurenti, 1768) in aquatic systems of Zimbabwe. *Global Ecology and Conservation*, 29, e01743. DOI: [10.1016/j.gecco.2021.e01743](https://doi.org/10.1016/j.gecco.2021.e01743)
- Van Weerd, M. (2010). Philippine crocodile *Crocodylus mindorensis*. Crocodiles: status, survey and conservation action plan. Third edition. Darwin: Crocodile Specialist Group, 71-78.
- Venter, F. J., and Gertenbach, W. P. D. (1986). A cursory review of the climate and vegetation of the Kruger National Park. *Koedoe*, 29(1), 139-148. DOI: [10.4102/koedoe.v29i1.526](https://doi.org/10.4102/koedoe.v29i1.526)
- Verdade, L. M., Pina, C. I., and Araújo, J. L. (2006). Diurnal use of space by captive adult broad-snouted caiman (*Caiman latirostris*): Implications for pen design. *Aquaculture*, 251(2), 333-339. DOI: [10.1016/j.aquaculture.2005.06.030](https://doi.org/10.1016/j.aquaculture.2005.06.030)

- <sup>1</sup>Viljoen, D., Webb, E., Myburgh, J., Truter, C., and Myburgh, A. (2023). Remote body condition scoring of Nile crocodiles (*Crocodylus niloticus*) using uncrewed aerial vehicle derived morphometrics. *Frontiers in Animal Science*, 4:1225396. DOI: [10.3389/fanim.2023.1225396](https://doi.org/10.3389/fanim.2023.1225396)
- <sup>2</sup>Viljoen, D., Webb, E., Myburgh, J., Truter, C., and Myburgh, A. (2023). Disturbance assessment identifying the drone model and flight altitudes for a morphometric assessment of farmed breeder Nile crocodiles. *Frontiers in Animal Science*, 4:1225396 (Supplementary Material). DOI: [10.3389/fanim.2023.1225396](https://doi.org/10.3389/fanim.2023.1225396)
- <sup>3</sup>Viljoen, D. M., Webb, E. C., Myburgh, J. G., Truter, J. C., Lang, J. W., and Myburgh, A. (2023). Adaptive thermal responses of captive Nile crocodiles (*Crocodylus niloticus*) in South Africa. *Applied Animal Behaviour Science*, 106098. DOI: [10.1016/j.applanim.2023.106098](https://doi.org/10.1016/j.applanim.2023.106098)
- Wallace, K. M., and Leslie, A. J. (2008). Diet of the Nile crocodile (*Crocodylus niloticus*) in the Okavango Delta, Botswana. *Journal of Herpetology*, 42(2), 361-368. DOI: [10.1670/07-1071.1](https://doi.org/10.1670/07-1071.1)
- Wallace, K.M., Leslie, A.J., Coulson, T. and Wallace, A.S. (2013). Population size and structure of the Nile crocodile *Crocodylus niloticus* in the lower Zambezi valley. *Oryx*, 47(3), 457-465. DOI: [10.1017/S0030605311001712](https://doi.org/10.1017/S0030605311001712)
- <sup>1</sup>Warner, J.K., Combrink, X., Calverley, P., Champion, G. and Downs, C.T. (2016). Morphometrics, sex ratio, sexual size dimorphism, biomass, and population size of the Nile crocodile (*Crocodylus niloticus*) at its southern range limit in KwaZulu-Natal, South Africa. *Zoomorphology*, 135, 511-521. DOI: [10.1007/s00435-016-0325-8](https://doi.org/10.1007/s00435-016-0325-8)
- <sup>2</sup>Warner, J.K., Combrink, X., Myburgh, J.G. and Downs, C.T. (2016). Blood lead concentrations in free-ranging Nile crocodiles (*Crocodylus niloticus*) from South Africa. *Ecotoxicology*, 25, 950-958. DOI: [10.1007/s10646-016-1652-8](https://doi.org/10.1007/s10646-016-1652-8)
- Webb, G. J. W., Reynolds, S., Brien, M. L., Manolis S. C., Brien, J. J. and Christian, K. (2013). Improving Australia's Crocodile Industry Productivity: Nutritional Requirements, Feed Ingredients and Feeding Systems for Farmed Crocodile Production. Rural Industries Research and Development Corporation. ISBN 9781742544878.
- Webb, E.C., Veldsman, D.M., Myburgh, J.G. and Swan, G.E. (2021). Effects of stocking density on growth and skin quality of grower Nile crocodiles (*Crocodylus niloticus*). *South African Journal of Animal Science*, 51(2), 142-150. DOI: [10.4314/sajas.v51i2.1](https://doi.org/10.4314/sajas.v51i2.1)
- Whitaker, N., and Srinivasan, M. (2018). Preliminary observations on deep body temperatures in female mugger crocodiles (*Crocodylus palustris* Lesson: 1831) in a captive facility. *International Journal of Current Microbiology and Applied Sciences*, 7(12), 2835-2842. DOI: [10.20546/ijcmas.2018.712.322](https://doi.org/10.20546/ijcmas.2018.712.322)
- Yangprapakorn, U., Cronin, E. W., and McNeely, J. A. (1971). Captive breeding of crocodiles in Thailand. In Proceedings of the 1st Working Meeting of the Crocodile Specialist Group. IUCN-The World Conservation Union, Gland, Switzerland, 98-101.
- Zhang, H., Wang, C., Turvey, S. T., Sun, Z., Tan, Z., Yang, Q., Long, W., Wu, X. and Yang, D. (2020). Thermal infrared imaging from drones can detect individuals and nocturnal behavior of the world's rarest primate. *Global Ecology and Conservation*, 23, e01101. DOI: [10.1016/j.gecco.2020.e01101](https://doi.org/10.1016/j.gecco.2020.e01101)



Zhang, H., Wang, E., Zhou, D., Luo, Z., and Zhang, Z. (2016). Rising soil temperature in China and its potential ecological impact. *Scientific reports*, 6(1), 35530. DOI: [10.1038/srep35530](https://doi.org/10.1038/srep35530)

Ziegler, T., and Olbort, S. (2007). Genital structures and sex identification in crocodiles. *Crocodile Specialist Group Newsletter*, 26(3), 16-17. Corpus ID: 45917809

Zweig, C.L. (2003). Body condition index analysis for the American alligator (*Alligator mississippiensis*) (Doctoral dissertation, University of Florida).

<https://cites.org/eng/app/appendices.php>

<https://www.krugerpark.co.za/krugerpark-times-5-7-kruger-devastated-by-climate-change-24943.html>

<https://www.thethingsnetwork.org/docs/lorawan/what-is-lorawan/>

## 9. Appendix



**Figure A1.** Aluminium pole with a concrete base for central water body temperature logging.



**Figure A2.** Holes drilled in the aluminium pole for Hobo pendant placement, secured by a cable tie.



**Figure A3.** The various tubing used for iButton force-feeding.



**Figure A4.** The hard tube securely taped into a crocodile's mouth.



**Figure A5.** Measuring and marking the second piece of tubing, ensuring crocodile safety



**Figure A6.** 3D Printed iButton holder, top view.



**Figure A7.** Tail punch used to create the attachment points for the iButton holders.



**Figure A8.** Liquid Armour encased 3D printed iButton.



**Figure A9.** A faulty iButton that did not survive MD 2.5. The lid cracked open, and the Liquid Armour encapsulation was no longer present.



**Figure A10.** Liquid Armour (bottom) and 3D printed polypropylene (top) encapsulated batteries.

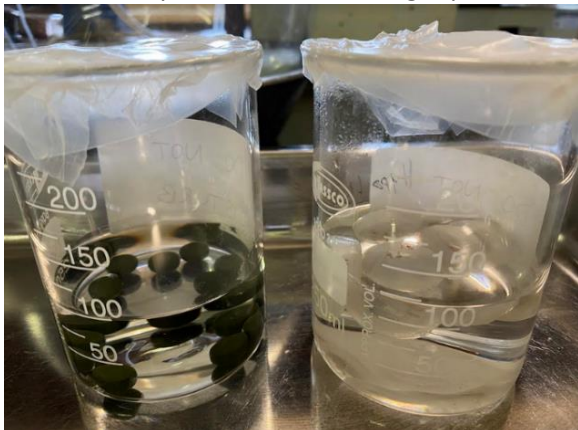


**Figure A11.** Encapsulated batteries in HCl solution with parafilm lids.



**Figure A12.** Precipitates in the final week of the assessment from the Liquid Armour beaker.

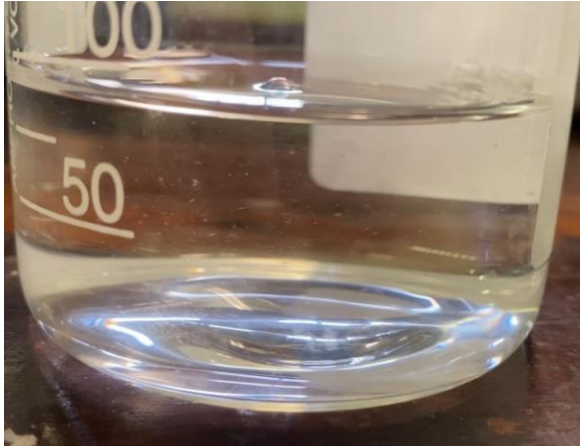


**Figure A13.** Precipitates in the final week of the assessment from the polypropylene beaker.



**Figure A14.** LHT65 LoRaWAN logger placement in the apex of the pyramid mould, prior to concrete addition.



**Figure A15.** The steel pole in a concrete base design, with the LHT65 logger box secured up top, before being pulled into the waterbody.

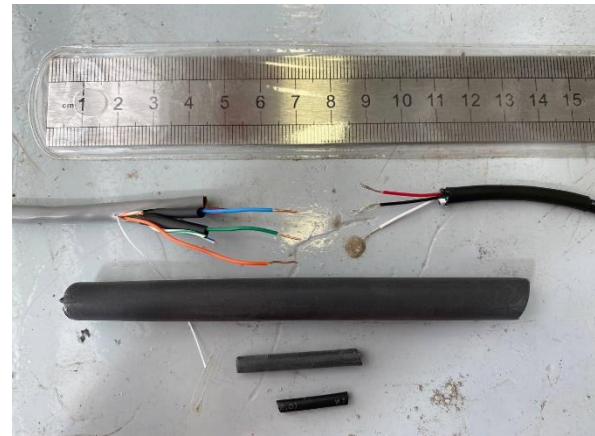


**Figure A16.** The spliced wire addition to extend the LHT65 logger's cable. Various heat shrink tubing was lined up to seal each splice point.



**Figure A17.** Point markers showing a Nile crocodiles' back (red) and positional (yellow) temperature measurement points in RGB (Mavic 2 Enterprise Dual drone).

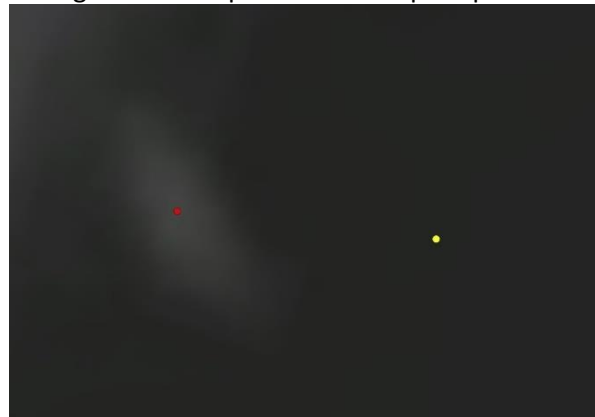


**Figure A18.** Point markers showing a Nile crocodiles' back (red) and positional (yellow) temperature measurement points in thermal image (Mavic 2 Enterprise Dual drone).



**Figure A19.** Baited cage trap containing a Nile crocodile.



**Figure A20.** Noose trapping of a Nile crocodile.



Figure A21. Stainless steel threading under nuchal rosettes.



Figure A22. WW1500AS unit attachment via steel threading under nuchal rosettes.



**Figure A23.** Force-feeding pipe secured in a Nile crocodile's mouth (left), and the soft stomach tube through which the WW0500 unit was administered (right).



**Figure A24.** Profile of the force-feeding pipe and tube application, cloth temporarily removed for picture.